Listening to Rivers: Using sound to monitor rivers

WILLIAM ALEXANDER OSBORNE

Listening to Rivers

Using sound to monitor rivers

Wm. Alexander Osborne

A thesis presented for the degree of

Doctor of Philosophy

Department of Geography

Durham University

United Kingdom

January 2022

“There is something delicious about writing the first words of a story. You never quite know where they’ll take you.

Beatrix Potter ”

Blank

Listening to Rivers

Using sound to monitor rivers

Wm. Alexander Osborne

Abstract

From a babbling brook to a thunderous torrent, a rivers' soundscape can be described by many onomatopoeic words. Using sound produced sub-aerially by a river to calculate its stage is an entirely novel idea, designed to be used in an environment that is seldom monitored, headwater catchments. In these environments it is difficult to use traditional methods of automatic stage gauging, such as pressure transducers and ultrasonic depth monitors. I propose a cost-effective, simple to install sound monitor which can be simply placed beside a river that is making a noise. I develop a method of how to take the tempest that is river sound and filter it to a usable component using data collected from around the North East of England during Storm Ciara and Dennis, 2020. Understanding where river sound is generated from and the mechanisms behind it are key to developing sound monitoring which is why I use an experiment at a white water course to investigate the link between sound and river topography. Using an artificial channel and obstacles I investigate the link between obstacle height and configuration on the production of sound. To use river sound as a proxy for river stage, there has to be a process of how to setup and calibrate sound. I present a method of how one may go about setting up a sound monitor and the usage it may have in water resource management. Finally, I apply the method of sound filtering, river placement, and calibration at a catchment scale to determine its validity in river monitoring. Although novel, using sound to monitor a rivers' stage is practical and deployable.

Supervisors: Dr Rebecca Hodge and Prof Gordon Love

Acknowledgements

As my favourite expression goes, "tick tock, goes the clock, and all the years they fly" is an apt description of a PhD.

I must exclaim my thankfulness to Dr Rebecca Hodge. Without her help and guidance over the past 3 years, I wouldn't be in the position I find myself in now. All the mentorship in applying for grant money, to attending conferences and writing academic publications has been invaluable. Foremost has been the belief in fostering my little ideas, and helping to turn them into the project we see today. I also want to thank Prof Gordon Love, who is able to find a missing axis label a mile away and for becoming part of the Geography club. Together they have provided me with the help and guidance that all PhD students would dream of. Thank you!

I wouldn't have done the PhD without the company behind it all, Evolto, with Peter and Ruth Hawkin. I have now been to the centre of Britain, the wonderful Haltwhistle, and can only advise anyone reading to visit. The project evolved over the years and through the work done may be in a position to use sound monitoring in the future.

I must also thank the team in the laboratory in the Geography department, especially Eleanor, Merv and Chris who have enabled me to get to this position.

During the darker times of writing a PhD I thank both my parents and my friend Rebecca (different Rebecca) for helping me through. Especially in finding the correct colour schemes.

Contents

Declaration

The work in this thesis is based on research carried out at the Department of Geography, Durham University, England. No part of this thesis has been submitted elsewhere for any other degree or qualification, and it is the sole work of the author unless referenced to the contrary in the text.

Some of the work presented in this thesis has been published in journals and conference proceedings - the relevant publications are listed below. I declare that the contributions of the co-authors in these papers are limited to editorial advice.

Publications

Osborne, W.A., Hodge, R., Love, G., Hawkin, P., and Hawkin, R. (2021). Babbling brook to thunderous torrent: Using sound to monitor river stage. *Earth Surface Processes And Landforms*. doi: 10.1002/esp.5199

Osborne, W.A., Hodge, R., Love, G., Hawkin, P., and Hawkin, R. (Submitted). A sound rating curve: Using sub-aerial sound to calculate river stage. *Journal of Hydrology*.

Osborne, W.A., Hodge, R., Love, G., Hawkin, P., and Hawkin, R. (2022). The influence of in-channel obstacles on river sound. *Water Resources Research*. doi: 10.1029/2021WR031567

List of Figures

List of Tables

Acronyms

ADCP acoustic Doppler current profilers

Defra Department for Environment Food and Rural Affairs

DEM Digital Elevation Model

DFT discrete Fourier transform

EA Environment Agency

FFT fast Fourier transform

IoT Internet of Things

LLFA Lead Local Flood Authorities

LMF lowest median filter

LSPIV Large Scale Particle Image Velocimetry

LSPTV Large Scale Particle Tracking Velocimetry

PIV Particle image velocimetry

RH relative humidity

RE roughness element

RSZ river sound zone

SEPA Scottish Environmental Protection Agency

SGD stream gauge density

SGN self generated noise

SPL sound pressure level

UAV uncrewed aerial vehicles

UDM ultrasonic depth monitors

WWV white water value

"...suddenly he stood by the edge of a full-fed river. Never in his life had he seen a river before—this sleek, sinuous, full-bodied animal, chasing and chuckling, gripping things with a gurgle and leaving them with a laugh..."

Kenneth Grahame
The Wind in the Willows

Chapter 1

Introduction

1.1 Overview

Rivers are dynamic and evolving features of the landscape, from the source to the sea, tumbling and flowing through the environment. When a river floods it causes significant damage and cost (Kummu *et al.*, 2011). In England alone, there is a 1 in 6 risk of a property flooding from a combination of river and coastal sources (Environment Agency, 2009). During this project there have been 20 named storms that have contributed to flooding in the UK, with recurrence intervals of 1 - 20+ years (Met Office, 2021). It is predicted that with the effect of climate change, the UK will see a 10% increase in rainfall by 2100, with a focus on more intense heavy rainfall. If left unchecked, the cost of flooding in the UK could increase by 15 times by 2080, from around £1.4 billlion currently (IPCC, 2014). River monitoring has been deployed to target resources, such as temporary flood barriers, and provide warning, but still there is only one monitor for every 130 km of river network in the UK (Marsh, 2002). Therefore there is a need to monitor these flood events in a way that will not incur significant cost and can be implemented throughout a river network, to alert as many people as possible. Even with better monitoring, significant cost will still be associated with flooding and the best long term solution is to reduce our contributions to climate change. However, strategies to adapt to a changing climate must also be met, with the IPCC (2014) stating that since 1950, there is a likelihood that storms have increased in frequency.

The monitoring of aspects of the hydrological cycle, hydrometry, encompasses river flow and behaviour. The onus is on the Department for Environment Food and Rural Affairs (Defra), the Environment Agency (EA) in England, Scottish Environmental Protection Agency (SEPA) in Scotland, Natural Resources in Wales, and Lead Local Flood Authorities (LLFA) to monitor

the risk associated with flooding in the UK (Environment Agency, 2013). However there is no combined single body responsible, meaning that there is a juxtaposition between national and local strategy even though they are required to follow the Flood and Water Management Act 2010. A LLFA is responsible mainly for smaller water courses and their flood risk, with the EA or national equivalent being responsible for flood forecasting and activity on main rivers. There is however a gap when it comes to individual property protection, which goes under the umbrella term flood responsibility, with their own safety falling to them, the riparian owner. Communities can also come together to form a flood action group, with 50 in 2004, increasing to over 234 as of 2017 (Trell *et al.*, 2017). As this scale of responsibility moves lower and lower, cost-benefit becomes more necessary: a project that protects 1,000 homes will be chosen over one that benefits 100 for the same cost (Sugdon, 2004). The UK Goverment forecasted that increasing the EA budget by an extra £20 million a year, would in turn save £180 billion over a century (Bennett and Hartwell-Naguib, 2014). That saving amounts to nearly 10% of UK GDP annually currently, which when spread over 100 years is quite small, meaning for such an investment the savings is large, but in context of national income is small.

Currently there are direct and indirect measurements from a river that are used in flood management, which are derived from emerging and existing technology. River stage (distance between a reference elevation and the water surface), discharge (volume of water passing through a section at a specific time interval), and velocity of the river are the most common metrics used (Schaefer, 1972). Commonly, the easiest to understand and recognisable measurement is river stage, being easily understood by the public, and professionals as we can imagine what 1 m is for example. Stage is measured mainly through the use of pressure transducers, situated within the river. Pressure transducers are a well proven system of reliable stage measurements, but does require infrastructure and careful placement of them. The cost of this permanent infrastructure for use in the national flood network is £80,000 on average for a gauge station, and is focussed in areas where it is easier to access (Environment Agency, 2015). Other types of monitors are also used, which are more cost effective and are discussed in Section 1.6.There are therefore substantial proportions of the river network that are not monitored and where cost effective monitoring solutions would be beneficial.

The aim of this project is to determine if we can use sound as a method of monitoring a river for use in flood management using only the natural soundscape. The term "soundscape" is the sounds that can be heard when if by a river, from the tumbling of the flow, to the birdsong and the wind. I use sound as a proxy for river stage, whilst trying to identify a sound-stage relationship and creating a sound-stage ratings curve. I target the smaller, headwater catchments, which make up 70 - 80% of the total catchment area since they are seldom monitored conventionally (Gomi *et al.*, 2002). The monitor is situated out of the water, therefore not using hydrophones, but instead a simple microphone. Ease of deployment is key, and the monitor needs to provide reliable measurements that can be easily be situated to any part of a river system. It is intended to be simple to deploy and leave, with limited calibration needed. The monitor is not designed to replace current river monitoring strategy, but to act along side and target areas not currently widely monitored. I show a new, innovative way of using sound to monitor a river. I split this work into three main parts:

How?

Can river sound be related to stage through filtering the soundscape around a river?

Why?

Can I determine what produces sound in a river and how it relates to in-stream obstacles?

What?

What can river sound monitoring be used for and where can it be implemented?

Chapter 2 is a published paper which investigates whether there is a relationship between river sound and flow stage. It shows my method of how to extract a single component of sound that relates to stage. It goes onto present data collected from Storm Ciara as an example of how well sound and stage form a relationship. Chapter 3 is a submitted paper on how to generate a sound-stage ratings curve for field calibration. Chapter 4 is a submitted paper which investigates which components of a river channel need to be present to generate a sound-stage relationship using a white water course to simulate at a real-world scale. The source of the sound is identified through the use of image analysis. Chapter 5 is a test of a network of sound monitors in the River

Gaunless catchment and shows the steps necessary for future deployments of this method in water resource management. Chapter 6 is a concluding chapter which sums up the progress made in sound monitoring and its possible usage in the future.

The next section of this chapter gives an introductory overview on what sound is, and the challenges faced in linking this to a river. I then review the current state of river monitoring using sound, and examine the causes of sound within this environment. Finally I examine the suite of technology being deployed to help with flood mitigation and explore the topic of "big data".

1.2 Sound fundamentals

A fundamental knowledge of sound and how it interacts with itself and the environment is needed to understand the complexity of a river soundscape and dictates what I can and cannot measure. This section introduces what sound is and how factors such as attenuation can limit sound.

1.2.1 What is sound?

Sound is generated when something vibrates, with its energy moving through a medium such as air, water or even the ground as a longitudinal pressure wave (Hall and Crockford, 1973; Rossing and Fletcher, 2004; Khairetdinov *et al.*, 2020). When these pressure waves hit something that is listening, such as your ear or microphone, the differences in pressure generated by these waves cause a diaphragm to move, allowing something to be heard through electrical signals (Hudspeth, 1989; Huang and Shiu, 2015). As to what is heard, sound is split into two main constituents, with the interplay of amplitude and frequency. A sound wave is a oscillating signal, with how many times it repeats within a second giving its frequency in Hertz, with the more cycles giving a higher pitch. The loudness of a sound is determined by the amplitude of the signal. Amplitude can be measured in pressure, decibels (a logarithmic scale), or a direct electrical signal in volts depending on how the signal is captured and processed (Figure 1.1).

A pure tone signal would look like a sinusoidal line, however, sound can be made up of many waves of different amplitudes and frequencies, with the superimposition of these creating constructive and destructive interference (Figure 1.2). With different frequencies, the resultant waveform can look complex. In dealing with a natural source, we expect the signal to be complex with the added complication of multiple sound sources coming together.

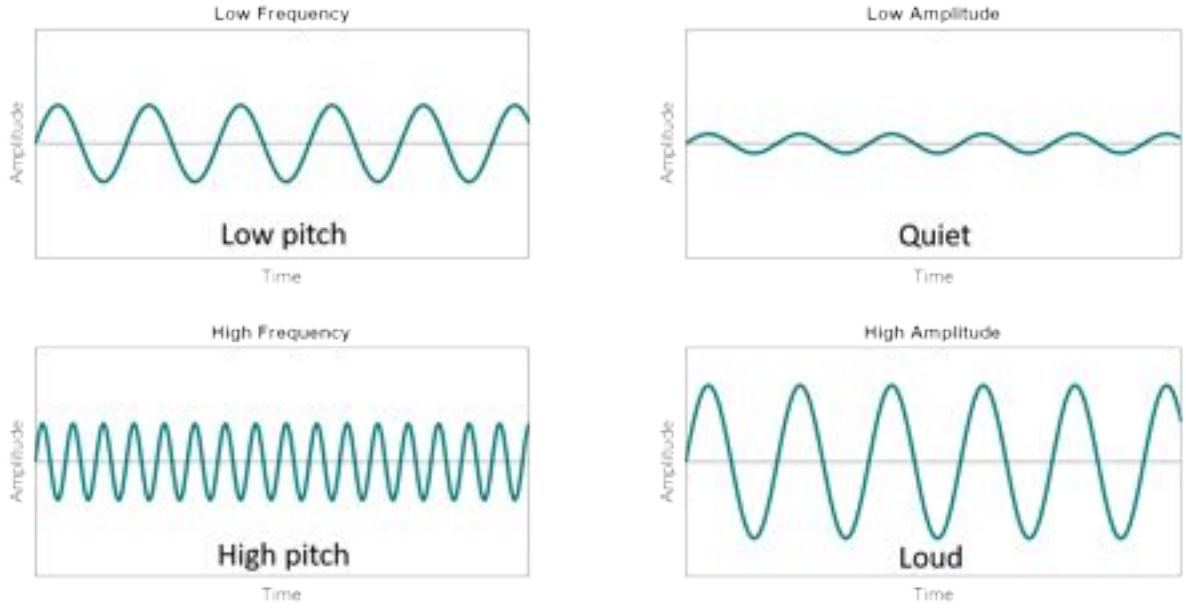

Figure 1.1: The affect of how frequency and amplitude effect a sinusoidal wave. With a reduction in the period between complete cycles, a higher frequency will be observed and an decrease in wavelength. An increase in the amplitude of a wave will create a louder sound.

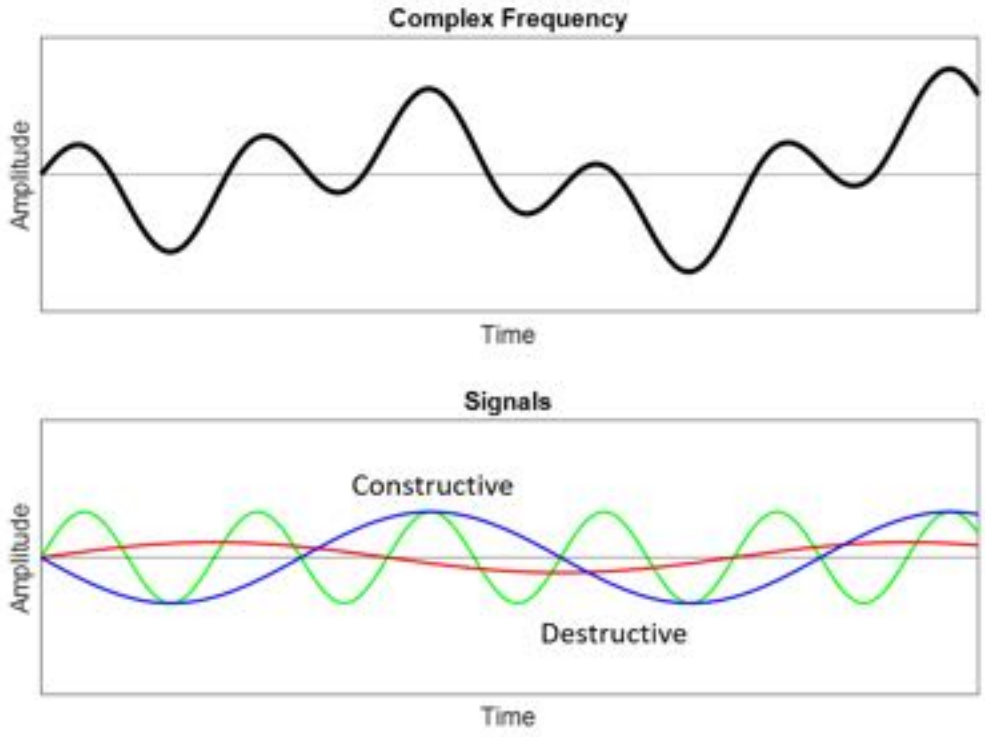

Figure 1.2: Three different frequency waves with one another causing a resulting pattern of destructive (wave amplitudes become smaller) or constructive (wave amplitudes become larger) interference.

1.2.2 Signal processing

Viewing audio data in a meaningful way for acoustic research has relied upon using an idea introduced in the 19th Century to categorise frequency within the frequency domain, called Fourier analysis. With constructive and destructive interference, trying to figure out the types of frequencies present in a signal is all but impossible by just looking at the shape of the waveform. Fourier (1878) theorised that any function can be decomposed into an infinite sum of sinusoidal functions using,

$$f(\theta) = a_0 + \sum_{n=1}^{\infty}(a_n \cos\, n\theta + b_n \sin\, n\theta) \tag{1.1}$$

$$f(t) = a_0 + \sum_{n=1}^{\infty}(a_n \cos\, n\omega t + b_n \sin\, n\omega t) \tag{1.2}$$

where f is frequency, a is amplitude and ω is angular velocity. The idea has been developed into a powerful tool which in its simplest form is changing the perspective of the data, from one in time, to that of frequency (Figure 1.3). The complexity of performing this analysis, a discrete Fourier transform (DFT), requires the sequentialisation of large amounts of data. The time taken to perform a DFT means that a faster alternative method is preferred using improved algorithms, a fast Fourier transform (FFT) which imposes different limits on the data. Imagine you have a signal made from the addition of a number of sine waves - so the signal is quite complicated. If you take the FFT of the signal it will tell you the amount of each component present. So the FFT of a sine wave is a delta function. The FFT of the sum of 2 sine waves is 2 delta functions as shown in Figure 1.3.

FFTs are used in numerous aspects of signal processing (Oppenheim and Weinstein, 1972), encompassing image analysis (including the processing of a Digital Elevation Model (DEM)) (Burt, 1981), sound filtering (Bishop *et al.*, 2020), spectroscopy (Pacholski *et al.*, 2005) and magnetic resonance (Irarrazabal and Nishimura, 1995) to name some practical applications.

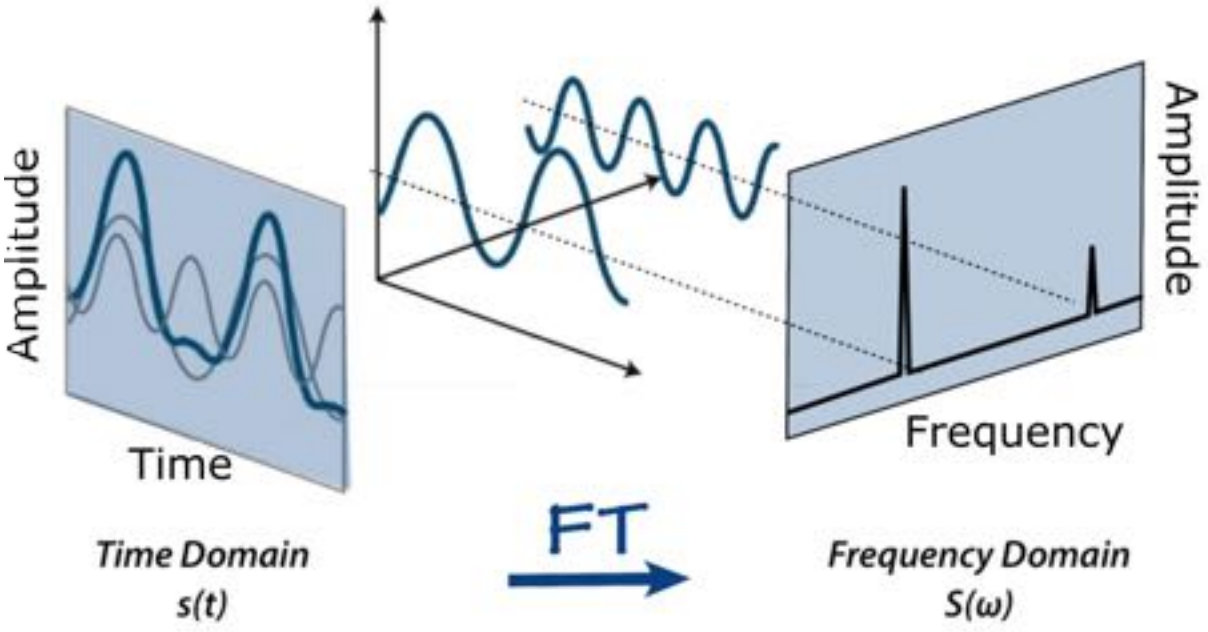

Figure 1.3: Transformation of a complete complex waveform in the time domain via a FFT which splits the complex into its constituent parts. The result from a FFT is a conversion into the frequency domain, showing what was combined to form the time domain signal. (Adapted from AAVOS.com, 2021)

1.2.3 Sound attenuation

It was said by Marconi, the credited inventor of radio, that sound never dies, simply decays. He then stated that theoretically you could hear into the past, listening to quieter, and quieter sounds, with his aim to hear the Sermon on the Mount (Hayes, 2009). Since energy cannot be destroyed, and we sadly cannot hear into the past, the energy must dissipated and be transformed. Through sound attenuation, sound energy is transformed into ultimately heat energy, with the yelling human voice generating 0.001 W of energy at 80 dB, meaning it would theoretically take 2 million people to get a kettle to boil water (Long, 2014). Like a splash in a puddle, sound energy dissipates from the source until it is completely transformed. Along with the absorption of energy, sound scatters in other directions from the original path, which increases the perception of sound, allowing something to be heard indirectly. Being omnidirectional does reduce the ability of sound to travel further. Equal spreading loss in decibels, A_s, is given by

$$A_s = 20g \log\left(\frac{r_2}{r_1}\right) \tag{1.3}$$

in which r are the relative positions of the source and measuring point and g is the wave propagation characteristic. The frequency of the wave also affects how far it can be heard from the source. Lower frequencies are the least attenuated over distance, hence why thunder can be heard as a low rumble from miles away (Bedard, 2005; Ziemann *et al.*, 2013). How far sound travel also depends on what it is propagating through. Earthquakes generate sounds that can be monitored seismically all over the Earth (teleseismics), but you can't hear one from the other side of the planet through the air (Dziewonski and Romanowicz, 2015). In a fluid, such as air and water, the ability of a sound to travel through it is known as Stoke's Law,

$$\alpha = \frac{2\eta w^2}{3\rho V^3} \tag{1.4}$$

where α is the attenuation coefficient, η is the fluid viscosity, w is the rate of change of the wave, ρ fluid density and V the speed of sound in the fluid. In air, temperature and relative humidity (RH) controls how far sound will transmit by changing the ρ , with warmer air temperatures allowing sound to travel further, negating the fact of refraction (the changing of the direction of a wave when passing through a medium), and higher humidity also aiding sound transmission (Figure 1.4).

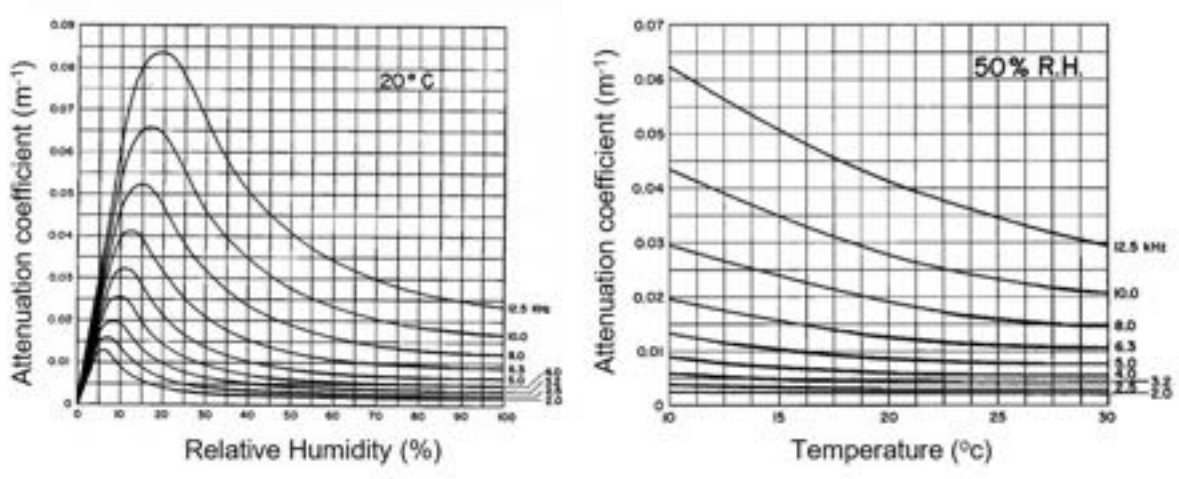

Figure 1.4: The effect of RH and air temperature on sound attenuation (Harris, 1966).

How RH and temperature affects the propagation of sound is due to how it changes the speed of sound, by changing variables in Stoke's Law, such as fluid density, since cold air is denser than warm air for example (Panda *et al.*, 2016). Low frequencies, <2 kHz, are the least affected by

changes in RH and air temperature. In a UK outdoor setting, RH is on average between 70-90% , and air temperature, 4-18 °C, meaning the greatest form of attenuation on sound will primarily be from temperature. The most challenging places to monitor sound at a distance would be both cold and with low RH. The heterogeneity of the atmosphere therefore makes calculating models of attenuation difficult, with the simplification of a sphere of sound propagating from the source being inadequate (Royle, 2018).

1.2.4 Harmonics and resonance

A fundamental frequency is the frequency at which an object resonates when it vibrates, for example hitting a gong. All objects have a fundamental frequency, as it is the reaction to an external force on the object, but the frequency depends on what is being struck and how well it dampens the sound (Matson, 2016). Often in association with a fundamental frequency there are subsequent harmonic frequencies (Figure 1.5). The harmonic frequency is a multiple integer of the fundamental, for example, a 100 Hz signal will have a 200 Hz, 300 Hz, etc... harmonic. When a gong is first hit, the fundamental frequency is dominant, but as time goes on, a time-decay takes over, allowing the various harmonics to appear (Hayes, 2009). Overtones, which includes harmonic frequencies, are alternative frequencies that can appear that are above the fundamental. The interplay of these additional frequencies is what make a tone feel "rich", with each overtone being lower in amplitude to the preceding one.

We see the behaviour of harmonics and overtones in natural settings, not only with musical instruments.Jousset *et al.* (2003) found while monitoring volcanic tremors that repeated peaks at higher frequencies from a seismogram at steps from the fundamental frequencies. It was assummed this was down to internal resonance structures within the ground facilitating this. Dziak *et al.* (2008) found during hydrophone monitoring of underwater tremors that the fundamental frequency was 3 Hz, with harmonic spacing seen at every 3 Hz until being undetectable after 18 overtones as they either become too quiet. Detecting overtones utilise the FFT approach, with being able to see the peaks occurring over the frequency domain, when the peaks begin to go into background noise then they are indistinguishable.

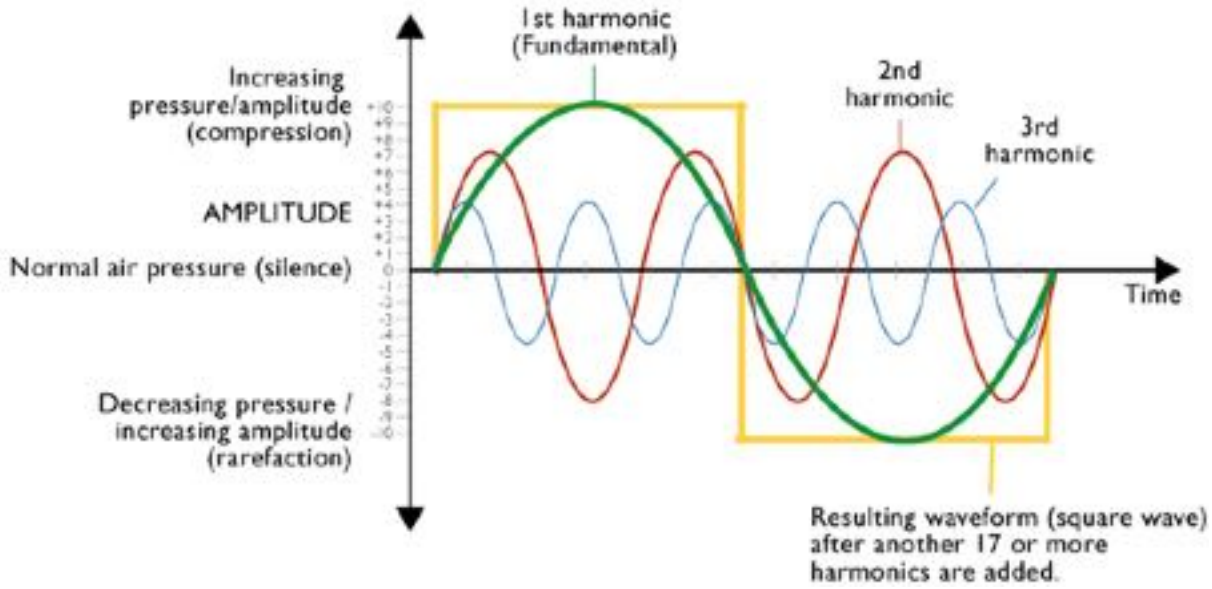

Figure 1.5: The fundamental frequency (Green) with its subsequent harmonics, 2nd (Red) and 3rd at lower amplitudes (Blue) (Ottewill, 2013).

1.2.5 Section summary

Understanding the basics of sound and how it interacts with its surroundings is crucial when it comes to beginning to monitor a river soundscape. Sound can be broken down into the frequency domain using a FFT, meaning that sections of a soundscape can be identified and studied. The environmental impact of RH and air temperature adds another complexity to monitoring outdoors and the impact of that needs to be assessed. Knowing that sound can be multilayered, with fundamental frequencies and overtones means there is a likelihood sound can be studied at different frequencies, or over a range of them.

1.3 Sound and rivers

Research into the sound produced by rivers was first published in 1933, with the first recorded example of Minnaert (1933) using the sound of sediment impacts on a pipe to characterise bedload movement. Two main fields of river sound were then spurred, hydrophone and geophone monitoring. With a history and research spanning more that 80 years, the insights gained from these two techniques is overwhelming. This section looks into the current field of river monitoring using sound, including how sound is generated and how geomorphology impacts this.

1.3.1 Hydrophone - Underwater sound

A hydrophone is a sensor which listens to the sound waves travelling through water. Hydroacoustic monitoring measures sound signals within the water, allowing non-invasive, long term observation (Figure 1.6) (Linke *et al.*, 2018). Hydrophones were first created in the aftermath of the Titanic disaster as an early form of sonar, and since then have been used in ecology, geomorphology and geophysics (Krohn and Chen, 1992; Frost, 2001; Simpfendorfer *et al.*, 2002; Belleudy *et al.*, 2010). In the context of sediment derived sound, it is categorised as self generated noise (SGN), and is composed within the boundary of water, with turbulence and sediment transport (Manasseh *et al.*, 2006). The speed of sound is much faster in water than in air, at 1,480 m s^{-1} compared to 343 m s^{-1} in air due to water being denser, allowing energy to be passed along easily (Del Grosso and Mader, 1972). So when a sound is created underwater, the flow of the river for example cannot prevent the transmission of sound upstream, and spreads out omnidirectionally, meaning you can hear equally as well from upstream and downstream so long as new sound sources aren't introduced such as turbulent noise acting on the hydrophone or impossibly the river flows faster than the speed of sound.

1.3.2 Hydrophone - Listening to sediment

Sound is not a direct measurement, but is continuous, i.e. sound is always being produced in a river (unless dry), and it changes through the influence of other factors such as rainfall.

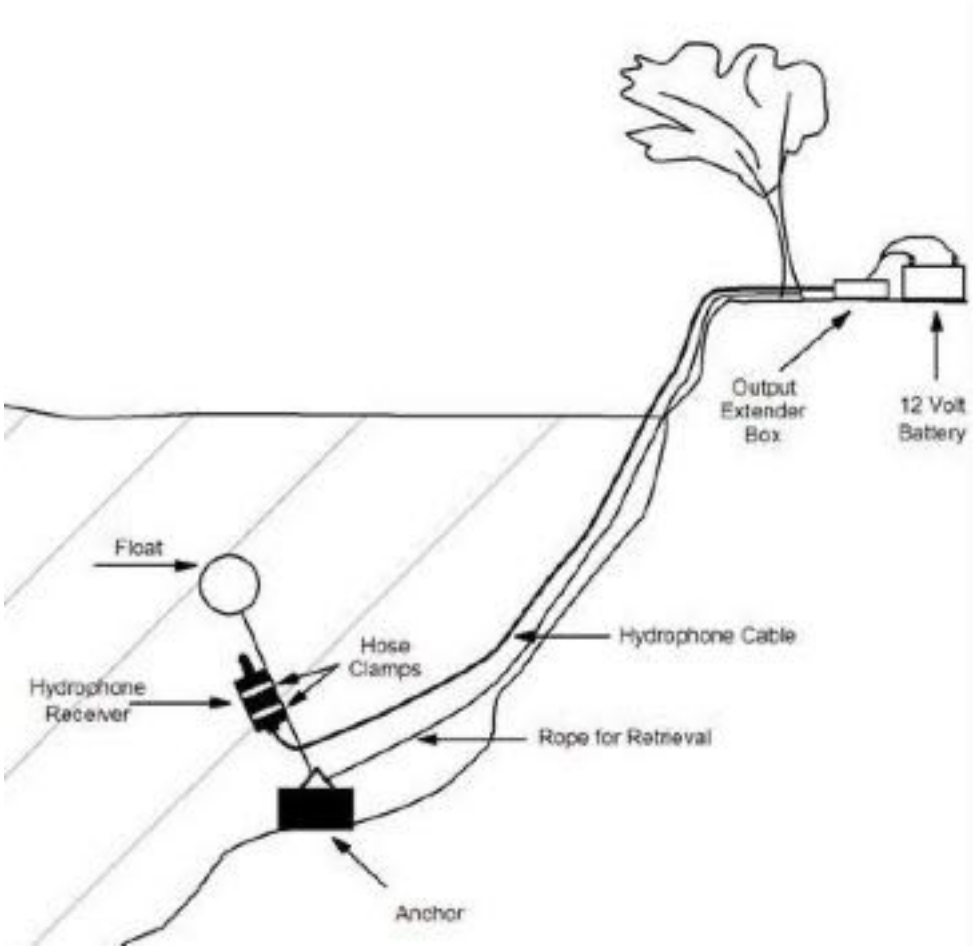

Figure 1.6: A typical hydrophone setup beside a river (Vogel, 2006).

Hydrophones are used in scenarios in which the direct measurement of a river process is either too dangerous or the processes happens without prior knowledge. Bedload measurements, identifying when the sediment become mobile, what size and how much of it, is difficult to directly measure without infrastructure (Ergenzinger and De Jong, 2003). Although this project is not about sediment, there is a longer history of using sound to monitor sediment (compared to flow), and thus start by presenting this. The Erlenbach stream, Switzerland, pictured in Figure 1.7 has been fitted with an automatic sediment basket allowing sediment transport rates and grain size distribution to be measured (Rickenmann *et al.*, 2012). Sediment collection bins, Birkbeck-type pit bedload samplers, can also be installed within the channel to monitor bedload flux, as with the Tordera River, Spain (Garcia *et al.*, 2000). These structures are not placed at the whim of the researcher, but require significant resources and time to install. It is said that these sampling methodologies are destined to become redundant, and only used for calibration when continuous and reliable alternatives mature. These include direct measurements using acoustic Doppler current profilers (ADCP), sonar and radar and passive using hydrophones and impact

columns (Gray *et al.*, 2010). Depending on what is needed to be measured, some techniques are better suited to certain grain sizes. Le Guern *et al.* (2021) was interested in sandy-gravel beds and used a combination of both a hydrophone and ADCP to quantify it.

Figure 1.7: The Erlenbach sediment monitoring station, with a zoomed in image of the sediment catching baskets (Rickenmann *et al.*, 2012).

An early form of bedload monitoring used the sound generated from a grain impacting a steel plate on the ground, and counted the impact sound to determine the rate at which grains hit the plate. In 1986, the Erlenbach was monitored using this method, with now the addition of the baskets (Banziger and Burch, 1990). Results from a storm event showed that there were two peaks of bedload movement, one at maximum water runoff and a second during the falling limb (Figure 1.8). The issue concerning this method is that the sensor was only able to hear small flood events, in which individual grain impacts could be heard. Higher magnitude events cause suspended particles, covering the sensor and resulted in less impacts being measured. Turowski and Rickenmann (2009) found that the tools and cover effect, with a grain either being used to contribute to bed erosion, or protect and cover it, can impact acoustic impact measurements, leading to a high degree of scatter between events of similar discharge. The scatter in data is primarily down to how the a sediment grain interacts with the plate and its mode of transport, with the monitoring technique itself shown to be reliable. Additional sound signals such as from the rolling and sliding of sediment instead of impacting has been shown to influence the signal (Krein *et al.*, 2008).

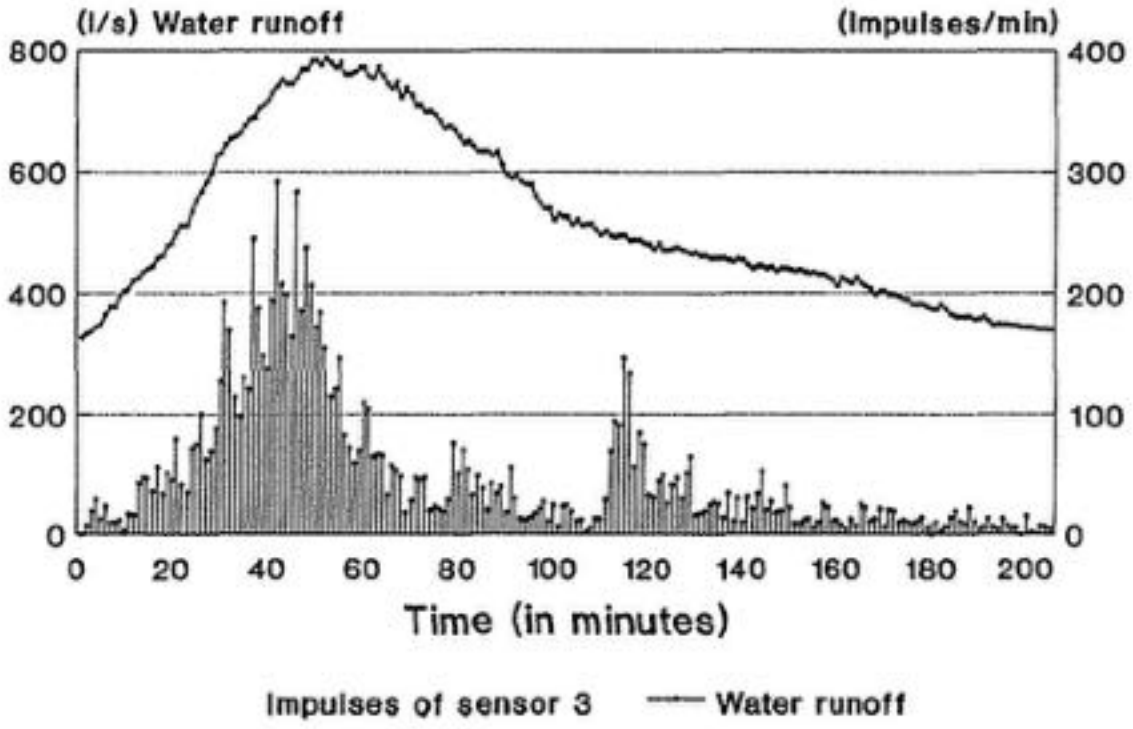

Figure 1.8: Number of recorded impacts on the plate vs. the measured water discharge (Banziger and Burch, 1990).

Krein *et al.* (2016) used a hydrophone under a steel plate to investigate how bedload changed in different energy regimes (increased water stage). Instead of counting impacts on the plate, they used the spectrum of sound to calculate bedload flux. The signal produced by the hydrophone is related to sediment impacts, with the louder the sound, the larger or more of the impactor. The frequency remained broadly the same, at between 0.1- 3 kHz, with intensity changing the most. It means that the increase in water stage caused changes in the acoustic field, due to an increase in bedload. Although the experiment was only over 0.04 m of water depth, it does give a continuous record.

These heavy infrastructure systems employed here are beyond what most can hope to achieve, and similarly to the infrastructural costs that the EA face when building gauges, alternative means are always sought after. The easier impact plate method also does not provide conclusive results with bedload, due to issues concerning the movement and behaviour of the sediment, such as becoming suspended. Therefore, for sound to be useful as a surrogate for direct measurements of bedload, it has to be able to be as good as in-channel measuring, while not creating additional issues.

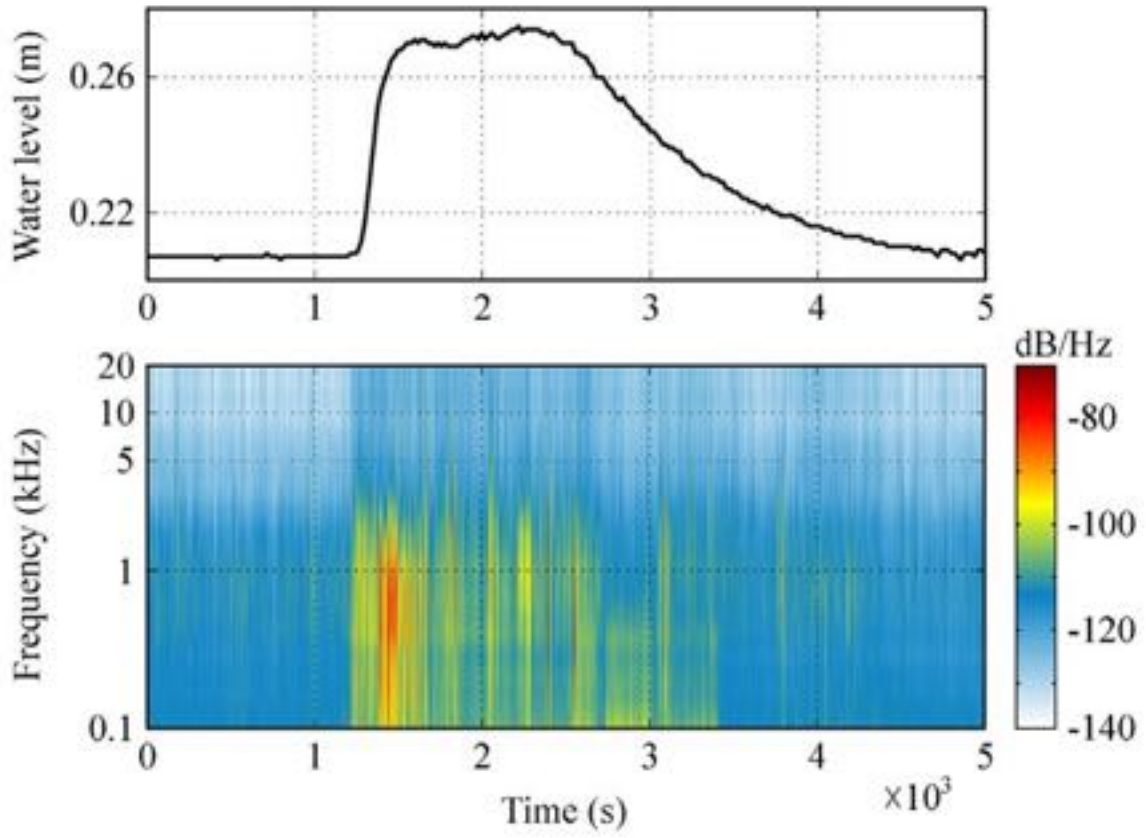

Figure 1.9: Hydrograph generated from a discharge event with the time series spectrogram showing the frequency and amplitude of the sound generated from impacting grains (Krein *et al.*, 2016).

1.3.3 Hydrophone - Underwater soundscape

Monitors that are easy to deploy, especially in large rivers with extreme hydrologic and hydraulic conditions and for continuous collection are advantageous (Geay *et al.*, 2019). A passive acoustic approach to determine bedload was demonstrated by Bedeus and Ivicsics (1964), while lowering a so called acoustic indicator (hydrophone), into the water without the need of steel plates or other infrastructure. Their results in Figure 1.10 show that they were getting variation in the sound, but it was very noisy and also didn't particularly correspond well with the bedload sampled or water depth. A hydrophone does not only pick up the sediment moving and impacting, but a whole suite of water induced noise, and without a way of filtering out and isolating this, your results will be poor. Aural review, listening to the sound by the ear, was seen as an effective means of distinguishing sound sources (Camp and Farwell, 1972).

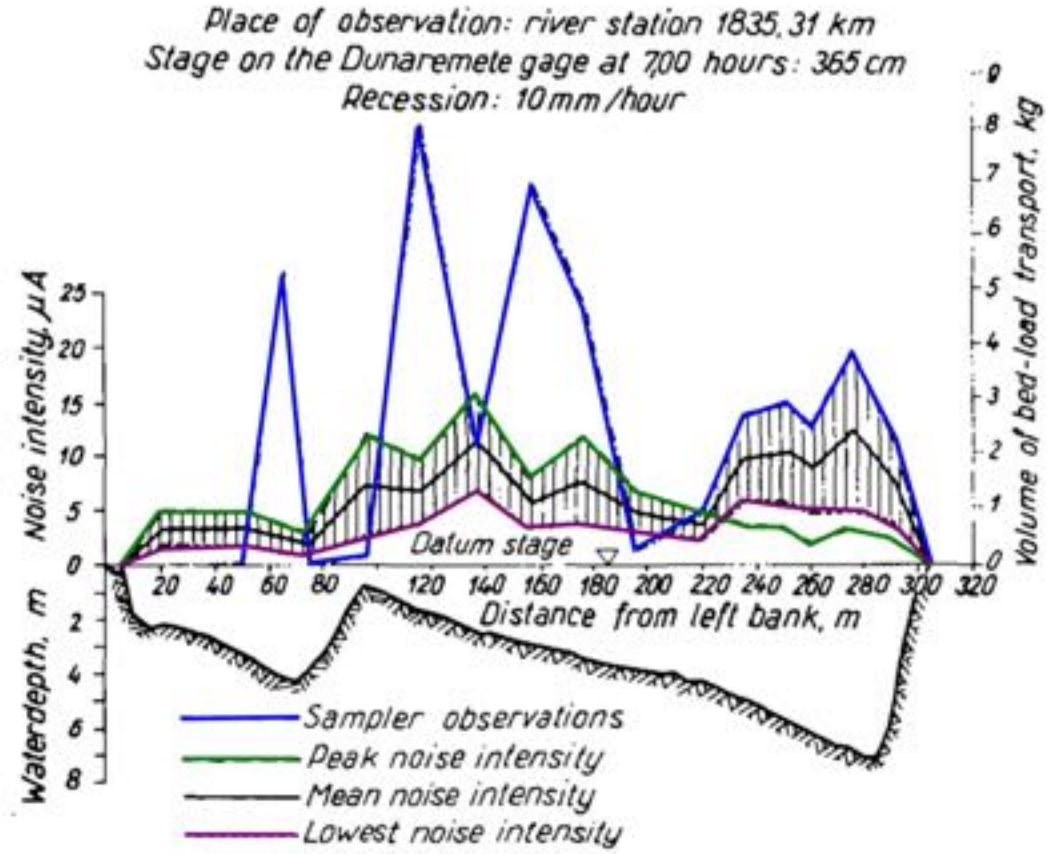

Figure 1.10: Water depth with the sound captured using a hydrophone with the measured in-channel bedload transport rate (Adapted from Bedeus and Ivicsics (1964)).

Studies using flumes and natural experiments found that certain SGN are classed in domains, specific sections of the spectrum. Linke *et al.* (2018) found that frequencies >1 kHz were related to how turbulent the water was and <1 kHz was the sound produced when sediment moved when monitoring freshwater ecosystems. Tonolla *et al.* (2009) found that during flume experiments investigating the sources of underwater sounds, that the most excitable part of the spectrum was between 0.125 - 2 kHz when obstacles began to be submerged. The signal to noise ratio is very close to each other in flume experiments, with external noise such as turbulence and pump noise being filtered out, which was aided by using two instead of one hydrophones (Tonolla *et al.*, 2009). The reason why particular parts of the sound spectrum are more excited than the others was explored by Thorne and Foden (1988) when looking at the sound generation of impacting glass spheres. It was found that the the deceleration of the impactor to the impactee generated sound depending on their density, size and speed. The peak frequency, f produced is found using

$$f_{\text{peak}} = \frac{224}{D^{0.9}} \tag{1.5}$$

when grain diameter, D, is with uniform-grain distribution (Thorne, 1986). Meaning that sediment with a size of between 10 and 20 cm will theoretically have a frequency range spanning 0.9 - 1.7 kHz. When viewing hydrophone data of bedload noise, Figure 1.11, Petrut *et al.* (2018) found the low frequencies are noisy, and without form, but above 1 kHz there is more homogeneity, then sound at these frequencies should correspond to particles of 20 cm. Hydrodynamic processes generated sound from 0.01 - 1 kHz, and 1- 50 kHz was truly showing bedload SGN. In comparison to Figure 1.10, the action of being able to filter the data using power spectral density has helped delineate a signal.

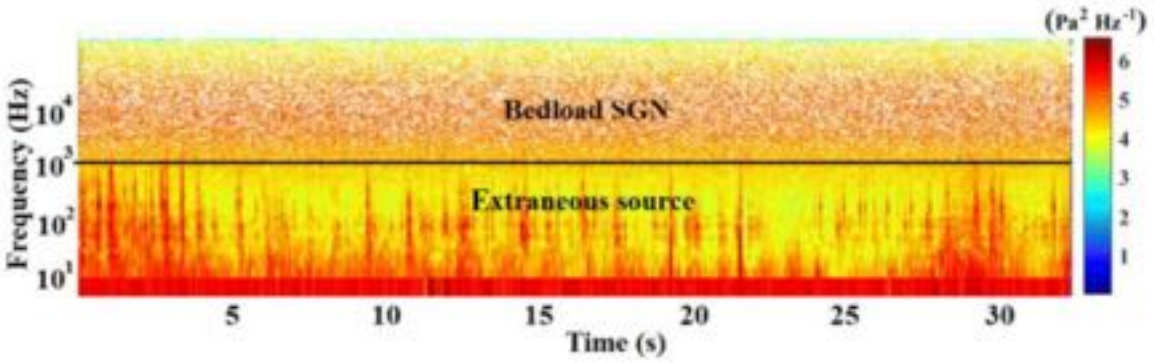

Figure 1.11: Spectrogram of underwater sound with the sections split between hydrodynamic noise and bedload sediment generated noise using a hydrophone (Petrut *et al.*, 2018).

Barton *et al.* (2010) found that when researching high energy bedload transport, their hydrophone monitoring had acoustic spikes and noted that within the bedload community large uncertainties were acceptable given the use of current methods of quantifying bedload. Signal analysis is therefore the key to unlocking the potential of hydrophone data, that is not linked to impact plates. It was found that the root mean squared of acoustic pressure, P_{rms}, is related to bed load transport, M, with

$$P_{\text{rms}} = \beta M^{\gamma} \tag{1.6}$$

where β and γ are parameters based on what is being measured, and by what (Rouse, 1994; Geay *et al.*, 2019). These experiments were run in so called "mountain type rivers", with areas such as riffles and pools able to mix the water. Larger rivers such as the Danube were monitored

by Vračar and Mijić (2011) over ten years, and without the agitation of the river bed found that frequencies below 100 Hz are most linked to flow rate and speed of the river. Higher frequencies were found to be related to increasing anthropogenic activity on the riverbanks.

For hydrophones to be seen as reliable in bedload measurements, key details need to be known, including the frequency released by the grains, grain size distribution and that the ambient noise is constant and able to be removed (Marineau *et al.*, 2015).

1.3.4 Hydrophone - Sound generation

Hydrophones are not only used for bedload monitoring, but can also pick up turbulence of the water itself. Turbulence causes extraneous noise which is filtered out when looking at bedload, since the frequency is within the same range, from 0.5- 2 kHz (Lugli and Fine, 2007). Turbulence will be generated from the flow itself, or induced by the wind generating surface waves, broadly in the 0.1 -1 kHz region (Zakarauskas, 1986). The trapping of air within water, causing bubbles, is thought to be the main source of the acoustic signal, within and outwith the water. The breaking of waves, moving floating objects and rainfall can also create sub-surface bubbles, which release sound when they burst (Bolghasi *et al.*, 2017a). The sounds of splashing, pouring and streaming are easily identifiable by humans, but do not have any distinctive features (Van Den Doel, 2005). Water is largely soundless by itself and needs an external force and to be moving (Bragg, 1921). Ronan (2017) studied how changing Froude numbers affects the acoustic field generated underwater. They found that as Froude number increased from 1 to 1.7 there was a change of sound when the flow regime changed from an undular to hydraulic jump. The frequency with which a bubble fragments is a function of surface tension, hydrostatic (transference of energy by pressure) and hydrodynamic (transference of energy through motion) forces (Leighton, 2012). The frequency of a bubble bursting was explored by Minnaert (1933), who was interested in reducing the complexity in the sound of the "humming of the sea" or the "roar of a cataract" to a more elementary state. Chicharro and Vazquez (2014) wrote the equation as

$$f_0 = \frac{1}{R_0}\sqrt{\frac{3\gamma P_A}{4\pi^2\rho}} \tag{1.7}$$

where, f_0 is frequency, r_0 is bubble radius, P_A is absolute liquid pressure, ρ is liquid density and γ is specific heat ratio. The bubble radius therefore assumes the bubble is spherical, and without observing individual bubbles is broadly accepted to work. Bubbles are influenced by the flow measured by the Reynolds number and surface tension with gravity measured by the Eötvös number (Figure 1.12) (Clift *et al.*, 1978). The shape is therefore not always a sphere.

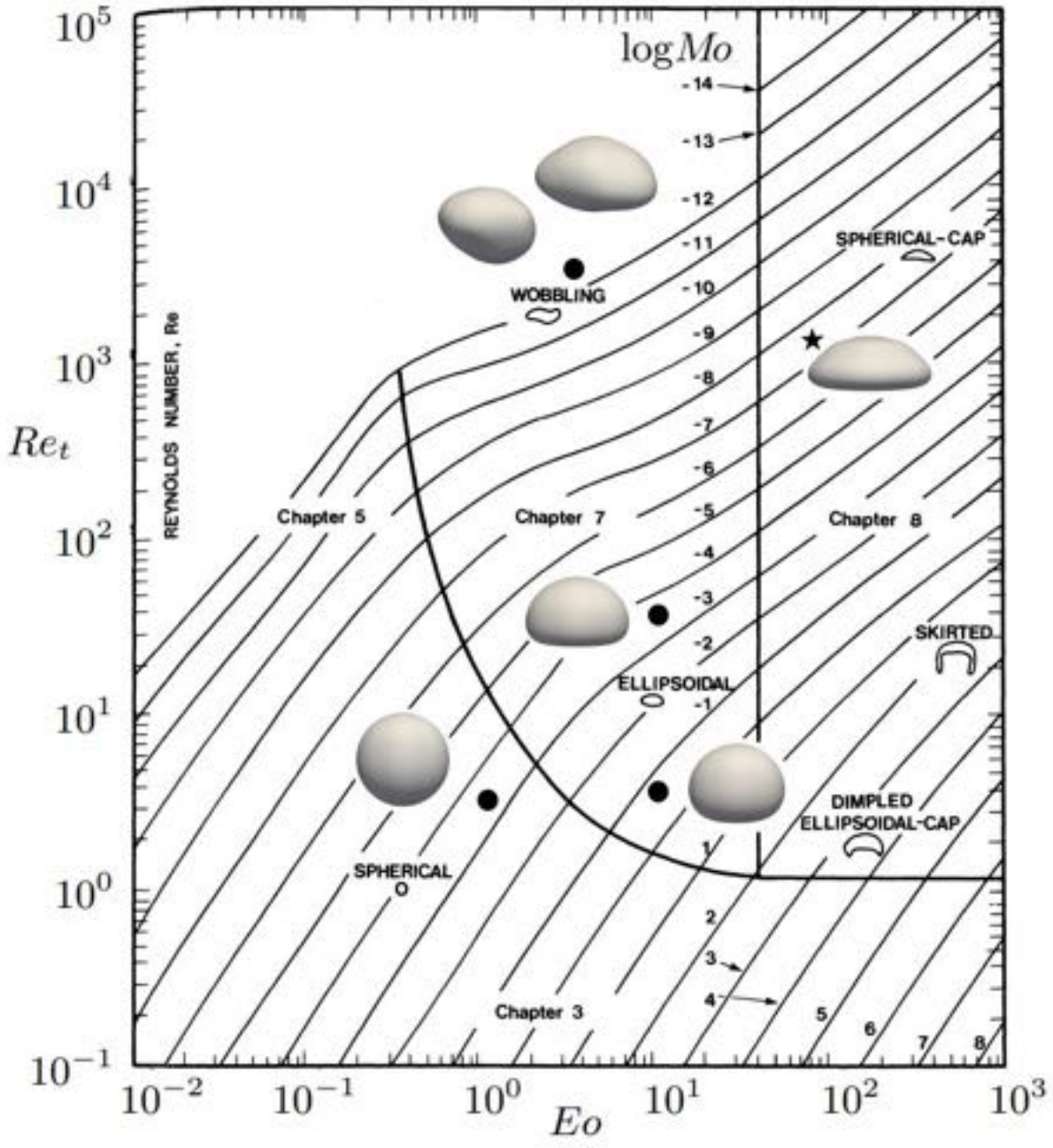

Figure 1.12: How a changing Eötvös and Reynold number can have on the shape of a bubble (Krull *et al.*, 2016).

Trying to measure the sound frequency produced by a single bubble, given the circumstances

needed to form them is highly complex and not readily studied (Frizzel, 1987). Bubbles interact with one another, such as two bubbles coalescing into one also releases sound happening as quickly as 0.1 ms (Manasseh *et al.*, 2007). We therefore take the Minnaert resonance as an idealised frequency, without the effects of fluid dynamics (Ammari *et al.*, 2017).

Experiments by Leighton *et al.* (2005) looked at the physics of breaking waves and showed that most bubbles burst at a frequency of between 0.4 and 2 kHz. They compared the detection of this from a hydrophone and a microphone. In doing so they showed that it was possible to pick up the sound of a bubble bursting first in water, then in the air due to the differences in the speed of sound and acoustic attenuation reducing its amplitude. The signal itself was shown to decay faster compared to in the water.

1.3.5 Geophone

A geophone is used to monitor ground vibration (known as seismic signals), with a signal being created when a mass moves inside the device between magnets (Iskander, 2018). The frequency of seismic data is lower than compared to that measured hydrophone and microphones, and depending on the type of geophone can be from 0.001 Hz to 2 kHz (Xiao *et al.*, 2018). Burtin *et al.* (2016) describes how seismic monitoring can be used in geomorphic activities, at landscape and streamside scale to measuring surface processes, not only limited to earthquake monitoring. Seismic data was first used in fluvial studies by Govi *et al.* (1993) to measure coarse sediment delivery mechanisms during flood events, with the microseismic signals found able to be related to bedload transport mechanisms. Fluvial seismology is relatively new with Hsu *et al.* (2011) being able to monitor seismically the impacting of grains during a storm event. Tsai *et al.* (2012) observed that the seismic data scaled with the size of grains and their velocity. The behaviour of how bedload sound changes over a discharge cycle was investigate by Barrière *et al.* (2015) and showed hysteresis of the sound, with the sound becoming quieter after peak flow. Seismic research has mainly been focused on bedload processes, as direct methods of collecting data are challenging, especially during large floods when the bulk amount of sediment transport occurs, similarly to the themes introduced in Section 1.3.1 (Roth *et al.*, 2017). Gimbert *et al.* (2014) have subsequently found that amplitudes in the region of 0.001 – 0.1 kHz formed a relationship with discharge when modelled for determining the sound of turbulent flows, with Anthony *et al.*

(2018) narrowing the range to between 0.0004 – 0.045 kHz.

Understanding what is generating the seismic signal is imperative to being able to filter out the component that is needed. Schmandt *et al.* (2013) found three distinct fluvial sources for seimic noise; bed load transport at 15 - 45 Hz, fluid traction on the bed at 0.0073 kHz and waves at 0.006 - 0.007 kHz. Figure 1.13 has spectrograms showing a relationship between a discharge of 300 to 1300 cumecs, on both seismic and infrasound (low frequency microphone). Burtin *et al.* (2011b) also linked changes in the 0.003 - 0.009 kHz region of being linked to river level, and assumed a linear relationship between seismic noise and water level, with seismic monitors within 50 m of the river. The limit imposed on the relationship between seismic noise and water level is whether the river reaches bankfull, with the relationship only being formed if the water level is kept below bankfull.

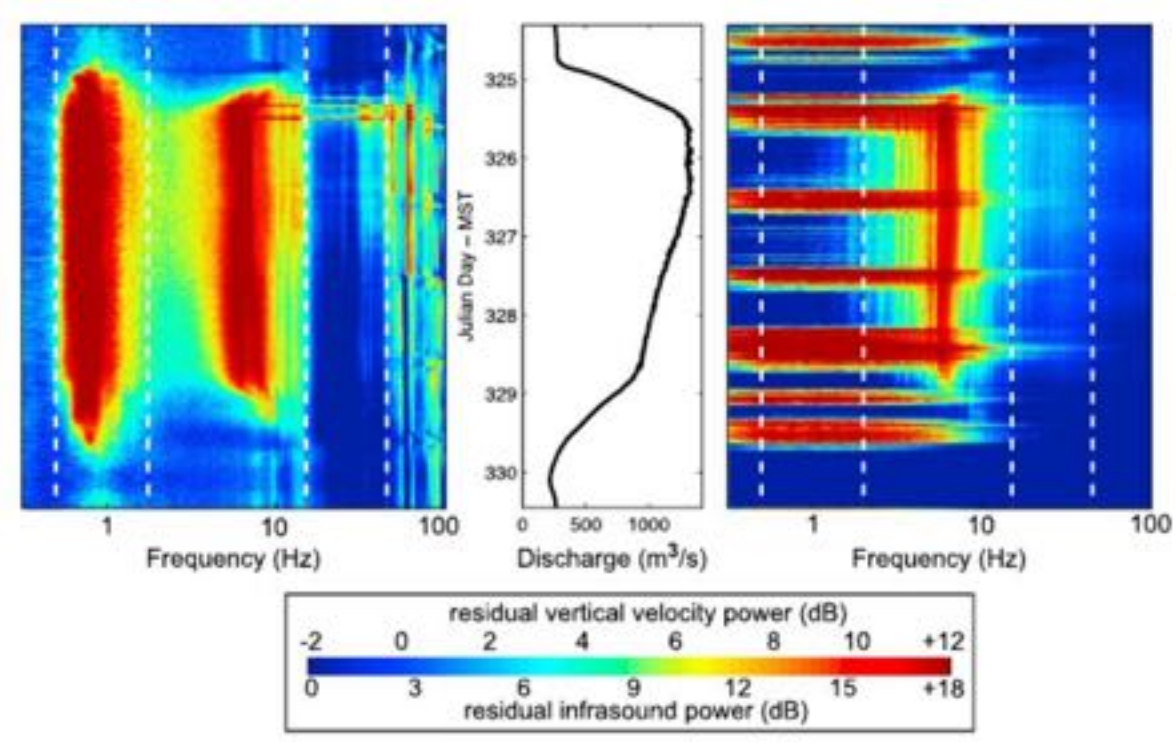

Figure 1.13: (Left)- Geophone data, (Right)- Infrasound data during a discharge event. Event time goes from top to bottom (Schmandt *et al.*, 2013).

Gimbert *et al.* (2014) suggests that noise generated by the water itself can be translated into seismic waves, from processes occurring such as cavitation in the water. Ambient monitoring, in which the geophone is not located within the channel gives the ability to monitor these additional

sources, as well as being easier to access for maintenance (Burtin *et al.*, 2016). Evidence of additional sources of sound being found is seen in Figure 1.14, in which Burtin *et al.* (2008a) found a hysteresis effect on the seismic signal. The data show that for the same water level, the seismic signal is higher at the start of the season, because of increased bedload transport rates. Without bedload data they are however not able to categorically say it was due to this.

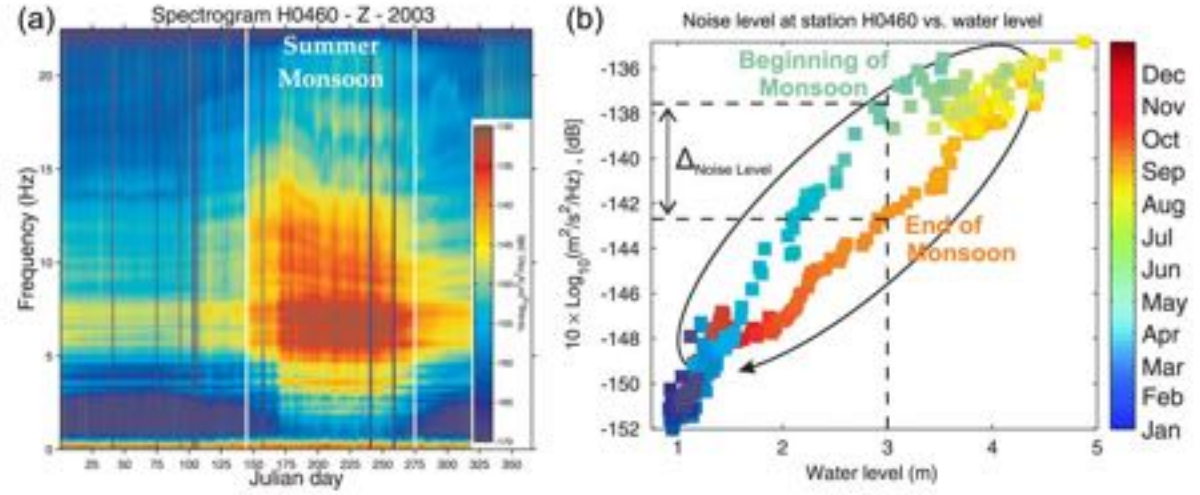

Figure 1.14: Clockwise hysteresis effect on seismic signals from a seasonal perspective during a monsoon season (Burtin *et al.*, 2008a)

Changing the temporal scales from seasonal to event based, Hsu *et al.* (2011) was also able to find hysteresis within seismic data. However, they suggest that without the effect of bedload, a similar loop can be generated by either the effect of the flood wave pressure changing from with the flow or with the channel shape itself changing. Schmandt *et al.* (2017) took a new approach to seismic monitoring, but looking at event timing, at a reach scale level by placing a 76 element array around a 700 m stretch of river. They were able to control the flow and gravel injection into the river, meaning they could hold the discharge constant and also introduced their own timed gravel. By being able to hold discharge at a given level, they were able to determine the fundamental frequency of the river at that discharge, and also to find a region of the spectrum that only changed due to an input and subsequent sediment transport.

1.3.6 Section summary

The sound a river makes has been shown to be linked to the processes happening within the river itself, with both hydrophone and seismic data being able to infer bedload transport. The size and shape of the grains contribute to the frequencies produced, through their ability to move

and in generating more turbulent flows. The research shown in this section goes to show that sound generated by a river is dependent at least underwater and seismically to river condition.

1.4 Geomorphic resistance

In the previous section it was found that the size of the grains had an affect on the soundscape produced underwater and seismically. This section explores the relationship between the geomorphology of a river channel and how it may impact the soundscape through its impact on flow and energy.

1.4.1 Flow resistance

When trying to describe geomorphology in relation to how it affects the rivers' flow, a quantitative approach is needed (Piégay, 2017). Flow resistance relationships are used to try and understand why one reach may behave substantially different from another that looks similar. It is essential to be able to predict channel flow resistance as they are required for prediction of flow depths, velocity, shear stress distribution, flood routing and mitigation (Bathurst, 2002; David *et al.*, 2011; Powell, 2014; Lamb *et al.*, 2017). Therefore, it is crucial for studies concerning geomorphological, sedimentological and hydroengineering research (Ferguson, 2010). Many studies have focused upon lowland rivers, however, some have begun to look at how mountain streams compare to existing relationships. Defining a mountain stream differs between authors, with slopes of between 0.1 and 41% being considered (Bathurst, 1985; Nitsche *et al.*, 2012; Schneider *et al.*, 2015). The qualitative definition is that there is coarse bed material (cobbles and boulders), relatively immobile grains and topographic variability (Bathurst, 2002; Monsalve *et al.*, 2017).

The significance of flow resistance is that it can be thought of in terms of energy dissipation, with the energy to overcome it converted to heat and most importantly, sound (Powell, 2014). Although there is a generic river sound, it can be different from low to high flow, or when there are obstacles or not present.

1.4.2 Relative submergence

Any obstacle in a river will have relative submergence which is the measure of the height of the obstacle relative to the depth of the water. Depending on the relative submergence different

mechanisms of flow patterns can develop related to depth which is why it is important in trying to link river depth to sound.

Boulders create flow pathways, increasing flow resistance especially at lower flows (Bathurst, 2002). This boulder-flow interaction can trigger turbulence, hydraulic jumps or plunging jet flows, allowing air to be mixed into the water, generating white water. It is by this method that bubbles are produced, and as mentioned in Section 1.3.4 these produce different frequency peaks when burst. Studies have linked bed roughness to energy loss within the flow, with complex 3D flow patterns between obstacles (Yen, 2002). However, once these obstacles are submerged, the ability of them to cause the trapping of air sharply diminishes and in turn turbulence is reduced (Kucukali and Cokgor, 2008). The response in the soundscape will therefore be linked to this threshold. The drag caused by boulders sometimes referred to as morphologic drag, due to the immobility of them is seen as the main mechanism of flow resistance (Lamb *et al.*, 2017).

If the free-surface is disturbed, caused by obstacles, was found by Flammer *et al.* (1970) to be related to relative submergence of obstacles. The free-surface effects are primarily responsible for the generation of white water (Brocchini and Peregrine, 2001). However, Flammer *et al.* (1970) found in an experimental drag simulation that there are stages to the free surface effects, pronounced, gradual and negligible, i.e. there is a lot of white water, to very little white water. To quantify how boulders and immobile objects interrupt flow, a relationship between the flow depth of the river and the height of the object has been formed. For sediment, the size chosen in a reach is usually D_{84} which is the 84^{th} percentile size from a grain size survey of the entire reaches river bed. With a measure of how river depth in relation to the objects in the flow, the corresponding resistance function can be calculated. Figure 1.15 shows this relationship found within a mountain stream.

Most river reaches will not have a single protruding boulder within a channel, but will have a mix, with the flow moving around one boulder being compounded by any other nearby (David *et al.*, 2011). Therefore boulder concentration needs to be included within flow resistance calculations as the total wake interference resistance is not equivalent to if the boulders were added up individually (Ferro, 2003). A method suggested by Kucukali and Cokgor (2008) to measure the

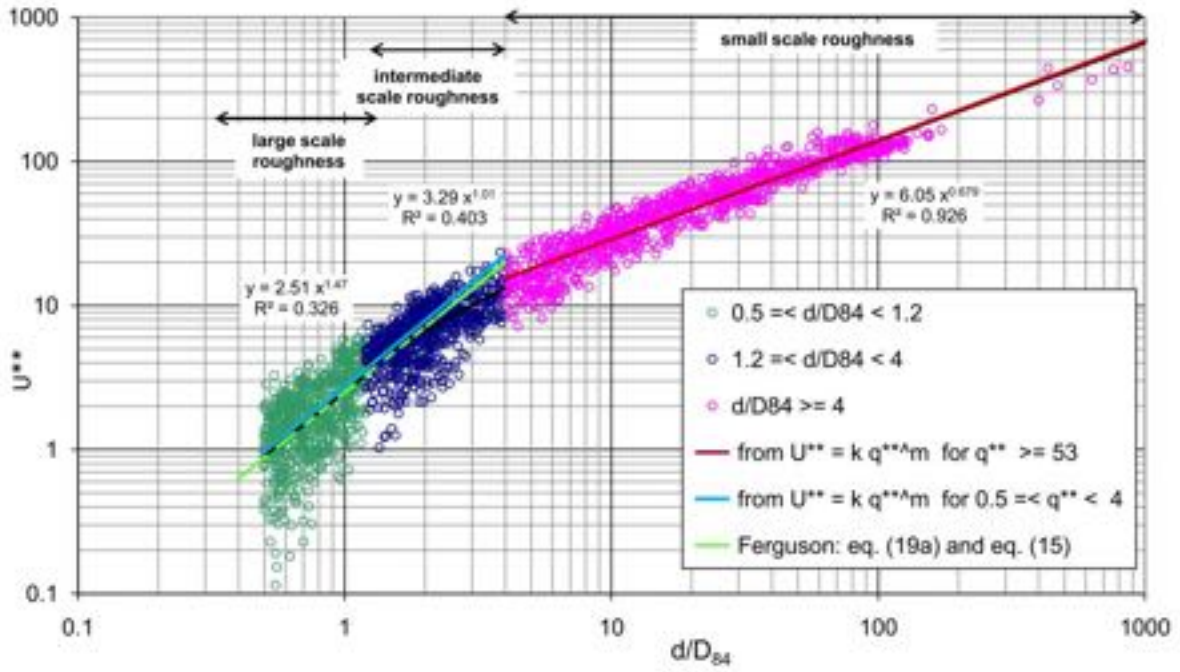

Figure 1.15: The difference of flow resistance depending on the scale of relative roughness, between large scale (depth and obstacle height are similar) and small scale (the depth is greater than the obstacle height) (Rickenmann and Recking, 2011).

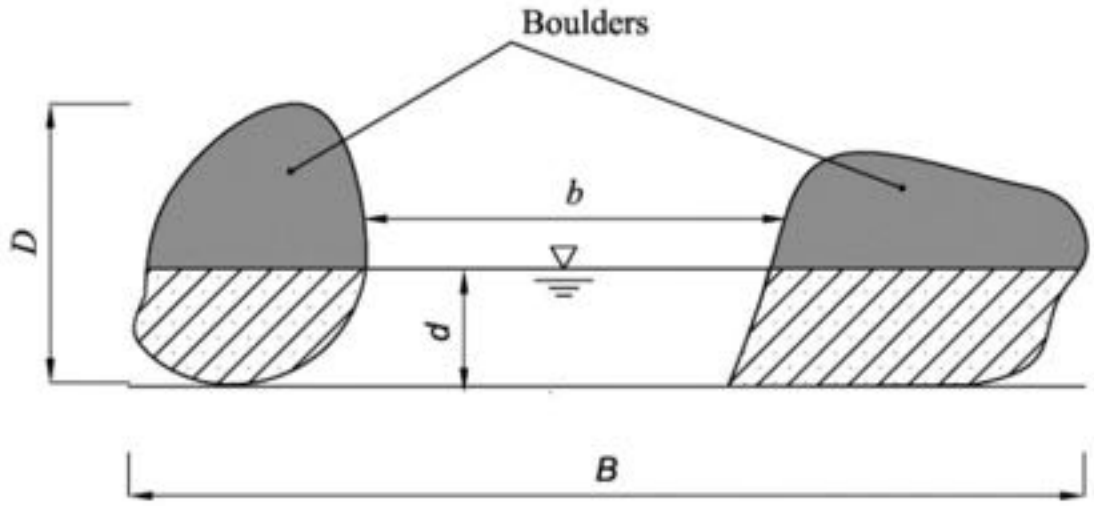

Figure 1.16: The blockage area (diagonal lines) in respect to the total surface area opposing flow as a function of depth. Where, D is boulder height, d, is water depth, B is boulder spacing and b is space between boulders (Kucukali and Cokgor, 2008).

impact of boulders on flow involves taking cross sections across a river reach and comparing boulder area facing upstream to the area of flow, known as the blockage ratio (Figure 1.16) .The relationship found was to compare the blockage ratio against aeration in the water (turbulence) and showed a strong correlation. Therefore the more of an obstacle to flow there is, then the more free-surface effects that could be expected. Linking this with the project it means that for

there to be white water, there has to be geomorphic resistance.

1.4.3 Section summary

In this section there is evidence that the disturbed free-surface and the white water, bubble producing medium, is linked to the relative submergence of an obstacle. The size and the amount of the flow that is obstructed is linked to flow resistance and energy being released.

1.5 Monitoring of rivers

In this section the idea of what needs to be monitored and how well is examined for rivers. The use of networked sensors and how many of them are required to build robust monitor network are considered.

1.5.1 How do you solve a problem like river monitoring?

Kundzewicz (2016) argued that if a flood happens, it should not be taken as a failure, and also not a success if flood prevention worked, i.e. you shouldn't be complacent. The flood warning system is only as strong as its weakest link, with the success of the system dependent on everything being satisfactory which may have worked one time, but might not the other. Perera *et al.* (2019) found that 75% of responses from the UN Office for Disaster Risk reduction indicated that their river basins did not have satisfactory hydrological network coverage such as depth gauges, with this most felt in developing countries. Significant numbers of stations in developing countries are staffed, with manual physical measuring and 50% having deficient technology such as from poor maintenance. The problem with river monitoring comes down to cost, with either being too expensive to have to begin with, or too expensive to build up an adequate enough network. The location, the density and the type of station are all important decisions to take when developing a network (WMO, 2008).

WMO (2008) describe the minimum network stream gauge density (SGD) required to have an operational system, to minimise the chances of miscalculations. Within hilly/undulating land, which we assume is most of the UK, the recommendation is 1 monitor per 1,875 km^2 of watershed area, but the UK is very dense with 1 monitor per 161 km^2. The UK's network is as dense as the EA has to understand its complex drainage density, climate, geology, land use and water utilisation (Marsh, 2002). The recommend amount does not take into account population density or socio-economic factors (Philip and McLaughlin, 2018). Whereas Benson (1965) did take into account these variables, including variables such as relief, population growth and water abstraction, with the nuance that a network fit for purpose now, may not be as it evolves. The lower the network density, the better the quality of data that needs to collected from them with Mishra and Coulibaly (2009) describing how to operate a low density network:

1. Choose a primary site that is useful to multiple socio-economic groups
2. Identify which of these primary stations are needed to keep errors low
3. Rank stations on how they perform in combination with each other which give low overall error
4. Look at how expensive the stations are in rank order, and decide if continuing at the site is required.
5. Select the combination that can improve network performance without requiring much additional resources.

On the other hand there is also a need for stream gauge network optimisation, as there is little point having 10 stations on a river, when it really only requires 4 for your purpose. Yoo *et al.* (2011) examined the Hantan River basin, Korea and found that the 27 stations in operation could be reduced to 7 through modelling. Splitting the station network into a dendrogram as a way to visualise them to show redundancy in the system and has the focus on tributaries instead of the main channel (Figure 1.17).

Joo *et al.* (2019) also found that a similar basin with 18 stations, performed optimally when there were only 12. Counter intuitively the more stations that are in a basin does not necessarily provide a better outcome. Again, upstream stations were seen as being more important than main channel which is what this project is focussed on. Joo *et al.* (2019) does mention that although hydrologically these stations are significant, it does not take into account flood mitigation strategy, such as monitoring before a significant population.

The monitoring of parts of the water cycle requires high frequency observational data, from different sources to aid in research, water management, modelling and forecasting (Tetzlaff *et al.*, 2017). In a survey of 336 hydrologists, Blume *et al.* (2016) found that to advance research there was consensus that small (<10 km^2) to medium (10 - 100 km^2) catchments would have the most significant impact to advance the science as they have been less well studied. Smaller, plot size and large scale (>1000 km^2) were seen as having the least impact. New monitoring equipment and techniques had a very strong need, with the addition of the current network being

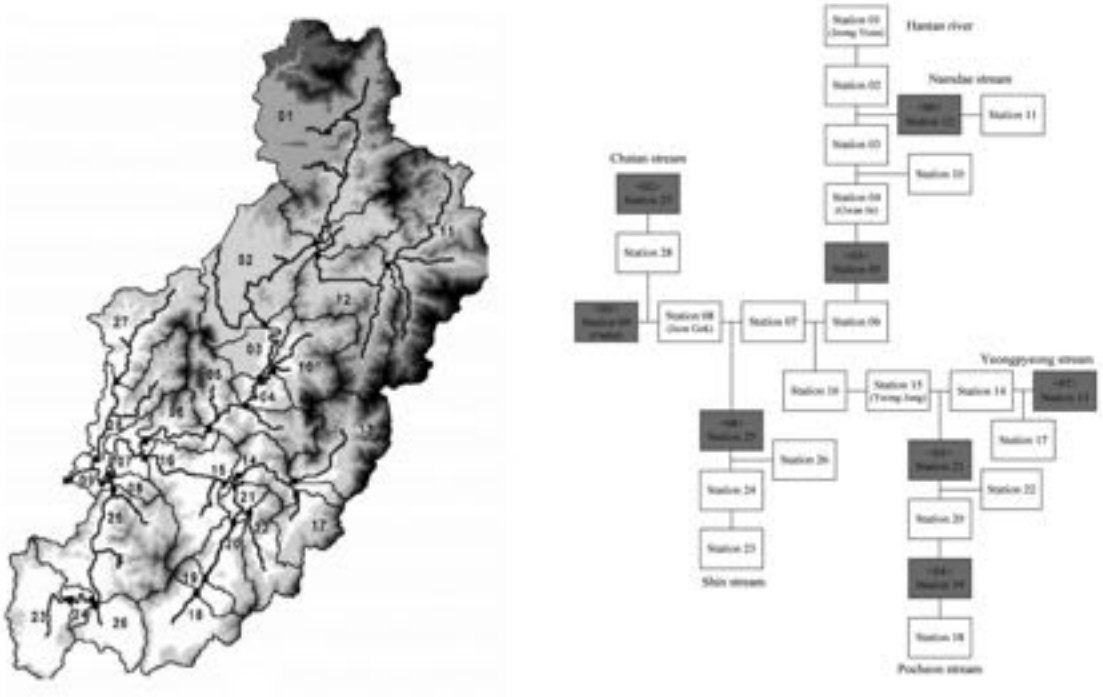

Figure 1.17: Catchment drainage network map with the station network map. Significant stations highlighted (Yoo *et al.*, 2011).

maintained, rather than more modelling. Real time monitoring is crucial in flood monitoring in particular as knowing the current condition of the river aids in refining any forecast and actionable alerts (Moreno *et al.*, 2019). At the medium catchment scale, river flooding can be dictated by numerous processes, such as where the rain falls, how saturated the ground is and what the land use may be (Figure 1.18) (Gaál *et al.*, 2012; Rogger *et al.*, 2017). With any changes in these variables having a different effect on the potential flood (Viglione *et al.*, 2016).

Localised variations of these variables can have a profound impact on the flood response, with antecedent conditions influencing the possible flood (Norbiato *et al.*, 2008). Within a season, the input conditions can have different catchment level responses, with simple and complex hydrographs (Harvey, 1971). In river forecasting, the river tributaries can be based upon conceptual models and in this sort of system forecasts for upstream and small catchments is lacking (Javelle *et al.*, 2010). Zoccatelli *et al.* (2011) found that neglecting the fact of rainfall spatial variability, influenced the catchment response time by -30 - 72%, showing that catchments have great spatial responses. The system of flooding is highly interlinked, with what happens in downstream, more densely populated areas being the resultant of upstream conditions (Seher

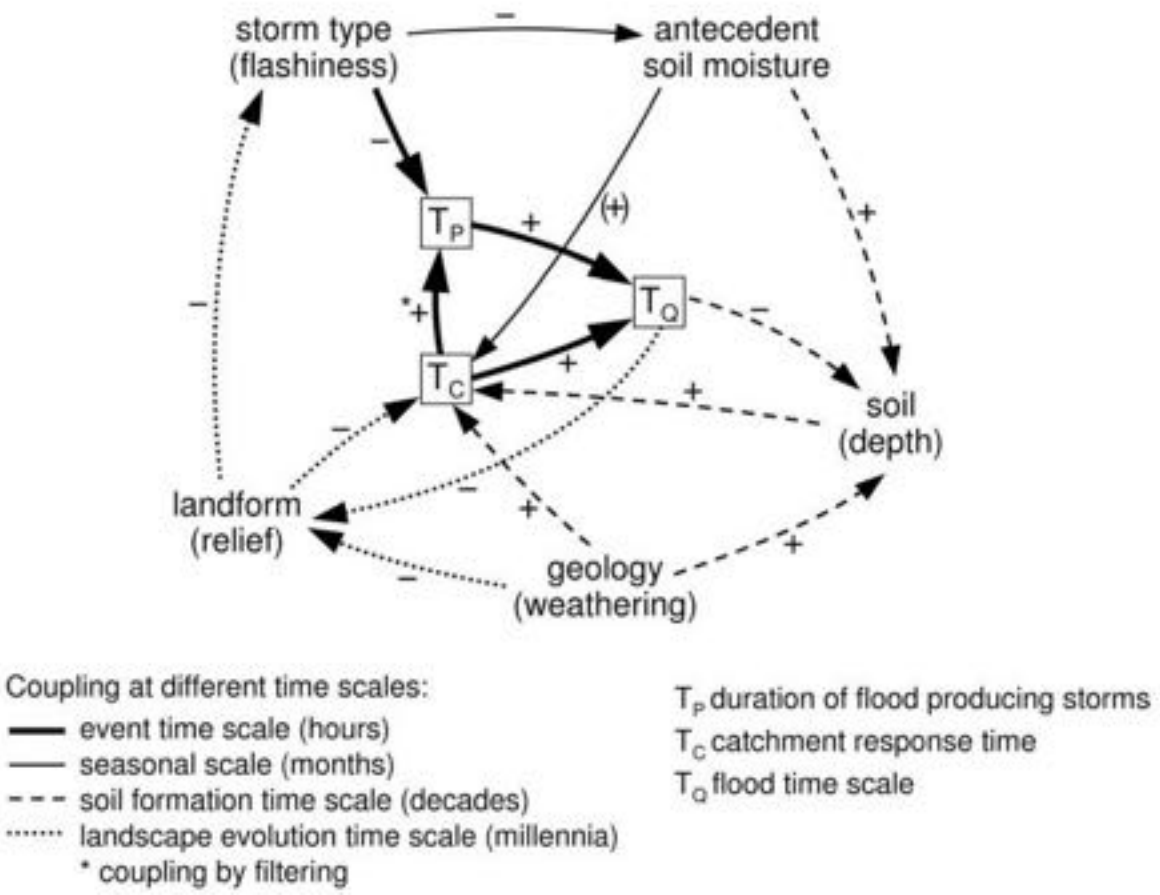

Figure 1.18: Feedback mechanisms of how aspects of the hydrological system can either positively or negatively impact flooding prediction (Gaál *et al.*, 2012).

and Löschner, 2018). The contribution of these individual reaches and section (hydrodynamic dispersion), coupled with geomorphological dispersion dictate how a flood event may unfold, if these are constant (Rinaldo *et al.*, 1991). However, the celerity of the flood wave should not be thought of in terms of space and time singly, with variation of flow depth and how this reacts to geomorphology (Dixon *et al.*, 2016). With high spatiality variation in response in these upper catchments, the onus is on how hydrological monitoring might be able to fill these voids.

1.5.2 Section summary

The key message from this section is that the monitoring of headwater catchments aids in the modelling of floods. Although too many monitors can be counter intuitively bad for modelling, having more upper catchment monitors are good. With 75% of respondents to a survey stating that small and medium level catchments offer the best research prospects, this area is prime for monitoring.

1.6 Internet of Things

The Internet of Things (IoT) is an umbrella term to group together a new generation of technology with the interaction of "things" being shared through a network (Figure 1.19)(Atzori *et al.*, 2010). The main aim behind the IoT is to enable people to gain access to technology that would otherwise be too costly or too difficult to setup themselves, such as smart home appliances. It is purported that by 2025 there will be 21.5 billion devices connected through the IoT, compared to only 9.9 billion in 2020 (Lueth, 2018).

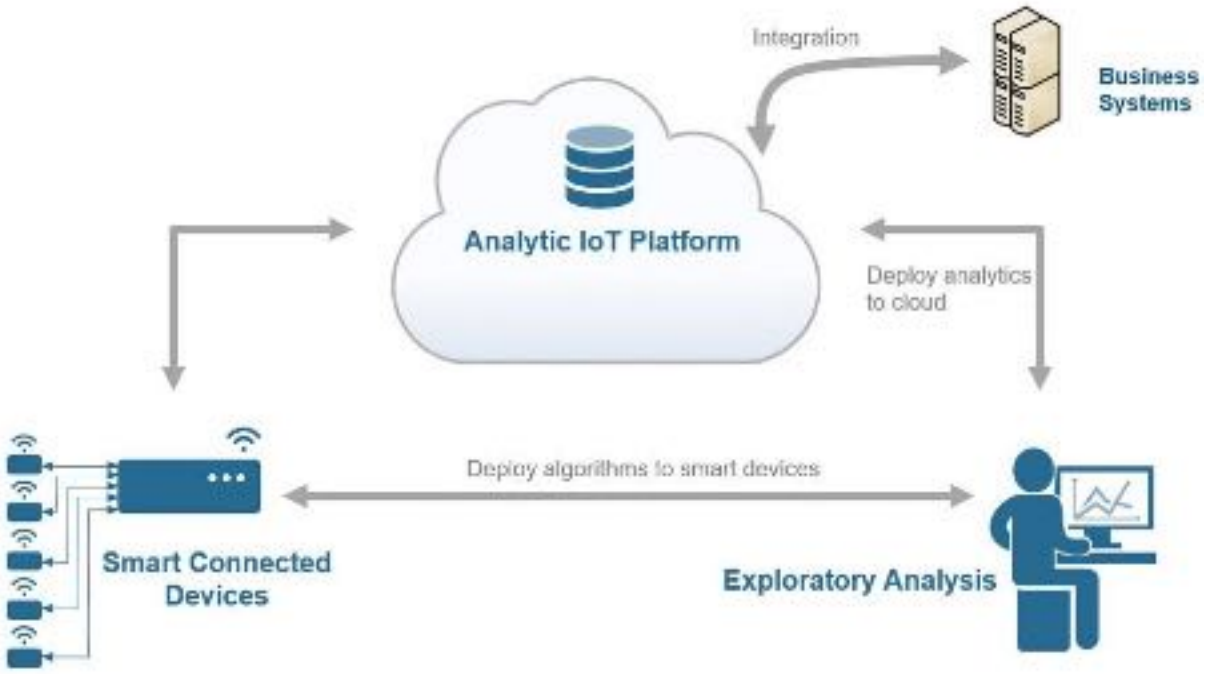

Figure 1.19: Diagram of how the internet of things connects to each part of the system (MathWorks, 2021).

1.6.1 Rivers and Internet of Things

In river monitoring IoT has enormous potential and growth. IoT sensors are essentially "dumb" according to Hughes *et al.* (2006) since they are only nodes in a system, recording and transmitting data, with the analysis done off site, such as how they used nodes to measure flow depth. Smith *et al.* (2009) presented a smarter flood warning system in which the sensors (pressure or conductivity) were proactively determining what they were recording, adapting, such as increasing measurement time, or to turning on advanced features such as cameras. Although

an adaptive sensor seems like a good idea, since 2009 there has been no update on the river monitoring technology, since perhaps it has became easier due to communication upgrades to enable this enhanced feature remotely, keeping sensors "dumb". Dimakis *et al.* (2006) noted that individually, they are cheap and unintelligent sensors, with them deriving strength from numbers to provide reliable and robust information. Indeed, the drive for cheaper, easier to deploy devices make it less necessary to provide precisely tuned data. The "dumb sensor, smart sink", with a sink being a main processing unit, has been the working paradigm of sensor technology for large-scale networks (Meng *et al.*, 2006).

The development of cost effective, low-power, data capturing IoT devices has reached the point that high quality observational data is obtainable and aiding in flood risk mitigation (Horsburgh *et al.*, 2019a). With systems being lower cost, this means that they can be scalable, allowing more data sources to be utilised. In flood detection there are two important factors, perception (is it really happening), and speed (enough time for action to be taken) (Yuliandoko *et al.*, 2018). Connecting these devices from remote areas is challenging, with mobile signal as one possibility being directly influenced by rainfall intensity, which is not promising when rainfall and flooding go hand in hand (Geng *et al.*, 2019). Other communication types such as LoRa use localised WiFi to connect devices in remote locations, through a centralised gateway (Ragnoli *et al.*, 2020). Lauridsen *et al.* (2017) found that all communication types have the possibility of outages regardless of specification.

Marin-Perez *et al.* (2012) describes the four main requirements for hydrologic applications of IoT sensors:

Power

Connection to convential power sources are often missing near areas of hydrological interest. Renewable sources such as solar and wind are susceptible to vandalism and theft. Sensors must therefore be of low power consumption, have standard batteries and last at least one hydrologic cycle (2 - 6 months).

Hardware compatibility

The data logging component of the system should be able to connect to more than one type of instrument to increase flexibility and adaptability. Power supply must be easy to change and adapt to the draw downs from the components to have optimal power management and performance.

Reliability

The system should be able to withstand the conditions it is built for, i.e. a flood monitor must be able to communicate and function during heavy rain storms. Backup systems must be present to avoid information losses.

Communication

Sensors are often in remote areas, the type of communication should adapt to the conditions. Peer to peer connections between each of them should be possible to extend monitorable range.

There are three main IoT monitor types that are specialised for monitoring river depth: ultrasonic depth monitors (UDM), optical and depth loggers. In this section we will explore the rationale behind these technologies and examine the sort of data these can provide.

1.6.2 Depth loggers

The most common type of monitor are depth loggers which calculate river depth by recording the difference between atmospheric and in-stream pressure (Sorensen and Butcher, 2011). First used from the 1960's, they were designed to replace a mechanical approach to automated depth recording using floats and counterweights (Freeman *et al.*, 2004). Installation of loggers may need enhanced power supplies, robust infrastructure and an alternative is just to download the data at the site instead. It can be said that the EA gauges are already part of the IoT system, with their pressure monitors instantly connecting to their servers via a fixed phone line or mobile network and running off of battery power (Environment Agency, 2011). However, the inflexibility of this setup, with reliance on permanent infrastructure make it costly, with costs for a basic setup and maintenance at £1,000pa, so perhaps not at true IoT approach. These devices can however produce accurate water depths with precision of 0.001 m, but do require constant compensation between the hydroststic and air pressure (Bączyk *et al.*, 2017). Companies such as VanEssen and HOBO make ready-to-go solutions that use depth loggers and pre-built portable stations using network signal, but with a cost in excess of £1,000. These pre-built systems offer ease of use and operation, aimed primarily at the industrial and research level.

An example of a true IoT device using a depth logger is a FreeStation, and as the name implies, the foundations of this system are free, with the end user paying for their own parts and time, with the parts costing less than £100 (Figure 1.20A). Chan *et al.* (2020) found when comparing their own £16 pressure transducer based sensor to a £600 commercially based when measuring stilling well depth, had an R^2 of 0.94. However, this was within a relatively stable environment of a well, with depth changes of 20 cm. Whether or not this system will be suitable for a river environment has not been stated, however, these results are encouraging. A more modular and DIY orientated project is known as the EnviroDIY, which also has the ability to attach a DIY pressure transducer (Figure 1.20B) (Horsburgh *et al.*, 2019b). Designed as a DIY environmental science station it can also be used to gather atmospheric data. Folz *et al.* (2018) used the station and gathered convincing results that this monitor was able to monitor river level, albeit with the station facing power and connectivity issues requiring weekly site visits. The haphazard approach to infrastructure also caused problem with high water and winds knocking over stations due to flimsy construction for the conditions to be expected.

Figure 1.20: Examples of DIY pressure transducers. (Top)- Freestation presure transducer with integrated pressure monitor and Arduino and (Bottom)- EnviroDIY pressure sensor only hidden inside a bolted pipe (Horsburgh *et al.*, 2019b; Chan *et al.*, 2020)

.

There is a lack of use of DIY station data within the literature, either due to being in its infancy, or still lacking credibility. There is no lack of data with the EnviroDIY network consisting of 2,811 stations (405 hydrology) and the FreeStation network of 382 (46 hydrology).

1.6.3 Ultrasonic depth monitors

In contrast to depth loggers, UDMs are non-contact monitoring devices, meaning they do not need to be fitted within water. Lo *et al.* (2015) describes how depth loggers have a high associated maintenance, because they are at risk of being buried in sediment or being destroyed. UDMs are devices that look down onto the river, sending out a pulse of ultrasonic sound, and listening

for the reflection back (Rahmtalla *et al.*, 2014). By measuring the time between the pulse and the return, the algorithm can work out the distance to the water surface. The system relies upon a direct line of sight to the water surface, and for variables such as RH and temperature to be known, for estimating the speed of sound, for reliable measurements which requires a separate sensor (Panda *et al.*, 2016). The most common sensor used, the HC-SR04, does however only have an accuracy of 96.6% compared to a pressure transducer at 99.9% (Nasution *et al.*, 2018). The theoretical sensing range of the HC-SR04 is between 0.02 m to 4 m, and the practical range of 0.02 m to 80.8 m, with a dispersion angle of 15 °(Indoware, 2013). The practical vs. theoretical range is due to the ultrasonic cone generated by the sensor, rather than a direct laminar pulse, it spreads out (Figure 1.21) (Escolà *et al.*, 2011).

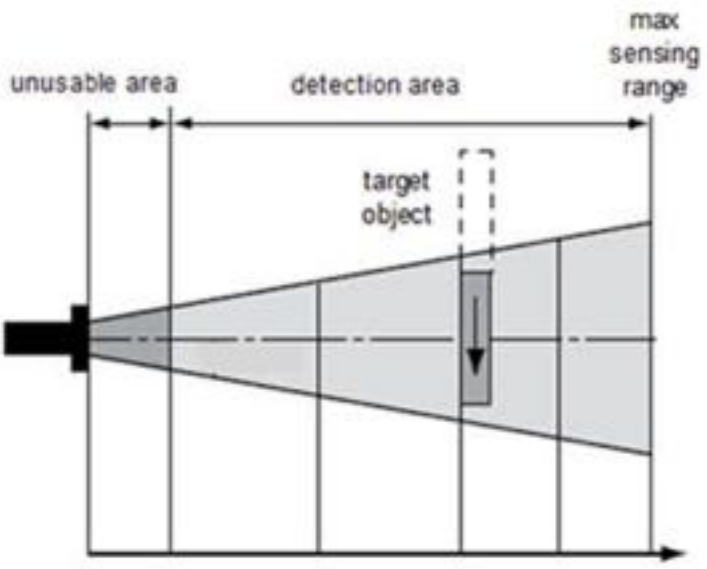

Figure 1.21: Ultrasonic cone demonstrating the zone which is useful and also the spread of the cone (Molnar, 2004).

The use of UDMs is widespread among the IoT driven river monitors, far more so than pressure monitoring in terms of published work. UDMs are more widespread as they are outwith the river, so easy to install and only requires one sensor instead of two pressure sensors to calculate water depth. Commercial and consumer units are available with this technology, being utilised more in the community flood resilience sector. RiverTrack, RiverCore, Libelium, BMRSS and the FreeStation are but a few of the devices available on the market (Figure 1.22). Mohd Sabre *et al.* (2019) uses an integrated network of UDMs and the IoT to create localised flood alerts. The underlying technology behind the sensing is all but identical.

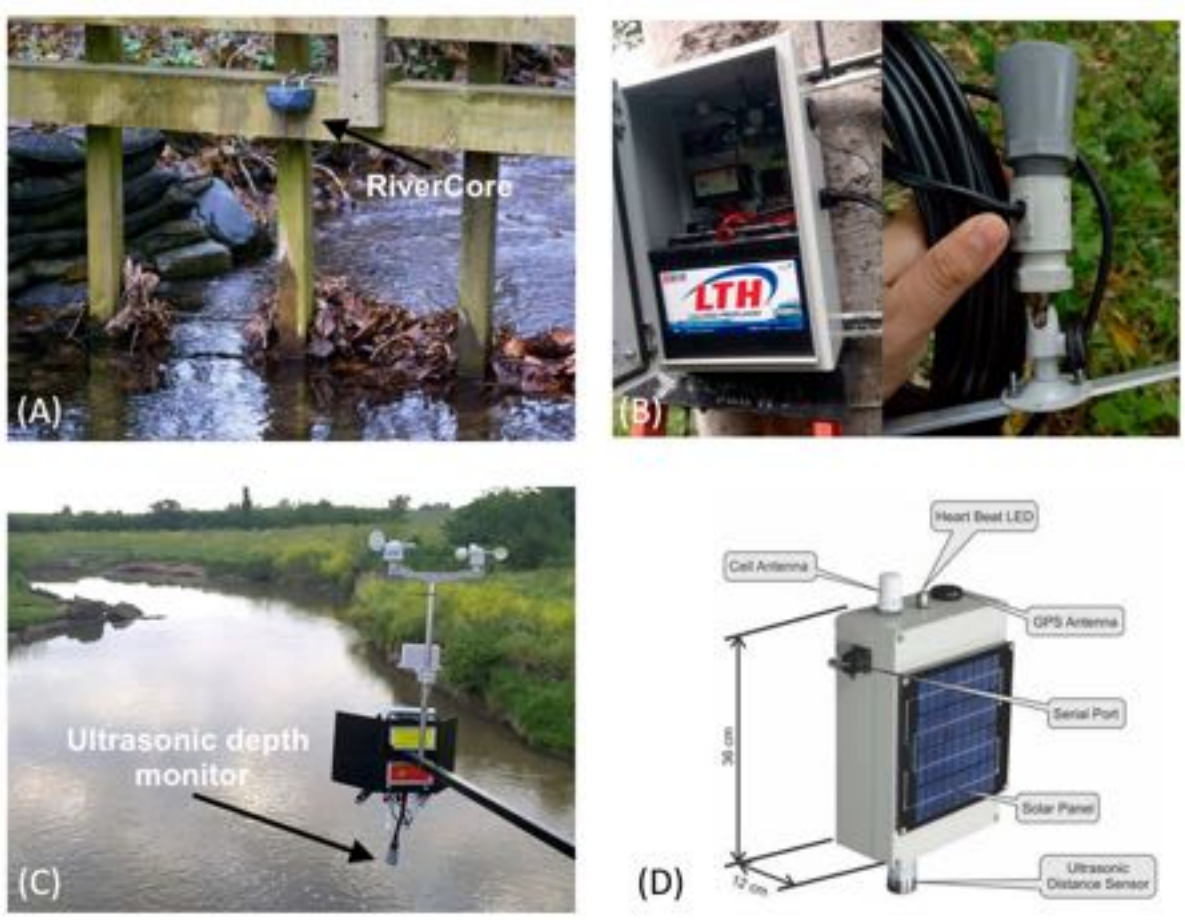

Figure 1.22: (A)- RiverCore with the small, low profile sensor attatched to a bridge, (B)- RiverTrack internals with the battery and computer, (C)- Libelium station over a low order stream on a bridge and (D)-BMRSS (Bridge mounted river sensor system). (GOV.scot; Moreno *et al.* (2019); libelium.com and Kruger *et al.* (2016))

For these devices to work well, Kruger *et al.* (2016) recommended a sturdy mounting point, with access to line of sight to the water surface. Kruger *et al.* (2016) chose to mount their UDMs onto bridges, since not only did they span rivers, they also were easy to get to. The added benefit at mounting to bridges are that the structures need to be checked to see if river levels may impact the bridge users safety. Being able to look vertically down on the surface is needed, given the ultrasonic cone dispersal. Moreno *et al.* (2019) examined the use of a "drifting" sensor, which is suspended over a channel by guide ropes. The data gathered showed that during calm conditions the measurements from the sensor to the surface fluctuated between 0.84 m and 0.96 m. In contrast, the fixed mounting system by Kruger *et al.* (2016) utilised the step of repeated short duration measurements of 5 groups of 5 over 15 seconds, with the highest average of these being taken. The results are incredibly close to that of the government operated site nearby (Figure 1.23).

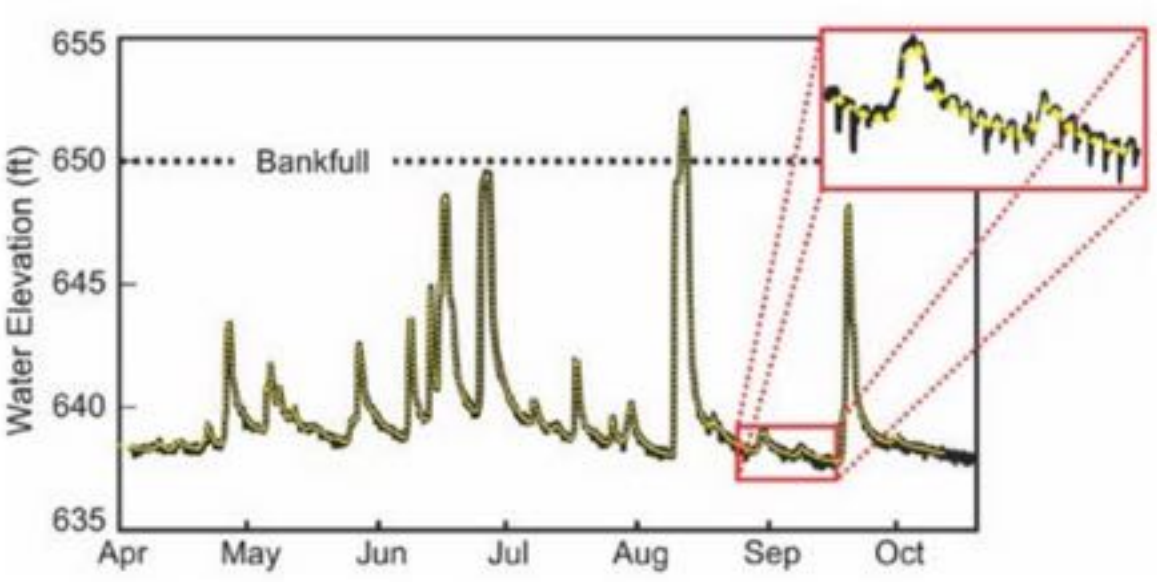

Figure 1.23: Comparision of the water stage data from a USGS station (yellow) and the BMRSS (black) (Kruger *et al.*, 2016).

1.6.4 Optical

A simpler method for calculating water stage is to read a value from a stage board, which can either be done in person or with the aid of cameras. Unlike with UDM which has other variables that need to be recorded for an accurate measurements, such as temperature, RH and incidence angles and is required to be placed over a river, camera based systems are simple (Kim *et al.*, 2011). Water level recognition can be achieved through image processing, rather than someone observing it (Shin *et al.*, 2007). Issues can still persist with with images, however, another benefit of the technique is that someone can visually check the data, something that couldn't be done with a depth logger or UDM without visiting (Gilmore *et al.*, 2013). The reason to image process is that it is tricky to tell by eye what the water level is, especially at high flow with depending on the surface (Takagi *et al.*, 1998). Takagi *et al.* (1998) developed a method that has a stage board and a slanting metal strip to help determine what the water interface was like, as if it was mirror like then the measured height would be incorrect. That method of image processing is however is problematic due to special apparatus needing to be installed, such as a stage board and its sensitivity to detritus (Kim *et al.*, 2011).

Iwahashi and Udomsiri (2007) set out a method for water level detection without the use of any in-situ river equipment based upon detecting the boundary between water and land. The

process of adding additional frames together as a method of removing raindrops and waves, i.e. combining 30 frames of a video into one frame and averaging, has the effect of being able to clear the image of noise, but also create a firm boundary (Figure 1.24). Alternatively, Sakaino (2016) believed that the heavy computational cost with sequencing multiple frames is unnecessary and developed a technique using a single frame to increase accuracy and speed. By breaking the image into a histogram of pixel intensity from black (0) to white (255) and comparing these values before and during an event they found a cross correlation of 0.87 between their method and a UDM. Opportunistic measurements, by close to river CCTV cameras was explored by Lin *et al.* (2018) in which they managed to get a level resolution of 1 cm using utilising principles of photogrammetry to create control points to stabilise the image in the case that the camera moved. Neural networks have been used by Pan *et al.* (2018) as an alternative to the "difference" method (frame comparing) to generate water level data, with the difference method performing at 0.046 m of error against 0.009 m of error with a nerual network. Combining CCTV data and neural networks, Moy de Vitry *et al.* (2019) found as a proof of concept that 75% of images correlated with water level after training the neural network with 1218 flooding images. These camera images were not only from river images, but also roads and from cars.

The previous studies have looked at rivers in a more urban setting in channels that are hydrologically indistinctive, with no bed or bedload being visible. We therefore begin to look at optical based water level detection in more challenging areas.

There are however difficulties with optical based margin measurements in more remote areas which were found by Young *et al.* (2015) when using images from Iceland. Illumination changes caused by the sun tracking across the sky, changing the contrast of images, meant that the difference in colour between the water and the surrounding landscape was not strong enough to separate the two. Furthermore environmental factors such as snow, fog and rain obscured the camera and the edge of the bank was highly textured, with no smooth surfaces to find a measuring point. In light of these challenges they adopted a manual approach to measuring, which had an enormous consequence on the data gathered.

Eltner *et al.* (2018) identified the need for small-scale and headwater catchments to be gauged, and thought that imaged based gauging could be the answer. In addtion to a fixed camera setup,

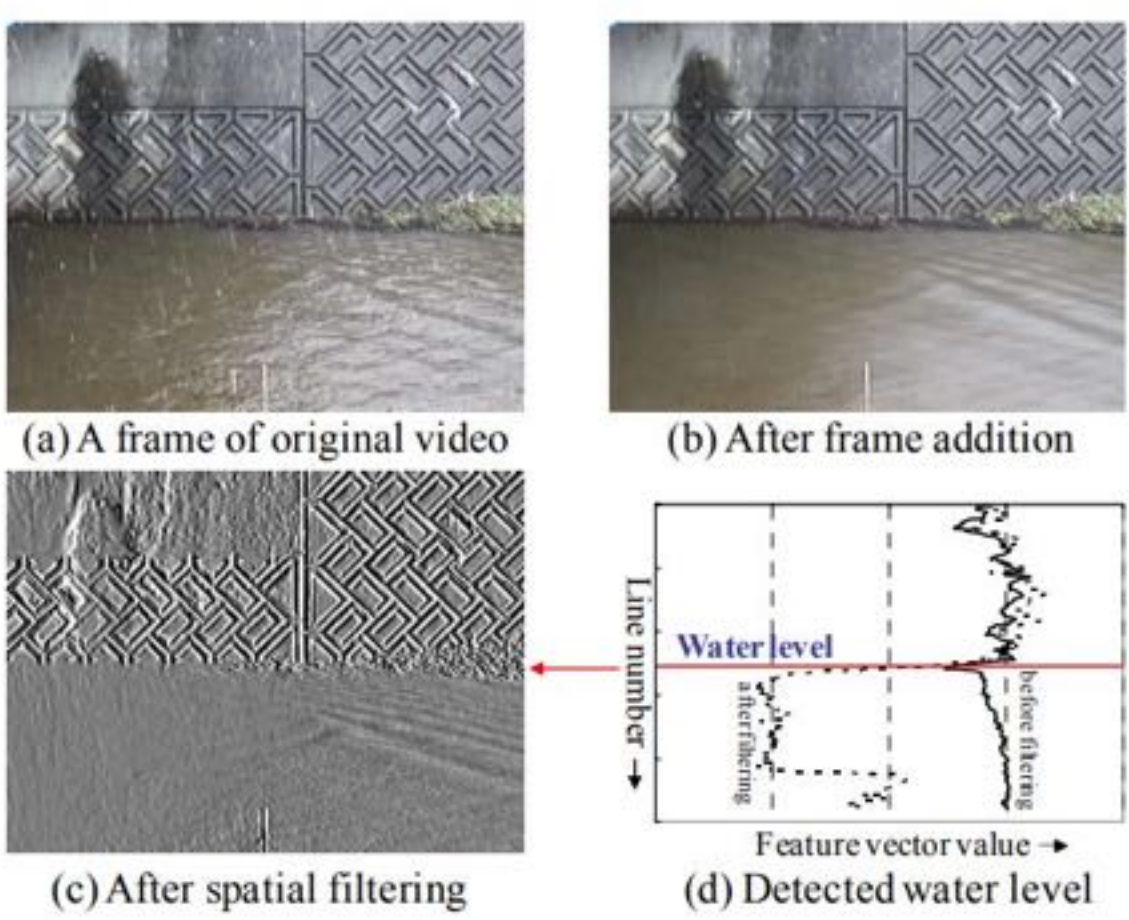

Figure 1.24: Image workflow from a single frame, to a combined frame. With after being filtered a water level can be established (Iwahashi and Udomsiri, 2007).

structure from motion was utilised to construct the channel in 3D, which stitches together photos. Their results yet again do not have night time collection, yet they conclude that it performs well (Figure 1.25). Leduc *et al.* (2018) found an R^2 of 0.91 based from a pressure transducer against their camera based monitor, however, they also do not have the facility to use night time images and argue that non- continuous data is still useful for channel hydraulics. Night vision cameras have been shown to be effective in measuring water level, however, though using a specially adapted stage board (Zhang *et al.*, 2019b). Challenges occur however with now more complex lighting scenarios, such as at twilight, and with the use of artificial lighting causing glare and shadows (Zhang *et al.*, 2019a).

Broadening the use of image based water level detection, Kröhnert and Eltner (2018); Elias *et al.* (2019) have developed a method for smartphone cameras to be used incidentally to measure water level. Without the need of any sort of infrastructure, a user can take an image, and have

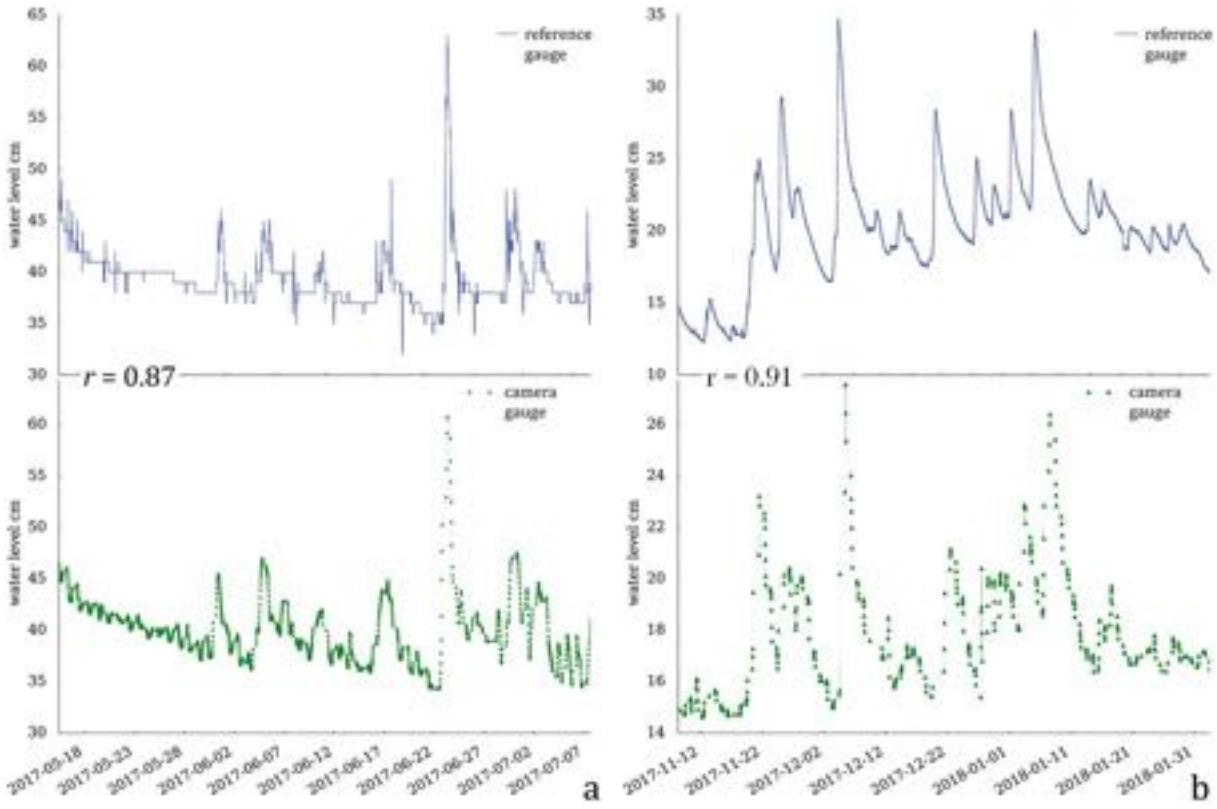

Figure 1.25: Hydrographs obtained from traditional gauges (blue) and the optical system (green) (Eltner *et al.*, 2018).

that converted into a water level measurement, and has 0.02 m accuracy up to 20 m away. The caveat being that a 3D image of the survey site needs to be known in advance in order to project the 2D image onto a 3D surface.

1.6.5 Particle image velocimetry

As a subset of optical measuring, there is also the opportunity to not only gather water level data but also flow velocity, which can be combined to let the user calculate discharge. Hauet *et al.* (2008) mentions how combining the two techniques is possible and is seen as the natural progression (Elias *et al.*, 2019).

Stream velocity measurements in high discharge scenarios, and with gradients greater than 0.1% being tricky due to shallow flow and turbulence (Jarrett, 1984; Lu *et al.*, 2006). Organisations such as the EA and USGS need to maintain and extend ratings curves to characterise the flow, but can put personnel at risk (Legleiter *et al.*, 2017). Particle image velocimetry (PIV) is an

optical, low-cost, non-contact based approach for measuring stream flow using sequential images to determine temporal evolution of surface flow velocity (Willert and Gharib, 1991; Patalano *et al.*, 2017). These systems can either be fixed CCTV type cameras or from uncrewed aerial vehicles (UAV)s (Tauro *et al.*, 2017; Thumser *et al.*, 2017). Adrian (2005) noted that PIV can be an accurate, quantitative measurement of fluid velocity, which is challenging and complicated. PIV is split into two camps, Large Scale Particle Image Velocimetry (LSPIV) and Large Scale Particle Tracking Velocimetry (LSPTV), and is used to determine water surface velocity and discharge estimates (Figure 1.26) (Patalano *et al.*, 2017). LSPIV uses Eulerian frame of reference and LSPTV uses Lagrangian frame of reference. Eulerian is when the image changes in the fixed field of view, with Langrangian being the frame of reference changing instead enabling particle trajectory to be monitored (Rapp, 2017). LSPIV is a more widely adopted monitoring strategy, with Fujita *et al.* (1998) being among the first to adapt PIV for use in environmental settings, rather than a laboratory (Dramais *et al.*, 2011). Admiraal *et al.* (2004) states that LSPTV is unbiased compared to LSPIV, and is more efficient in high velocity gradient zones.

LSPIV requires five components: flow visualisation, illumination, image recording, image processing and orthorectification. From these components it is possible to determine mean velocity, streamlines, vorticity and all other statistical moments and cross-products (Muste *et al.*, 2008). Discharge however requires the bathymetry of the channel and flow depth, which either needs to be measured once if it is not changing, or repeatedly if it is and an assumption between the surface velocity and average stream velocity. Genç *et al.* (2015) found that there was an error of 4.08% between using surface velocity and in-stream discharge measurements. Le Coz *et al.* (2010) found that during flash flood events, in discharges of near 300 m^3 s^{-1}, they were within 10% of the discharge measured by an ADCP and in discharges from 300 to 2500 m^3 s^{-1}, within 20%. Significant problems occurred when conditions for taking the images were poor or if the flow became unsteady, contributing to errors of between 30-80%. LSPIV can be used with UAVs, to survey rivers that are seldom measured due to their sporadic nature of response and practical difficulties of getting there fast enough (Tauro *et al.*, 2016). Perks *et al.* (2016) measured a 1 in 200 year flood event using drone imagery, and were able to determine flow velocity and direction, with an error of $\pm$ 0.15 m s^1.

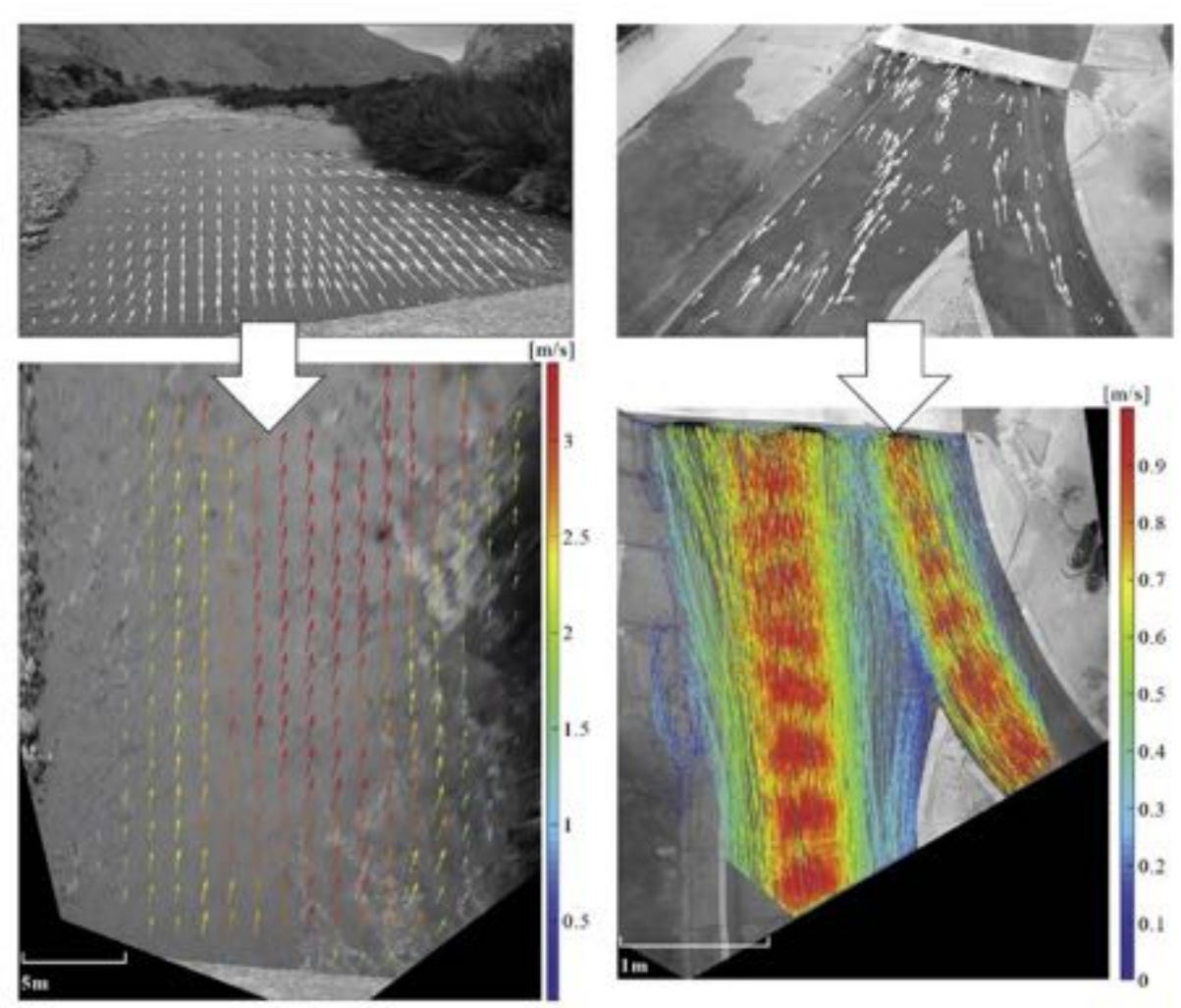

Figure 1.26: Comparison of the different PIV techniques with LSPIV on the left, with each coloured arrow on the left is an average velocity for an area and LSPTV on the right, and each coloured line tracks an individual particle (Patalano *et al.*, 2017).

Using commercial available cameras, Hortobágyi *et al.* (2019) has been able to feature track debris in a river, such as foam, wood, and turbulence structures, to determine vectors of water velocity, using LSPTV. Tracking of these objects is comparable in field and laboratory conditions, with adequate accuracy, with LSPTV most efficient during periods of low to medium flow (Patalano *et al.*, 2014; Mella *et al.*, 2019). This method is particularly advantageous in low flow conditions, as traditional measuring with an ADCP is limited in shallow water (Gordon, 1989). In comparison to LSPIV, (Tauro *et al.*, 2017) found that LSPTV provided closer to the actual velocities rather than underestimating. Lightning (reflections of the sunlight) and the wind (moving the particles) are environmental factors that effect the use of LSPTV in particular (Patalano *et al.*, 2014). Conversely, LSPIV has lighting and seeding related issues, and generally underperforms in adverse condtions (Tauro *et al.*, 2017).

PIV techniques can also be combined with techniques that measure water depth from images (Section 1.6.3). Ran *et al.* (2016) gathered both surface velocity and water level from a DIY camera recorder, which had a water level accuracy of 3.7 cm and within 10% of values from measured velocity. From the ungauged station, they were able to construct a convincing ratings curve with an R^2 of 0.94 (Figure 1.27). However, the monitoring period was only during daylight hours due to no artificial illumination. Illuminating for night monitoring was shown to be effective by Chaves (2012), with the use of a pulsed LED, and retro-reflective fabric to help bounce back the light to the camera, providing a large number of valid field vectors to measure.

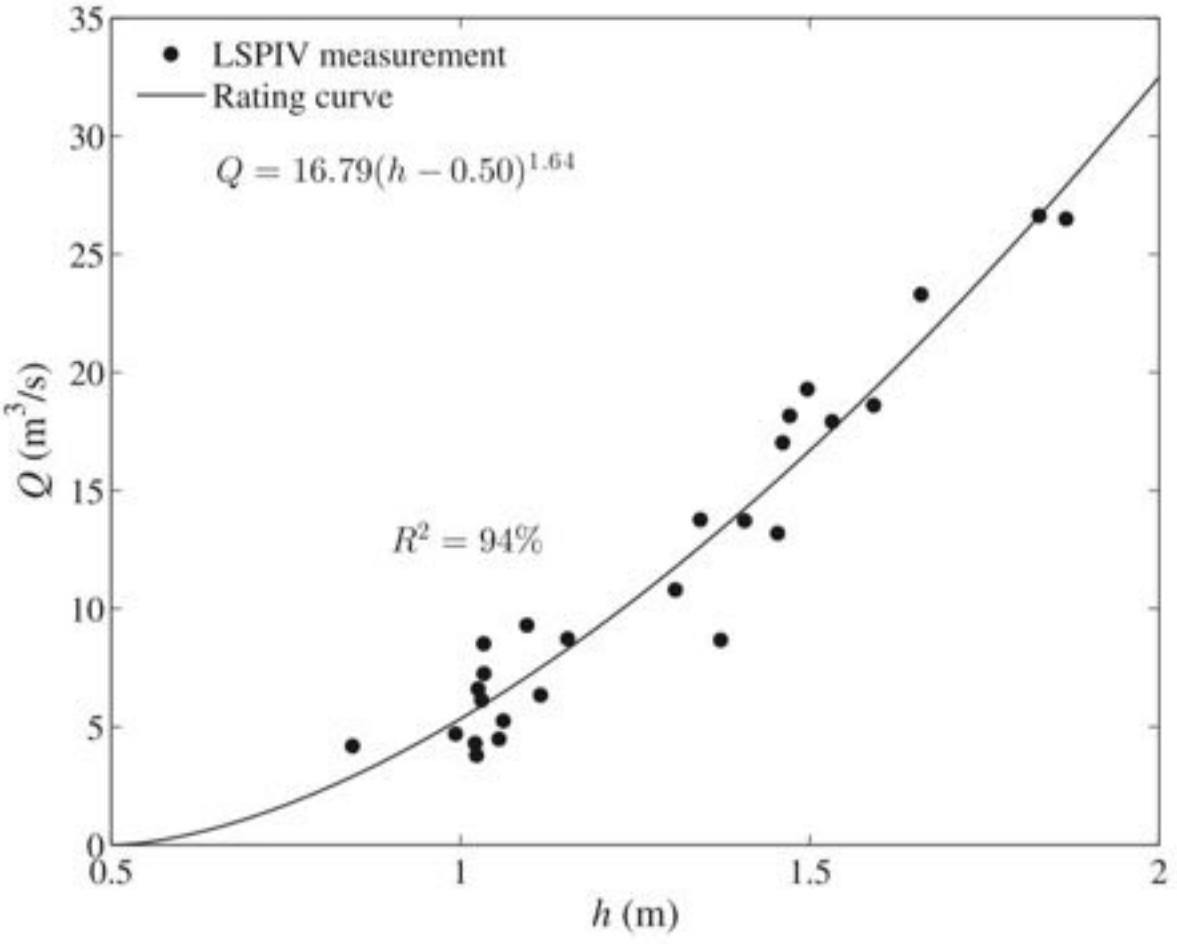

Figure 1.27: Ratings curve using data only acquired from a PIV system and stage data from 3D stereoimaging (Ran *et al.*, 2016).

Often during flood events, there is rain. Authors do not go into detail about the effect of rain on image acquisition, often calling it optical noise. Zhang *et al.* (2013) noted how rain and fog can blur an image, due to increased airborne particles, dulling the image. Raindrop impact on the

surface can impact the motion vector estimation, but not significantly enough. If the river cannot be seen, either being obscured by rain or bad lighting, optical based monitoring breaks down.

1.6.6 Section summary

Depth loggers, UDM, optical and PIV are all innovative solution to monitor a river, with stage and surface velocity being able to be measured or calculated. Each of these technologies have pros and cons, which sound can potentially overcome. Depth loggers require to be placed within the river, with infrastructure, meaning headwater catchments and their bed topography meaning fixing is difficult. As sound is omnidirectional and can travel away from a river, it does not need to be place within a river. UDMs need a direct line of sight to the river surface and to be steady to get a clear measurement, sound again is not required to be placed over a channel. Both optical and PIV require illumination if to work at night time, requiring power, whereas sound is just as loud at night as in the day.

1.7 The Data

1.7.1 Citizen science

Data accuracy and availability issues persist at a local level, with localised catchments being spatially and temporally complex (Starkey *et al.*, 2017). Citizen science is a relatively new endeavour, and in the environmental sector allows the public to make observations, contributing to the hierarchy of decision making at local levels (Ferri *et al.*, 2019). Hydrology has the potential to become a major citizen science project since it enables diverse observations from areas which may have been out of bounds, such as in another country or at a national level (Nardi *et al.*, 2021). Ferri *et al.* (2019) found that the cost vs. impact of the recording of river conditions carried out, which when measured was a 2 to 1 outweighing at reducing the expected flood damage. Buytaert *et al.* (2014) states that the development of new sensing technology, data processing and analysis are allowing this public engagement with science to become viable. The internet has been the enabler for this new wave of scientific endeavour, with the layperson being able to build their own sensors, instead of needing a University education and high-tech equipment (Wildschut, 2017). Cost effective sensors allow relative amateurs to collect data with the IoT allowing this data to be delivered to large databases, which has been setup and maintained by someone. Buytaert *et al.* (2016) also sees a trend from hydrometry being measured by formal institutions (EA) towards a diverse array of decentralised data collectors.

Diverging from the norm of traditional data collection, the accuracy of data collected using of citizen science has been called into question. Hunter *et al.* (2013) claims that the limited training, knowledge and expertise can lead to bad data. A juxtaposition behind the greater science community regarding citizen science as a poor, and not that trustworthy, is in stark contrast to the scientists themselves wanting this data. It is dependent on how well the citizen scientists are trained and how well the project is setup. Cuff *et al.* (2008) labelled two main concerns with this form of data collection, "observer effect" and "junk data". The collection of data from cheap, unverified, uncalibrated sensors can be seen as "junk data", with no pretence of neutrality or comprehensiveness. The "observer effect" is essentially when someone becomes so engrossed in a subject to work, they lose objectivity, change their behaviour and alter the data. Rather than being nihilistic, Sheppard and Terveen (2011) broke down the argument into how

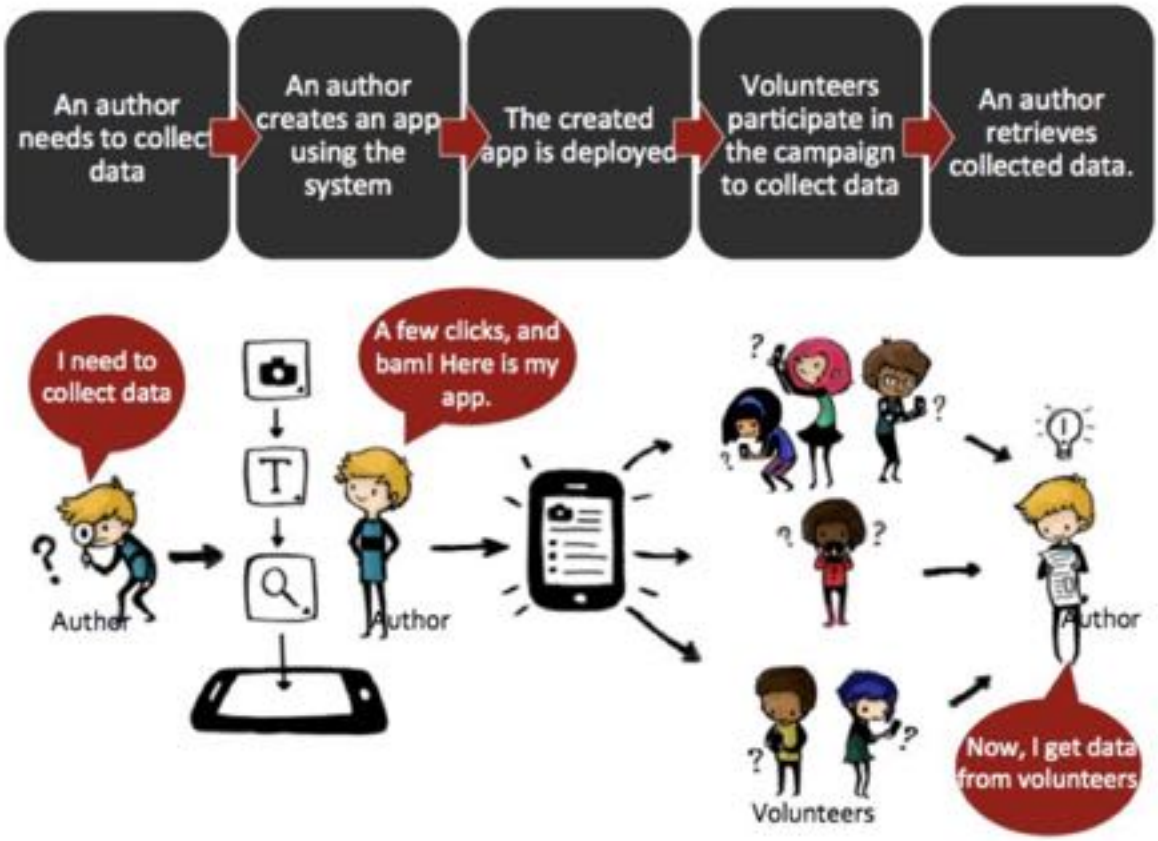

Figure 1.28: Workflow of a citizen science project (Kim *et al.*, 2013).

data quality can be defined, maintained and balanced. The data you get from citizen science is only as good as the effort and design that is put in in the first place, high quality data requires a defined collection strategy, rigorous quality control and an atmosphere where participants are engaged.

1.7.2 The Big idea

With the IoT and citizen science approach the number of stations will become far greater (Towe *et al.*, 2020). So what is the big idea with this? Big data. To define something as big data, it has to satisfy the three V's; volume, velocity and variety. High volumes of low density information, such as river levels, the speed of data collection in near real time and the variety of data, coming from different source in an unstructured way (Gandomi and Haider, 2015). The data stream does not necessarily need to be data points from monitors, but also from indirect sources such as tweets and generic CCTV (Ranjan *et al.*, 2017). Accurate flood warning systems are to benefit from this big

data, with advancements in IoT and machine learning providing the tools to analyse the real-time data, producing a system that is as near to real-time warning as possible (Donratanapat *et al.*, 2020). Mathematical models, predicting flood peak and duration for example, are increasingly updated with observations from physical sensors to reduce model uncertainty and improve forecasting (Mazzoleni *et al.*, 2017). Hydraulic models may not perform as expected if calibrated to low flows when an unexpected event takes place (Unduche *et al.*, 2018). A solution to improve the sparsity of gauge data is to deploy DIY sensors in the data assimilation process, albeit with the caveat that the data itself may have high uncertainty (Fava *et al.*, 2019). Mazzoleni *et al.* (2017) found that with even limited and uncertain hydraulic data can improve the flood prediction of models. Real-time data assimilation combines the complementary model and observational data into an optimal estimate (Reichle, 2008).

Sood *et al.* (2018) put catchments into discrete clusters, grouping together weather data, river data and ground data (forest density, soil type and drainage systems) within a 200 m area. When one cluster begins to notice change, the surrounding clusters are put into enhanced mode, making more frequent observations. Mitra *et al.* (2016) proposed a mesh connected wireless sensor network , composed of water level, humidity, pressure, water flow and rain intensity and to train an artificial neural network to detect flooding. Using a pre-obtained data set, with 65% of the data being used to train and the remaining for validation, Mitra *et al.* (2016) had a R^2 value of 0.99 for prediction if there was a flood. The authors themselves state that that the model might not be complex enough, and when a data set from a IoT is used this may need significant modification to train the neural network to new situations. Towe *et al.* (2020) raises the argument of what you want and need a model to do dependent on the time. Fast response decisions need a model to be operationally fast and robust with the ability to take real-time data, in contrast to longer term decisions, which are more flexible and generate more probable outcomes. A recent report by the EA recommended that for regional to national flood modelling, there has to be synergy between all data sources and for regional models to all use the same type of input data to allow a national forecast to be made (Robson *et al.*, 2017). Importing new types of data into flood mitigation is seen as important, but trying to determine how these complex and mixed up data sources can be used is still lacking (Demir and Krajewski, 2013).

Big data , with aiding traditional data sources is seen as a solution in crisis management, when

there is a simultaneous information overload and "information dearth", due to not enough sensors where you need them, and too many where you don't (Restrepo-Estrada *et al.*, 2018). Procuring from the citizen science methodology, georeferenced social media is a supplement to flood modelling that is becoming popular, as the data is linked to the people who are experiencing a flood, "human sensors", moving the conversation from numbers to a more personal approach (Fraternali *et al.*, 2012). Calling it human computation, Quinn and Bederson (2011) introduces the concept that instead of relying on a computer model to make decisions solely, human intelligence or intuition is far better at collecting the results that are needed. Figure 1.29 displays a sample workflow for data gathered from traditional hydrometric sources and from the human aspect data. In practice, by adding this social media aspect, (Restrepo-Estrada *et al.*, 2018) seen an increase from 39% accuracy when determining rainfall using only traditional monitors to 71% accuracy by including social media (nearly 16 million tweets), based upon more data was being received from areas that were seldom monitored. Moving from reactive to proactive is seen as a way of mitigation to minimise disruption and protect people (Barr *et al.*, 2020).

Looking towards the future, McCabe *et al.* (2017) mentions that it is unclear whether current models are able to usefully ingest the numerous new streams of data, or whether this new data is going to simply be superfluous to modelling, with petabytes (million gigabytes) of data coming in. Remarkably, Feng and Sester (2018) was able to pick out the peaks of rainfall events with only images and texts supplied on Twitter. McCabe *et al.* (2017) stated that non-traditional sources will expand the spatio-temporal representation of existing networks. However in theory Fonstad and Zettler-Mann (2020) sees that current analytics are lagging behind new big data, with the analogy of "new wine in old bottles", with new data with old analysis.

1.7.3 Section summary

In this section the acquisition of data is shown to be important, with the caveat that the data has to be of good enough quality to be used. Utilising citizen science in which it is both beneficial to the citizen and a researcher is seen as a motive for sound monitoring.

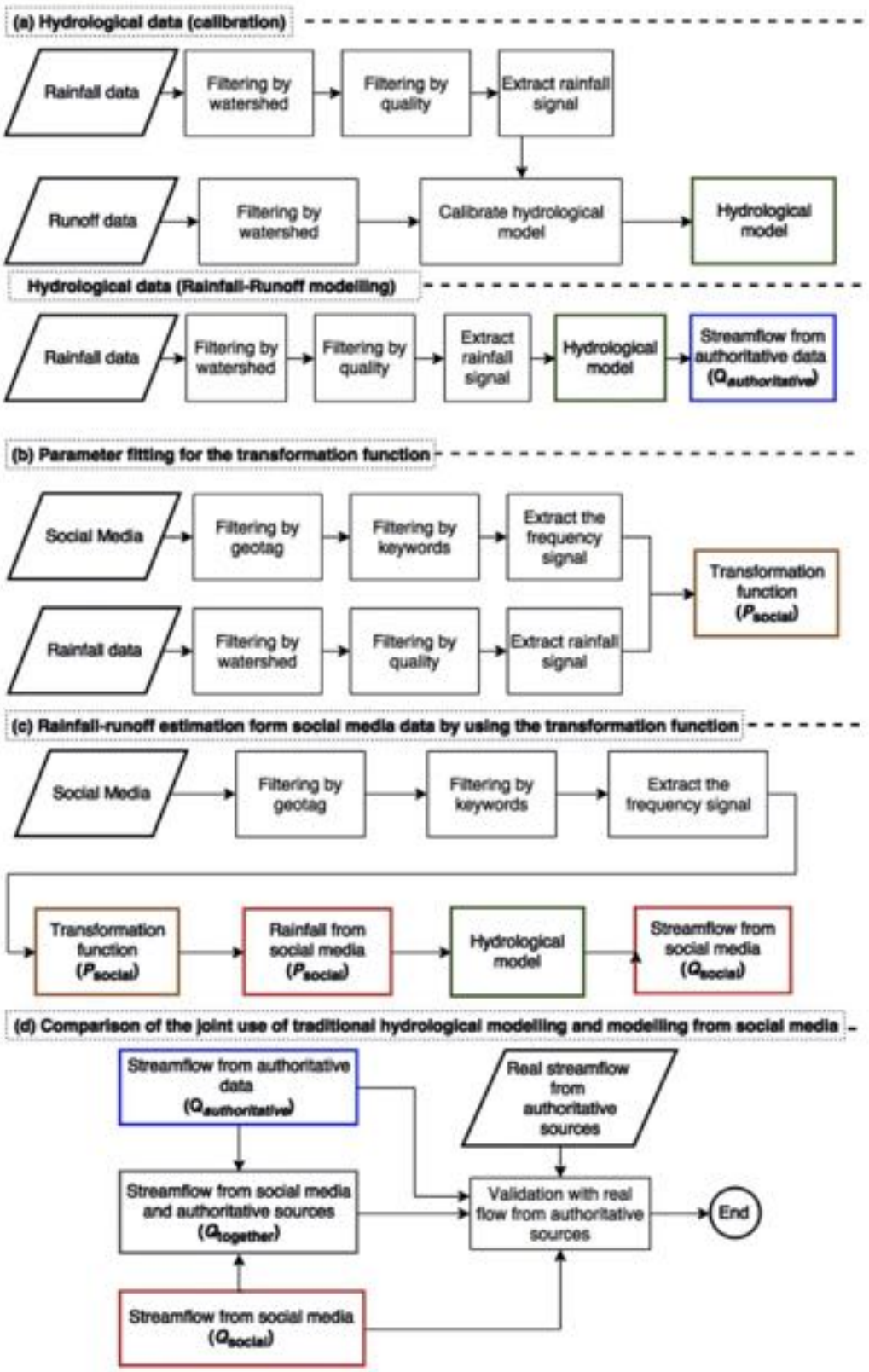

Figure 1.29: Workflow of how different data streams can be used to construct a working hydrological model (Restrepo-Estrada *et al.*, 2018).

“Sometimes, if you stand on the bottom rail of a bridge and lean over to watch the river slipping slowly away beneath you, you will suddenly know everything there is to be known.

A.A. Milne”

Chapter 2

Babbling brook to thunderous torrent: Using sound to monitor river stage

Chapter has been published in Earth Surface Processes and Landforms.

Expanded work is highlighted when not found in the original published paper.

Osborne, W.A., Hodge, R., Love, G., Hawkin, P., and Hawkin, R. (2021). Babbling brook to thunderous torrent: Using sound to monitor river stage. *Earth Surface Processes And Landforms*. doi: 10.1002/esp.5199

Abstract

The passive, ambient sound above the water from a river has previously untapped potential for determining flow characteristics such as stage. Measuring sub-aerial sound could provide a new, efficient way to continuously monitor river stage, without the need for in-stream infrastructure. Previous published work has suggested that there might be a relationship between sound and river stage, but the analysis has been restricted to a narrow range of flow conditions and river morphologies. We present a method to determine site suitability and the process of how to record and analyse sound. Data collected along a 500 m length of the River Washburn during July 2019 is used to determine what makes a site suitable for sound monitoring. We found that sound is controlled by roughness elements in the channel, such as a boulder or weir, which influences the sound produced. On the basis of these findings, we collect audio recordings from 6 sites around the North East of England, covering a range of flow conditions and different roughness elements, since 2019. We use data from those sites collected during storms Ciara and Dennis to produce a relationship between this sound and river stage. Our analysis has showed a positive relationship between an R^2 of 0.73 and 0.99 in all rivers, however, requires careful site selection and data processing to achieve the best results. We introduce a filter which is capable of isolating a rivers' sound from other environmental sound. Future work in examining the role of these roughness elements is required to understand the full extent of this technique. By demonstrating that sound can operate as a hydrometric tool, we suggest that sound monitoring could be used to provide cost effective monitoring devices, either to detect relative change in a river or, after more research, a reliable stage measurement.

2.1 Introduction

Hydrometry, the measuring of components of the hydrological system such as river flow characteristics, is crucial in flood mitigation strategy and monitoring (Chacon-Hurtado *et al.*, 2017). The methods by which rivers are monitored are ever evolving with new techniques such as PIV and ADCP measuring flow velocity, and UDM measuring stage (Muste *et al.*, 2004, 2008; Kruger *et al.*, 2016). There is a drive for greater ease of use of this kind of technology, being spurred on by the IoT to create an easy to use framework that everyone can contribute to (Moreno *et al.*, 2019). These approaches are designed to supplement the 1,500 hydrometric stations currently operational in the UK (Marsh and Hannaford, 2008). Although the UK network of government agency hydrometric stations is dense, this equates to one monitor per 130 km of the river network (Marsh, 2002). All of these technologies, both existing and emerging, have infrastructural issues to overcome to work efficiently, such as power, direct line of sight and calibration, limiting their wider implementation. There is a need for an innovative, non-invasive, cost-effective method for monitoring river stage, which could be distributed throughout parts of catchments that currently are not monitored.

Imagine being beside a river, what do you hear? In this study we propose that sound can be used as an alternative method to calculate river stage and track flood peaks. The use of sound is based upon the assumption that a river gets louder as its depth increases, such as a babbling brook becoming a thunderous torrent, generating a soundscape that is dependent on river condition. We focus on sound because it has a number of potential advantages over alternative methods for measuring river stage. Measuring sound is power efficient as the monitor measures passively, rather than actively generating a signal, such as an ultrasonic pulse from an UDM. PIV requires illumination at night, which can be a significant drain on energy. Sound can be measured from the banks of a river, reducing the need for extensive in-stream infrastructure. Despite its potential advantages, we do not currently know under what range of conditions sound can be used to monitor river stage. A method that works across a wide range of conditions is necessary for this technique to be used to manage flood risk.

The sound of a river has been studied through the use of seismic (ground), infrasonic (air) and

hydroacoustic (water) surveying, examining how sound production can be linked to sediment transport, flood processes and turbulence within a natural environment (Manasseh *et al.*, 2006; Ronan *et al.*, 2017; Schmandt *et al.*, 2017). The sub-aerial sound of a river is primarily produced by the entrainment and collapse of air bubbles in the flow, through turbulent features such as hydraulic jumps, rapids or waterfalls generating waves and whitewater (Bolghasi *et al.*, 2017b). Minnaert (1933), first described how the sound of "musical" air bubbles and running water were complex in nature. The Minnaert resonance is the idealised sound frequency at which a bubble bursts, without the effects of surface tension, viscosity of the liquid and the thermal conductivity of the gas (Gaunaurd and Überall, 1981). Bubbles monitored underwater were found to burst in the frequency range of 400 - 2000 Hz, with bubble radius determining the frequency (Chicharro and Vazquez, 2014). The larger the bubble, the lower it's corresponding frequency, such as a 10 cm bubble radius has a frequency of 32 Hz and a 1 cm radius of 326 Hz (Leighton, 1994). We expect that this frequency range will determine the frequencies in the sound made by rivers sub-aerially.

The relationship between sub-aerial sound and stage level has been investigated by Morse *et al.* (2007). They concluded that as stage changes, then sound pressure, the deviation of air pressure from ambient, will change in unison. The presence of geomorphic features, such as a cascade or riffle, were found to affect the sound pressure ranges. The study, however, had limited observations, with 6-8 sound points over a range of flow conditions that did not include flooding, nor were the mechanics of what controlled the sound considered. The extrapolation of a relationship found during low flow to high flow has not been tested, with high flows having an inherently different flow regime, with surface turbulence structures emerging (Chanson, 1996). A relationship between seismic noise, sediment transport and river discharge was found by Govi *et al.* (1993); Anthony *et al.* (2018) and with river stage by Burtin *et al.* (2008b) , determining that hydrodynamics were the most probable source of the signal. Infrasound monitoring by Schmandt *et al.* (2013) suggests that waves on the water surface generated sound, showing a link between discharge and sound. The use of passive sound above the water is also seen as an emerging way of measuring the air-water gas exchange velocity (K), which is essential for ecological processes (Morse *et al.*, 2007; Klaus *et al.*, 2019). Klaus *et al.* (2019) found that there was a positive relationship between sound pressure and K in the frequency range 31.5 Hz - 1000 Hz. The riverbed morphology had a significant control over the sound produced by each reach, with

large scale roughness element (RE), such as boulders, having a larger effect than a gravel bed. A large obstacle will also cause the most deflection of the water, called form drag, at low and high flow (Bathurst, 2002). Looking at the self-aeration process, the mixing of gases from the atmosphere into the water, Kucukali and Cokgor (2008) found that there was a relationship between the blockage ratio (upstream area blocked by an obstacle) and aeration caused by turbulence. With a relationship between the size of an RE and turbulence, this supports the idea that REs are important to sound generation. We therefore seek to expand our understanding about a link between sound and REs and whether this has any influence on sound and stage relationships.

The aims of this paper are to: (1) identify sites suitable for sound monitoring; (2) determine if river sound can be isolated from a complex, seasonal soundscape, outwith clement conditions; (3) investigate how factors such as REs may influence a relationship between sound and stage.

2.2 Methods

We first introduce our process for determining site suitability and the techniques to record and analyse sound data from rivers. We then examine the relationship between the recorded sound and river stage, and explore the factors that contribute to the relationship.

2.2.1 Sound collection

All audio from our field locations (introduced below) was recorded in the WAV format at 16 kbps as it preserves more data in a recording compared to a compressed format such as MP3. Mennitt and Fristrup (2012) used consumer level recorders for outdoor audio recording and found that although MP3 allowed long, continuous recordings to be made, it did reduce the frequency resolution that could be used. Recording at a sampling rate of 44.1 kHz, with the Nyquist frequency of 22.05 kHz, the recording captures all data in the frequency range between 1 Hz and 22.05 kHz, which is greater than the range of normal human hearing of 20 Hz to 20 kHz (Horii *et al.*, 2018). However, because of limitations in the response of consumer grade microphones to low-frequency sound (Table 2.1) and due to power-source noise, we only consider frequencies >

Monitor	Microphone	Directionality	Frequency range	Singal to noise ratiio (dBA)	Sensitivity (dB) (1 kHz at 94 dB, 1Pa)
River Washburn	RØDE VideoMic	Supercardioid	40 Hz - 20 kHz	79	-38
Bushnell E3	ECM-60C	Omni	50 Hz - 13 kHz	40	-64
Raspberry Pi	CMA-4544PF-W	Omni	20 Hz - 20 kHz	60	-44

Table 2.1: The monitors and their associated microphones units within them. Technical specification of the microphones is freely available online. Values that are important to the study are frequency range, signal to noise ratio and sensitivity. These determine the range we can measure at and also the conversion into sound pressure level. Each microphone has a quasi flat response to frequency as per the technical specifications but was not tested in this study. Any frequency bias will have a negligible effect on our data.

50 Hz in this study. We define river sound as the sound that can be audibly heard by a person since we expect that someone can audibly tell the difference between a river at low and high flow. Infrasound, below 20 Hz, is not considered as consumer microphone frequency ranges rarely go below 20 Hz and with the frequency humans can hear at, a change of rivers sound is audibly noticeable. Bubbles would also need to be bigger, at greater than 30 cm diameter to produce sound below 20 Hz (Leighton, 1994).

In this study, three types of microphone are used, with their technical specification shown in Table 2.1. Although less than ideal to use different microphones, once converted into sound pressure level (SPL), our sound value is measured in decibels of SPL (dB SPL) in reference to $20\,\mu\mathrm{Pa}$. Understanding how the sound changes is more relevant to our study and not why one river is louder than another since other factors such as sound attenuation would need to be accounted for for direct comparison. All microphones were recessed within an enclosure to protect against wind and rain, but not blocked to the environment.

2.2.2 Site suitability

In order to identify the most suitable sites we need to know how the sound produced by a river channel changes spatially and what river features influence it. We deem a site suitable if (1) we can hear the river and (2) if there is a significant response in the sound between river stages. We addressed this at the River Washburn, Yorkshire, UK, where there was a unique opportunity to record audio in the same day during a low compensation discharge of 0.08 m^3s^{-1} and a high continuous discharge of 8.55 m^3s^{-1}. The Washburn is a natural river channel connecting a series of reservoirs, and occasional high discharges move water between the reservoirs. These releases

are used for whitewater sports, and the channel has been managed by introducing rapids and boulder gardens (REs), altering it from what it would have been naturally.

To investigate site suitability an acoustic map along 500 m of the river was generated to help us identify regions that had a markable change in sound from low to high flow. Markers were placed at 10 m intervals along the course of the river, and each point was referenced using a dGPS. Recordings were taken at an elevation of 1.5 m above the bank during high and low conditions from the marked location. An additional section of the river was identified for a more in depth examination which had a flat floodplain around a RE to examine how sound behaves at different monitoring points around a channel. Mapping the sound at 10 m intervals along the river, and at 1 m points away from the river we are able to describe how sound behaves. Audio was recorded for 8 seconds at each location, using the RØDE VideoMic (supercardioid) with a sensitivity azimuth of 210° which is more directional in comparison to omnidirectional microphones at 360°. We used a supercardioid microphone to record the majority of sound produced by each specific section of the channel, and to limit sound from sections further up/downstream. However, components of upstream and downstream will still remain.

Photographs of each marker section were taken to assess what was generating the whitewater at each reach and to designate if a section had: no REs (Rank 1), small REs (Rank 2), or large REs (Rank 3). Qualitative ranking of the REs is used as direct measurements of these obstacles was not possible. Determining rank was done by eye, with rank 2 and 3 differentiated by if there was a large RE (height approximately >1 m) and how the REs were dispersed, such as how directly in the flow they were. It was assumed that a RE in the middle of the flow will have more impact on the flow than at either bank side.

2.2.3 Sound analysis

With the sound captured, we needed to find a way to filter any noise from our expected river signal. Audio clips were converted from the time to frequency domain using a FFT in MATLAB R2020a. To examine at a resolution of 1 Hz, a minimum sample length of 1 second is required.

We aim to identify a river sound zone (RSZ), which is the frequency range that best correlates with river stage. To derive a single sound value for each recording, which can be compared against the corresponding river stage measurement, we use the spectral centre (median) of the data. The median is calculated from all values of SPL within a certain frequency range, known as a bin. As the FFT produces a SPL value for every 1 Hz, we have 22,050 individual sound values, with 0 Hz being the mean of the data. Therefore when we calculate a median from a 1 kHz bin, it is calculated from 1000 values. We use this instead of the spectral centroid (average) or maximum volume, because the median of the data yields a more representative signal that is not skewed by erroneously large or low values in the frequency range. Median filters are useful in scenarios where periodic patterns are found (Ohki *et al.*, 1995). The first bin of 1 - 1000 Hz is clipped to 50 - 1000 Hz, as due to the switching power supply used, noise from the power supply affects readings below 50 Hz.

It is unrealistic to assume that the only sound source is the river. To further constrain the RSZ, other environmental noise needs to be removed. Certain frequency domains that may be of influence are: the human voice in mainly the 100 Hz - 8 kHz range; birdsong at 1 - 8 kHz; and vehicles at 0 - 4 kHz (Monson *et al.*, 2014; Liu *et al.*, 2013; Slabbekoorn and Ripmeester, 2008). These noises will primarily affect monitoring during low flow conditions as during high conditions these will either be absent, or drowned out. Figure 2.1 shows the spectrogram of each of these individual noises. Each sound has its own unique fingerprint, compared to a pure river signal. Birdsong has excitable chirps and trills, car sound is a wideband, flat noise, and talking is in pulses of speech. To reduce the number of noise related errors the RSZ will have to be both strongly linked to the river, while maintaining its independence from these other environmental noises.

Wind and rain are not associated with a certain frequency range, and are dependent on intensity instead. The fluctuating nature of wind and rain intensity makes this sound known as Brownian noise, with a rumbling, roaring sound (Yackinous, 2015). Rain was found by Burtin *et al.* (2011a) to have caused a seismic signal when landing on rocky debris near monitors. Wind can be the most intrusive sound on a recording and if the wind is constantly louder than the river, blowing out the microphone, then it is not possible to extract a river component. In a remote location

away from cultural noise sources, wind has also been recorded on seismic monitors at the surface, contaminating the recorded signal at speeds of only 6.5 mph (Withers *et al.*, 1996). Ronan *et al.* (2017) found wind to be the most probable source of high power, low spectral coherence noise on infrasound recordings. With Anthony *et al.* (2018) suggesting that without wind filters and if deployed close to a river, infrasound acoustic signals were likely unsuitable for smaller river systems. To reduce wind impact on the monitor, the microphone can be placed in the opposite direction to the prevailing wind or placed in an area with adequate wind baffling from trees or shrubs. But, even with adequate protection, wind can still be heard in some recordings. Figure 2.1B shows a spectrogram of a gusty signal, with the bright peaks caused by intermittent wind spreading into the higher frequencies. If the entire recording was run through the FFT code, then these peaks spanning the entire frequency range would dominate the results.

To remove the impact of the wind we apply an additional filtering step to our data (Figure 2.2). We record each sample for as long as possible as it provides a better chance of getting a continuous section of recording without wind noise. Changing the recording length is subject to the site and how confident we are that we can filter out the wind physically. In this study we considered a minimum recording length of 5 seconds to be necessary. To filter out the wind noise, we split the recording into 1 second rectangular windows, with 0.5 second overlap between them. We do this to allow a frequency resolution of 1 Hz to be maintained through the FFT, as this matches our sampling rate. A rectangular window also does not smooth out the boundaries of the clip. Reducing the total recording length reduces the number of windows, and thus the potential samples to get the lowest median from. The overlap is to increase the number of windows that can be taken from any given recording. The audio data from each of these new windows are processed with the same FFT code, resulting in one median value per frequency bin for each window. The minimum value for the RSZ, the region of frequencies found to have the maximum correlation with stage, from across all the different time windows is chosen. We take the minimum value from all the different time intervals because it is expected that river sound is constant in any recording and will always be the loudest of any constant base sound but will also be quieter than sporadic noises caused by wind, thunder etc. By taking the minima of each audio sample in the RSZ, we can significantly improve the processing of noisy recordings. We call this the lowest median filter (LMF). When assessing this technique to determine any bias in the window that is chosen, we found that the window with the lowest value is equally

taken from across all the windows and one is not preferentially choosing one.

The following section introduces our workflow of collecting and processing river data, which was applied to all study sites and is the basis for any future work or different sites (Figure 2.2).

2.2.4 Study site monitoring

Six sites were selected for monitoring between November 2019 and February 2020 based upon the findings of data collected at the River Washburn for site suitability, chiefly the occurrence of REs (see Figure 2.3 and Table 2.2 for characteristics). These locations were selected to be typical of many rivers and not highly specific. Sites A-C were deemed to have good site suitability. Sites D-F were not explicitly chosen for good suitability, for instance many have small REs and site F has a large amount of wind noise. They are predominantly alluvial rivers but include two bedrock channels (site D and F), and range between 8.0 - 34.5 m wide. Stage at Sites A-C was measured using a pressure transducer (TD- Diver), calibrated to atmospheric pressure, and Sites D-F were EA operated gauges recording at 15 minute intervals.

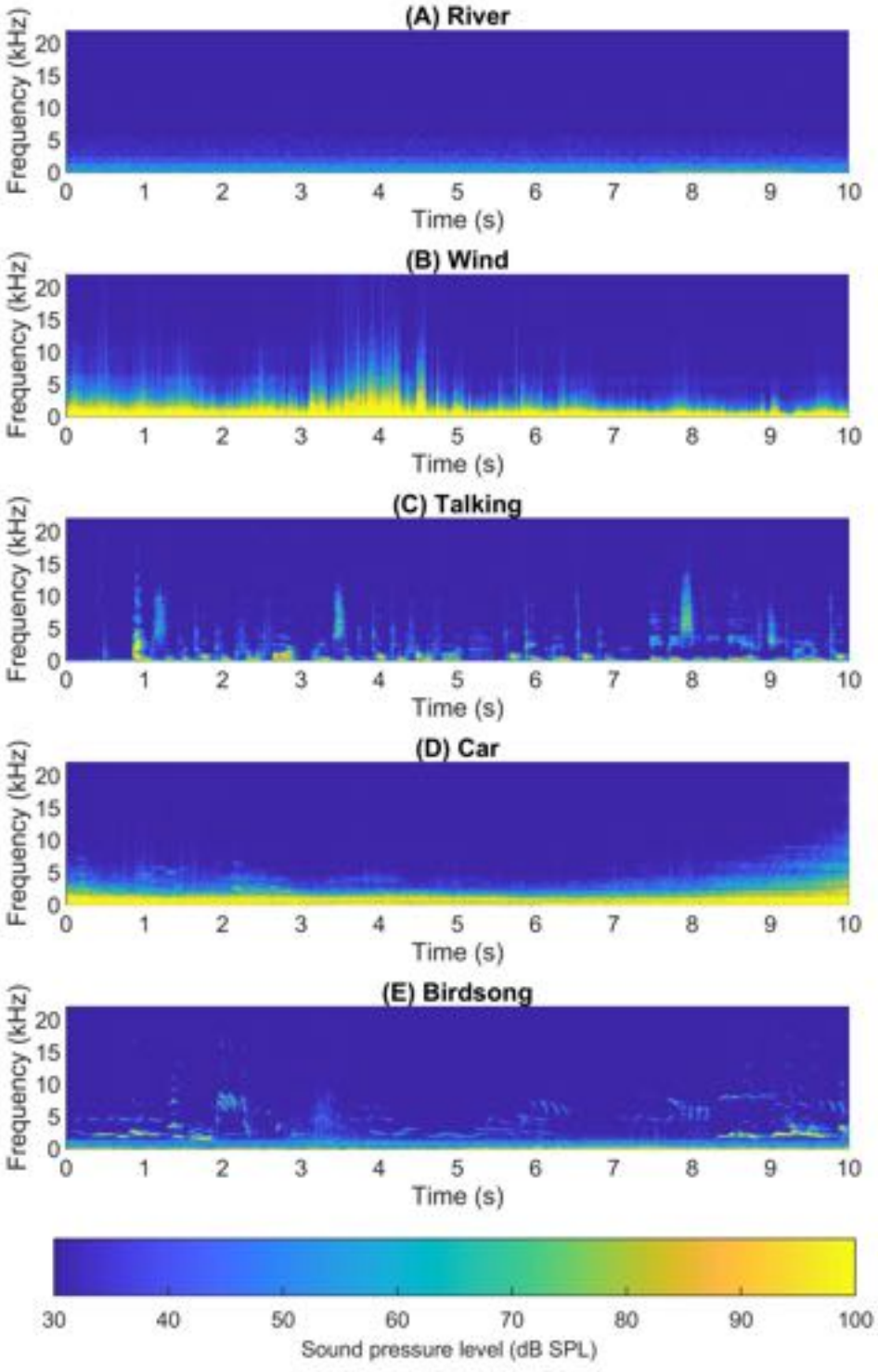

Figure 2.1: Spectrograms for different sources of environmental noise. Each recording is only of that sound. (A) Chainley Burn during average flow condition on a calm day, (B) Trout Beck, County Durham during continuous high wind, (C) Reciting of the alphabet, (D) main road with cars going past and (E) Black bird. Plots are produced by the spectrogram function using short-time Fourier transforms, which allows both frequency and the time domain to be viewed concurrently. Bin width is set to 1 Hz to show a finer resolution of data.

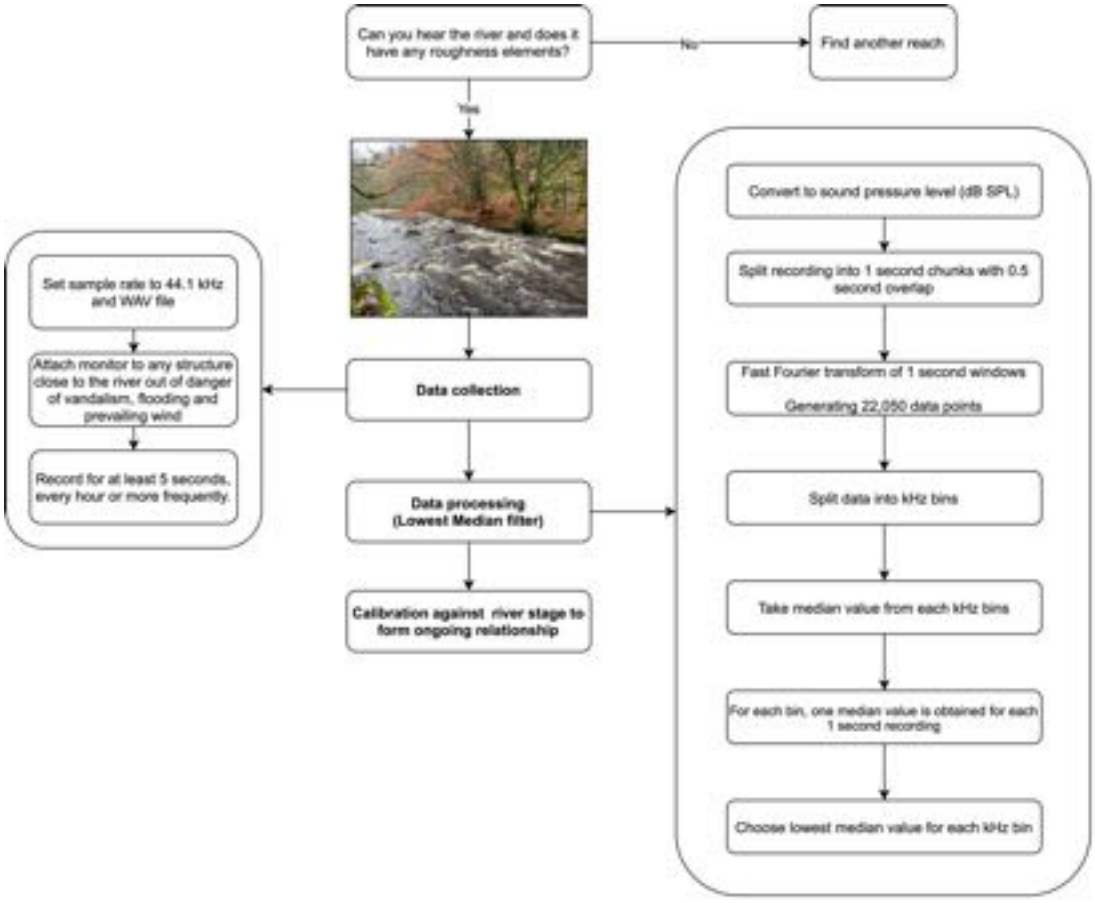

Figure 2.2: Our workflow of how to monitor a river using sound with the required steps needed to perform lowest median filtering.

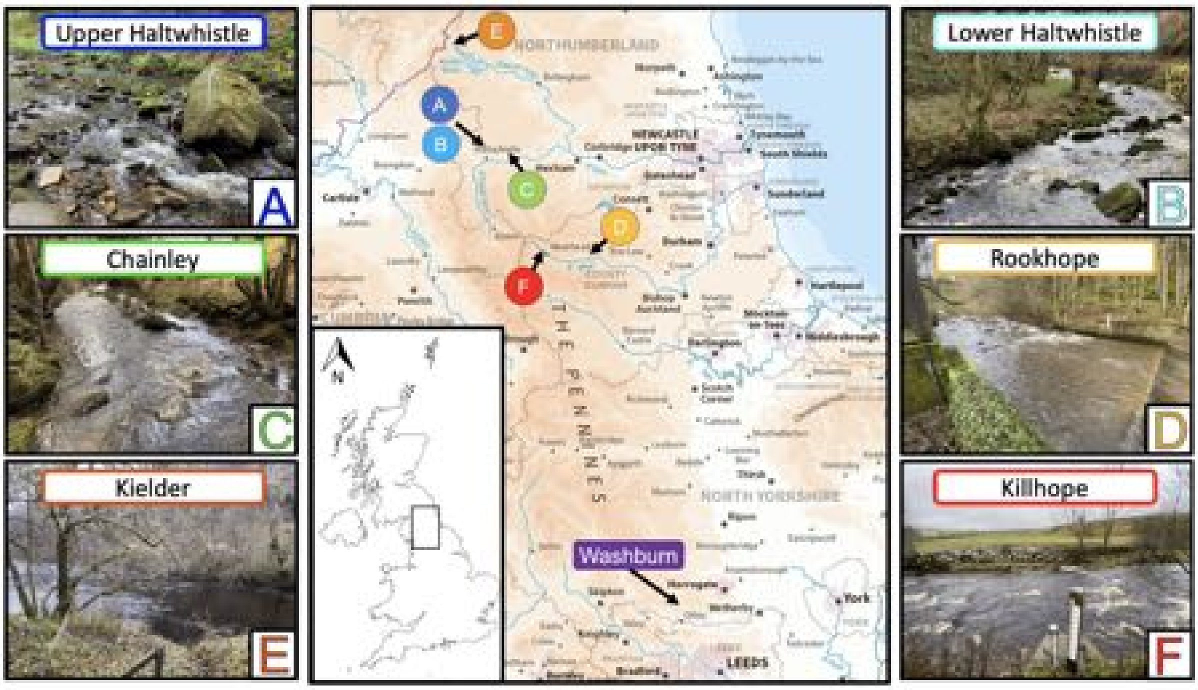

Figure 2.3: Map of study site locations with corresponding photographs taken from each site showing the morphology of the river and the general surroundings. A-D were taken during low river levels, with E-F taken during above normal levels. Approximate channel widths A: 6.0 m, B: 6.0 m, C: 5.0 m, D: 8.0 m, E: 13.5 m and F: 5.0 m.

Site	River	Coordinates	Data collection period	Gauging	Distance from monitor to river bank (m)	Bankfull depth (m)	Bankfull width (m)	Substrate
A	Haltwhistle Burn (Lower), Northumberland	5458′43.5"N 227′40.6"W	24/07/2019 -19/02/2020	Diver	1.0	1.6	14.3	Cobble
B	Haltwhistle Burn (Upper), Northumberland	5458′47.2"N 227′36.4"W	28/01/2020 -19/02/2020	Diver	5.0	1.1	19.9	Cobble
C	Chainley Burn, Northumberland	5458′51.1"N 221′22.7"W	6/12/2020 - 19/02/2020	Diver	1.5	1.4	9.8	Cobble
D	Rookhope Burn, County Durham	5444′51.0"N 204′31.0"W	27/11/2019 -14/02/2020	EA	4.5	0.8	8.0	Cobble/ Bedrock
E	Kielder Burn, Northumberland	5513′50.9"N 234′54.0"W	27/11/2019 -16/02/2020	EA	13.0	1.5	34.5	Gravel
F	Killhope Burn, County Durham	5445′11.7"N 213′27.5"W	27/11/2019 -18/02/2020	EA	7.5	0.8	8.7	Bedrock

Table 2.2: Study site location properties.

A Bushnell E3 trail camera was used to record sound at Site A as this provided a "ready to go" setup at the start of the project. A purpose built monitor was created from a Raspberry Pi Zero, a CMA-4544PF-W microphone and a WittyPi Mini (timer) for use at all subsequent sites. Monitors were attached as close as possible to the river on existing structures and out of danger of high water. At Site A sound was recorded for up to 10 seconds, once an hour due to running off of AA batteries. A reading once an hour is the minimum frequency to monitor at, as anything longer than this becomes unconducive for meaningful flood monitoring. Higher frequency sampling rates of every 15 minutes were achieved with the Pi Zero at Sites B-F, allowing comparison against the 15 minute interval EA station data. Each device has a finite number of recordings it can take, due to the size of battery used, meaning it can either sample at a high rate for a short time, or last longer and only sample every hour. Using a 7 Ah, 12 v lead acid battery allowed up to 1,400 recordings to be made with the Pi. The length of individual recordings varied due to power saving management, with the wildlife camera varying between 8- 10 seconds and the Pi Zero, 9-10 seconds.

With exception of the acoustic mapping, an omnidirectional microphone was used in the monitors as this captures audio from an identified reach, without the need to target the microphone during installation. There would be a risk of a supercardioid microphone moving during any long term experiment, which would incur an extra source of error. The ambition to make a sensor that can be widely deployed means that it is advantageous if it can use cost effective and easily procured components. Higher resolution and frequency response data could be captured with a higher specification microphone and digital audio recorder, but with the problems of power and cost becoming an issue. We expect that the frequencies that will be of interest are less than 15 kHz, so the microphones used should be sufficient (Klaus *et al.*, 2019).

During our monitoring, the UK was subjected to substantial rainfall in February 2020, with Storm Ciara on $8^{th} - 9^{th}$ February, and Storm Dennis on 15^{th}- 16^{th} February. These events produced river levels that reached the highest levels monitored in some of our stations, and higher than levels reached from Storm Desmond (5^{th}- 6^{th} December 2015) for others but not quite beating long standing records. Having both storms back to back was an incredibly rare opportunity. We use the data from the storms as our primary dataset, because it ranges from very low to very

high levels, and therefore can be used to test the range of conditions across which sound can be used to predict stage. We supplement this data with a longer dataset collected at Site A from 24th July 2019 to 20th February 2020.

We test the fit of any sound-stage relationship using a Nash-Sutcliffe efficiency (NSE), comparing our observed and simulated stage data. Nash and Sutcliffe (1970) developed a technique to test the fit of observed and simulated flow data, by determining how well it fits to a 1:1 line. NSE has a range of 1 to -∞, with the 1 being a perfect relationship. McCuen *et al.* (2006) showed that a NSE greather than 0.5 was a good fit. When comparing between observed and calculated stage we therefore show a NSE which will determine how good the fit is.

2.3 Results

We present our results in three stages: (1) analysing what features within a river may control the sound emitted and determine a suitable site, (2) demonstrating how the LMF helps to improve the data collected from the river and (3) examine whether the filtered sound data has any correlation to river stage.

2.3.1 Acoustic mapping

2.3.1.1 River Washburn

An acoustic map of the River Washburn is shown in Figure 2.4 during low and near bankfull flow. The River Washburn has a SPL of 30 - 60 dB SPL across its course during low conditions, with higher values at a weir and a constrained section. At high discharge certain reaches become very loud, where there are substantial REs with heights $>$ 0.5 m. When observing the photographs at each section, we found a correlation between the presence of whitewater and the SPL, with more whitewater being associated with higher SPL values, agreeing with (Ronan *et al.*, 2017). Every section of the river experienced a rise in SPL from low to almost bankfull flow. When comparing to the qualitative REs rankings in the channel: Rank 1 generates a median range of SPL between 40 - 60 db SPL; Rank 2, 46 - 64 db SPL and Rank 3, 45- 66 dB SPL (Figure 2.5). Therefore between low and high flow, SPL rises by around 20 dB SPL no matter what rank is

used. However, choosing the rank in which the loudest sound is produced is beneficial as it provides a higher likelihood of being louder than any possible environmental noise.

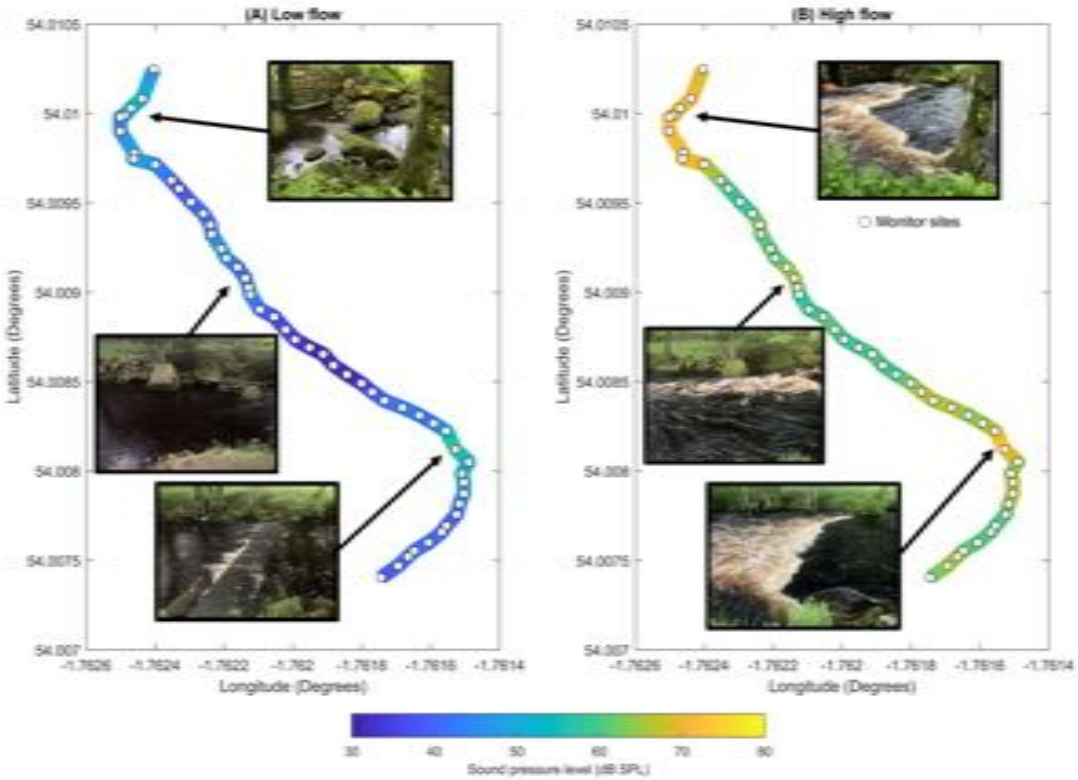

Figure 2.4: Acoustic map plotted of a 500 m course of the River Washburn during low and high flow. Markers show recording locations with the coloured line being a 1D interpretation between these points. Images shown highlight the main areas of change along with photographs of the sites. Sound values are obtained using the lowest median filter with a frequency of 0.05 -1 kHz. 0.05- 1 kHz is used due to the site being sheltered from wind meaning any sound generated will be purely from the river.

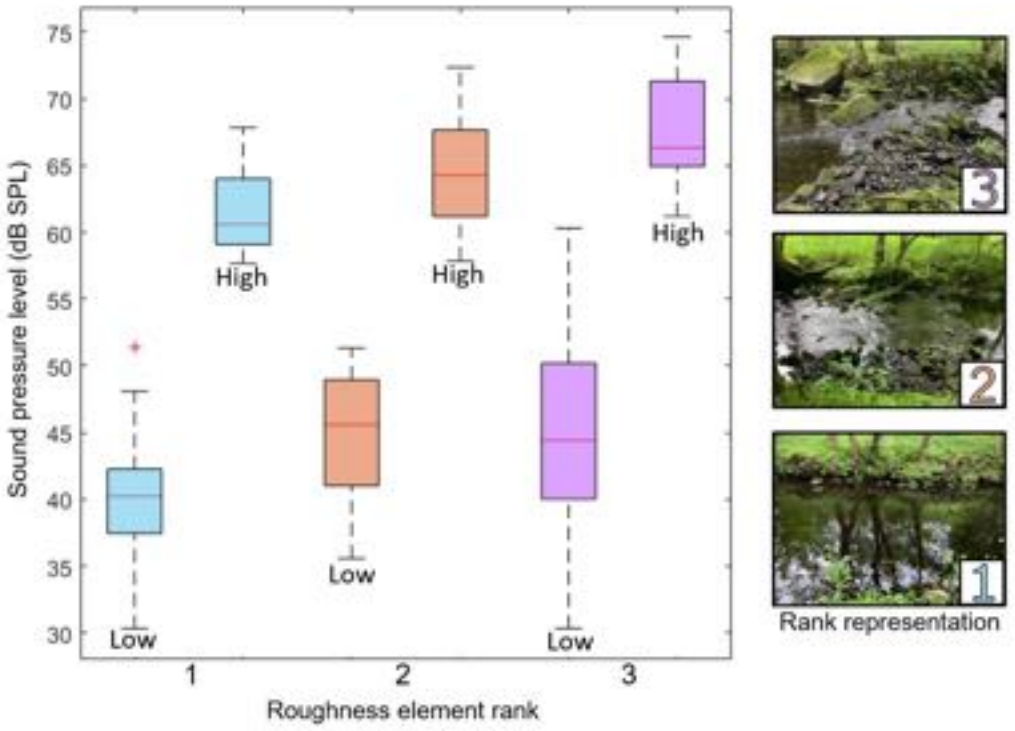

Figure 2.5: Box plot of normalised amplitude at low and high flow conditions, grouped by the qualitative rankings of roughness elements at the River Washburn. Photographs show a representative example of each rank. Roughness element rank is chosen by eye, with dominant REs, i.e. the largest element, being easily identifiable in Rank 3. Number of samples: Rank 1, 22; Rank 2, 15; and Rank 3, 13.

An in-depth look at a section of the river with an large RE, with a rank of 2, is shown in Figure 2.6. In Figure 2.6A , as we walk 10 m away from the river, the SPL drops from 66 to 55 dB SPL during high flow. At every point, the SPL measured at high flow is larger than that measured at low flow. Moving upstream or downstream, Figure 2.6B shows that SPL drops as we move away from the RE. The highest SPL is not at the RE as a tree was between the microphone and the RE. Without the tree we would expect a smooth convex shape to continue. Sound does not drop as much as when moving away from the river, with a 10 m movement causing a drop from 66 to 61 dB SPL.

2.3.2 Lowest median filter

2.3.2.1 River sound/ stage relationship

Long term audio data, recorded using the trail camera at Site A are compared against the river stage data from the pressure transducer in Figure 2.7. The audio data were processed to calculate

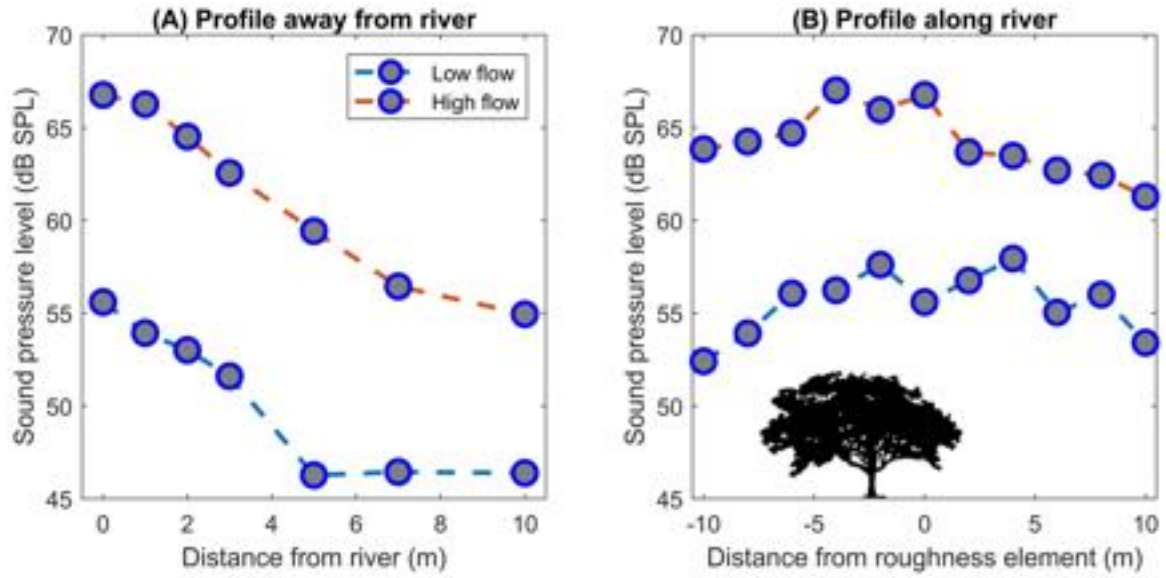

Figure 2.6: At the River Washburn, acoustic mapping was done around a dominant RE with a rank of 2. (A) moving away from the river and (B) along it. Recordings were done at the same points during low and high flow. Sound value relates to the 0.05 - 1 kHz band after lowest median filtering.

the median SPL within the frequency range 0.05- 1 kHz. The frequency range was chosen to illustrate how well the filter works, although may not be the best frequency range to use in the study due to the prevalence of wind. We call the resulting profiles of how sound changes over time sonohydrographs. In Figure 2.7A there is little similarity between the sonohydrograph and the actual hydrograph. In contrast in Figure 2.7B, after LMF, the sonohydrograph has the same shape as the hydrograph, with the steep sides of the rising limbs and the slower lowering of the falling limbs. In Figure 2.7A the wind noise produced by winter storms is clearly highlighted in the large fluctuations of the blue line such as on the 9th February 2020, with no clear signal being given during this time period. If used to interpret river stage, the river would appear to be in a state of flooding and sudden drainage repeatedly. In contrast, in the filtered data, there are no fluctuations. We therefore apply the LMF in all subsequent data analysis.

2.3.2.2 Wind noise

The Killhope Burn, at Site F, is a far noisier site in comparison to the more secluded locations such as Haltwhistle, with traffic and wind noise (Figure 2.8). As shown in Figure 2.1, these pollutants share the same frequency space as the river sound, meaning we needed to use a higher

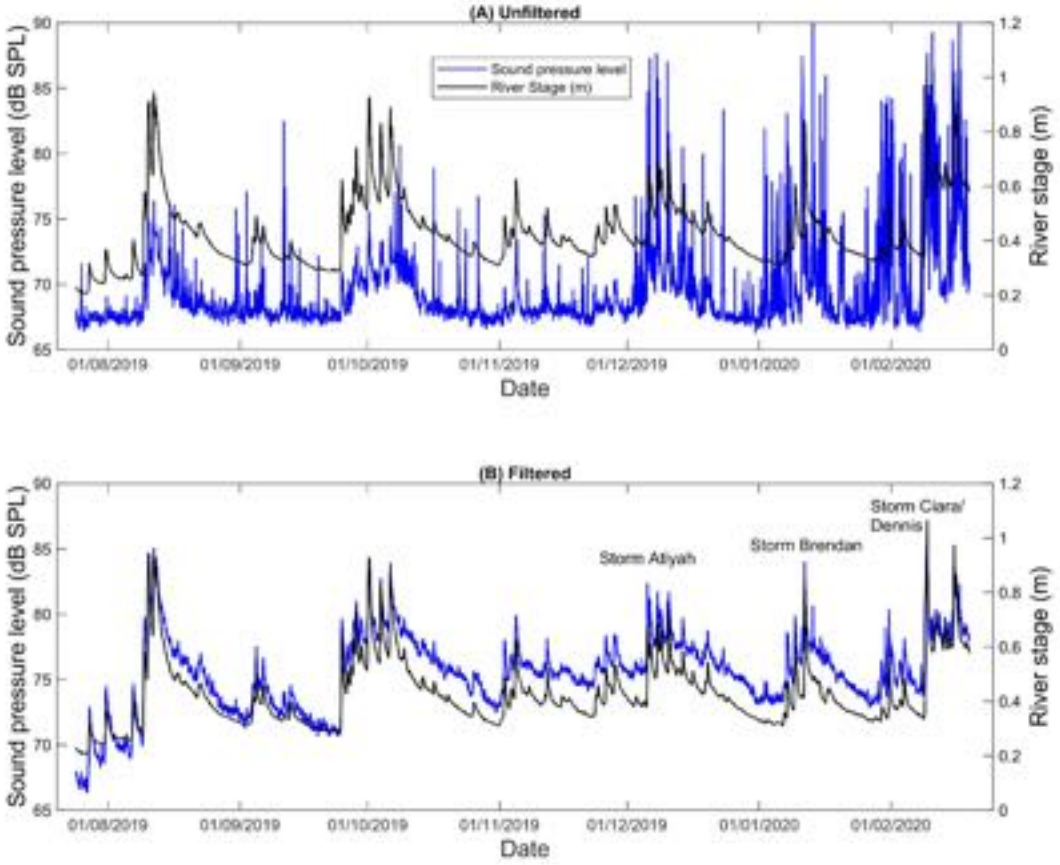

Figure 2.7: Sonohydrographs (blue) and hydrographs (black) of the Haltwhistle Burn over a Summer/ Winter season. (A) Unfiltered data at 0.05-1 kHz and (B) LMF filtered data at 0.05-1 kHz. Unfiltered data is a FFT of the entire audio clip, and the median taken from the 0.05 - 1kHz bin.

frequency range of 5-6 kHz as it was shown later in the study to be the best to use at this site. The readings are affected by wind even during periods of more settled weather, with Storm Atiyah, 8th- 9th December 2019. The filtering has an enhanced effect compared to Figure 2.7, removing most of the fluctuating readings and reducing the scatter of the data. We still have some wind noise artefacts in the data in Figure 2.8C, but significantly less than in Figure 2.8A. The number of points in the data where the SPL is an order of magnitude greater than the value of the previous point is reduced by 70% after application of the filter. The fit and smoothness of the sonohydrograph also improves, when viewed in relation to river stage. When we plot river sound and it's co-current river stage we are able to fit a function to this, with Figure 2.8B and D showing that an exponential relationship is able to be found, with a R^2 of 0.85 after the LMF, when before it was not possible. The wind noise that was persistent at low stages has all but been eradicated.

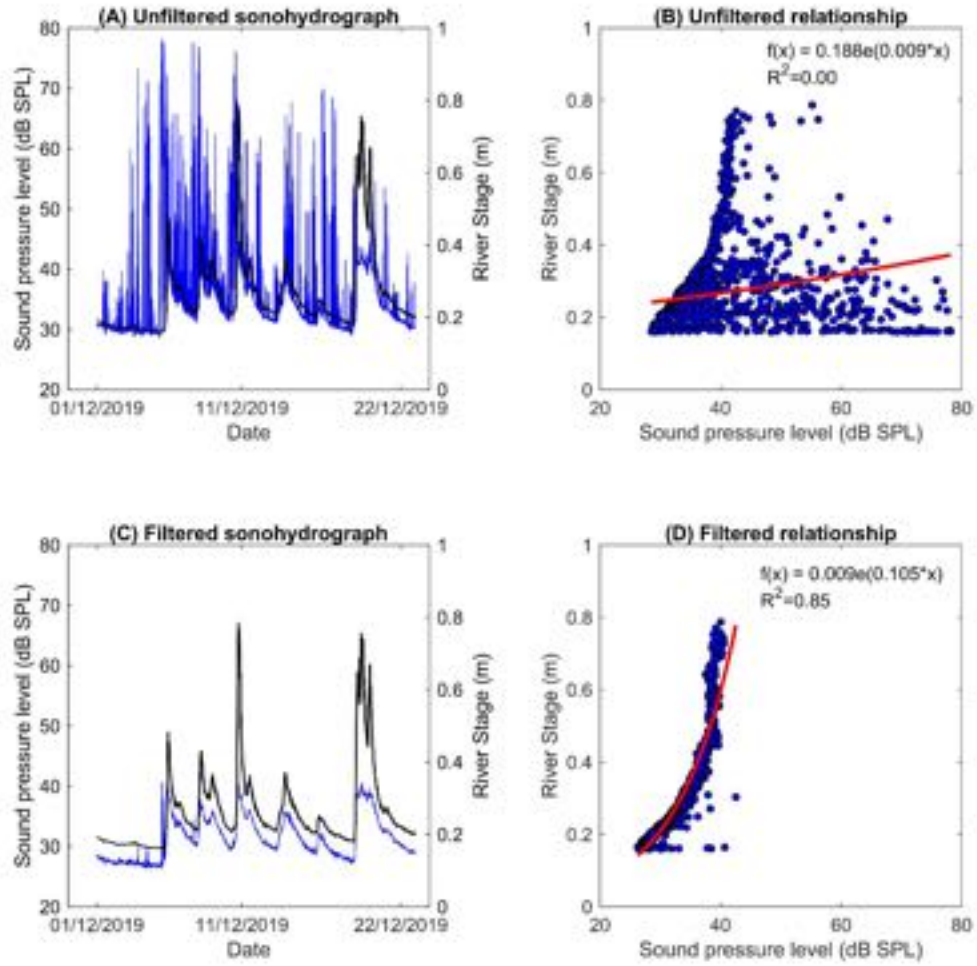

Figure 2.8: Comparison of river data with substantial wind noise from the Killhope Burn, Wearhead between 5 - 6 kHz. (A) Unfiltered sonohydrograph, (B) unfiltered river stage/ sound relationship, (C) LMF sonohydrograph and (D) LMF river stage/ sound relationship.

To allow the LMF to operate efficiently, a recording length has to be long enough to include a gap in any concurrent noise. We ran our LMF code with different lengths of recordings, from one second to total recording length. These new SPL values were then compared against stage, and the R^2 found of the best relationship between the two. In Figure 2.9 the difference between the calmer Haltwhistle and the windier Killhope site becomes clear. Haltwhistle is able to achieve a better relationship against river stage at very short recording times, with a one second recording giving an R^2 of 0.90 in the 1 - 2 kHz bin. Conversely a one second recording at Killhope only has an R^2 of 0.7. There is a upwards trend in R^2 against recording time for both sites, but this trend is more substantial at Killhope. At a total recording time of greater than two seconds there

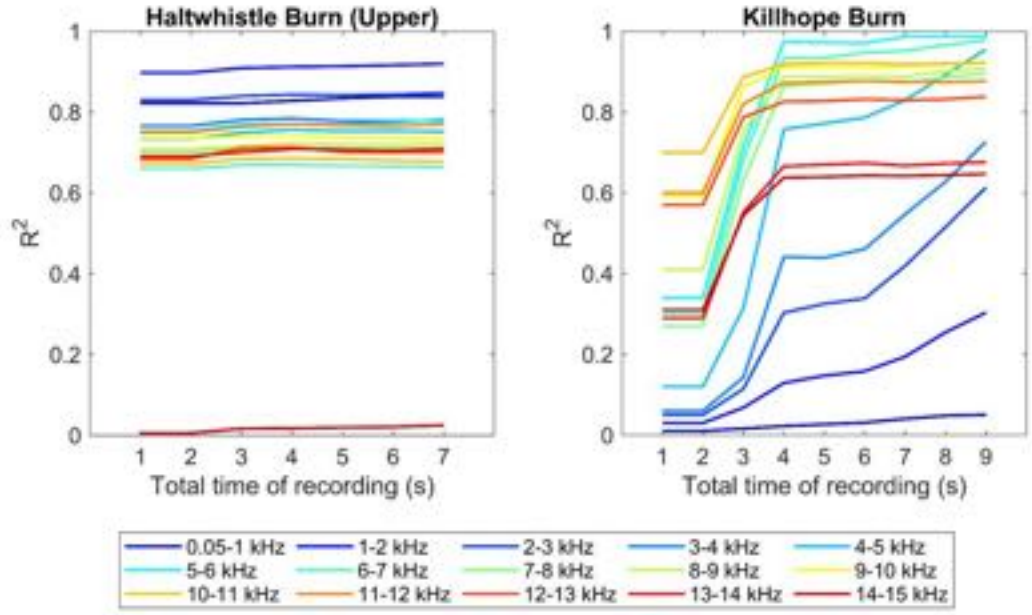

Figure 2.9: Sound data from Haltwhistle and Killhope filtered through the LMF using different total recording times and its affect on the stage/ sound relationship R^2 value. Haltwhistle burn uses a logarithmic function to fit to the data, and Killhope uses an exponential function.

is a substantial increase in R^2 in the Killhope data, with R^2 reaching 0.97. After four seconds there is a gradual increase of the fit. The filter is also improving the lower frequencies of the Killhope burn, however, longer recording times would be needed to match the mid-frequencies. This demonstrates that the LMF is effective at reducing the impact of wind noise on our data.

2.3.3 Storm Ciara and Dennis

Figure 2.10 represents February for the study sites located throughout the North East of England. For each site we calculated the median sound value after LMF filtering in bin widths of 1 kHz, plotted these values against river stage, and calculated an R^2 value of a logarithmic and exponential fit. Two fit options are used as some data fits better with an exponential compared to a logarithm. Our aim is to identify whether there is a relationship in the data, regardless of the form, rather than having a prior assumption about what the shape of the relationship should

be. The variations in R^2 values with frequency range are shown in the first column of Figure 2.10. We use all the sound data during February (inclusive of storms) to determine the RSZ that is most likely to be the best region to use going forward. Site D has relatively poor, but consistent correlations throughout the spectrum between 0.05 - 15 kHz. We see that the highest R^2 values occur in the 0.05 - 3 kHz range in 4 out of the 6 rivers (Sites A, C, D and E). The RSZ used subsequently for each of these rivers is the highest R^2 found from fitting a relationship. Two sites have their best relationship with a logarithm, and four with an exponential. The R^2 values can vary across the frequency range in each river, with some being very consistent (Site B), to others being less consistent (Site C).

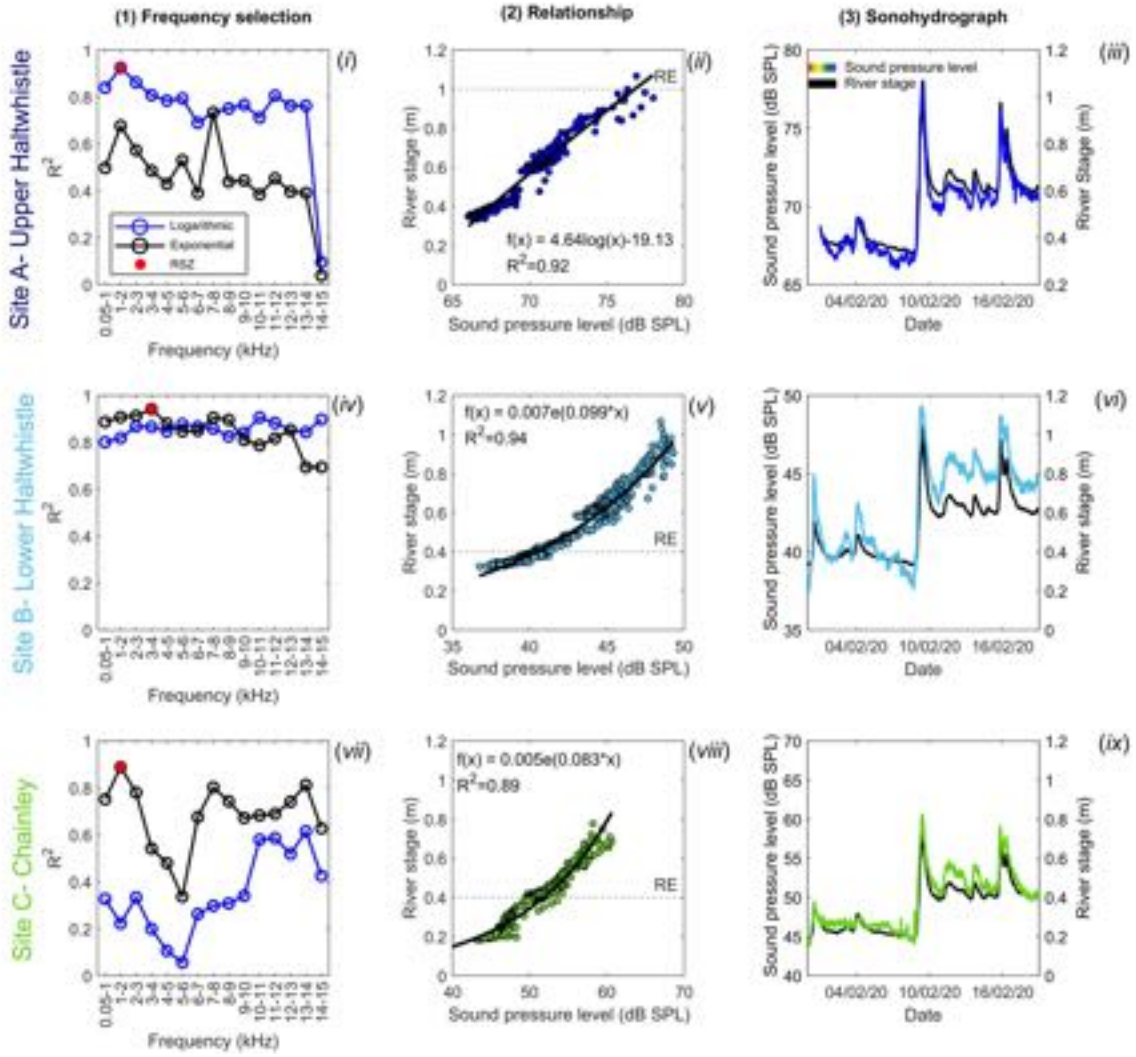

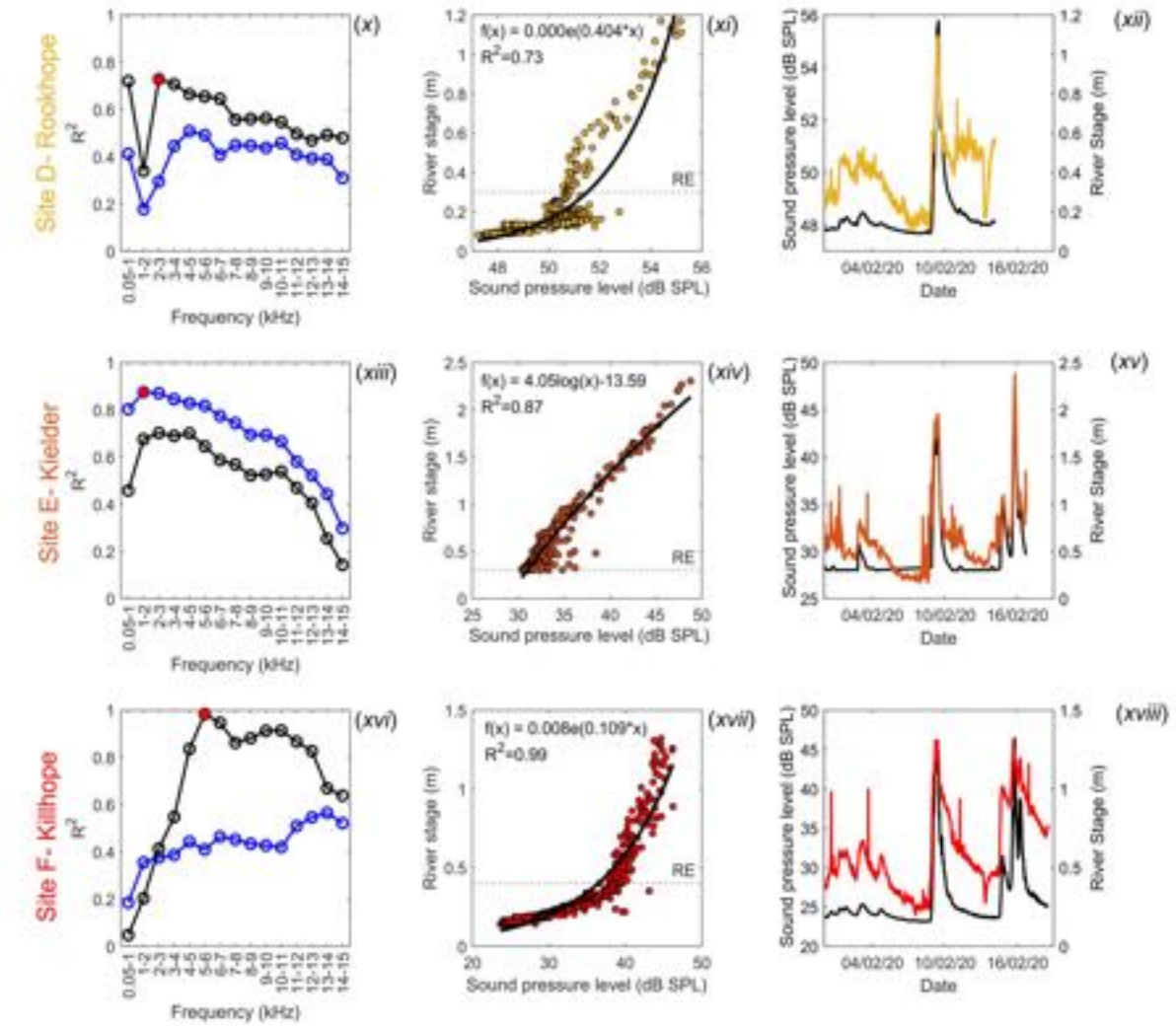

Figure 2.10: Workflow for identifying the best RSZ and obtaining the best river sound/ stage relationship for our 6 sites during Storm Ciara and Dennis. Column 1- the plotting of Storm Ciara/Dennis sound data against stage forming an R^2 value for both a logarithmic and exponential function. Highlighted point is the chosen RSZ for the rest of the figure which is the highest R^2 value. Column 2- The sound data and river stage plotted for the highlighted RSZ. Column 3- The sonohydrograph and hydrograph comparison for the RSZ. Horizontal dashed line shows the highest point of the largest roughness element found in the channel.

With the best RSZ determined, column 2 in Figure 2.10 compares the river stage data against the sound data recorded during February using the chosen bin (RSZ) highlighted in column 1. Each river shows a correlation between recorded sound and river stage, with certain reaches better than others. Sites A, B and C had very good site suitability and have been found to have amongst the highest and most consistent R^2 of between 0.89 - 0.94. In these sites stage modeled from sound is within 0.2 m of the actual stage at the 95% confidence interval. Sites D, E and F were not explicitly chosen for good site suitability but they do all still have a strong relationship, with R^2 of between 0.73 - 0.99. Data below 0.3 m at Site E has been removed since no comparable

river stage data is available.

The highest river level was recorded at Site E at 2.2 m. When the stage reaches 1 m, we see a large increases in SPL with subsequent increases in stage. Bankfull for this reach is at an average depth of 1.5 m, above which the river flows through riparian vegetation. At these levels any riverbed morphology will have been submerged, but other obstacles such as trees start to interact with the flow. Site E is the only site to have experienced significant above bankfull flow during this time period. Flow in other channels was kept within the banks by features such as built up footpaths and flood defences. Site D was located at a weir/ natural waterfall complex, with the shape of the graph perhaps reflecting this, with large variation of SPL below 0.25 m at 47 - 52 dB SPL. At low flow there may be two competing sound sources, the REs and the weir/waterfall. As river stage increases one sound source may become dominant, most likely the waterfall, and a less varied signal emerges.

Column 3 shows the hydrograph compared against the sonohydrograph. From the sonohydrographs we can see that there are a few peaks caused by wind, with some still found in Figure 2.10xv and $xviii$. High gusts of 50 mph, and a sustained wind speed of 30 mph, in combination with low river level are the likely cause. The general shape between the two curves are the same during flooding. There is divergence between the graphs in Figure 2.10xi at lower river levels, before the peak emerging at 0.3 m. Site E does not record stage below 0.3 m, however, we have included our sound data in the sonohydrograph to show that we were still able to measure sound below 0.3 m.

2.3.4 Nash-Sutcliffe

In Figure 2.11, when converted from sound to stage using the sound-stage relationship found in Figure 2.10 we are able to assess the how well the simulated data compares. We can see in all plots that the simulated data plots well against the observed data, with a NSE ranging from 0.80 to 0.95. There are no observable differences on whether a logarithmic or exponential function is used on the resulting NSE. The lower NSE of 0.80 at Kielder is due to the lack of observed data below 0.3 m.

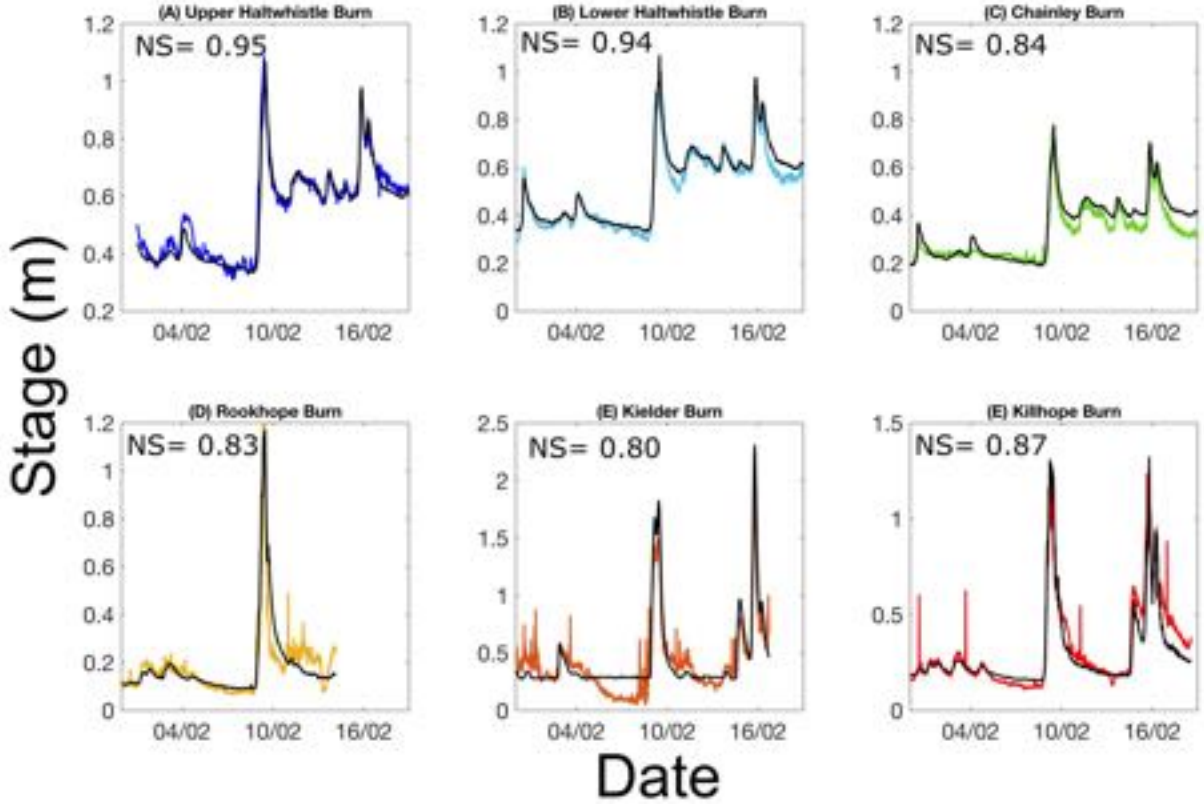

Figure 2.11: Storm Ciara and Dennis observed stage data vs. simulated data from using the sound-stage relationship found in Figure 2.10. Nash-Sutcliffe efficiency given between observed and simulated stage.

2.4 Discussion

We have shown that sound shows a strong correlation with river stage after determining the best frequency range. Consequently we think that it might be possible that given reliable sound measurements and site calibration, a corresponding river stage can be estimated. Producing reliable estimations of river stage from sound requires consideration of how the river sound can be isolated from ambient noise and how sound is produced by a river. Although this is preliminary work, it has shown promising results, albeit with requiring post processing at this stage.

2.4.1 Controls on sound generation

In order to be able to implement monitors at different locations without the need for calibration, we need to be able to predict the form of the stage/SPL relationship. We expect that this will be

a function of factors including the size of the largest obstacle, obstacle density, bankfull level, how close the monitor is to a RE, and if there are any barriers between them which was shown to impact sound propagation (Figure 2.6). Our Washburn dataset leads us to the conclusion that for a site to be suitable for monitoring it beneficial to have a RE within the channel since it produces the loudest sound. The variability in sound along the 500 m section is proposed to be entirely down to the REs presence, prominence or absence. The REs of these reaches impede the river, forcing flow around/ and or over. The river has to exert its energy to overcome these, and some of this is released as sound energy, from the entrapment of air and bursting of bubbles. When observing the photographs at each section (Figure 2.5), we found a correlation between the presence of whitewater and the SPL, with more whitewater being associated with higher SPL values. An entirely featureless reach, such as a culvert, would be less than ideal for this method, unless there was some sort of texture.

In our data we see upticks in the trend of the sound/stage data in Figure 2.10$viii$, xi and $xvii$. The interruptions occur when a RE feature has either been submerged or perhaps when a new RE is activated. Site D, with its weir and waterfall, is an alluvial channel, with boulders of between 0.2 - 0.3 m. We believe that once the boulders have been submerged the loudest sound is generated from the waterfall complex, which at low levels is quieter than the boulder sound. Site F's RE is from stepping within the bedrock channel, with step heights of 0.35 - 0.45 m. Similarly with Site D, once these features are submerged, the trend seen in the data shows an exponential trend in sound being produced, with an increase from 0.5 to 1.4 m, having a SPL range of 40 -45 dB SPL. The trend means that as stage increases, the SPL will increase, but not at the same rate as during lower levels at the RE submergence height. The continued upward trend in data is hypothesised to still be originating from these RE, however from a different mechanism arising from the higher discharges. Turbulence structures created by the changes in flow may be generating different bubble structures for example, with fluctuations in intensity. Standing waves are the most likely cause of new turbulence at higher stages with submerged boulders, with localised increases in Froude number (Comiti and Lenzi, 2006). The preference of a either an exponential or logarithmic function being fitted to the data is hypothesised to be linked to a self limiting part of the system, with a river reaching a point that there are no other sound sources being activated. Sites with an exponential fit have their REs covered at low levels, and do not activate new ones even at above bankfull. Sites with logarithmic functions have either not

had their REs covered or have broken their banks and activated new ones. To further test this hypothesis a river would have to be monitored at both in bank and over bank storm conditions.

In ranking the river reaches in Figure 2.5, sections without any REs still had an increase in SPL between low and high flow. We could conclude that generally there is noise bleeding in from sections up/downstream, or that there are other sound generating elements in a reach. Figure 2.6B has sound generated from an RE being observable 10 m up or downstream of it, which is within our 10 m sampling range. Therefore the change in sound observed at a site with smaller REs (Rank 1), may in fact be affected by REs further away. The design of the river means that there were REs found throughout, and attributing a specific RE for bleeding is difficult. Bank resistance is another possible source of sound, such as from protruding tree roots or alluvial deposits. However, we expect that REs are the main source of sound within a river environment. Our Washburn data suggests that the larger the RE in the river, the greater the SPL at high conditions. Being louder is seen to be beneficial to monitoring, since the river is more likely to be louder than environmental noise and is broadcast over greater distances, meaning monitors can be located further away. Rivers with smaller REs may still be able to be used, with the caveat of monitors perhaps needing to be more sheltered or closer to the river. In general we can say that the larger the RE, the louder it can become, and therefore opens more flexibility in the monitoring regime. Assuming that large obstacles are near permanent fixtures in the river, they remain stable even during high flow events. This stability should make any long term data and future extrapolation of stage far easier than if the environment was constantly shifting. A moving obstacle would have the same effect as moving the microphone (Figure 2.6), changing the sounds that are monitored. Further long term studies will need to be undertaken to determine how long a site's relationship remains stable, however, in Figure 2.7 over the course of 6 months the signal does not change drastically. Over this time, bedload will have been transported, but this movement did not change the signal we observed. In a more dynamic environment, a change in bed configuration may have a significant change in sound.

We can use the Storm Ciara data (Figure 2.10), where data were collected from channels with different REs, to determine whether a RE has any influence on a relationship. The data show that, regardless of RE size, a smooth relationship exists after RE submersion. However, the trend

of that relationship appears to be ultimately controlled by the RE, such as in Figure 2.10$viii$, xi and $xvii$. As all sites had REs, we cannot be sure if these sorts of relationships would still persist at sites without REs. We have shown that when using co-located measurements of sound and stage, we can derive a relationship to predict stage to within 0.2 m at the 95% confidence interval. However, the ideal frequency band used to get stage information and the nature of the relationships are both highly site specific, and so it is not currently feasible to predict the form of that relationship without some paired measurements of sound and stage. But, at all sites SPL has increased with increasing stage. Consequently the relative change in SPL of the river could be used, without calibration, to determine whether the peak of a flood has passed.

2.4.2 RSZ isolation

When trying to determine the best frequency range to use in our research, we defined the best zone as the RSZ. We found the RSZ to change between different rivers within the range 0.05 - 6 kHz, with no set zone for all (Figure 2.10). The RSZ is influenced by how noisy the signals fed into the LMF were. The greatest challenge faced by this study was the isolation of a river sound component from the ambient soundscape. Without the benefit of generating our own signal, we rely on the continuous burbling of a river and if this primary sound source is obscured by other noises we need to actively search for a clean signal, which is why the RSZ is influenced. We expect that the main frequency range for sound production in rivers is in the lower frequencies, < 3 kHz, as we experienced our most consistent R^2 values there, with one site B having a marginally better R^2 at 3 - 4 kHz but only by 0.03 compared to 2 -3 kHz. We do still have very high R^2 values in higher frequencies, and a very good 0.99 for Site F. However, 0.05- 3 kHz is heavily affected by wind noise, which if strong enough may require the switching to higher frequencies as observed at Site F. Potentially Site F may have had a strong relationship in the lower frequencies, but due to persistent wind noise we cannot identify it.

Research using hydrophones is consistent with our RSZ, with surface turbulence having a frequency range of between 500 - 2000 Hz over varying flow regimes (Geay *et al.*, 2017). Tonolla *et al.* (2009) examined how relative submergence of an obstacle influenced the sound, stating that a frequency swap may occur once a relative submergence limit is passed, such as a riffle producing mid-frequency noise during low discharge, changing to a low frequency at high discharge. We

do not see the complete abandonment of a frequency range after a RE is submerged, such as in Figure 2.10xiv and $xvii$, as there is still a relationship with stage present beyond RE submergence. A frequency switch might be causing the change in direction of a relationship once an RE is submerged, but we cannot be certain on this since the low frequency needed to confirm this at our sites that display this behaviour is obscured by the wind. Other sources of sound produced from within a river, such as sediment transport, can exist in the same frequency space as turbulence, around 1 kHz (Krein *et al.*, 2016). But, we have not seen any indication from our data of sudden changes in our trends at high discharges. It might be that our rivers do not generate bedload sound loud enough to overcome the sound of turbulence, but in other rivers it might be a different case. The sound from sediment moving is not strongly transmissible through the water to the air, with acoustic pressure reducing by 2000 times when sound transfers between the two, meaning either there has to be a lot of bedload movement or for the turbulence sound to be lower than it for it to be heard (Leighton, 2012).

We use a frequency range instead of a single frequency to measure river level because as river level increases, changes in the turbulence cause the bubble size to change, altering the frequency of the sound that is produced, the Minnaert resonance. Using a range also adds stability to the data. In the frequency range of 0.05 - 3 kHz, we are in the Goldilocks zone for sound production from surface turbulence, with filtering helping to remove any environmental noise. Within this range, each river has a different most efficient frequency to look at. But, not all rivers have their best efficiency in this region, so the RSZ may need to be altered subject to analysis of previous data. We do however see that the sites chosen for good sound potential, (Sites A and C), have the RSZ in the 0.05 - 3 kHz region. The reason for better stage/ sound relationships being found at higher frequencies when the lower frequencies are polluted, despite sound being produced in the 0 - 3 kHz region, is perhaps down to harmonics. If there is a fundamental frequency of 1.5 kHz, we can expect to see upper harmonics at 3 kHz, 4.5 kHz etc. reducing in SPL magnitude at each jump. Similarly a range of fundamental frequency may have these harmonics. Kumar and Brennen (1991) showed that sound of bubbles bursting in water showed harmonics, with defined peaks occurring at higher frequencies above the fundamental frequency. It is perhaps with harmonics and overtones of the bubbles that we continue to see a river/ sound relationship at higher frequencies.

Having identified that sound production is focussed at < 3 kHz, we need to ensure that we are able to monitor this region as easily as possible. The basics of sound isolation lie in the design and placement of the monitor. Eldwaik and Li (2018) noted that wind noise was notoriously difficult to filter in an outdoor environment, due to its time varying nature and broadband frequency. We show that our LMF can help to reduce noise from the wind (Figure 2.8), but better still would be to not have the noise in the first place, achieved by having a microphone properly shielded from the wind. We recessed our microphones to protect them from the rain and wind, but still had wind noise present meaning without recessing our data may have been more affected. Adding a wind dampening sponge could also be used, having the effect of quietening down the recording, but also baffling the wind (Lin *et al.*, 2014). Even with these preventative measures, wind noise will still be present since it is part of the soundscape. Rivers that are however found in exposed areas, such as moorland that are subject to frequent low level wind, and placement of the monitor then becomes crucial. Placing a monitor as close to the river as possible has two benefits, the likelihood of hearing only the river, and also offering the highest range in sound, with a better resolution of data (Figure 2.6). We see that through acoustic mapping at the River Washburn, when the microphone is moved further away from the river, it begins to quieten. At every point, the SPL measured at high flow is larger than that measured at low flow. SPL decreases upstream and downstream of the RE, with the highest SPL near the RE. The decrease in SPL as you move up/downstream, is less than that observed when heading away from the river due to other sound components being introduced from the river. We do however acknowledge that placement beside a river is not always possible, and find that being within 5 m is advantageous, with being able to move up to 10 m and still having a difference between high and low (Figure 2.6). The limitation of how far a monitor can be placed is when the sound from high and low flow overlap, meaning you cannot monitor changes acoustically anymore. The distance of how far a monitor can be placed is determined by the river itself; larger, more energetic rivers, may be still within a zone of high relationship further than 5 m. Conversely, a smaller, less energetic river may need to have a closer monitor.

2.4.3 Sound as a hydrometric

We are encouraged by the trends between sound and river stage we see in each river that we have monitored. Currently we are able to model with certainty when river level is changing, with all sites in Figure 2.10 showing their flood peaks clearly from sound data. With NSE of between 0.80 and 0.95 we believe this to be a very good fit between observed and simulated data, with a score of 0.50 being described as a good fit. We acknowledge that an absolute measurement is not currently of a standard that could be used for essential management. Consequently we do not see sound as a method for absolute value monitoring, but rather a warning system, capable of detecting flood peaks when they occur or when the river might be starting to flood. If absolute measurements are needed, alternative channel monitoring techniques are available.

Sound varied with stage in all the river reaches that we monitored, and so we are confident that noisy rivers will have a relationship with stage. The more data that is collected and correlated with the river stage, the greater the confidence we have in sound being used as a measurement. On reflection on what makes a good section of river to monitor to measure sound, our Washburn data gave us ideas on sound generation from large obstacles, making lots of noise was shown to be largely correct. Further work will need to be undertaken to allow a SPL/ stage relationship to be predicted from the channel characteristics and without the need for previous stage data.

2.5 Conclusion

At the start of this study, we set out to isolate river sound from a soundscape. The isolation of the river from the soundscape was achieved through the use of the LMF, which is capable of turning a poor, windy relationship, into a promising, predictable signal. A perfect scenario, with no wind or rain noise, is still advantageous, but we have shown that even with these sources that river sound is a monitorable source of river stage information. Future work will need to be undertaken to allow stage measurements to be calculated without the need of calibration. The relationship between sound and a river's stage has been shown to have a strong relationship, with positive correlation seen in every site chosen. River morphology was shown to influence the sound that we were able to measure and find relationships from. Our results suggest that

there is significant geomorphic control on sound production and that sound is unique to each river, like a fingerprint, but it is still able to be monitored after site calibration.

When assessing the usefulness of this technology, it has to be considered in the benefits it may bring to some places that require some sort of monitoring. The technology may not be used to determine an exact river stage, but to show if a flood peak has past or if the river is rising or lowering. Using sound as a method for measuring a river is a novel approach to remotely monitor rivers. Established methods of gathering hydrometric data are not going to be abolished thanks to this, but can work in harmony, with a larger catchment scale network envisioned, made up of several IoT devices that each work in their own specialised sector. Sound can fill the gaps where other hydrometric stations cannot be deployed, either due to infrastructure or cost. With continued research into this field, it may be possible to embed sound monitoring into a network scale approach to river flood management, rather than isolating it to a sole source of information.

Acknowledgements

This work was supported by Durham University, the European Regional Development Fund - Intensive Industrial Innovation programme Grant No.25R17P01847 and Evolto Ltd. We also acknowledge the help of the Environment Agency, from Victoria Crichton and John Lamb, and Yorkshire Water for their allowance to monitor the River Washburn.Contains OS data © Crown copyright and database right 2021. We thank the anonymous reviewer for their invaluable comments and suggestions on the manuscript.

“The River...Whether in winter or summer, spring or autumn, it’s always got its fun and its excitements. When the floods are on in February...

Kenneth Grahame
The Wind in the Willows”

Chapter 3

A sound rating curve: Using sub-aerial sound to calculate river stage

Chapter has been submitted to River Research and Applications.

Osborne, W.A., Hodge, R., Love, G., Hawkin, P., and Hawkin, R. (sumbitted). A sound rating curve: Using sub-aerial sound to calculate river stage. *River Research and Applications*.

Abstract

The sub-aerial sound of a river can be used as a proxy for stage, enabling the monitoring of catchments that may seldom be studied with traditional techniques. Our previous work has shown that the relationship between sound and stage is dependent on the number and size of obstacles in the channel, and cannot easily be predicted. Previously, we calibrated relationships between sound and stage using data sets with thousands of paired measurements. However, collecting so many stage measurements is generally not feasible, and defeats the point of developing an alternative method for measuring stage. The aim of this paper is to determine the minimum number of paired stage and sound measurements that are needed to produce a ratings curve that will give a robust prediction of stage from sound. We use sound-stage measurements from the Haltwhistle Burn, Northumberland and Killhope Burn, County Durham, during the 2020 Storms Ciara and Dennis as our data set. We find that as the number of points used to generate a rating curve increases, from 3 to 7, then the relationship formed becomes more robust. However, adding a condition that there has to be a minimum stage range between all points used is more important than the number of points. We recommend that sound-stage ratings curves are produced from a minimum of 6 pairs of sound-stage points, and/or data that covers a 0.5 m variation in stage.

3.1 Introduction

Directly measuring a stream characteristic, such as stream discharge, is challenging. Instead, indirect methods are often used to calculate them (Ocio *et al.*, 2017). Osborne *et al.* (2021) found that the sub-aerial sound produced by a river can be related to its stage. That was achieved through the continual simultaneous measuring of stage and sound, with stage being continuously monitored with pressure transducers. We found that the relationship between the sound and stage could be approximated by a log or exponential relationship, which could be used to predict stage at times when stage was not being measured directly. But, in order for this technique to be widely applied, we need to establish how to implement it in locations without continual independent stage gauging. An alternative way of measuring stage is to measure stage manually. Without the continual stage measurements to compare sound against, we address the question of whether a relationship can be formed from limited concurrent sound-stage measurements to form a rating style curve. Developing a sound-stage rating curve would enable sound monitor calibration without the need of instream infrastructure such as stilling wells. In this paper we will be testing whether a sound-stage ratings curve can be established and examine the best practices in doing so in regards to the minimum number of points required.

Knowing the uncertainties around the production of a ratings curve is essential for hydrometry and water resource management, and they are broken into three classes: natural, knowledge and data uncertainties (Jalbert *et al.*, 2011). A natural uncertainty is the understanding that some processes in nature are random, such as turbulent flow dynamics, the vegetation changing seasonally or the river freezes (Di Baldassarre and Claps, 2011). A knowledge based uncertainty is that there are processes occurring that you are unaware of, such as backwater or hysteresis effects (McMillan and Westerberg, 2015). Finally, data uncertainty is how accurate your measurements taken are and if they are consistent over time (Jalbert *et al.*, 2011). A ratings curve boils down to drawing a smooth curve between points, but depends on what those points are, and how accurate they are (Herschy, 2008). Rating curves are typically built up over years of monitoring, with a back catalogue of stream flow measurements helping to reduce all the classes of uncertainties. When developing a curve for an entirely new field location, it was shown by Pool and Seibert (2021) that sample periods of between 1 and 6 months can produce a robust curve. Alternatively, taking several point measurements during peak flow events can produce a valid ratings curve

(Perrin *et al.*, 2007). Having a field campaign to gather as much data over an event can be used to create a ratings curve in otherwise data scarce environments, for example going out during a storm event (Pool and Seibert, 2021). This suggests that with careful design, it is possible to develop a rating curve with a small number of points.

A ratings curve is only as reliable as the data that it is developed from. A ratings curve's uncertainties may become more prevalent and amplified after it is extrapolated beyond the last data point (Di Baldassarre and Claps, 2011; Pedersen and Rüther, 2016). The ramifications of uncertainties are dependent on how the data is used by the end user, with a potential of great damage and cost if improperly used, such as for stream flow estimations (Petersen-Øverleir and Reitan, 2009). Di Baldassarre and Montanari (2009) found that when extrapolated beyond the maximum measured value, that at higher and higher discharges the extrapolation uncertainty greatly increased, with a 14% error on stream flow discharge. Quantifying or excluding uncertainty therefore needs to be taken into account to avoid increased costs or incorrect decisions being made (Westerberg *et al.*, 2020).

3.2 Method

3.2.1 Sound rating curve

To determine the minimum number of concurrent sound-stage measurements that are necessary to produce a robust sound-stage ratings curve, we use our data set from the 2020 Storm Ciara, from the Haltwhistle Burn, Northumberland (gravel bedded river, with a channel width of 19.9 m and bankfull depth of 1.1 m) and Killhope Burn, County Durham (bedrock river, with a channel width of 8.7 m and bankfull depth of 0.8 m). The data set has over 1000 sound-stage measurements over a flood event in which stage rose by over 1 m at both locations, during a 1 in 10 year flood event. Stage data was measured in stream using a TD-Diver pressure transducer at the Haltwhistle Burn and stage data was acquired from the Environment Agency pressure transducer at Killhope. Sound data was collected at both sites using a custom built Raspberry Pi operated sound monitor, using an omnidirectional microphone. Sound data is filtered using

the lowest median filter, which uses a fast Fourier transform to convert the sound data into the frequency domain (Osborne *et al.*, 2021). The filter removes any extraneous noise, such as wind, and enables the rivers' sound to be measured in decibels of sound pressure level (dB SPL) within a given frequency range. Osborne *et al.* (2021) found that sound at certain frequencies correlates best with river stage, and from that study the frequency range used in this study are 1 - 2 kHz for Haltwhistle and 5 - 6 kHz for Killhope. Stage and sound data were collected at 15 minute intervals.

To identify what combination of sound-stage measurements are needed as a field campaign style calibration, we subsample the complete sound-stage data sets from the rivers. We fit rating curves to subsamples containing between 3 and 7 pairs of points. We use two approaches to sample the points: random sampling and sampling such that there was a proscribed minimum difference in stage between the minimum and maximum recorded stage, which we varied between 0.1 and 0.5 m. We do not test higher than a 0.5 m range, as we want a method that could be implemented using manual stage measurements, and realistically during floods there shouldn't be anyone within or near the river. Each combination of number of points and sampling strategy is repeated 100 times, and a curve fit to each set of points. We compare these curves to the curve produced when all sound-stage measurements are used with a 95% confidence interval, which represents our best prediction of the actual relationship between stage and sound. The fits to all data have an R^2 of 0.92 for Hatlwhistle and 0.99 for Killhope (Figure 3.1). Osborne *et al.* (2021) found that for the Haltwhistle Burn, a logarithmic function formed the best relationship and for the Killhope an exponential fit. The different fits is presumed to be a result of the roughness element sizing in each. Therefore, each data set is fitted with their respective curve. We further compare the resulting equations by producing a sonohydrograph (a hydrograph produced from sound), from the equations and the entire time series of sound data. To compare between the different sonohydrographs, the peak stage is taken from each sonohydrograph and plotted in a box plot to show the range of peak stages produced and how that compares to the actual recorded peak stage.

We define a robust ratings curve as one which meets the following criteria: (1) As sound increases, stage increases; (2) There is a proportional increase in stage with sound, i.e. stage does not increase by 1 m over only 1 dB SPL and (3) the curve has to have reasonable ends, such as stage is not measured higher than could be generated, e.g. a small stream having a stage of over 2 m.

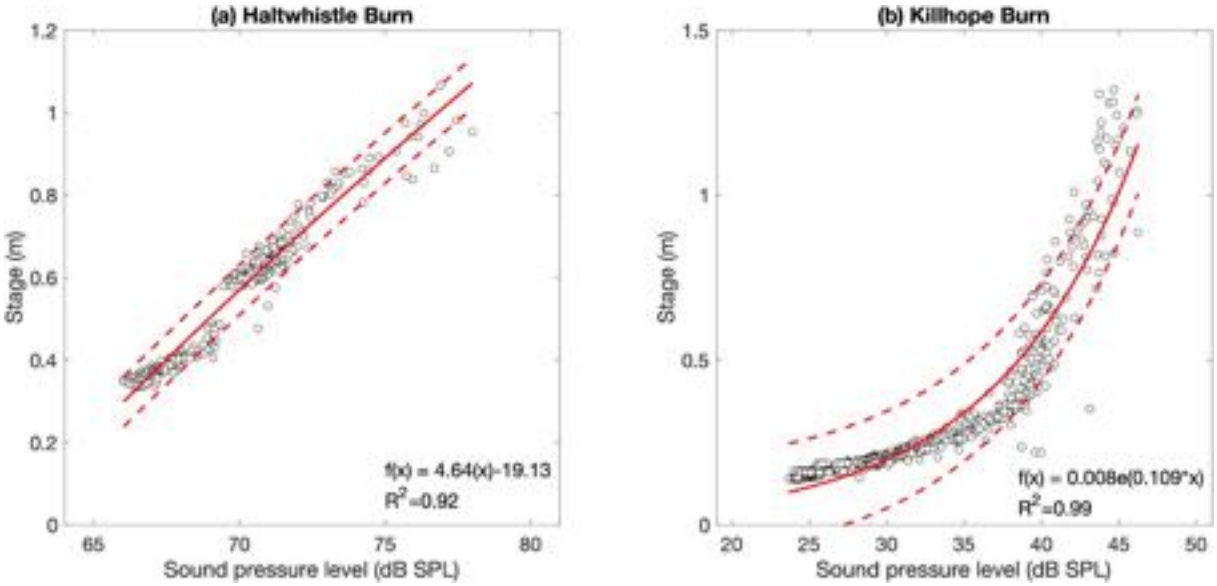

Figure 3.1: Sound-stage ratings curves for the Haltwhistle and Killhope Burn during Storm Ciara and Dennis. Red curve is the relationship formed from the sound-stage measurements with the dashed red lines being the 95% confidence interval.

3.3 Results

3.3.1 Sound-stage curve

Sound-stage curves for 100 runs were generated from the Haltwhistle and Killhope Burn data set as shown in Figure 3.2 and 3.3. Sampling only three data points at random and fitting a curve (Figure 3.2.a and 3.3.a) produces many curves which greatly differ from the red curve, including scenarios in which stage rises and sound falls. These lines couldn't be correct given what is known about how sound and stage interact. The unfeasible rating curves, ones that are beyond the confidence interval from the red curve, may be generated from three very close or identical sound-stage measurements. Increasing the number of data points used in the model runs (Figure 3.2.a-e and Figure 3.3.a-e), without any minimum range, begins to reduce the number of lines that are unfeasible, from 22 to 14 at Haltwhistle and 89 to 52 at Killhope. The number of curves that are falling out of the confidence interval are still high, especially for Killhope, giving a near 1 in 2 chance of the curve being unfeasible even with seven points being used.

Once the condition of needing a minimum range between values is applied, then nearly all the

Haltwhistle rating curves are within the 95% confidence of the entire data set value curve. When the minimum range between values is set at 0.5 m and 7 data points are used at Haltwhistle, both the spread is reduced and the number of unfeasible lines is reduced to 8. However, at Killhope there are still lines that fall outwith the 95% confidence interval. When curves are fitted to only three points at Haltwhistle and Killhope, but there is a minimum range of values set at 0.5 m, there is still an improvement compared to curves fitted to three points selected at random. Even though the curves are beyond the 95% confidence interval, they are still close, and within a 90% confidence interval.

3.3.2 Sonohydrographs

Reconstructing river stage from sound recordings using the sound-stage curve constructed from relationships found previously are shown as sonohydrographs in Figure 3.4 and 3.5. When compared to the red hydrograph line, which was measured by pressure transducers in the channel, we show that the shape of the sonohydrographs match the hydrographs, with rising and falling limbs. When an unfeasible relationship is used to calculate the sonohydrograph, the resulting sonohydrograph is either reversed or exaggerated beyond what the river's stage was at that time. In Figure 3.4 the range of the river is 0.4 to 1.1 m, so for example a range of between 0.8 to 2.6 m can be described as unfeasible. As the sonohydrographs are derived from the relationships formed in Figure 3.2 and 3.3, they follow the same pattern of improvement with increasing the number of points or increasing the minimum range between values. With the Killhope data set the sonohydrographs are more likely to be exaggerated, due to the use of an exponential function compared to a logarithmic function at Haltwhistle.

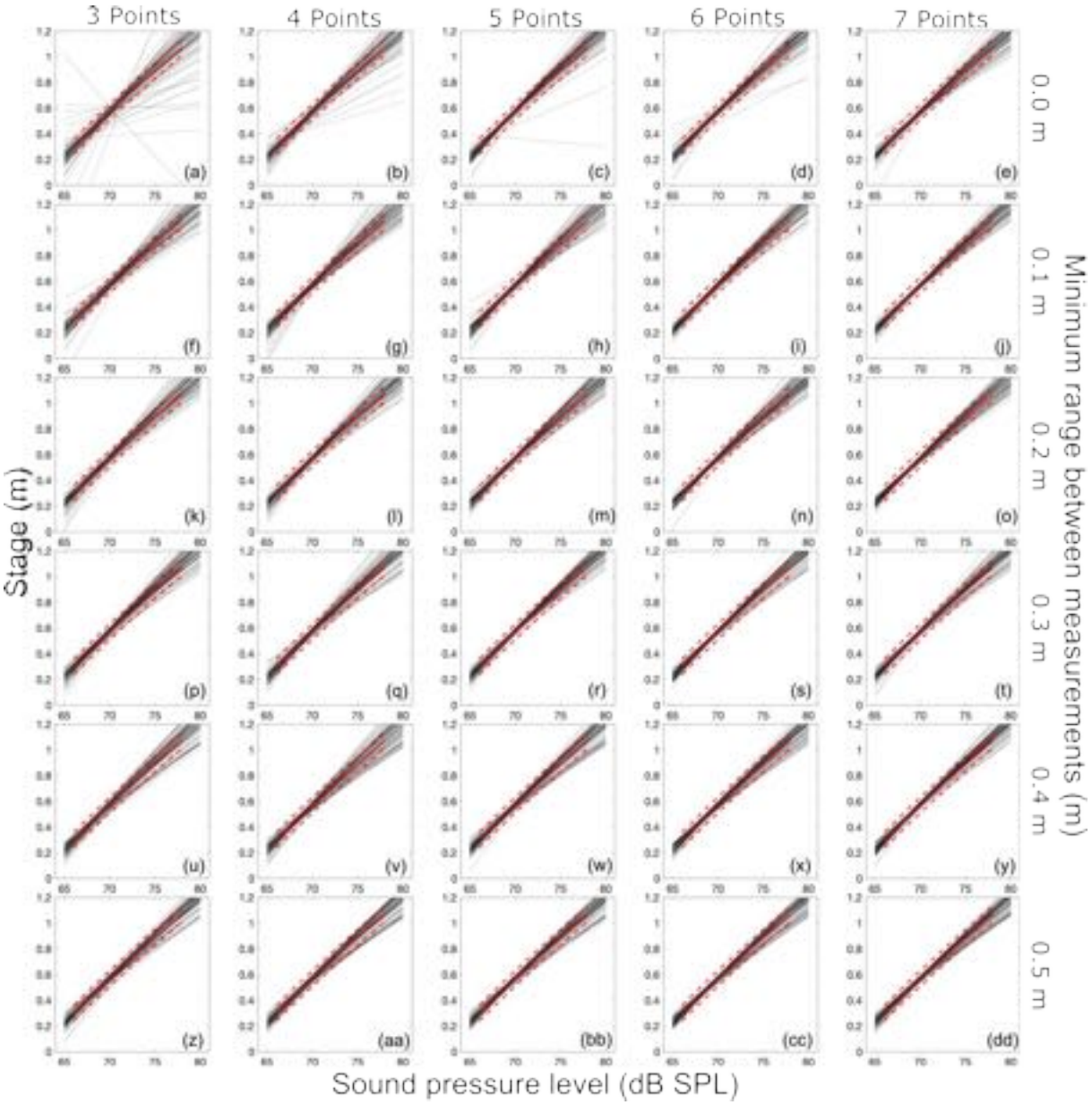

Figure 3.2: Sound-stage ratings curves for the Haltwhistle Burn during Storm Ciara and Dennis. Columns are related to the number of sound-stage measurements used to form a curve and rows are when there has to be a minimum range between stage measurements. Red line- Curve fitted to 1,000 data points, Red dashed line- 95% confidence interval and Grey lines- each model run with set parameters.

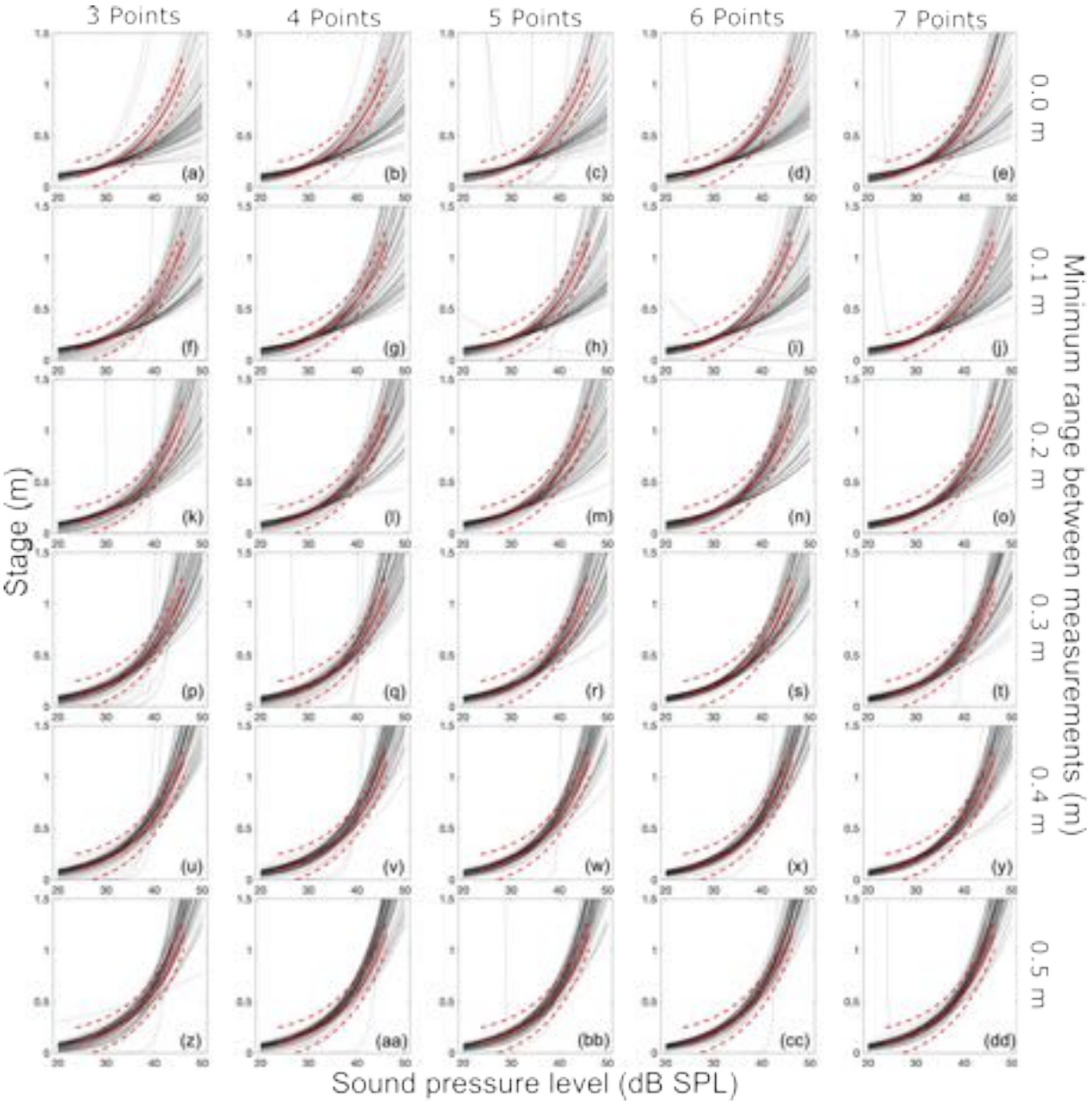

Figure 3.3: Sound-stage ratings curves for the Killhope Burn during Storm Ciara and Dennis. Columns are related to the number of sound-stage measurements used to form a curve and rows are when there has to be a minimum range between stage measurements. Red line- Curve fitted to 1,000 data points, Red dashed line- 95% confidence interval and Grey lines- each model run with set parameters.

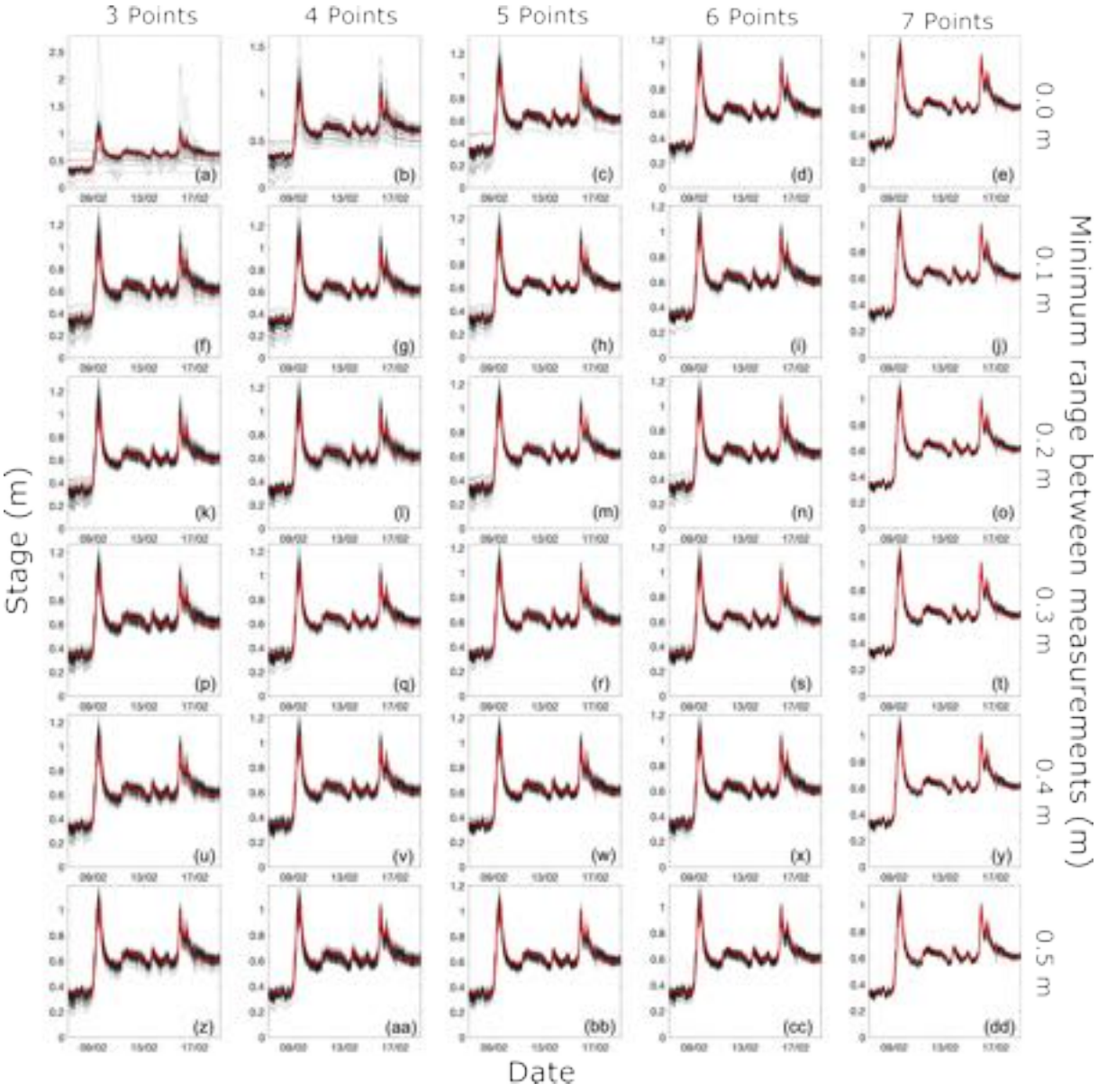

Figure 3.4: Sonohydrographs for the Haltwhistle Burn during Storm Ciara and Dennis. Columns are related to the number of sound-stage measurements used to form a curve and rows are when there has to be a minimum range between stage measurements. Red line- Hydrograph from in stream pressure transducer, and Grey lines- each model run with set parameters.

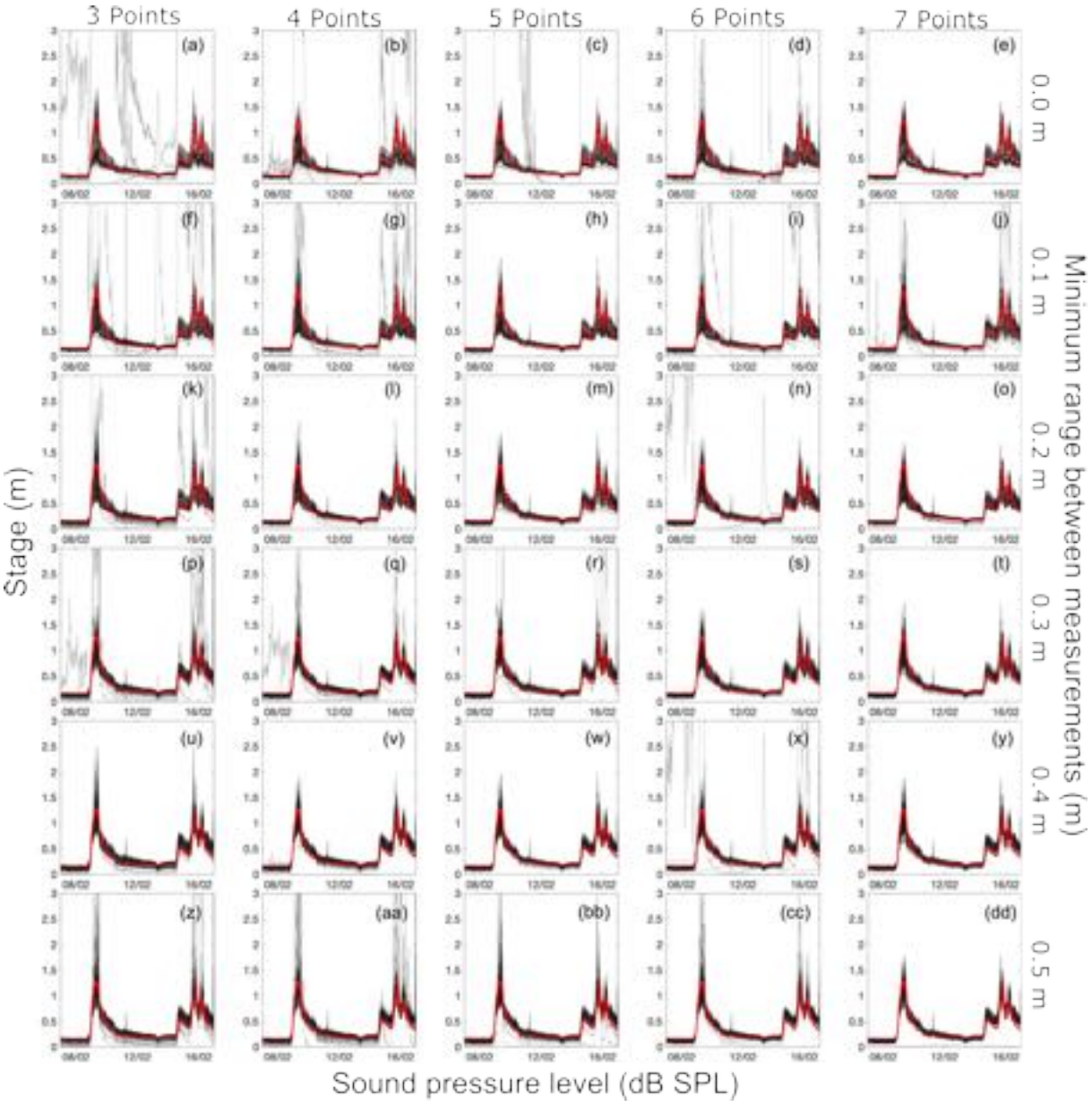

Figure 3.5: Sonohydrographs for the Killhope Burn during Storm Ciara and Dennis. Columns are related to the number of sound-stage measurements used to form a curve and rows are when there has to be a minimum range between stage measurements. Red line- Hydrograph from in stream pressure transducer, and Grey lines- each model run with set parameters.

3.3.3 Nash-Sutcliffe

Converting river sound using the rating curve relationships to a stage value is shown in Figure 3.6 and 3.7. The previous comparison between hydrograph and sonohydrograph shows how well the shapes and peaks match. However to compare how well the observed stage data matches the corresponding calculated stage requires the use of Nash-Sutcliffe efficiency (NSE) to determine if there is a good fit between sound-stage and stage. In Figure 3.6 at Haltwhistle regardless of run, we see a NSE above 0.68. When a minimum difference in stage is implemented or the number of points increased, the NSE increases to a stable 0.88 to 0.95, with the closeness of the boxplots showing broadly NSE are high. Figure 3.7 at Killhope has a poorer NSE, ranging from 0.22 to 0.90, with outliers at 0.17. Increasing the number of points, with no minimum range does little to improve the NSE. Only when the minimum range of stage is implemented do we see an increase in the NSE. With only 3 points at 0.5 m minimum range, the NSE median is 0.80.

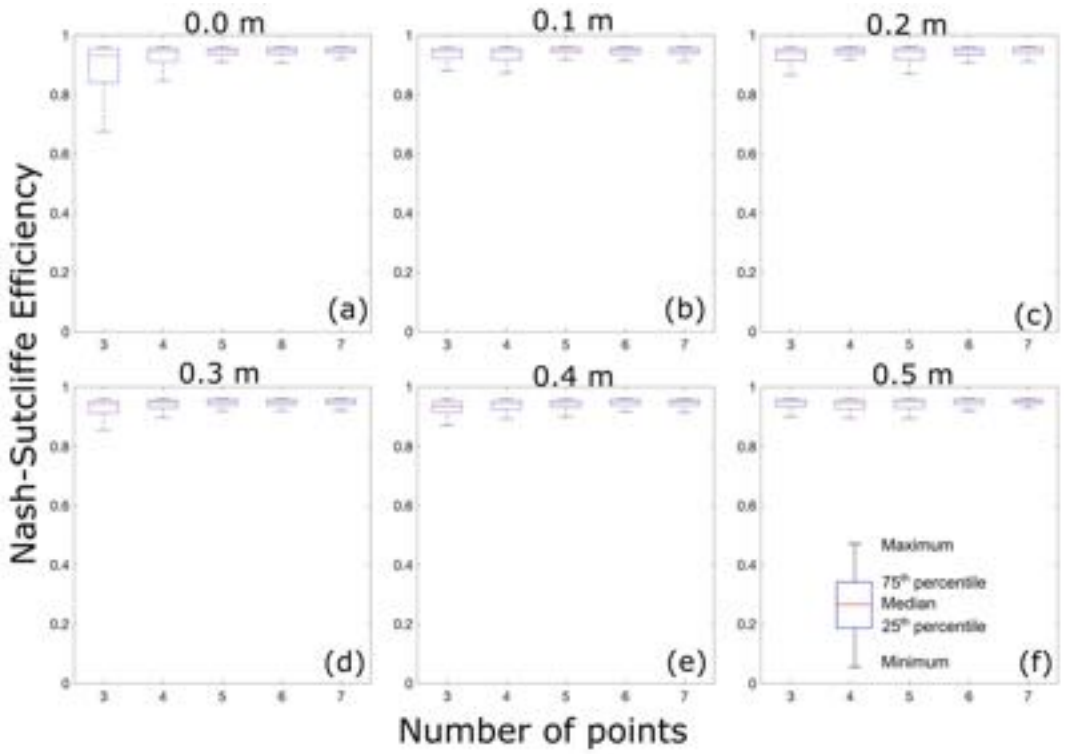

Figure 3.6: Box plots of the Nash-Sutcliffe efficiency of the Haltwhistle Burn calculated from the observed and simulated hydrographs.

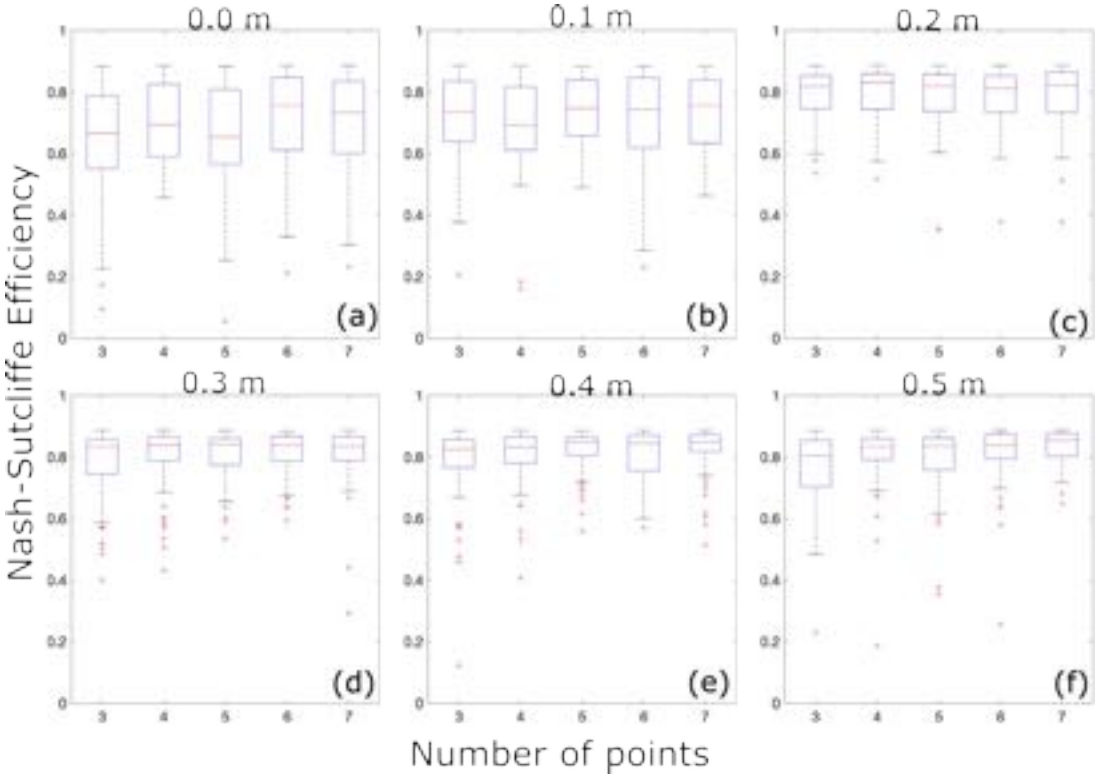

Figure 3.7: Box plots of the Nash-Sutcliffe efficiency of the Killhope Burn calculated from the observed and simulated hydrographs. Outliers shown as red crosses.

3.3.4 Peak stage

When using the peak stage from Storm Ciara we assess how well the relationships formed from only a few data points behave in determining water stage (Figure 3.8 and 3.9). Using the peak stage from the sonohydrographs we use a box-plot to assess how spread out the peak stage data is in relation to the peak stage taken from the hydrograph. When only three points are used in curve fitting at Haltwhistle, the predicted peak stage varies from 0.75 to 1.4 m (with the 25^{th} to 75^{th} percentiles of the predictions being 1.05 to 1.2 m), compared to an actual peak of 1.06 m (Figure 3.8.a). Similarly at Killhope, the predicted peak stage varies from 0.25 to 1.2 m (with the 25^{th} to 75^{th} percentiles of the predictions being 0.52 to 0.8 m), compared to an actual peak of 1.3 m (Figure 3.9.a). However, as the number of points increases and minimum range is introduced, the range of stage at Haltwhistle improves to 0.95 to 1.2 m (with the 25^{th} to 75^{th} percentiles of the predictions being 1.08 to 1.15 m) when 7 points and a minimum range of 0.5 m is used (Figure 3.8.f). At Killhope, the predicted stage range is 0.9 to 1.7 m (with the 25^{th} to 75^{th} percentiles of the predictions being 1.2 to 1.4 m)(Figure 3.9.f). The effect of introducing more data points and a minimum range between values is more apparent at Haltwhistle, in which the range of peak stages narrows as they are introduced. However, even with the no restrictions, the median of the predicted peak stages is almost always the same as the measured peak stage. Killhope improves more from the conditions placed on point selection, with limited conditions of 3 points and no minimum range producing a median value up to 1 m less than measured.

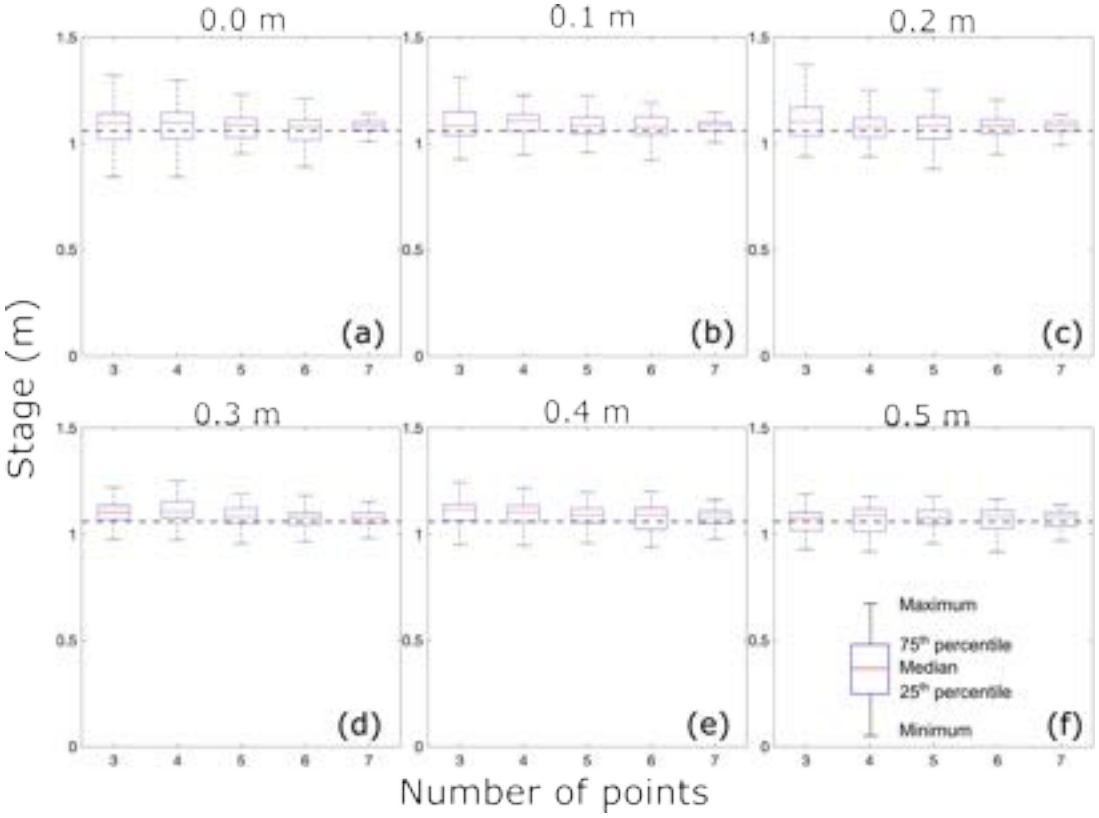

Figure 3.8: Box plots of the peak stage of the Haltwhistle Burn taken from the sonohydrographs using the sound-stage ratings curves. Dashed line- Peak stage recorded from the in stream pressure transducer.

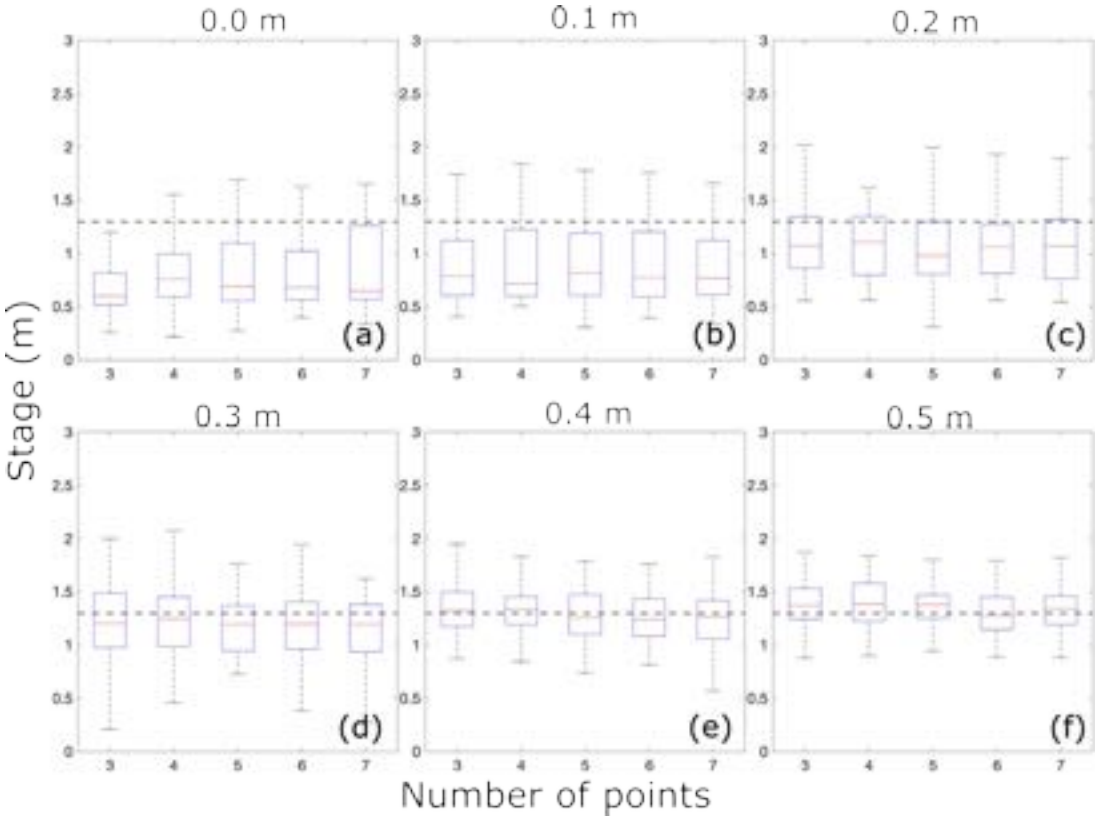

Figure 3.9: Box plots of the peak stage of the Killhope Burn taken from the sonohydrographs using the sound-stage ratings curves. Dashed line- Peak stage recorded from the in stream pressure transducer.

3.4 Discussion

3.4.1 Sound-stage curve

The setting up of a sound-stage monitor comes with the challenge of calculating a stage value from the recorded sound. Figures 3.2 and 3.3 demonstrated that the more concurrent sound-stage values that are recorded, the more likely the relationship generated from them would be reliable. As noted by Perrin *et al.* (2007), several points are all that can be needed to form a robust relationship, as long as those points are taken at the right time. The more data points that are added reduces the chances of errors within the data, as a sound point either higher or lower than anticipated, i.e. 20 dB SPL instead of 10 dB SPL, would skew the relationship, and make the resulting stage calculated higher or lower. The errors associated with individual depth measurements are small, and therefore there is less need to have lots of depth measurements to smooth out errors in individual data points. Without a conditional range required between values however, the points may all be recorded around the same stage. Having a narrow range of stages is detrimental to the ratings curve as it means that a larger proportion of the rating curve will be extrapolated outside the range of the data. However, if the stage data are manually collected, some extrapolation may be inevitable as the Environment Agency warn against the collection of data during a flood peak based on the grounds of health and safety (Ramsbottom and Whitlow, 2003).

To mitigate errors of the fitted curve, we recommend that at least 6 distinct points are taken. When less than 6 points are taken, then the resulting curves can be unreliable (Figures 3.2 and 3.3). Ibeje (2019) suggested that taking random subsamples of existing data can aid in determining uncertainty, meaning our approach in using fewer measurements to identify what is required in our rivers to produce a robust rating curve. If only three points are used then the curve fitting is poorly constrained, and the final curve is unlikely to represent the curve fitted to a larger data set. Only by increasing the number of sound-stage points above 5 do the curves begin to coalesce, getting closer to the entire data set curve, with the best improvement from 3 to 4 points. Five or more randomly sampled points are already likely to have a wide range of stage values. Kiang *et al.* (2018) found that extrapolating data beyond the largest measured stage was always going to cause uncertainty, and recommended to use a range when extrapolating using

stage to calculate discharge. To reduce the uncertainty caused by extrapolation, we examined what happens when a condition on the sound-stage measurements is used, with a minimum difference of stage between values. Figures 3.2 and 3.3 show that when a condition is added, even with three data points, the number of unreliable curves reduces. The sound produced by a river is proportional to its stage, so with three points at low and higher stages, means the extrapolation between them is possible. For Storm Ciara, the predicted range of peak stage for Haltwhistle was calculated at 0.95 -1.2 m and Killhope at 0.9 - 1.7 m (Figure 3.8 and 3.9). The narrower range of Haltwhistle indicates that the relationships being formed have lower uncertainty, with the larger range from Killhope indicating that there are other factors influencing the relationship.

3.4.2 Sonohydrographs

The intended purpose of a sound-stage ratings curve is to derive a stage value from sound, for example in order for it to be used in flood management or real-time forecasting. Figures 3.4 and 3.5 show the hydrographs and the sonohydrographs for Storms Ciara and Dennis. The shape of the sonohydrographs begin to closely match that of the hydrographs once either more points or a conditional range is implemented on the data. From an unreliable rating curve, the timings and shape of the sonohydrograph will still be known, but actual stage values would be highly inaccurate. There is a difference between if a logarithmic function or an exponential is required to fit the data and how it affects the ratings curve. An exponential by definition experiences more rapid increase in stage as sound increases, and for Killhope (Figure 3.5) predicted maximum stage values were reaching upwards of 40 m. Exponential curves are rarely found in stage-discharge rating curves, but are more common in sediment rating curves (Vaughan *et al.*, 2017). Even when more points are chosen and a condition applied, there are still sonohydrographs that exhibit unrealistic stages. If a rating curve predicts stages above what could ever be expected then the data should be examined to see if there are any data points which are erroneous. If a logarithmic function is being used to form a curve, then, as shown in Figure 3.4, once more points or a condition are applied, the resulting sonohydrographs are comparable to that of the hydrograph.

When comparing between observed and calculated stage it becomes clear again that an exponential relationship behaves poorly opposed to a logarithmic function (Figure 3.6 and 3.7). A good fit (> 0.5 NSE), is found with all logarithmic function runs, regardless of minimum range or number of points used. That shows that with minimal data points, the resulting sound-stage relationship is of a good fit. However, when the exponential function is used with Killhope there is greater spread of NSEs and therefore when used to convert sound to stage will provide unreliable results. The poorer fit may be due to the spread of sound-stage measurements at lower stages due to the wind. Increasing the number of points and a minimum range improves the NSE, but still can lead to outliers, leading to a poor fit.

To understand how well a ratings curve is working, comparing the peak stage calculated and measured allows us to assess if curves are more or less prone to inaccuracy dependent on the data value used. The box plot of predicted peak stage straddles the actual peak stage measured (Figure 3.8). As more points are added, the box plot reduces in size, meaning more of the calculated values are falling with the actual peak stage. The rating curves used seem to be overestimating the peak stage more than underestimating. The overestimating may be due to fewer sound-stage measurements near the peak of the flood, so curves are fitted to data from lower stages. Noting that the correlation between stage and SPL is weakest in the lower stages. If these rating curves were to be used for flood monitoring then the possibility of predictions only being 5 cm over the actual peak stage is encouraging. Figure 3.9 shows the need to have a range of stage measurements, as when data from a limited range of stages is used to produce a curve, the peak stages are around 1 m lower than observed at Killhope. When a minimum stage range is used, the resulting peak stages are close to the observed peak.

3.4.3 Implementation

For our method of stage gauging, a stage value is required to compare against sound and there are alternative methods to calculate stage without the need for in stream measuring. We suggest that in addition to taking several sound-stage measurements, that they are taken across a flood peak where possible, with a minimum difference in stage of 0.5 m between them. It may be beneficial to use data from multiple flood events to account for the uncertainty caused by changes in channel morphology during an event. To apply this method to other rivers, the difference

between the minimum stage range will be dictated by the expected stage of a river during a flood. For example, if a river is expected to flood upwards of 2 m, then having a sound-stage measurement of nearer the expected peak stage is advantageous to reduce extrapolating. For both the Haltwhistle and Killhope their bankfull depths were around 1 m, therefore a minimum stage range of 0.5 m was adequate. Our analysis was based upon previous work, allowing us to know if the data would be best fitted by a logarithmic or exponential relationship. In a new location, we recommend the use of a logarithmic function at first to generate a ratings curve, with the proviso that when further data points are added, then the user might want to also try an exponential fit. Having a baseline relationship, using stages below a peak will at least enable a range of peak stages to be produced, which can then be further added to during a flood peak. Extrapolation of a ratings curve beyond the last value is difficult, and many approaches rely upon the use of hydraulic equations, until bankfull is reached, at which point the hydraulics of a river changes. Without reaching bankfull, the ratings curves we have determined may reach the same boundary. Therefore the extrapolation of a sound-stage ratings curve is limited by bankfull stage. The Environment Agency plot their ratings curves in 2 - 5 year time periods to determine if there has been any change and we therefore recommend the same approach if sound monitoring is used over more than one season.

3.5 Conclusion

The aim of this paper was to determine the minimum number of concurrent sound-stage points to form a rating curve. We have shown that by having more than three measured points, with at least 0.5 m difference in stage, then a ratings curve can be generated. However, adding more sound-stage measurements is beneficial at reducing any uncertainty around the collection of the data and any changes of condition over time. It is hoped that by using a sound-stage ratings curve that sound monitoring for flood management could be implemented without the need to have a coupled stage monitor at all times. We see the method for generating a sound-stage curve as a robust method which can easily be implemented.

Acknowledgements

This work was supported by Durham University, the European Regional Development Fund - Intensive Industrial Innovation programme Grant No.25R17P01847 and Evolto Ltd. We also acknowledge the help of the Environment Agency, from Victoria Crichton and John Lamb.

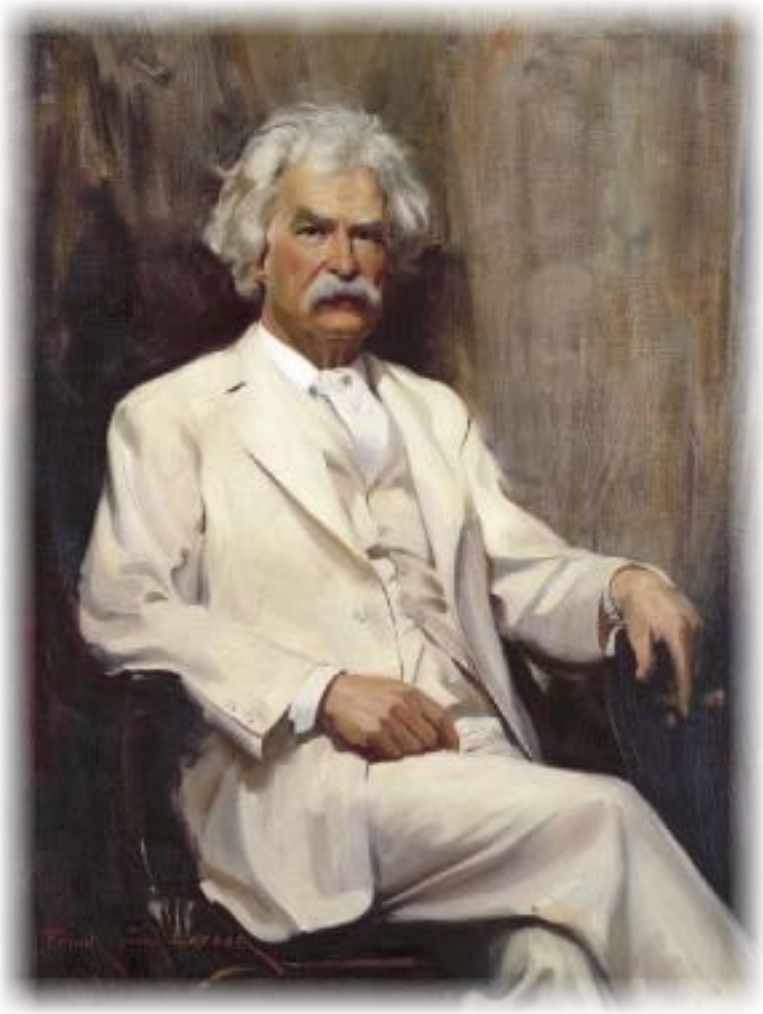

> “The river has great wisdom and whispers its secrets to the hearts of men.”
>
> Mark Twain

Chapter 4

The influence of in-channel obstacles on river sound

Chapter has been published in Water Resources Research.

Expanded work is highlighted when not found in the original published paper.

Osborne, W.A., Hodge, R., Love, G., Hawkin, P., and Hawkin, R. (2022). The influence of in-channel obstacles on river sound. *Water Resource Research*. doi: 10.1029/2021WR031567

Abstract

The sound of a river can change from a babbling brook to a thunderous torrent, and we have previously shown that there is the potential to predict river stage from the river's sub-aerial sound. Here we examined how alterations in channel configuration can change the relationship between stage and sound pressure level using a white water course to simulate a real world scale channel. By using blocks as roughness elements (RE) we were able to customise the course's obstacles, creating towers of different heights and placements. We then ran a varied flow discharge of up to $10\,\mathrm{m}^3\,\mathrm{s}^{-1}$ through. We used data collected from microphones, a hydrophone and cameras to monitor the flow and to understand the processes occurring. In addition to sound processing, we used image analysis to calculate the area of white water on the surface of the water to determine the mechanism for sound production. Our analysis showed the likeliest source of sub-aerial sound is from white water being produced from the flow's interaction with the REs, with the relationship between white water value and sound relationship having an R^2 between 0.35 and 0.82.. In terms of influence on sound, we found that the height of the REs is more important than their spatial distribution, with the taller the RE, the better the logarithmic relationship between sound and stage. We suggest that monitoring in a natural setting will work best in the places with the tallest obstacles and that the quality of the sound-stage relationship is dependent on RE height.

4.1 Introduction

Rivers can be variable, noisy environments, able to change from a babbling brook to a thunderous torrent. There is evidence to suggest that the flow controls the range of sounds produced by a river, including seismic (ground vibrations), hydroacoustic (underwater) ,infrasonic (sub-aerially at < 20 Hz) and human-audible acoustics (sub-aerially at 20 Hz - 20 kHz) (Manasseh *et al.*, 2006; Morse *et al.*, 2007; Ronan *et al.*, 2017; Schmandt *et al.*, 2017; Osborne *et al.*, 2021). Human-audible sound produced sub-aerially has been shown to correlate with a river's stage, providing a non-intrusive way to monitor a river (Osborne *et al.*, 2021). Using sub-aerial sound to monitor a river's stage is potentially a non-intrusive method of measuring, such as for flood monitoring, when other methods such as pressure transducers or ultrasonic depth monitors aren't safe to deploy. This method could be especially useful in the seldom monitored headwater catchments, which make up 70 - 80% of total catchment area, whose morphology is characterised by rough beds (Gomi *et al.*, 2002). The sound of the river is determined by the interaction of the flow with the bed topography. Our previous work has demonstrated the role of roughness elements (RE) in producing noise, but we do not know how factors such as RE size and spacing affect noise production. To determine the effect of the bed topography on the flow, and the sound it produces, we designed an experiment using a white water course (WWC), allowing the channel bed to be altered through the addition of REs. Our findings will aid future work using sound to monitor stage as it will identify sections of a river that will provide the best chances of finding a sound-stage relationship. We turn to two areas of hydraulics that introduce aspects of how the bed topography of a river can influence its flow; flow resistance and white water generation.

Flow resistance is formed by features within a channel that oppose the flow, generating turbulence, and depends on channel topography and bed texture and discharge (Venditti, 2013). Understanding flow resistance is critical for applications including flood prediction/ management and channel design, such as in civil engineering (Ferguson, 2010; Powell, 2014). The flow resistance of a river channel is likely to be linked to the production of sub-aerial sound. We collected audio data from a range of different rivers, and we found that REs have an effect on the sound produced sub-aerially and suggested that they are the probable cause for sound production in a river (Osborne *et al.*, 2021). To compare between different rivers, relative submergence is used as a way to determine the scale of an object relative to the flow depth (Weichert *et al.*, 2006). Herbich

and Shulits (1964) suggested that resistance at flow depths greater than RE height is related to the pattern and spacing of the REs. Bathurst (1978) noted that unless all the taller REs protrude from the flow, then there will be spatial differences in the flow regime, with the wake from one RE affecting the flow around downstream REs. Water will be forced around an obstacle (producing buffer waves) when relative submergence is low, but as stage increases, the water's path will begin to change and will eventually overtop the RE (producing recirculating waves) (Kean and Smith, 2006). Therefore sound may be dependent on how closely REs are spaced and if they protrude from the flow. We take account in our experiment that the size, distribution and state of protrusion of the obstacles can have an effect on the flow resistance.

Sub-aerial sound is primarily generated from the surface of the water, and is formed from turbulent structures such as standing waves and eddy currents forming white water (Bolghasi *et al.*, 2017b). Air becomes trapped within the water, known as self-aeration, when there are flow discontinuities generating white water locally, which is both air trapped within the water, and air coated in water (Rodi, 2010; Chanson, 2012). In flume studies of supercritical flow, where flow was forced to diverge or overtop a structure, air cavities built and led to "loud noises" being formed (Chanson and Toombes, 1998). In terms of energy, we can think of this as a turbulent energy cascade, in which the initial large scale eddies break down into progressively smaller and smaller eddies until they are small enough that friction removes the remaining energy (Kolmogorov, 1949). In doing so, the bubbles generated from turbulent eddies break up further into smaller, and smaller bubbles (bubble-mass cascade) (Chan *et al.*, 2021). Bubble size and eddy size are intrinsically linked, with large eddies advecting bubbles and small eddies being unable to break them up (Chanson, 2012). Advected bubbles are then released when the shear becomes low enough. Bubbles and sound are linked with the Minnaert resonance, with the larger a bubble, the lower its corresponding frequency, such that a 10 cm bubble radius has a frequency of 32 Hz and a 1 cm radius bubble has a frequency of 326 Hz (Minnaert, 1933; Leighton, 1994). These white waters are drivers of air-water gas exchange, especially in mountain streams, where turbulence and bed roughness means that the gas exchange rate can be 96 times greater than for low-sloped, gentler rivers (Hall *et al.*, 2012; Ulseth *et al.*, 2019). Underwater sound production can be generated from the collision of bedload as sediment is transported downstream (Marineau *et al.*, 2015). However, since there is no mobile bedload in our experiment, then that is not generated. While we can determine the source of the sound, there is no current way of linking

the white water to the sub-aerial sound that is being produced and how it is related with RE size or configuration. Our experiment will examine how the area of white water found on the surface relates to the sub-aerial sound.

Our focus here is with the sub-aerial sound produced by a river and how that is connected with REs. However, in our experiments we also record underwater sound as a basis of comparing if what is observed on the surface is the same as underwater sound. The aims of our paper are to investigate if : (1) there is a link between the sound produced and the height of a RE; (2) layout of REs has any control on sound production and (3) there is a relationship between the white water area and sound pressure level (SPL).

4.2 Methods

Experimental setup

The Tees Barrage International White Water Centre, Stockton-on-Tees was chosen to simulate a real scale river. Figure 4.1 shows photographs of the course when used for sport. The course has substantial advantages over a conventional indoor flume such as removing the need for recirculation pumps which produce noise that would obscure the audio signal. It is at a scale which is comparable to a river, but retains the same control over flow that you get in a flume (Barton *et al.*, 2005). Being at real life scale means our data are comparable to real world river systems. The experiment was run over two consecutive days, 9th - 10th December 2020, on which there were cloudy but settled weather conditions.

The section of the course that we collected data in is $7.5\,\mathrm{m}$ wide, with a slope of 0.005, and is lined with concrete. Within the channel obstacles can be created from RapidBlocs™ which are interlocking, stackable blocks that are able to be attached firmly to the channel bed in different configurations and can quickly be rearranged into new designs. Blocks are 1.0 m x 0.50 m x 0.25 m and are capped with a rounded lid of 1.0 m x 0.50 m x 0.08 m. We used these blocks to alter the channel bed, simulating different REs. Water was run through the course with a discharge up to $10\,\mathrm{m^3\,s^{-1}}$. Within the channel, the water was released using a digitally controlled and

monitored bear trap gate, allowing fine control of $0.1\,\mathrm{m^3\,s^{-1}}$ in discharge and was able to sustain the desired discharge due to the large body of water being held upstream.

Our experiment involved changing the blocks within the channel and then quickly increasing the flow from zero to full discharge, before gradually ramping down the discharge. The course was initially configured for white water sports, with blocks arranged to create alternating runs and hydraulic jumps. We reconfigured the upstream part of the course to remove the obstacles that created the hydraulic jumps, and to minimise the backwater effect of downstream obstacles (Figure 4.1C and D), creating a clear run which was maintained for $50\,\mathrm{m}$. To increase the flow depth in our experimental section we created a pinch point upstream and downstream of the test site, which constrained the channel. The addition of these side blocks allowed a stage above $1\,\mathrm{m}$ to be achieved (Figure 4.2A). Although these blocks are an additional RE in our measurement section, their influence will be consistent through all runs.

To monitor the WWC, 4 microphones were setup in an array around and above the channel (Figure 4.2B). In addition to sub-aerial recording, a hydrophone was placed within the channel to record underwater sound and two pressure transducers (TD-Diver) were attached to the floor

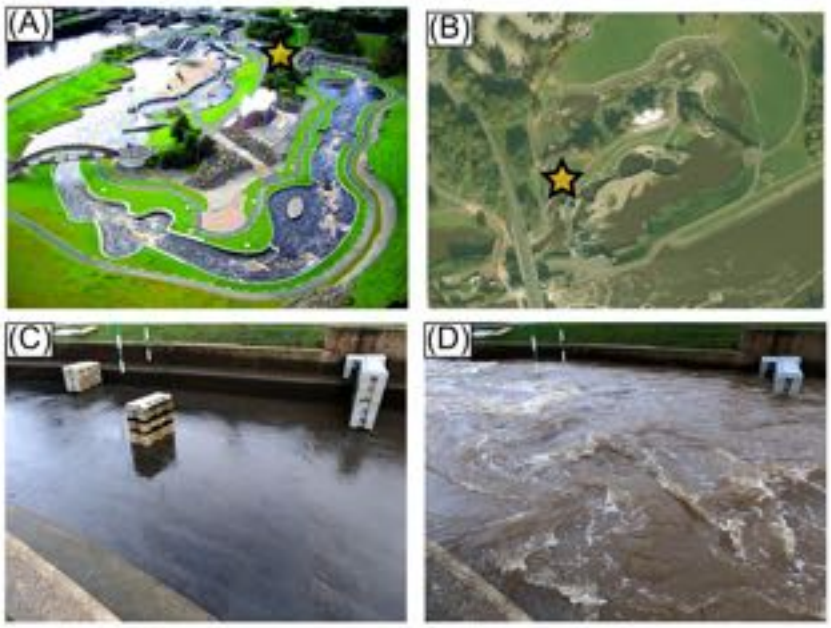

Figure 4.1: Star represents the area chosen for the study. (a) Aerial image of the course during full flow, (b) aerial image of course during no flow, (c) section of course used during no flow and (d) section of course during high flow. Image (a) is produced with permission of the Tees Barrage International White Water Centre and (b) OS data Crown copyright.

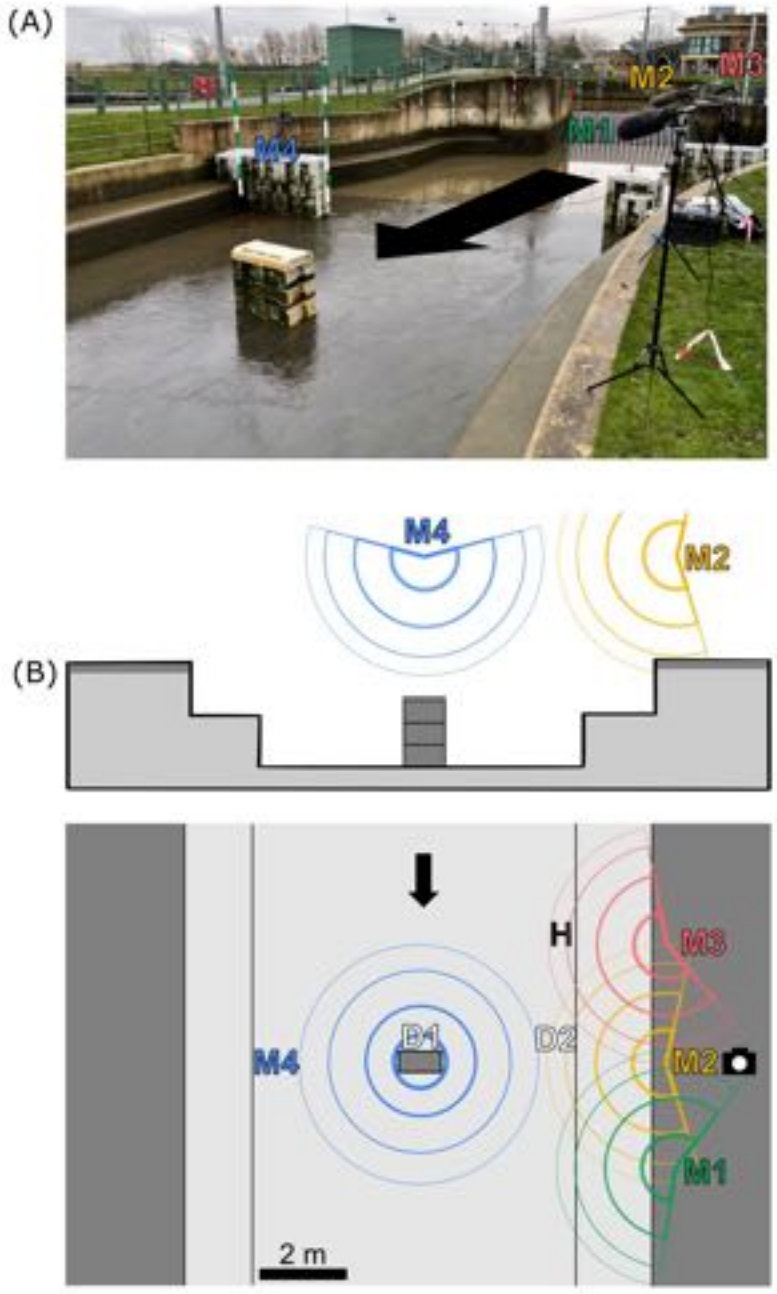

Figure 4.2: A- Photograph of the white water course during experimental run F3 showing the proximity to the bear trap gate. B- Schematic of the experimental setup and locations of equipment. Microphones:Downstream (M1), central (M2), upstream (M3) and over-channel (M4). Hydrophone (H), camera, and central diver (D1) and bank diver (D2). The pickup angle of the microphones is shown with the concentric circles.

in the centre (D1) and the bank (D2) to monitor stage. One microphone was suspended above the centre point (M4) of the test site from guide wires, with the other three located downstream (M1), centrally (M2), and upstream (M3). All the microphones were directed to the centre of the test site. The microphones were covered with a windshield primarily to prevent water splashes from hitting them, but also to reduce any wind noise. Wind was however limited during the experiment at less than 5 mph. We used RØDE NTG2, which is a mid-high level supercardioid microphone, with a rejection of $150°$ to the rear, with a sensitivity of -36 dB re $1\mathrm{v}$/Pascal at 1 kHz. The hydrophone used was an Aquarian H2a, an omnidirectional hydrophone with a sensitivity of -170 dB re $1\mathrm{v}$/Pascal at 1 kHz. Due to the different reference values between water and air, the SPL values between them cannot be directly compared. The hydrophone was shielded from the direct flow of the course by situating it behind a set of blocks upstream of the measurement site. All microphones and the hydrophone were connected to a Zoom F6 field recorder and so could be operated at the same time. For the first two experimental runs the hydrophone was disconnected, therefore no data is presented for these runs. The Zoom F6 recorded each microphone simultaneously at 32-bits at 44.1 kHz in the WAV format. Our sound data is presented in sound pressure level (dB). During each run, a time lapse video was recorded from the bank of the channel near M2 using a GoPro MAX 360 at a frame rate of one per second.

4.2.1 Experimental run

An experimental run typically took 15- 20 minutes including both the increase and decrease in flow, and the rearrangement of the blocks. The blocks were setup in the following ways (Figure 4.3) and hereunto configurations will be referred to by the letter of the configuration, and the number of blocks, i.e. $\mathrm{LF}_{2.2}$ would be blocks with their long face perpendicular to the flow in a side by side arrangement with each side being two blocks tall and LF_{n} refers to all scenarios with a single tower of heights between 1 and 4 blocks. We used configurations of between one and four towers of blocks, and each tower was between one and four blocks tall. The run types are broken into two groups, simple and mixed. In simple runs, all towers had the same height, whereas in mixed runs different towers had different heights. A run started with a dry course, and consisted of a rapid flow release of $10\,\mathrm{m}^3\,\mathrm{s}^{-1}$, followed by a period of time to allow the flow

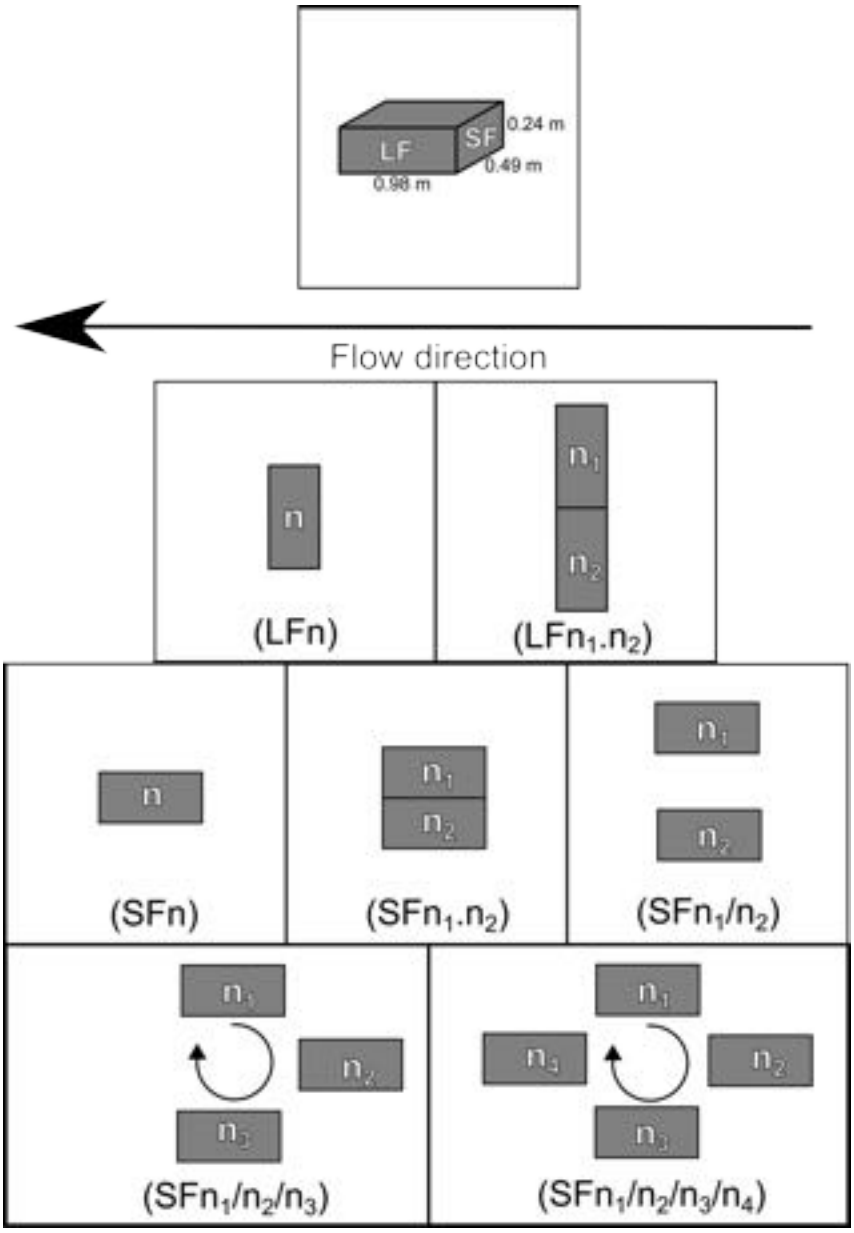

Figure 4.3: Block configurations when placed in the channel. LF- longest face, SF- shortest face, n- number of blocks in the tower.

to steady, which averaged from around 30 - 60 seconds. The discharge was then dropped in $2\,\mathrm{m^3\,s^{-1}}$ increments, with again time being given to allow the gate to move and for the discharge to drop, averaging 1 minute. As the experimental section was within $30\,\mathrm{m}$ of the top of the course, the flow quickly adapted to any change in discharge. We stopped the run once the flow reached $2\,\mathrm{m^3\,s^{-1}}$, as after this point the noise of the gate draining obscured the sound produced by the REs as well as allowing foam to be produced.

4.2.2 Sound processing

Producing a sound-stage relationship requires a single value for sound, which is found by processing audio through a fast Fourier transform (FFT), giving SPL for each frequency. By splitting our continuous recording into 1 second clips, it allowed a frequency resolution of 1 Hz from the FFT, meaning an SPL for each hertz from 20 Hz up to 22.05 kHz due to the microphone frequency response. A single SPL value is found by binning into kHz ranges, i.e. 1-2 kHz, and then the median (spectral centre) of the 1000 SPL values within this range is taken (Osborne *et al.*, 2021). The spectral centre of the data is used as it yields a more representative signal that is not skewed by erroneously large or low values in the frequency range. Each kHz bin therefore had a single value, with the sound-stage relationship being dependent on the frequency bin chosen. Since there was no wind present during the experiments we do not need to preprocess the data to remove any extraneous ambient noises. In Osborne *et al.* (2021) we showed that the sound-stage relationship was strongest at low frequencies (< 3 kHz) and that not having wind noise significantly improves the data quality. We use our experimental data to test how sound-stage relationships are affected by microphone location, and whether the location affects the frequency that produces the strongest sound-stage relationship. As we are concerned with finding the best relationship possible, we needed to analyse all microphone recordings to chose the microphone that provided the best signal.

4.2.3 Image processing

We used image processing to measure how the amount of white water that was produced varied through each experimental run. Video was recorded from the same location as M2 on the bank of the course, which gave an oblique view to the channel. An above water view would have been preferred, but would have been difficult to record continuously and to set up. A drone was not appropriate because its rotor noise would then have affected our sound recordings. Beneficially, the experimental days were cloudy, giving equal lighting and no shadows or glare from the water. For each experimental run, we had one video frame per second, which matched the sound processing clip length of a second. Within a frame there were areas outwith the target area, such as the sky, that were first masked from the frame, leaving only the channel. Due to the top surface of the block being white, these were masked as well, whereas the other surfaces are dark

enough to not be considered white (Figure 4.4). The frame was then converted into greyscale and then binarised into black (0) and white (1) using $imbinarize$ in MATLAB 2021. A pixel was either assigned black or white given the threshold luminance value. Pilot tests showed that a luminescence value of 0.6 produced the best results as it kept the white water, but removed any light reflections. Noise was reduced in the binarised image, with white pixels being required to be connected to another white pixel. A connection value of 20, meaning a minimum block size of 20 white pixels, was found to be capable of removing pixels not related to white water but to also still capture small white water areas. The equation to calculate the amount of white water in an image is

$$WWV = \log_{10} \frac{W}{T} \tag{4.1}$$

where W = number of white pixels and T = total number of pixels, and WWV is the white water value. A log was taken for the WWV as it is to be compared against SPL, which is also in log form. Each frame had a WWV and collectively over an entire run a change in WWV can be observed.

4.3 Results

The results are presented in the following order: (1) analysing the experimental runs to identify what microphones and frequency ranges are the best to use, (2) investigating the effect of roughness element size and configuration on sub-aerial and underwater sound and (3) comparing how both sub-aerial and underwater sound relate to our image analysis of white water.

4.3.1 Microphone and frequency selection for sub-aerial sound

We present an example experimental run in Figure 4.5 to show the relationships between sound and stage for both the rising and falling limbs. Figure 4.5A shows SPL from M4 between 0.02 kHz to 1 kHz, and stage data recorded by transducer from D2. Stage data from D1 is not used since it was highly variable due to being placed in front of an obstacle. The figure shows that stage and SPL rise and fall concurrently, with the exception of increases in sound in the first

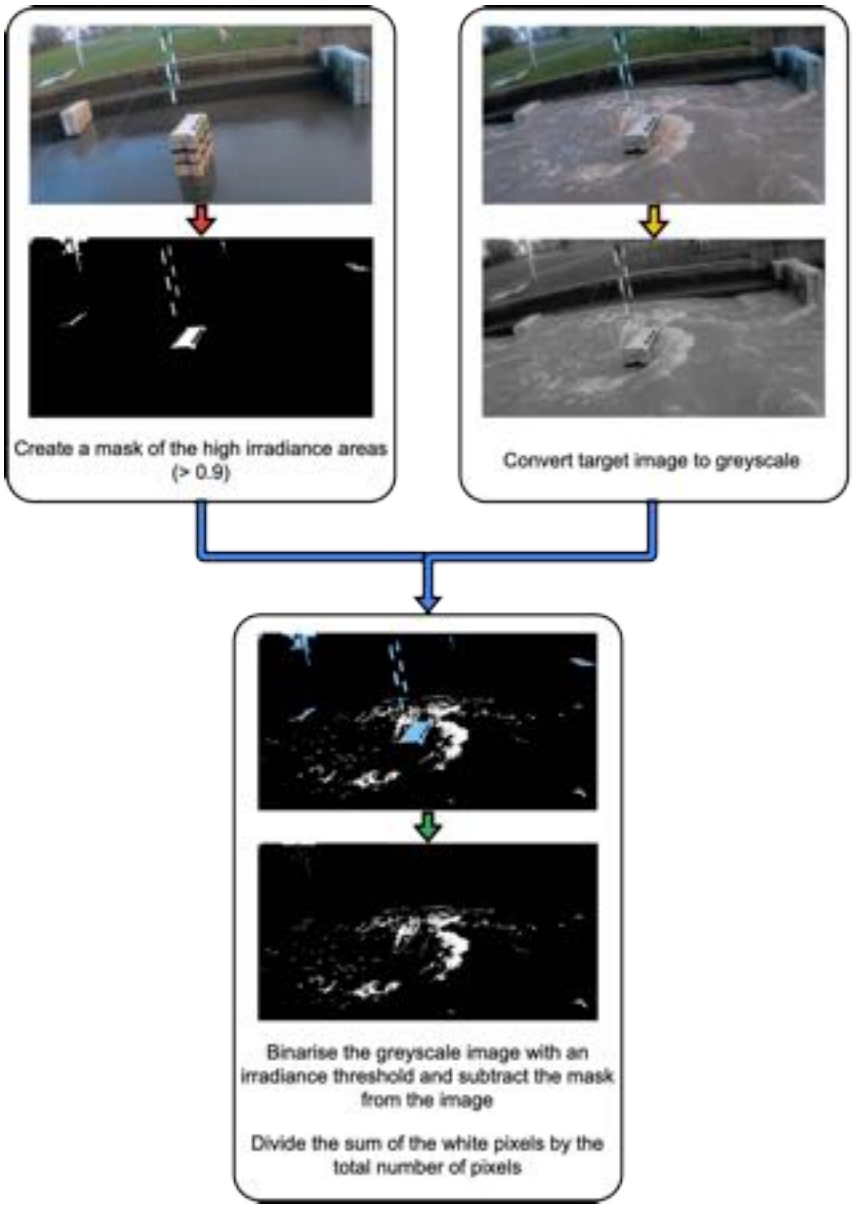

Figure 4.4: Flow chart of how the white water value is obtained from an image. Light blue shading indicates the masked area.

30 seconds which are noises from the bear trap gate opening and not from increases in stage. We therefore disregard increases in sound before stage in all data. Figure 4.5B shows that there there is hysteresis within the run, with the falling limb being quieter than the rising limb. The Froude number of the rising limb was 0.41 and the falling limb was 0.61 meaning subcritical flow occurred during the duration of the run. We focus our analysis on the data from the falling limb as it is more representative of a river, compared to the sudden increase of discharge with the rising limb. The longer time duration of the falling limb also means that this limb provides more data points.

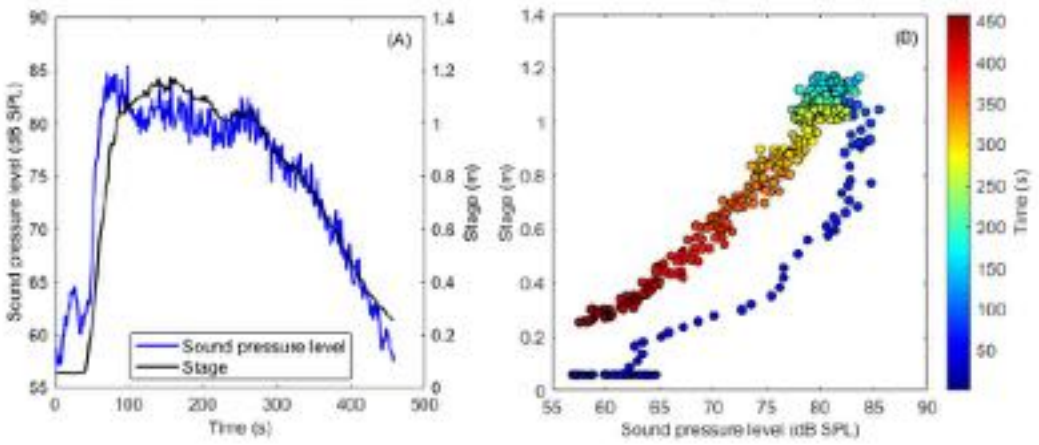

Figure 4.5: A- Sonohydrograph (blue) with the stage (black) recorded from the diver 2. B- Scatter between sound pressure level value and concurrent stage value.

To identify which microphone and frequency range to use in the subsequent analysis, for all runs and for every microphone we plotted the stage and SPL data (as in Figure 4.5B) and fitted a logarithmic function to it, and generated its R^2 value. For each of the 37 runs, we identified the microphone which produced the highest R^2 using a frequency range of 0.02 - 1 kHz (Figure 4.6A). Based upon the full data set of R^2 values, there is very little difference between the R^2 values from the different microphones. To determine what frequency range to monitor, we perform the same process as for choosing the microphone. The frequency range with the highest R^2 is counted for each run, for each microphone. Figure 4.6B and C show the results from microphones M3 and M4, and it is clearly seen that lower frequencies, < 2 kHz, have the highest R^2 values. M4 has 25 out of the 37 highest R^2 values in the 0.02- 1 kHz bin. We therefore chose the 0.02- 1 kHz bin for use in subsequent data processing. Generally the R^2 values drop as frequency range is increased, an observation made by Osborne *et al.* (2021).

With a frequency range chosen we can analyse how configuration of the blocks affects the R^2 values for M3 and M4 (Figure 4.6D and E). Both microphones have high R^2 values, with M3 ranging from 0.63 to 0.92 and M4 from 0.17 to 0.94. M3 shows similar R^2 values across all block configurations, whereas with M4 R^2 values are lower for shorter REs than for higher ones. M4 is chosen in the paper due to its position centrally over the channel meaning that it stays a more consistent distance from the obstacles, regardless of their configuration. We also select M4 as we think that M3 is more affected by the noise of upstream obstacles.

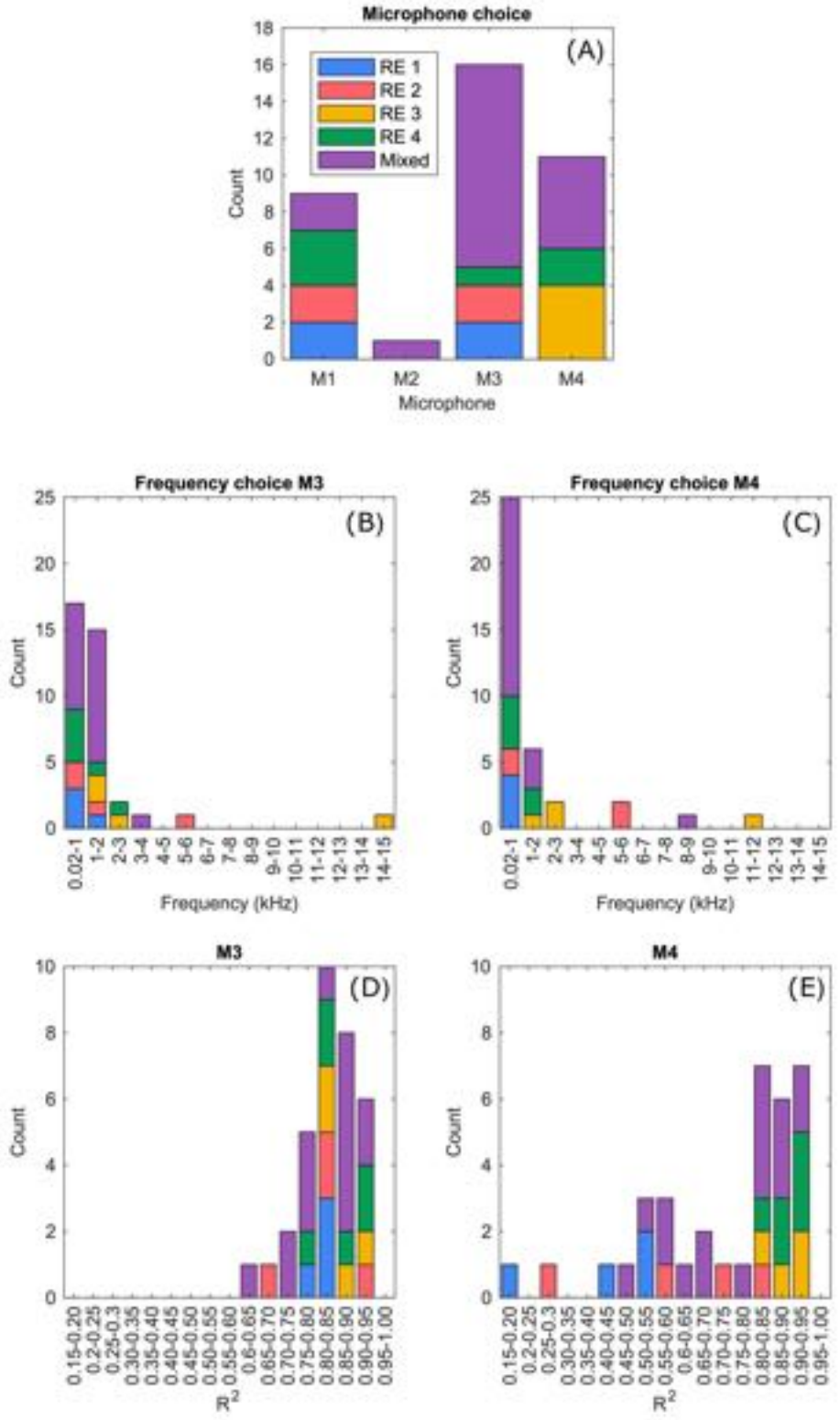

Figure 4.6: A- Histogram displaying which microphone has the runs with the highest R^2 values using the frequency range 0.02 - 1 kHz and categorised by the roughness element height used. B and C - Microphone 3 and 4 and the frequency range where the highest R^2 occurs. D and E- Microphone 3 and 4 and the R^2 obtained when using the frequency range of 0.02- 1 kHz.

4.3.2 The impact of roughness element height on sub-aerial sound

We break the runs into two groups, simple and mixed, and by the height of the REs, in order to clarify the results. The runs with a simple configuration show a clear relationship between sound and stage, which overall forms a logarithmic function (Figure 4.7). Within the overall logarithmic shape, some scenarios show kinks in the data at certain elevations. For configurations with a RE height of 1 the data is more scattered, with kinks in the data above the RE 1's height. Similarly we see a kink in the data from runs with REs of two blocks high, however, it occurs above the height of RE 2. The kink in data is not seen in data from runs with REs of 3 and 4. The scatter of the data reduces as RE height is increased and in turn the R^2 of the logarithmic fit increases. For example, with the simplest block configuration LF_n, (where $_n = 1$ to 4), R^2 increases from 0.52 to 0.91. Another factor to consider is the range of the data, and how loud the flow becomes. With an RE height of 1, SPL approximately varies between 60 - $75\,\mathrm{dB}$, whereas with a RE height of 4, SPL varies between 60 - $85\,\mathrm{dB}$.

4.3.3 The impact of roughness element configuration on sub-aerial sound

Having established that the RE height is important in the sound-stage relationship, we now see how this relationship is affected by RE configuration. Figure 4.8 shows all the other runs undertaken, comprising REs of varied heights, and different configurations. As with the previous configurations, as RE height is increased, the R^2 value also increases. However, the changes in R^2 as the height of the tallest RE varies from RE 1 to RE 4 is not as substantial as from the simpler configurations. The kinks observed above the submergence of an RE are still visible in the data, most notably when there are RE 1 heights. The spatial configuration has a negligible effect on the trends we are seeing, with the configuration with most blocks $\mathrm{SF}_{4/4/4}$ having the same loudness as $\mathrm{SF}_{4/4}$. There are differences between runs where the blocks were connected or separated, for example $\mathrm{SF}_{4.4}$ and $\mathrm{SF}_{4/4}$, with the latter being marginally louder. The only configuration with the same RE height, and only a change in location, SF_4 and $\mathrm{SF}_{0/4/0}$, has a reduced R^2 from 0.91 to 0.78. The reduction in R^2 can be attributed to the microphone being further away in $\mathrm{SF}_{0/4/0}$. The configuration with all RE heights in the channel, $\mathrm{SF}_{4/3/1/2}$, has a R^2 of 0.65, but it can be seen that the data kinks around the same points as when RE 1 and RE 2 are

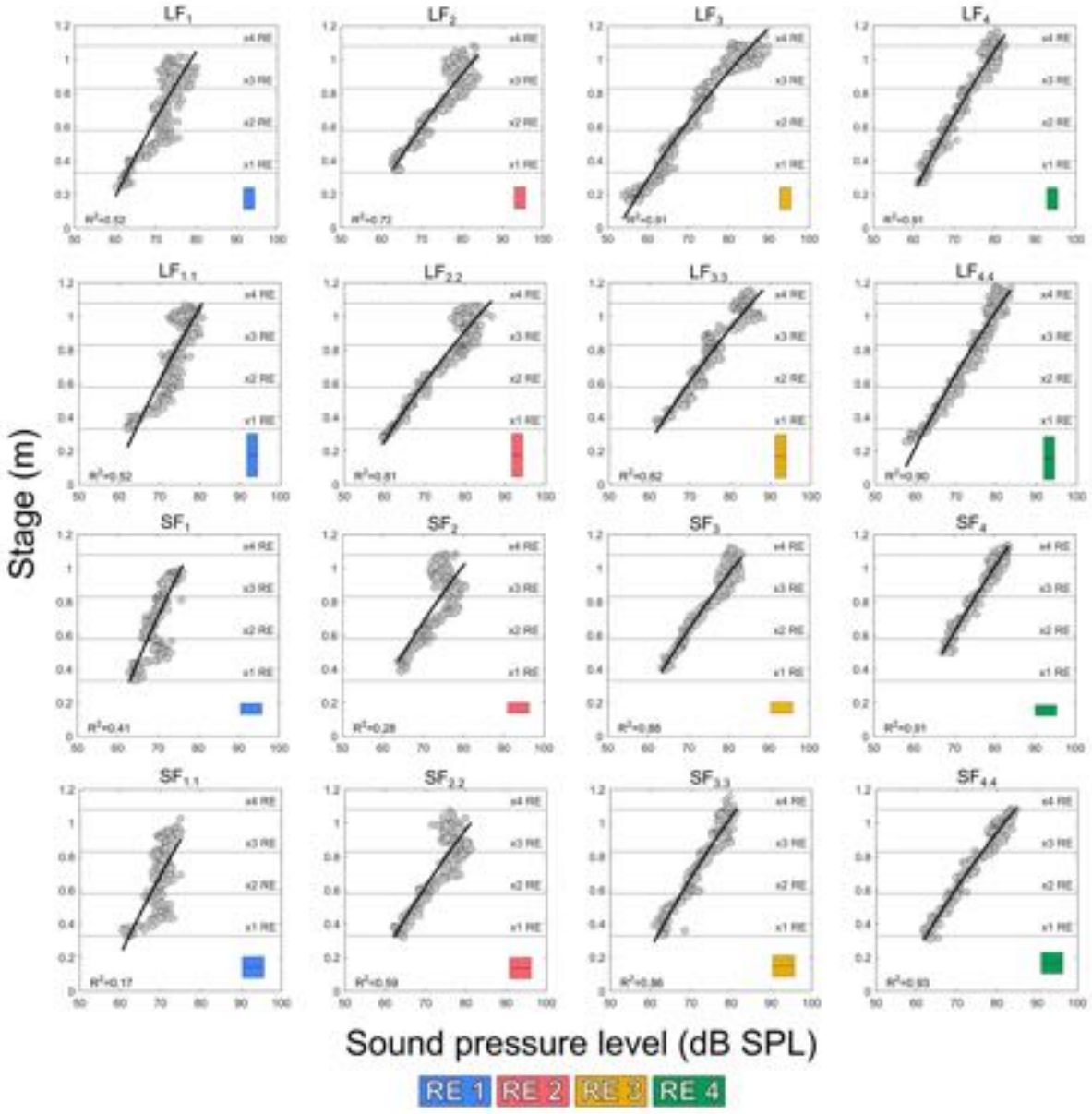

Figure 4.7: Plots showing the sound pressure level and stage recorded during the simple configuration experimental runs. Inset schematics have the block configuration colour coded to the towers' height. Black line is the logarithmic function fitted to the data and the associated R^2. Horizontal lines indicate the heights of the roughness element.

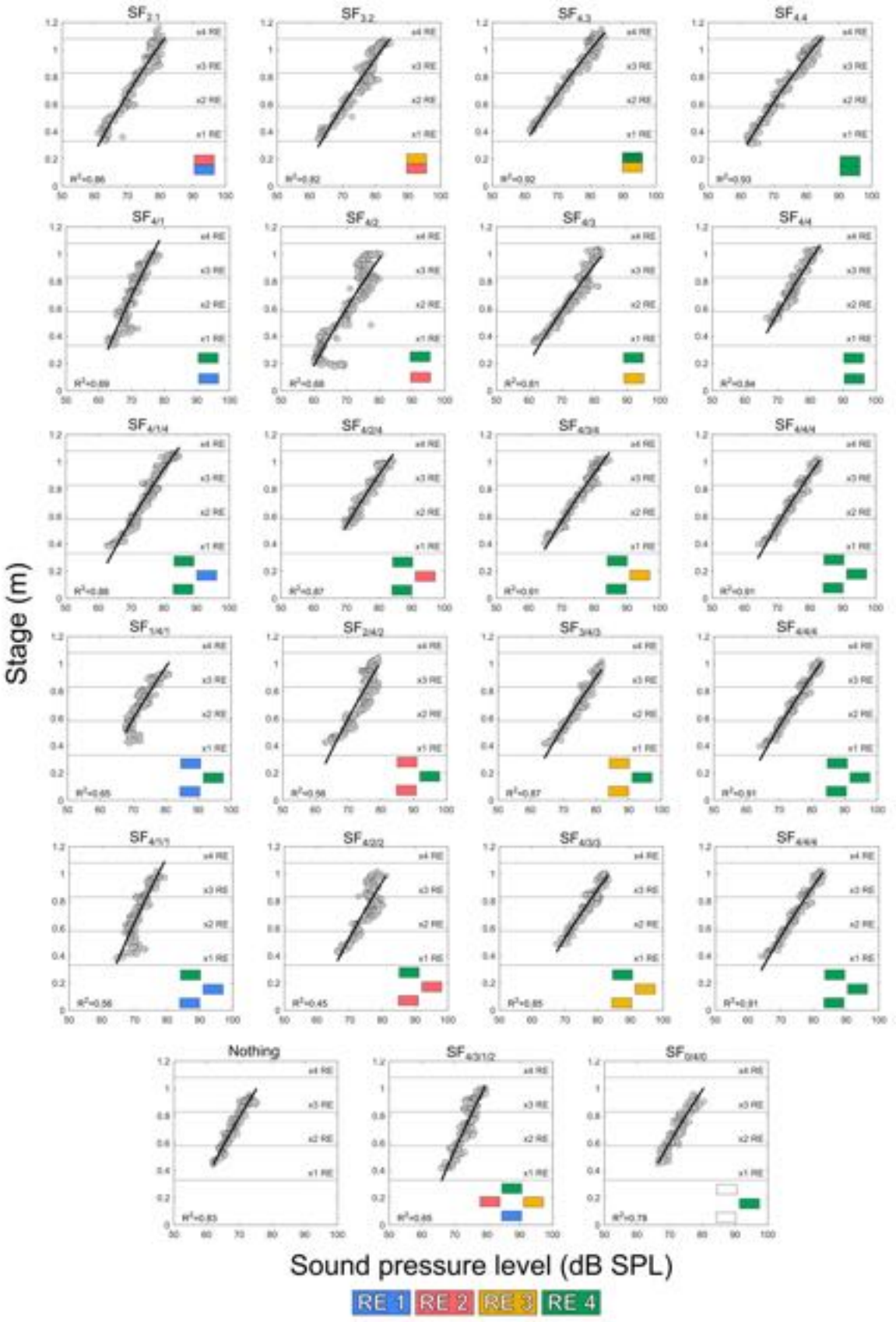

Figure 4.8: Plots showing the sound pressure level and stage recorded during the mixed configuration experimental runs. Inset schematics have the block configuration colour coded to the towers' height. Black line is the logarithmic function fitted to the data and the associated R^2. Horizontal lines indicate the heights of the roughness element.

submerged. Of interest is the run in which there were no REs within the experimental section. Sound was still generated by other obstacles downstream, which in turn generated a high R^2 of 0.83, with a SPL range of 60 - 75 dB. Although we have a high R^2 value, the loudness is less than in runs with obstacles in the section. Whenever an RE is within the vicinity of the microphone it will have the effect of becoming the main signal source due to proximity, and therefore will be what we are mainly listening to during out experimental runs.

4.3.4 The impact of roughness elements on underwater sound

We also evaluate how the underwater sound recorded by the hydrophone varies with RE number and spacing (Figure 4.9). The relationship between sound and stage is not as clear as that shown with sub-aerial sound. In each run there is a hook in the data as stage decreases from 0.6 to 0.4 m, in which sound becomes louder as stage falls. We do not have an increase in sound as stage decreases in the sub-aerial data unless there is a RE of a similar height present, but this pattern is visible in the hydrophone data at all RE height configurations. As RE height increases there is not an increase in R^2 (unlike in Figure 4.7), but we have decrease in R^2 in $LF_{4.4}$ and SF_4. There is significant scatter in the data, especially at high stages, for example a range of 15 dB at a stage height of 0.6 m in $SF_{1.1}$.

Figure 4.10 shows hydrophone data for the mixed RE configurations and, as with the change from sub-aerial to underwater, there are substantial changes. There is significant scatter of the data, with R^2 values between 0.01 and 0.68. The highest R^2 of 0.68 is found with configuration $SF_{4.3}$, with all experimental runs in the $SF_{n1.n2}$ configuration having high R^2 values between 0.59 - 0.68. With no RE in the channel, there is a positive relationship between SPL and stage up until a stage of 0.6 m. Above this, SPL is constant regardless of stage.

4.3.5 White water value

The white water value (WWV) was calculated from only runs using configurations LF_{n1} and $LF_{n1.n2}$ (where $_{n1}$ and $_{n2}$ = 1 to 4) due to the fall of darkness during other runs on the first day. During day 2 natural foam was generated from the Archimedes screw which severely impeded measurement of the white water produced by the REs. Figure 4.11 shows both the stage and

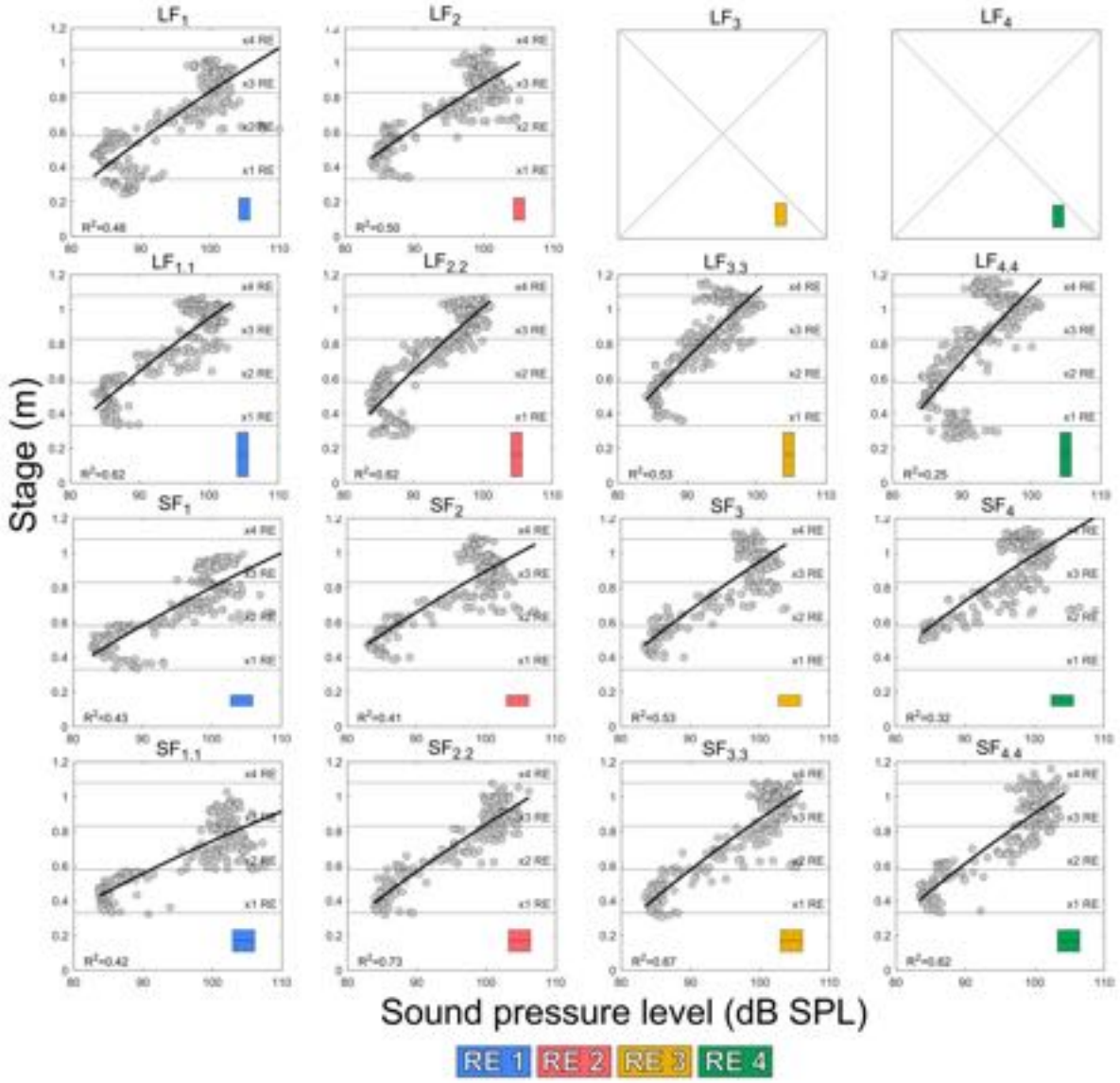

Figure 4.9: Plots showing the underwater sound pressure level and stage recorded during the simple configuration experimental runs. Inset schematics have the block configuration colour coded with the towers' height. Black line is the logarithmic function fitted to the data and the associated R^2 printed. Horizontal lines indicate the heights of the roughness element levels. No data indicates that the hydrophone was not on during these runs.

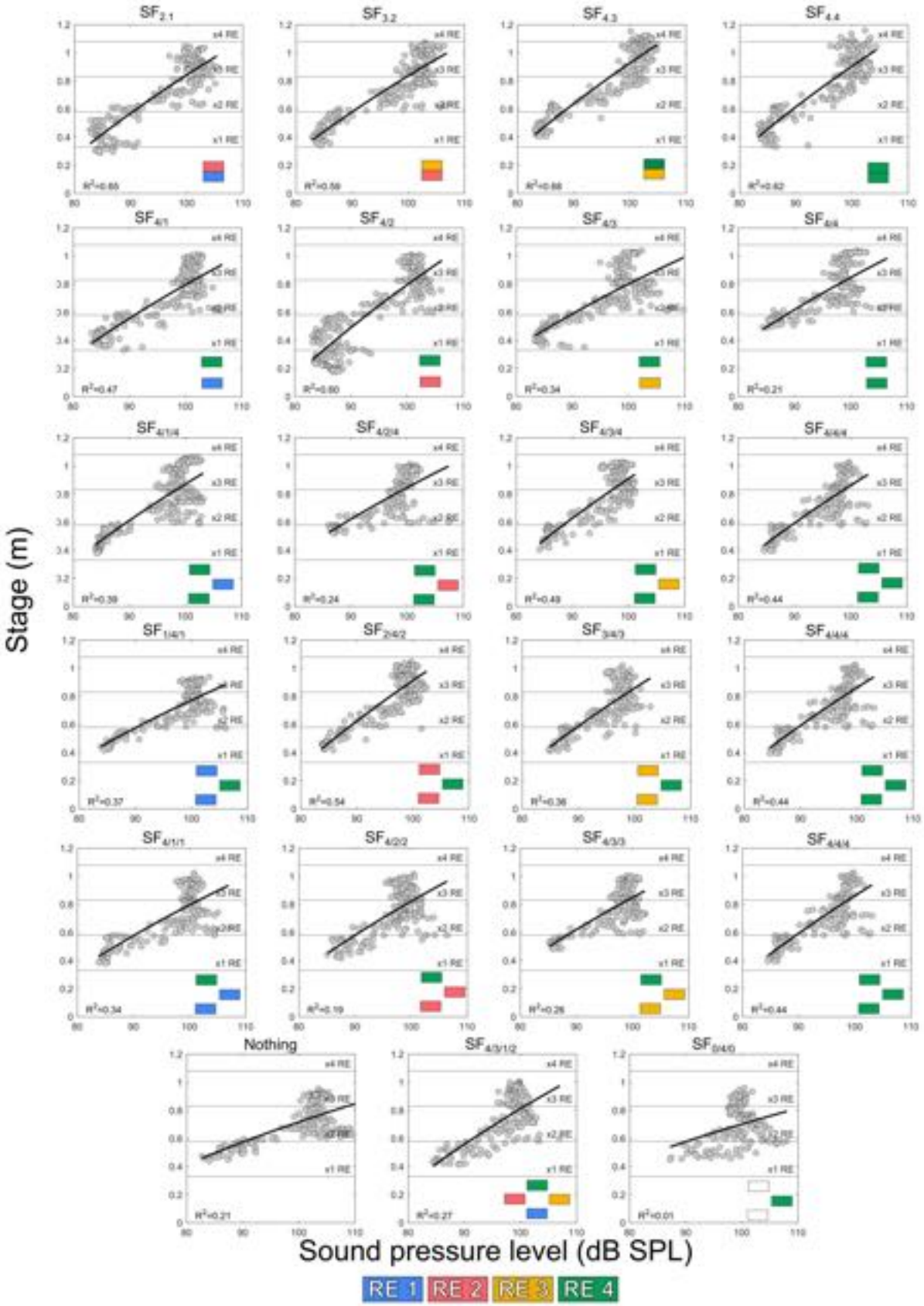

Figure 4.10: Plots showing the underwater sound pressure level and stage recorded during the mixed configuration experimental runs. Inset schematics have the block configuration colour coded with the towers' height. Black line is the logarithmic function fitted to the data and the associated R^2 printed. Horizontal lines indicate the heights of the roughness element.

WWV relationships for $LF_{4.4}$. WWV is a negative number due to being a log of a value less than one, so therefore the closer to 0 the WWV is, the more white water there is in the image. Figure 4.11A-C shows that the shape of a hydrograph, sonohydrograph (sound graph) and the aphrosograph (foam graph) is very similar. When plotted against SPL, WWV has an R^2 value of 0.73, compared to an R^2 value of 0.25 for the relationship between sound and stage for the same run (Figure 4.11D and E). The data shown here is for an entire run, complete with the initial ramping up of the course hence why there is a strong hysteresis effect. We compare an entire run, instead of only the falling limb as if sound is linked to white water, then that relationship should be true regardless of flow type and thus prove that white water is the source of sound. The hysteresis effect is lesser in the sound/ WWV plot, meaning that even during rapid increases in discharge and unsteady flow, the white water still correlates with the sound.

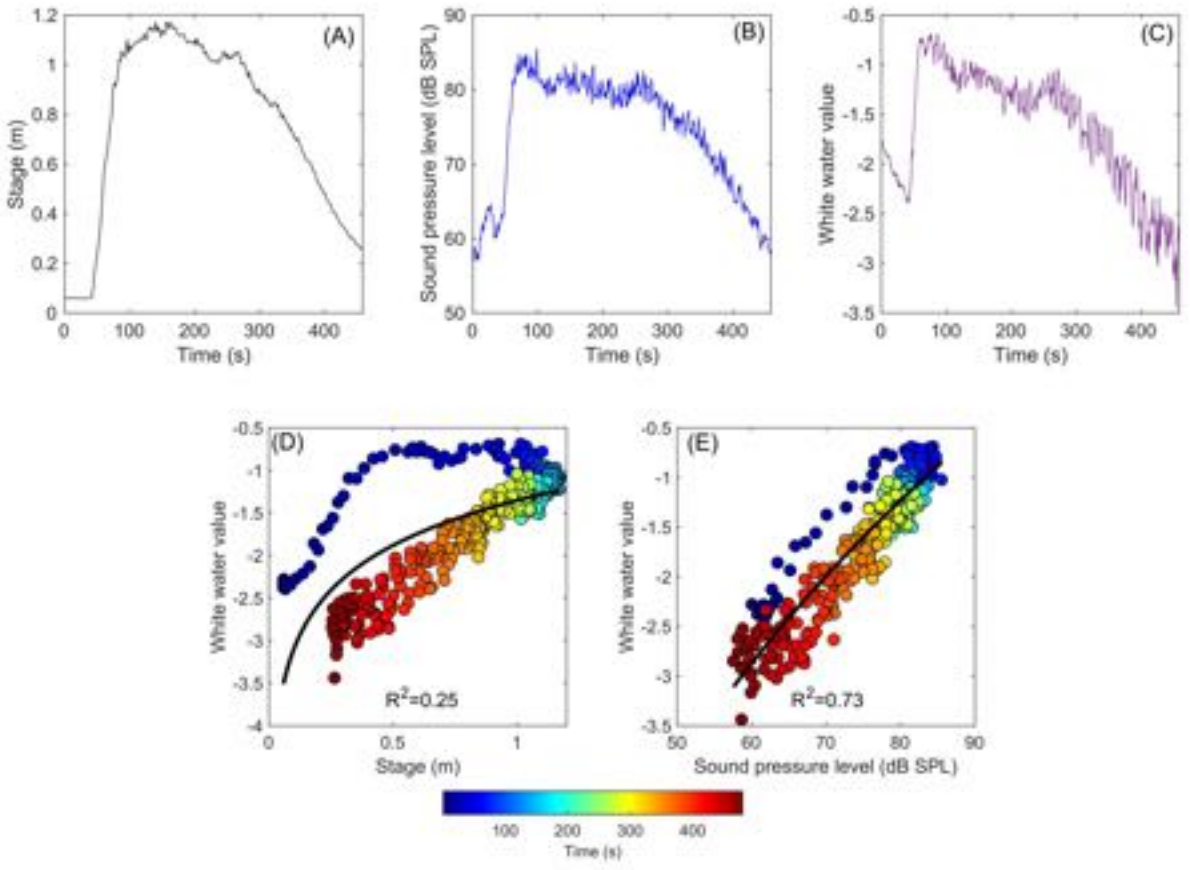

Figure 4.11: Data shown from experimental run $LF_{4.4}$. A- Hydrograph, B- Sonohydrograph (sound), plotting sound-stage, C- Aphrosograph (foam), plotting sound-WWV, D- relationship between stage and sound pressure level and E- relationship between white water value and sound pressure level. Black line is a logarithmic function fitted to the data.

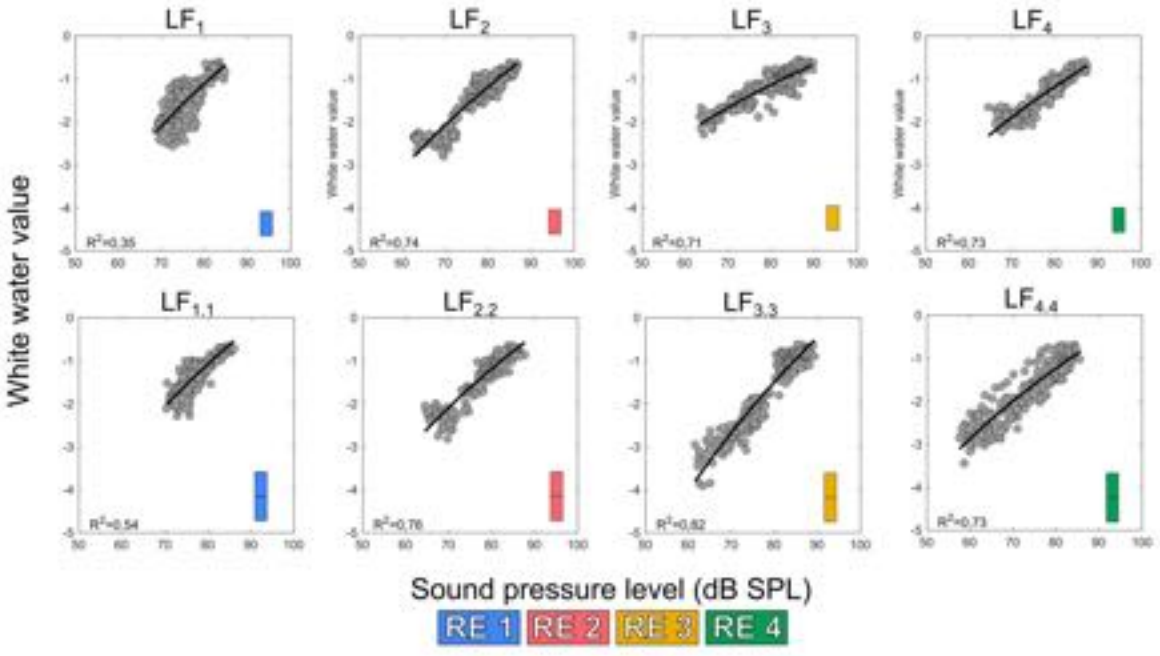

Figure 4.12: Plots showing the relationship between sub-aerial sound and white water value. Inset schematics have the block configuration colour coded to the towers' height.

When the sub-aerial sound and WWV are compared for different heights and configurations, we see a different pattern to that between sub-aerial sound and stage (Figure 4.7). Rather than an increase in RE height improving the relationship between sound and stage, Figure 4.12 has very similar R^2 of between 0.54 and 0.82 regardless of height. The only low R^2 value of 0.35 was with LF_1 in which there was a large range of WWV for a similar SPL. When there is low sound, < 70 db SPL, there is a hockey stick shape to the data, primarily in LF_2 and $LF_{2.2}$. At these lower SPLs, as they increased there was no substantial change in WWV, meaning at the early and closing stages of release, even as sound was being produced, there was little change in the WW being made. The data from LF_2, $LF_{2.2}$ and $LF_{3.3}$ has two distinct clusters of data, between low and high SPL, with gaps of WWV between them.

4.4 Discussion

4.4.1 Roughness element impact on sub-aerial sound

Our previous work linking sound to river stage indicated that the RE size was a determining factor on the relationship between sound and stage (Osborne *et al.*, 2021). Here we tested the hypothesis that the height of the RE was the main controlling factor on sound. By comparing the R^2 values from the different RE configurations (Figure 4.13a), we see that as the height increases, so does the R^2, which provides support for our previous work. The height of the RE, rather than the configuration of the blocks, appears to cause the R^2 of the relationship between sound and stage. We find that a RE does not become inactive in sound generation once fully submerged, and still has an influence on flow at higher stages, as seen by the sound data not rapidly quietening after RE submergence (Figure 4.7). As the stage rises it will first encounter the base of the block, and the flow is blind to the height of the RE, so we expect to see that below the submergence of a block, any sound-stage relationship will be the same. Our data (Figure 4.7 and 4.8) suggests we see this blindness, with nearly identical data paths from the taller REs (Figure 4.14). We see kinks in the data when the flow reaches the point where it encounters the top of the RE, for example, runs LF_1, $LF_{1.1}$, SF_1 and $SF_{1.1}$ in Figure 4.7, and causes a rapid loudening of the flow. The sudden change in SPL is linked to the height of the RE, with it occurring just after the flow overtops the block.

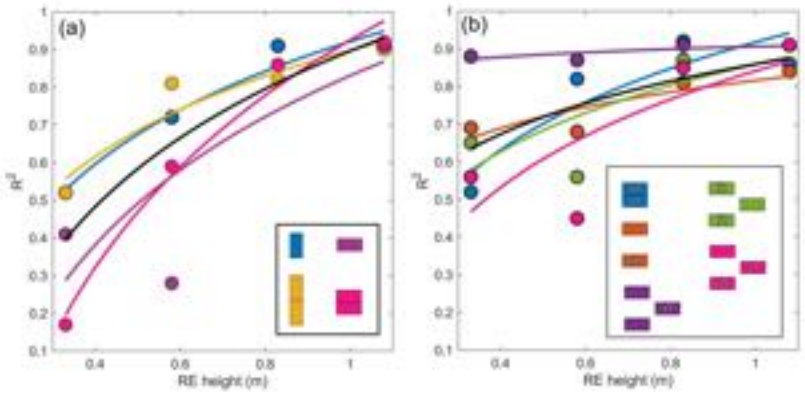

Figure 4.13: Synthesis figure of the R^2 values collected from each experimental run, broken into the simple (a) and complex (b) configurations. Complex configuration uses the block height that changed in each run. Black line indicates the average relationship found with increasing RE height.

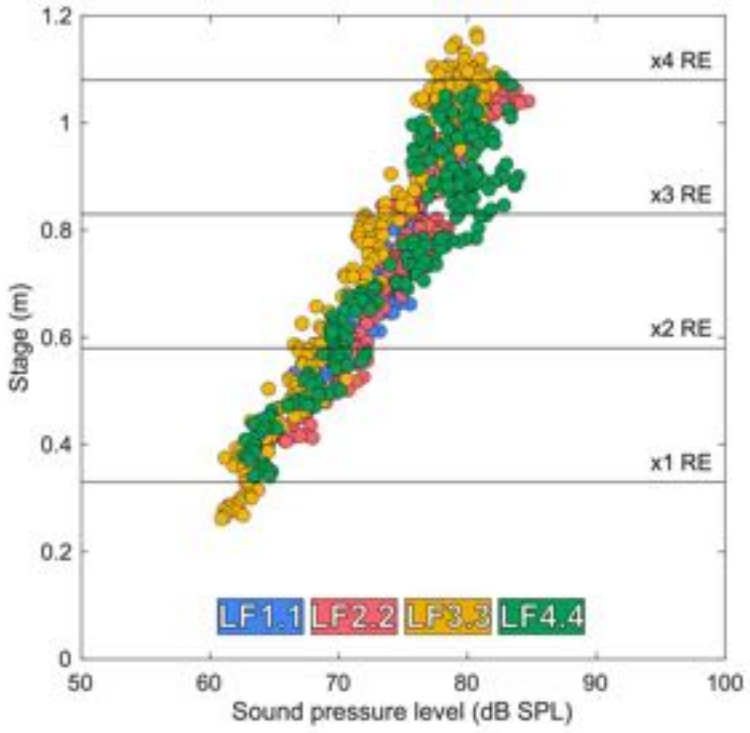

Figure 4.14: SPL plotted against stage for all $LF_{n1 \cdot n1}$ block combinations.

The free-surface is the dynamic and turbulent surface of the rivers' flow, and therefore is affected by flow disturbing REs (Muraro *et al.*, 2021). Flammer *et al.* (1970) observed that as relative submergence increased, the flow transitions between three phases of pronounced, gradual and negligible free-surface effects. These free-surface effects are shown to be white water generating structures such as surface waves and riffles (Brocchini and Peregrine, 2001). Lawrence (2000) found at the point of partial submergence that there was high flow resistance and that as the RE continued to be submerged the resistance gradually reduced. Therefore, as an RE is overtopped, we do not see a cessation to the free-surface effects, but continue to observe them. At our maximum stage, an RE with height of 1 has a relative submergence of 2.85, whereas a RE with a height of 4 has a relative submergence of 0.87. This means that at the max stage the RE1 and RE4 are respectively in the regions of gradual and pronounced free surface effects. At maximum stage, the RE of height 1 is still producing free surface effects, which would only become negligible at a stage of around 1.5 m. The larger RE 4 would require a stage of nearly 4 m to reduce any free-surface effects, therefore allowing sound to be measured beyond submergence. It is by the mechanism of REs becoming submerged, but still having free-surface effects, that we suggest why sound is produced, albeit at a reduced but stable rate, after the submergence of the RE.

The boundary layer is the region where a fluid flows over a solid body, such as our water over the blocks, in which velocity is zero at the boundary, and increases away from the boundary in a logarithmic velocity profile (Carling, 1992). After the submergence of a RE, factors such as RE arrangement and channel geometry were required for modelling the boundary. The kinked changes in SPL at the point when an RE is submerged (Figure 4.7) is from the mechanism of how the flow changes, as before submergence it could only go around the sides, forming a horseshoe vortex, and as stage increases, it can now overtop, creating a trailing vortex (Dey *et al.*, 2008; Ouro *et al.*, 2017). The change of vortex has an associated change in energy, with a horseshoe vortex releasing more energy than a trailing vortex (Zeman, 1995). The shape of the obstacle will influence the free-surface, generating drag, with Nardone and Koll (2016) finding that sharp angular obstacles (such as our block) produce the maximum amount of drag due to increasing flow separation. However, hemispherical object still produced drag and followed the same pattern of drag lessening as the RE became submerged further (Nardone and Koll, 2016). Simpson (1989) found that as flow separation occurs, turbulent flow forms and thus white water is produced, so the larger or more angular the RE, the more flow separation that will happen. That results in more white water, which was shown to be linked to sound. Relative submergence and sound can be linked, with the stronger relationships between stage and sound occurring when REs have a lower relative submergence at maximum stage.

When considering a natural river channel, we do not expect to see a single block in the channel, or for every boulder to be the exact same size or shape. So by looking at more complex channel designs, by including different heights of blocks and configurations, we can go someway to create a more naturalistic setup. With a single RE we find that RE height is the critical determinant of the sound-stage relationship, and so when there are a mixture of heights, we expect that the tallest RE will still be the most important. It is clear from the comparison in Figure 4.13 that the R^2 values are higher when there are multiple REs in the channel. Counterintuitively, creating less of an obstacle, makes the sound-stage relationship better. For examples, the addition of a split level block configuration with $SFn_1.n_2$, increases the R^2 with removing one block from $SF_{2.2}$ to make $SF_{2.1}$, increases R^2 from 0.59 to 0.86. We expect the presence of multiple heights act to smooth the abrupt transition from flow going around, to overtopping a RE, which created the sudden increases in SPL shown in SF_1 and $_{1.1}$. If that is played out in a natural environment, then a heterogenous mix of RE heights would have influence on the sound being produced,

helping to increase the correlation between sound and stage.

We cannot disregard the influence of shorter REs in a configuration, as although a mixture of heights may help smooth out the data, large varied heights may introduce scatter in the sound-stage relationship, e.g. 10 cm and 100 cm REs. With $SF_{4/1}$ and $SF_{4/2}$, there is a block of 4 in each, however compared to other situations with a 4 block high tower, the R^2 is lower. At lower depths the flow is again blind to the fact of smaller REs, with RE4 perhaps being a constant background sound, with the shorter RE acting independently as in SF_1. Without the smooth transition between two block heights, the sudden increases in SPL are back. In runs with an uneven distribution of block heights, the ability of taller blocks to dominate over the shorter ones becomes clear. For example, when 2 out of the 3 towers are 4 blocks high, the R^2 only varies between 0.87 and 0.91. Conversely, when only one of the towers is 4 blocks high, the shorter towers influence the sound-stage relationship greatly, with an R^2 range between 0.45 and 0.91. In an uneven distribution, the REs with the greatest number of similar heights may impose more of an impact than the spatial configuration of them. However, as the average height of the block increases, so does the R^2, meaning the taller the obstacles are, the better the relationship.

4.4.2 Roughness elements and hydraulics

The kinks in the data we see for example during runs LF_1, $LF_{1.1}$, SF_1 and $SF_{1.1}$ in Figure 4.7 may be able to be explained in terms of hydraulics. Papanicolaou *et al.* (2010) found during flume studies that when there is low flow, relative submergences effect on flow structures is governed mainly by localised flow structures and Froude number, and during high flow the Reynolds number. The kink in data could therefore be subject to the change in hydraulic governance. Shamloo *et al.* (2001) found that when relative submergence reached 1, overtopping produced an arching vortex from the combining of the horseshoe vortexes and defined regimes in which features such as surface waves appear and when different vortexes appear and change. The kink can be attributed to the changing through these regime changes. During low flow, Karman vortexes exist, generating backflow behind the block. As flow depth increases, the vortexes transition into horseshoe and arch types. The increases in flow increases the amount of energy in the system, and the kink could be the rapid transfer of energy when one vortex structure transitions into another.

In the flow there is an energy budget, through which energy is transferred from potential energy, into kinetic. However, the kinetic energy is transferred into other forms of energy, such as frictional loss due to flow resistance. It is the transfer of energy that enables a river to generate sound by the mechanism of transfer of energy. In our experiment, we enabled the transfer of the kinetic energy to sound using the RE blocks in the channel. The energy budget was therefore near identical during the experimental runs, with the only change occurring from the RE blocks. When increasing roughness, energy is transferred from the flow, into turbulence, which in turn slows the flow down (Carbonneau and Bergeron, 2000). If we were to measure flow velocity during the experiment, we would be therefore able to measure how different RE blocks affected flow speed, and in turn if this translated to changes in sound with a direct correlation between energy lost in the flow, and sound generated. We can intuitively see this when we increase the RE height, as the larger the face opposing the flow, the more energy is lost to overcome it, with when an RE is 1 tall, the sound generated is quieter than when it is 4 tall.

4.4.3 Sub-aerial sound generation

Knowing what is creating the sound we are trying to relate to stage will aid in the design of any future sub-aerial and river sound experiments. From the image analysis of a how white water changes over stage, we are able to determine that white water correlates with SPL and infer that it is the white water producing the sound. Figure 4.11 demonstrates that on both rising and lower limbs, white water and sound maintain a logarithmic fit, unlike the relationship between white water and stage when there is a split between the limbs. In Figure 4.12 there is an R^2 of between 0.35 and 0.82, the fit between white water and stage is not perfect, with scatter still across the data. The scatter of the data could be a result of the camera position being oblique to the flow, introducing error in the WWV, or that the sound also introduces scatter since there can be a range of SPL for a single stage. There may be variation in the white water calculations due to small changes of luminance in an image, meaning greater or fewer pixels are categorised as white or black. Given that we did not have a light meter to measure that, we cannot be certain if imperceivable changes to light may have occurred. We presumed there are two zones of river sound production, from underwater and on the surface of the water. As our experiment lacked any mobile bedload, then it cannot account for the scatter of the data. In real word examples in which there is mobile bedload there may be an opportunity for sound to transmit from the water into the air, but is dependent on the water depth, the frequency and amplitude of the collision (Geay *et al.*, 2019).

Some of the scatter between white water and sound may be due to the episodic nature of bubble formation and destruction. The exact moment between an image being taken and a recording being matched up could be out by milliseconds for example with bubble formations bursting within 10's of milliseconds, the data could be out of sync (Chicharro and Vazquez, 2014). Averaging sound over an entire second should help to reduce the impact of that, whereas for the WWV there is no averaging since only a frame was recorded per second. The recording of coastal breaking waves by Deane (1997) found air entrapment to generate sound underwater, with both the sound and breaking waves (creating white water when the air rises to the surface) occurring simultaneously. Peak sound production happened at the moment the wave broke, with it reducing as the wake decayed. A coastal wave is at a different physical and temporal scale to the waves generated in the WWC. Waves are being constantly being constructed and

destructed in the WWC, and interacting with themselves, so rather than an episodic splosh of a wave, it combines into a melodic form. With potentially multiple sound sources from different REs, of differing intensity, duration and frequency, taking a single video frame for reference may induce a minimal error but should not be completely out of sync.

4.4.4 Underwater sound generation from roughness elements

With no bedload, the hydrophone used in our experiment would have two possible sources of sound, with Tonolla *et al.* (2009) finding during underwater flume experiments noise was transmitted by white water at the surface, or from the pressure field formed around the hydrophone. We do not think that it is useful to construct relationships between stage and underwater sound because our data showed only a weak relationship between the two. Furthermore, in natural channels they would be affected by the noise of bedload transport. Bedload transport has been shown to be active in the same frequency range that we observe sub-aerial sound at, at between 500- 2000 Hz and dependent on bedload size (Geay *et al.*, 2017). Our data suggests that there is a direct correlation between underwater sound and stage up to a stage of 0.6 m, which may not be a good choice if concerned about flood monitoring for example, but could influence other forms of monitoring, such as bedload since the frequencies overlap. Tonolla *et al.* (2009) identified that relative submergence of REs may cause changes in the underwater soundscape, particularly in lower order streams. With that change in soundscape, we therefore may be seeing evidence as to why stage and underwater sound relationships are lesser than sub-aerial sound. Marineau *et al.* (2015) recorded the sound level of a flood event using a hydrophone, and attributed discharge in direct relation to the bed transport generated sound. Given that our data has underwater sound reacting in a similar manner without bedload it could mean that the influence of the sound produced by the flow needs to be considered in future works.

4.4.5 Controls on WWV and sound

Having identified where sound is being produced from, we now need to understand what in turn controls the white water production. Our experiment leads us to two conclusions regarding how the height of an RE and the spacing of them affects sound production. From our white water imaging (Figure 4.12), we see that as an RE gets taller, the R^2 of the sound-WWV fit increases

from 0.35 at LF_1 to between 0.71 and 0.74 at the other heights. The WWV is similar to the same SPL on these graphs, at -2 WWV having a SPL range of 65-71 dB. The nature of the scatter can be partially explained by the height of the REs, with the shorter RE (LF_1) being submerged almost immediately, but in doing so producing white water and sound, hence why it has a narrow range of SPL. At taller REs (LF_3 and $_4$), there is sound produced, but with less white water since water is forced around for longer, instead of over the top. The larger range of SPL is what allows a better fit to be found.

When comparing between a height change, but with larger block face there is a similar pattern, with the R^2 of the fit increasing from 0.54 at $LF_{1.1}$ to between 0.73 and 0.82 at the other heights. How the downstream length of the obstacle affect the white water is seen by comparing LF_3 & LF_4 and $LF_{3.3}$ & $LF_{4.4}$, with the amount of white water being less in the side by side REs. We suggest that even though LF4.4 provides a larger blockage to the flow compared to LF_4, it causes the flow to diverge more, which seems to reduce the amount of turbulence produced. The separation of data point clusters in $LF_{2.2}$ and $LF_{3.3}$ may be explained by the sudden generation of white water once these obstacles are overtopped, since there would be a significant rise in white water generation potential. From a white water and sound perspective we can determine that as RE height increases, the larger the SPL range becomes and that the configuration of the blocks mimics but could add a new delay to sound being produced.

4.4.6 Lessons for field deployment of sound monitors

A sound monitor can be used in areas where traditional monitoring techniques for stage measurements are not feasible, such as a lack of infrastructure. The need to understand what it is within a river that generates a strong sound-stage relationship is therefore vital if sound monitoring is to be of use in fields such as flood monitoring. From our WWC experiment we identify the following lessons that should improve a sound-stage relationship.

To draw comparisons between an entirely unnatural channel to a natural one has its drawbacks, such as that there is no active bedload, and that it condenses a hydroevent from hours into minutes. What we can take away is the interaction of flow and REs. The height of REs is important

in the sound-stage relationship, with the higher the RE, the higher the R^2. This does not mean that you need a 1 m tall RE in a stream that only reaches 0.5 m for example, as it all becomes relative to the flow itself. Our configurations with RE of 2 (0.58 m) high still can produce very good relationships in relation to stages of up to 1.2 m. So in a natural setting an RE equivalent or up to 50% less than the anticipated maximum stage will offer a strong chance of a relationship, with the proviso still that the taller the RE, the better the relationship can be. It will be highly unlikely that a natural channel will have simply one RE within it, meaning that channels are more likely to have a heterogeneous mixture of REs. In that situation having a distribution of REs will help to generate a smoother and more constrained sound-stage relationship.

If this experiment was conducted in a natural setting, using natural REs, the results would be different. Changing the uniformity of REs, from rectangular blocks, to more rounded boulders, would impact the sharp transition we see when an RE is overtopped. Instead of a definite overtop, there will be a gradual transition, from which it might not be capable to definitively see such a kink. Having a mixture of REs would therefore have multiple overtopping transitions happening at once, and as shown when mixed REs are used, they combine into a mixed signal, not several single, distinctive ones. The shape and orientation of a RE can also impact the flow resistance, and in doing so could influence the sound produced (Aberle *et al.*, 2022). We investigated how orientation of an RE can impact sound, with either the long or short face perpendicular to flow, and showed that when there is a longer surface for the flow to overcome (short face perpendicular to the flow), the sound generated is louder, in comparison to the same RE block when the long face is shown. Another factor of a natural river is that REs can move, and although in our experiment REs were fixed, the microphones downstream and upstream still provided a good relationship between sound-stage, simulating if the REs began to move away from the microphone. If there was sufficient energy in the system, then a completely new RE configuration could emerge, and then any existing sound-stage relationship would be void, and a new one needing to be formed. We therefore do not see sound monitoing being implemented in high energy environments, when there is potential for REs to move during an event.

The use of using image analysis to calculate the amount of white water on a river is a proof of concept, rather than a fully functional process. We advise that if the method was to be used in a comparative study that certain conditions would have to be kept. Aerial photography will provide the best view of the river, so therefore the use of a drone would be best, if the sound

produced by it was minimal. Despite the oblique view of our images, we were still able to find relationships, but obscuring by the blocks was possible. The field of view (FOV) of the river surface also needs to be considered, as you need to observe the full extent of the white water generated from an obstacle. Having a narrow FOV would cut off sections of the tail of a wave for example. Having too large a field is less of a concern unless other white water structures begin to appear that are not related to the RE being studied. We therefore recommend that the FOV is directly related to the size of the RE so as to observe its white water production without cropping out areas and not introducing other structures into it. To compare between rivers would require that the total area being monitored is similar to allow comparison. The ability to calculate the amount of white water in a river temporally could also be useful for other disciplines such as gas exchange or identifying areas of flow resistance.

4.5 Conclusion

Our paper aimed to determine the source of sub-aerial sound and how the REs within a channel can affect the sound-stage relationship. Through the use of a large scale experiment we were able to closely mimic a real river and generate sounds of a similar type. Sub-aerial sound is concluded to be predominantly produced by white water generated by the interaction of flow with the RE. Identifying the mechanism for the creation of the sound enabled us to begin to test what other factors could influence sound-stage relationship. The height of the REs within a channel is the primary control on the sound-stage relationships strength. In terms of relative submergence, the lower the stage that is required to be monitored up until, the better the relationship will be. A heterogeneous mixture of REs does not degrade the relationship, and instead improves it. An uneven distribution however will begin to influence the relationship, with more tall REs stabilising it, and more shorter REs destabilising.

Although the experiment was run at real world scale, it is not a complete analogue of a real river's behaviour. Sediment is not fixed to the bed like our blocks, but is mobile, meaning the configuration can change during a flood event. However, since spatial configuration is not a significant factor in the sound-stage relationship, and the sound from individual REs becomes melodic. If the balance of RE heights were to change, then that may begin to change

the relationship. With continued research into sound mechanics of rivers in relation to REs, such as our experiment but in a fully natural setting, the size and spacial distribution could be represented by a singular component, such as the maximum RE height in the channel. All of which could be aid in the possibility of being able to predict the sound so that you can use it as a proxy for stage.

Acknowledgements

This work was supported by Durham University, the British Society of Geomorphology, the European Regional Development Fund - Intensive Industrial Innovation programme Grant No.25R17P01847 and Evolto Ltd. We also acknowledge the help of the team at the Tees Barrage International White Water Centre for all their help and assistance. Contains OS data © Crown copyright and database rights, 2021.

Data availability statement

The data that support the findings of this study are available from DOI:10.17632/gxf5sy24kg.1.

> “We called it the "River of Silence"; for there seemed to be a hushing influence in its flow. No murmur arose from its bed, and so gently it wandered along...
>
> Edgar Allan Poe
> *Eleonora* ”

Chapter 5

A case study of the River Gaunless catchment

5.1 Introduction

When trying to build a comprehensive network of river stage monitors for water-resource, flood and environmental management it needs to adapt to the changing nature of future hydrometrics. With data the most scarce currently where it is most needed in smaller catchments (Hundt and Blasch, 2019; Wilby, 2019). There are limitations on the resources available and therefore monitoring is targeted where the most useful data can be collected from (Seibert *et al.*, 2019). Knowing if there is change in streamflow in an is crucial to water resource management and importantly to flood management when time is a critical component (Demeritt *et al.*, 2013). Having an easy to deploy and maintain system of hydrometric stations is therefore advantageous and could help to reverse the decline in stations when we are in a period of climate change (Ward *et al.*, 2019).

I developed a low-cost river stage monitor capable of being placed in upland river channels. The monitor records the sound of the rivers, which when filtered to produce a SPL I have shown to have a relationship with stage (Osborne *et al.*, 2021). The relationship between sound and stage is dependent on the number and size of REs in the channel. I will detail the method for deploying a network and then examine a case study of the River Gaunless network. My aims of this chapter are to show: (1) how to set-up and maintain a sound monitoring station, (2)

whether monitoring headwater catchments be achievable and (3) what benefits these additional stations have on water resource management.

5.1.1 Background

The use of sound has certain benefits over conventional and emergent river stage measuring techniques as shown in Section 1.6.1, such as not requiring in-stream infrastructure or needing to be placed within the river (Osborne *et al.*, 2021). Deployment is focused primarily in headwater catchments due to their compatible morphology, such as having a steep gradient and variable bed topography which generates the white water required for sound monitoring (Gomi *et al.*, 2002). Headwater streams are seldom monitored commercially due to the lack of resources and inherent difficulty to reach but are useful in understanding how fast water moves from the landscape to the river system (Benda *et al.*, 2005; Hundt and Blasch, 2019; Fritz, K., Johnson, R., and Walters, 2006). Headwaters are the most adaptable locations, being most impacted in the winter/spring, altering their discharge regime, even with slight variation in rainfall or snowmelt (Riley *et al.*, 2018). Although headwater rivers are small, being first and second order streams, they are 60 – 80% of the total length of the stream network, and up to 80% of its drainage area (Pažourková *et al.*, 2021; Benda *et al.*, 2005; MacDonald and Coe, 2007). These streams have potential to provide natural flood control and are also important ecologically, with controls on sediment and nutrient fluxes but are usually under represented in monitoring networks (MacDonald and Coe, 2007; Bradford and Marsh, 2003). The confluence of lower order streams and the continued increase of the drainage area adds complexity to what is influencing the channel more, the headwaters or the inputs downstream. Because of the number of channels, and both temporal and spatial extent of them, it becomes difficult to estimate their value and input into the channel and to separate out the contributions of individual tributaries to downstream flood peaks (Gomi *et al.*, 2002; Baattrup-Pedersen *et al.*, 2018). I therefore examine the difference in headwater channels and their impacts downstream.

Hundt and Blasch (2019) said that low-cost and practical stream flow measuring could be used by professionals or even citizens to provide a solution to the lack of headwater monitoring, such monitoring would be of value even if it only indicated the peak time and duration of a flood.

However, the quality of the data needs to be assured, since the data is to be used in decision making or warning local residents and also to potentially calibrate and test flood models (Wilby, 2019). The short lead times of minutes to hours in comparison to hours to days in larger rivers means there is less time to warn communities downstream, meaning that early warning systems need to be designed to mitigate risk (Borga *et al.*, 2014). Simulated flood models are an option to examine the risk to communities, with the understanding if during the conditions monitored, this outcome is likely (Cameron *et al.*, 1999). However, some models do not take into account the individual tributary catchment responses and group them together into a basin, raising uncertainty (Wang *et al.*, 2021). The use of stream gauging also causes the risk of errors, with assumptions on stage-discharge relationships being stretched due to a lack of temporal data, such as only daily stages (McMillan *et al.*, 2010, 2012). Rabie *et al.* (2017) found that for flood modelling to be useful, detailed information has to be included such as rainfall, soil moisture, land use and stream gauge data. The inclusion of data from headwater channels has to be weighed upon the benefit it gives, as their difficult to predict behaviour makes modelling significantly challenging (Kavage Adams and Spotila, 2005). Hydraulic models may not perform as expected if calibrated to low flows when an unexpected event takes place (Unduche *et al.*, 2018). A solution to improve the sparsity of gauge data is to deploy my sound monitors in the data assimilation process, albeit with the caveat that DIY data itself may have high uncertainty (Fava *et al.*, 2019). Mazzoleni *et al.* (2017) found that with even limited and uncertain hydraulic data, it can improve the flood prediction of models. Real-time data assimilation combines the complementary model and observational data into an optimal estimate (Reichle, 2008).

5.2 Method

I present our study area of the River Guanless and describe the headwater and tributary channels that make up the area. I explain the principle of setting up a sound network and the method used to get the most reliable data from it.

River	Coordinates	Gauging	RE (m)	Drainage Area (km^2)	Substrate
Hindon Beck (1^{st})	54°37′12.3"N 1°52′43.7"W	Sound	0.30	5.1	Bedrock
Cowclose Beck (1^{st})	54°37′13.5"N 1°52′43.2"W	Sound	0.35	2.4	Bedrock/ Cobble
Arn Gill (1^{st})	54°37′10.7"N 1°52′14.5"W	Sound	0.25	3.6	Cobble
Steele Gill (2^{nd})	54°37′13.6"N 1°52′2.4"W	Sound/ EA	0.21	12.1	Cobble
Crow Howle Beck (2^{nd})	54°37′29.5"N 1°49′45.9"W	Sound	0.30	8.5	Cobble
Highlands (3^{rd})	54°37′13.9"N 1°47′37.5"W	Sound/ EA	0.40	28.8	Cobble/ Boulder
Gordon Beck (2^{nd})	54°37′49.7"N 1°46′14.3"W	Sound	0.25	6.7	Cobble
Ramshaw (3^{rd})	54°37′45.2"N 1°45′31.6"W	Sound/ EA	0.20	41.4	Cobble

Table 5.1: Monitoring site location properties with river stream order. Roughness element (RE) is the height of the tallest obstacle within the channel.

5.2.1 Study area

The River Gaunless is located to the East of the North Pennines, travelling through County Durham before joining the River Wear (Figure 5.1A). It flows from the Woodland Fells, through smaller communities in its upper reaches before going through the town of Bishop Auckland. Gaunless means "useless" as original Viking settlers said it was unmanageable by boat, due its rough bed, and therefore resources could not be transported (Curtis, 2015). The River Gaunless was chosen primarily because of the existing infrastructure on the River, with three EA stage gauges within a 7 km reach of each other. The river has three gauges within a short distance because the local mining history has produced a substantial pollution risk and the gauges are used to calculate the pollution from different point sources. The Gaunless is a spatey river, being described by the EA as a highly connected drainage system allowing fast responses to rainfall.

The River Gaunless catchment is shown in Figure 5.1B, upstream of our lowest monitoring point. In total the catchment's drainage area is $41.4\,\mathrm{km}^2$. I have chosen to monitor five main tributaries into the River Gaunless: Hindon Beck; Arn Gill; Cowclose Beck; Crow Howle Beck and Gordon Beck based upon their increase to cumulative drainage area (Table 5.1). The order of the streams are based upon the definitions set out by Strahler (1957), with the highest order stream being the one which all others flow into. Other tributaries are present in the Gaunless but are not considered either due to being farm drainage or having very small drainage areas (< 1 km^2).

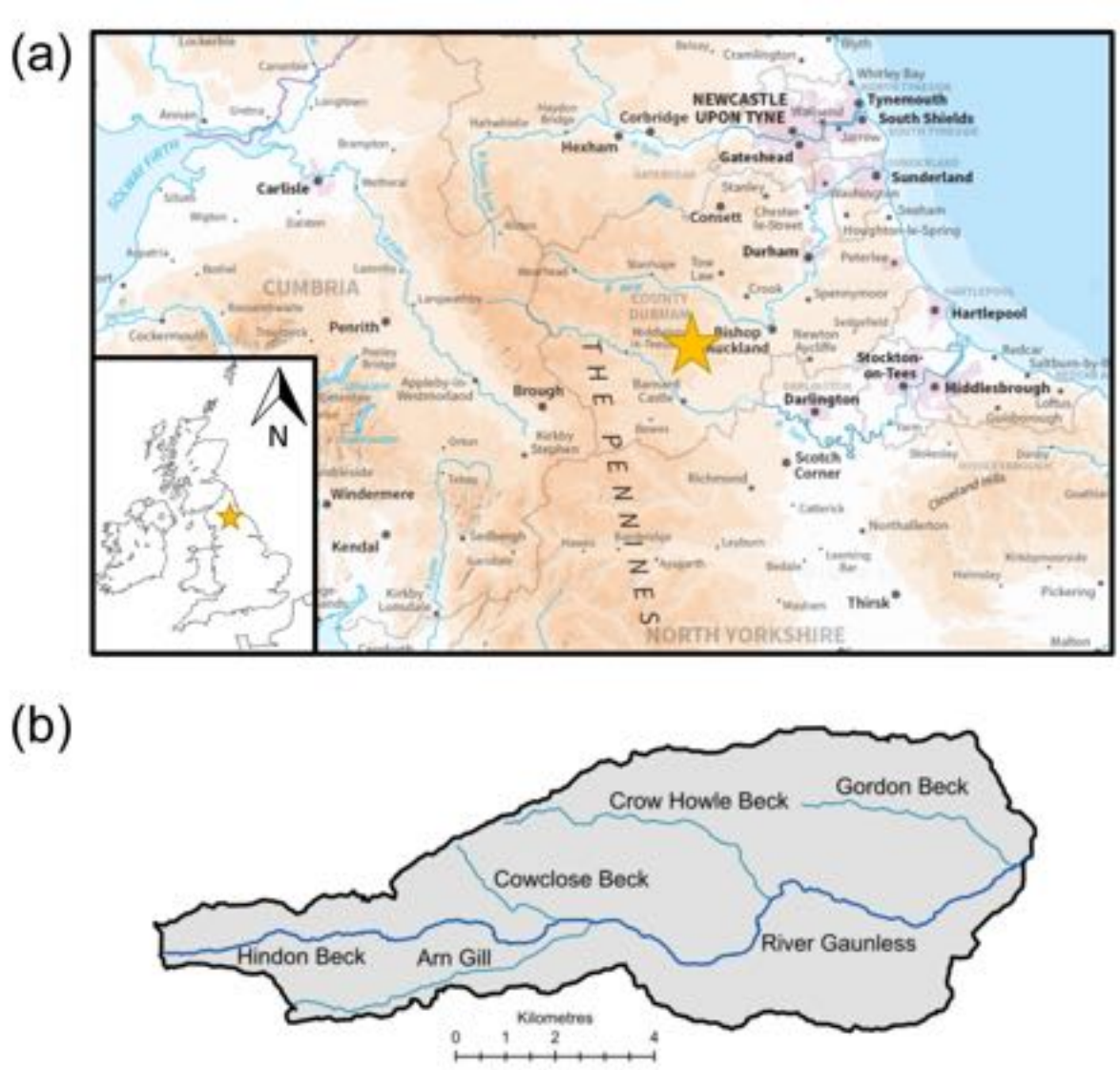

Figure 5.1: A-Map of the location of the River Gaunless study site. B- Catchment area of the River Gaunless from the lowest monitoring point. Main channel shown in dark blue, with tributaries in light blue.

5.2.2 River Gaunless network

A network of sound-stage monitors were deployed in the River Gaunless area. My network was setup in order to identify the contribution of each tributary to the River Gaunless. Although there are already three EA run stage gauges, these are found on the main River Gaunless at points after main tributaries join meaning that associating what tributaries are contributing more or less water to the River Gaunless is difficult. The sites chosen were not appropriate for traditional stage monitoring techniques, as examined in Section 1.5 due to a mixture of bed type and vegetation coverage as shown in Figure 5.2. I include the three EA gauge sites as sound-stage

monitor locations as the EA gauges provide an independent dataset with which to validate the sound monitor results. I use the Nash-Sutliffe efficiency as described in Section 2.2.4.

Each site was fitted with a sound-stage monitor which was capable of recording 10 seconds of sound every 15 minutes from February to June 2021, with a battery lasting up to a month. Sound data was then processed using the lowest median filtering method as outlined in our previous work (Osborne *et al.*, 2021). As five sites did not have stage measuring already installed, generating a relationship between sound and stage from using concurrent measurements was not possible. I therefore use the sound rating curve approach outlined in Chapter 3 to calculate stage, using 5 concurrent sound-stage measurements.

5.3 Results

5.3.1 Gaunless

I present data from a flow event on the Gaunless that occurred on the 11th March 2021 which caused three distinct peaks in the stage data. Figure 5.3 shows a storm hydrograph for the Steele Gill EA gauging station with rainfall data from the local Copley station. In total, 21.6 mm of precipitation was measured over three days causing the river to rise by 0.16 m, followed by two smaller peaks. During the rest of the monitoring duration monitoring there was a lack of significant rainfall, and so this was the largest event during this time.

With 3 sound-stage monitors placed at existing EA gauges I am able to assess the sound-stage relationships and to determine if the sound data was in unison with the stage data. In Figure 5.4 I have the hydrograph and sonohydrograph overlapping from which I can see that the timings of the peaks in the Steele Gill and Highlands gauge match. The sound-stage relationship is very good with an R^2 of 0.89 at the Steele Gill, with an R^2 of 0.70 at Highlands. However, the Ramshaw site does not show the expected relationship between sound and stage, and above a threshold stage of 0.15 m, the SPL drops. The Nash-Sutcliffe efficiency is equally as good, at 0.75 and 0.83 respectively.

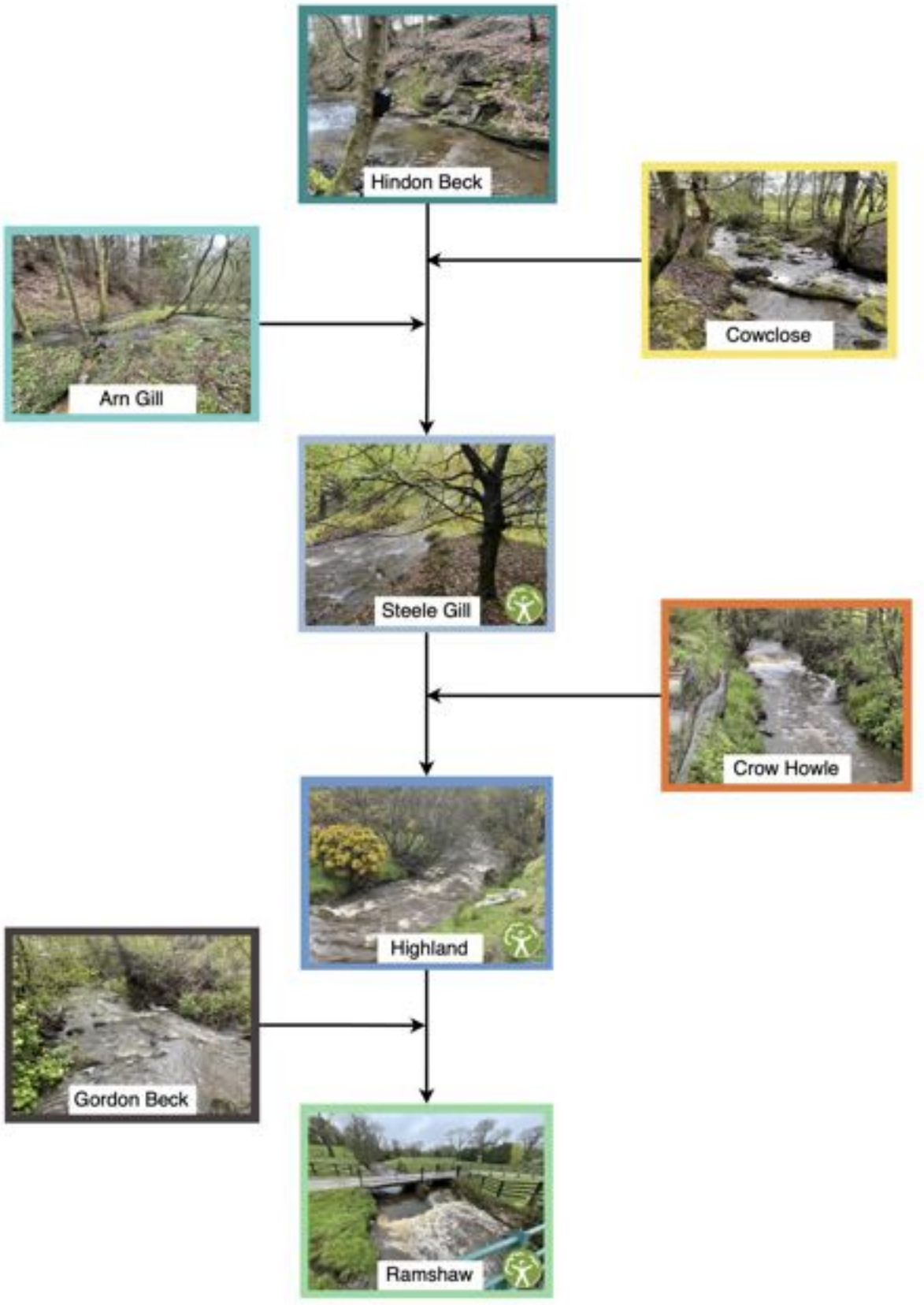

Figure 5.2: Network diagram of monitor locations with photographs of the rivers at representative low flow. Green Environment Agency logos symbolise locations where Environment Agency gauges are situated.

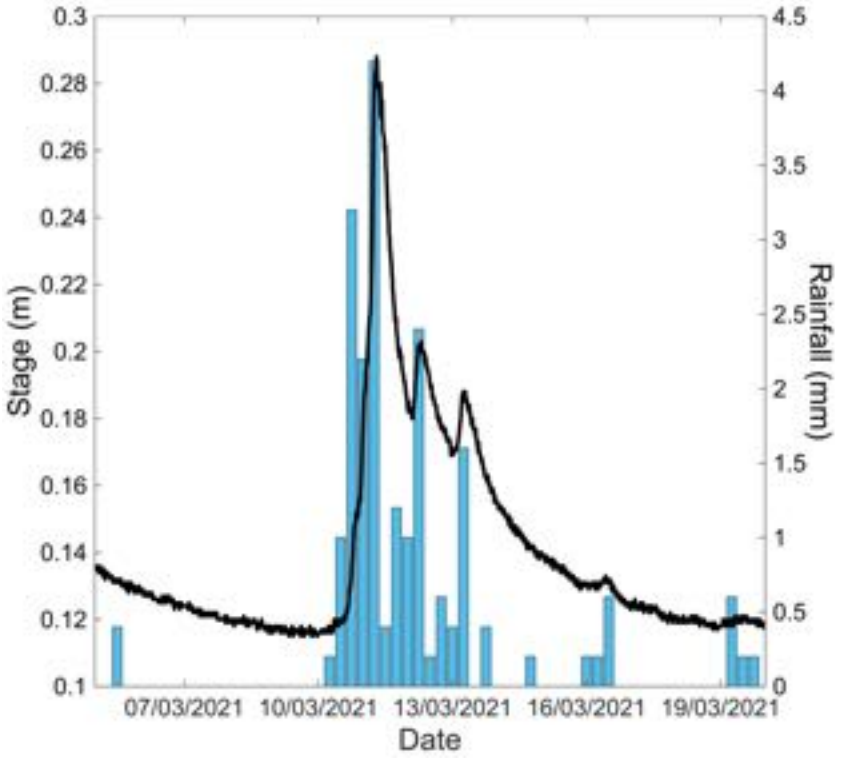

Figure 5.3: Hydrograph of the River Gaunless from Steele Gill site and rainfall data from Copley gauge during from the 6th- 20th March 2021.

My sites without conventional stage monitoring are shown in Figure 5.5, at which I have five concurrent sound-stage measurements taken during the event and at other times. With the five measurements I construct my sound-stage ratings curve. Using the equation I am able to input all our SPL readings and calculate stage. The R^2 values vary between 0.64 to 0.96 for the fit of the curve to the data. The sonohydrographs produced are similar to the EA gauge data with three peaks, with the exception of Arn Gill where the peaks are not clearly visible. The shape of Hindon Beck, Crow Howle and Gordon Beck are close to the sharp rising limb seen with the EA data. Cowclose has a more rounded shape, indicating that it held onto a higher stage after the peak. With the exception of Arn Gill, the sonohydrographs appear to be smooth, with around a 0.01 m oscillation in stage calculation. Arn Gill has a jagged line, which can be associated with the limited range of its SPL, only varying from 32 - 38 dB SPL. The other rivers have a larger range of SPL, with between 9 - 25 db SPL separating the highest and lowest recorded.

Table 5.2 shows the peak stage and time from all the stations during the 11th March 2021 flow event. Comparing the stations with both sound and EA monitoring, shows that Steele Gill has the sound peak 45 minutes later than the EA, and Highlands having a sound peak 2 hours earlier

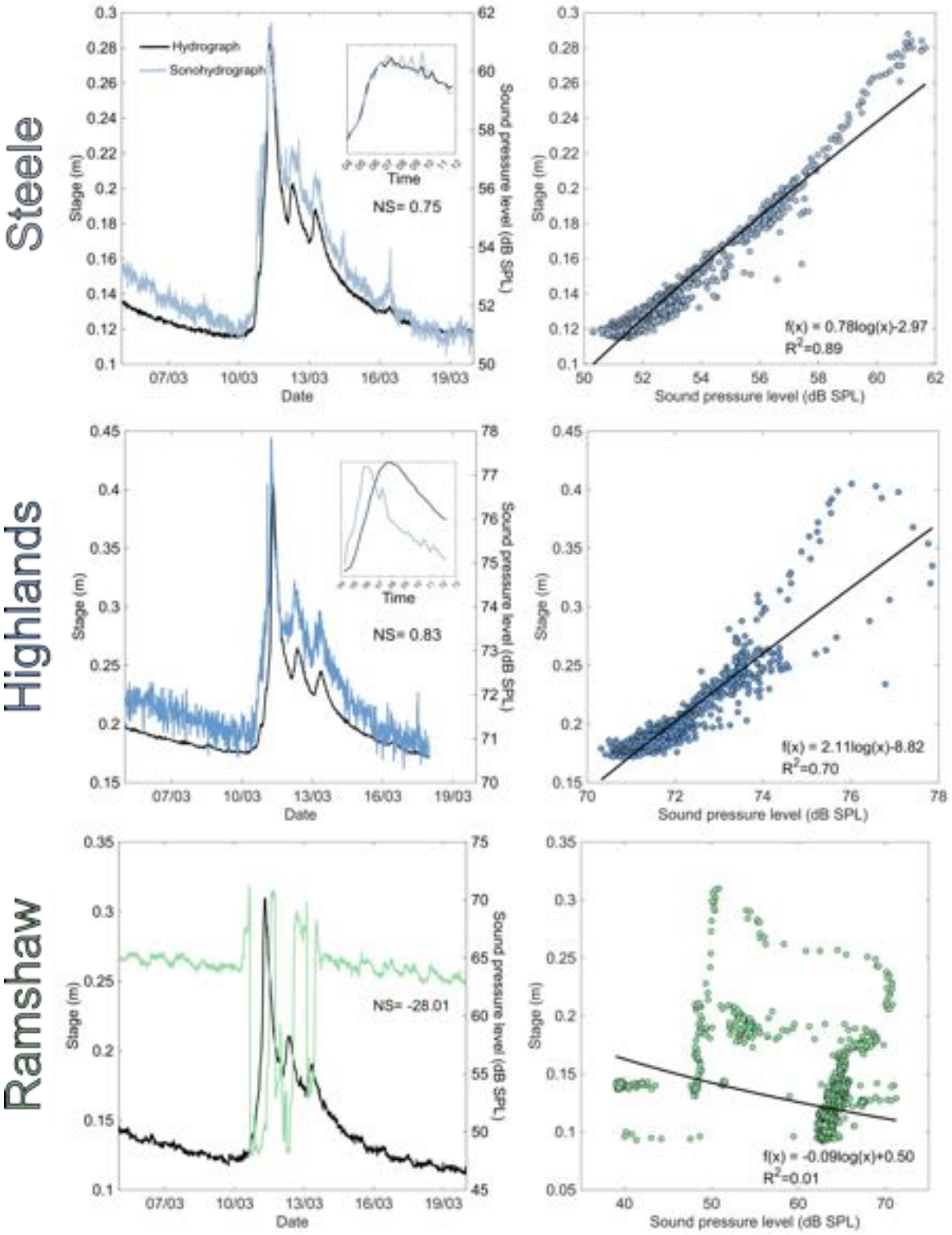

Figure 5.4: Column 1- Comparison between the Environment Agency hydrograph data and sonohydrograph data at 1 -2 kHz. Inset graph shows in detail the peaks. Column 2- Relationship between sound-stage with a logarithmic function fitted. Nash-Sutcliffe efficiency given between the observed and simulated stage taken from the sound-stage relationship.

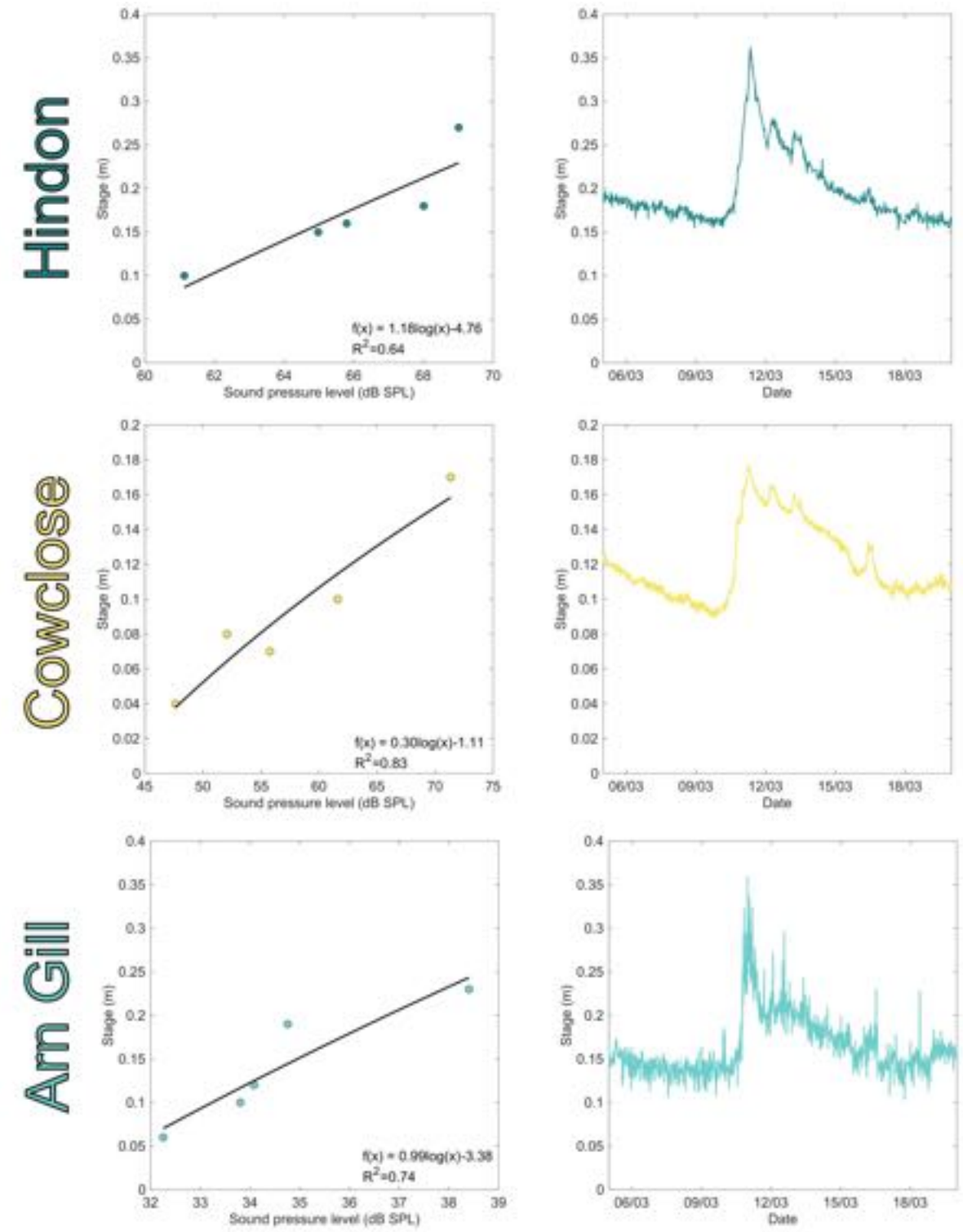
Hindon
Stage (m)
Sound pressure level (dB SPL)
f(x) = 1.18log(x)-4.76
R2=0.64
Date
Cowclose
f(x) = 0.30log(x)-1.11
R2=0.83
Am Gill
f(x) = 0.99log(x)-3.38
R2=0.74
06/03
09/03
12/03
15/03
18/03

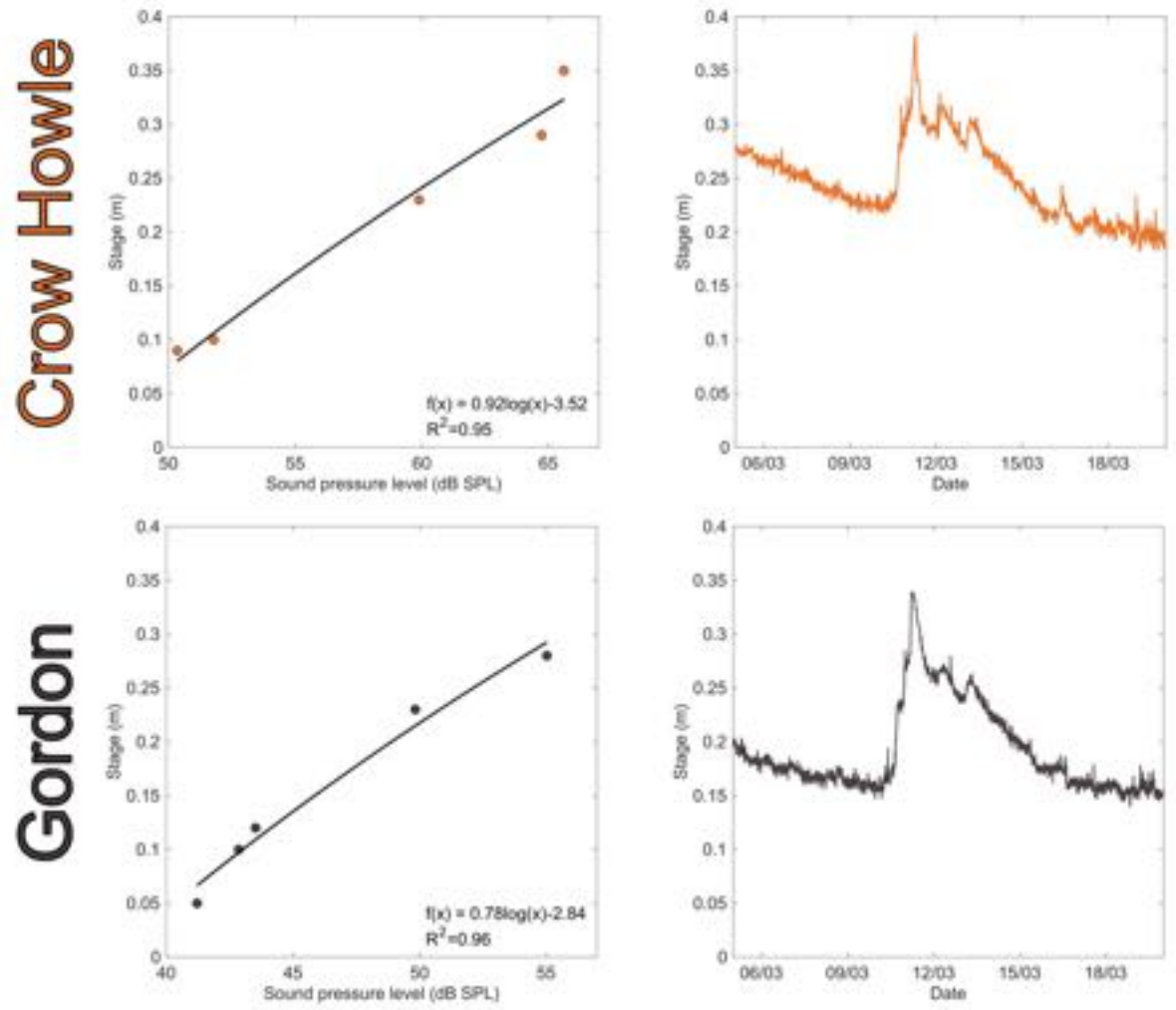

Figure 5.5: Column 1 - Sound-stage rating curve fitted from 5 concurrent stage-sound measurements using a logarithmic function. Column 2- Sonohydrograph constructed from the relationship found and applied to all other sound values.

than the EA. The peak stages from these stations are close, with the sound stage being 0.04 m lower than the EA at Steele Gill and 0.03 m lower at Highlands. With sound only monitoring the peak times are broadly similar to what the EA gauges record, with the exception of Arn Gill which recorded a peak around 8 hours earlier than the others. Peak stages of between 0.18 - 0.36 m are recorded in the upper rivers of the network, with similar stages of between 0.34 and 0.38 m.

With five concurrent sound-stage measurements being taken to form a sound-stage curve used to calculate the stage from our sound data, I look at what happens when the number of measurements are reduced. Figure 5.8 has the sonohydrographs for each sound only station, with

River	Monitor	Sound peak time	Calculated sound peak stage (m)	Gauge peak time	Gauge peak stage (m)
Hindon Beck	Sound	08:30 11/03/21	0.36	-	-
Cowclose Beck	Sound	06:45 11/03/21	0.18	-	-
Arn Gill	Sound	23:30 10/03/21	0.36	-	-
Steele Gill	Sound and EA	08:00 11/03/21	0.25	07:15 11/03/21	0.29
Crow Howle Beck	Sound	06:45 11/03/21	0.38	-	-
Highlands	Sound and EA	05:45 11/03/21	0.37	07:45 11/03/21	0.40
Gordon Beck	Sound	06:30 11/03/21	0.34	-	-
Ramshaw	Sound and EA	-	-	07:30 11/03/21	0.31

Table 5.2: Flow event data from the sonohydrograph data and comparison between the Environment Agency gauge data.

the progressive removal of the highest stage measurement. By simulating when someone only takes measurements during low stages, I can determine what affect it has on the sonohydrographs and how it affects the predicted peak stage. In Figure 5.4 and 5.5 there is not a clear effect from removing measurements, with Gordon Beck showing both over and under estimation, and Hindon Beck showing only under estimation.

The peak calculated stage when removing the highest stage consequentially has the greatest impact on Gordon Beck in which the removal of points leads to an increase of stage, changing from 0.34 to 0.49 m, a change of 44%. If the that trend was to continue, then a measured stage of 1.0 m would be shown as 1.44 m potentially. The other monitoring stations have the trend that when a measurement is removed, the peak calculated stage lowers, with Crow Howle changing from 0.37 to 0.21 m, a reduction of 43%. Consequentially if a flood was to occur using only these two points, then a stage measuring 1.0 m would be shown as 0.56 m.

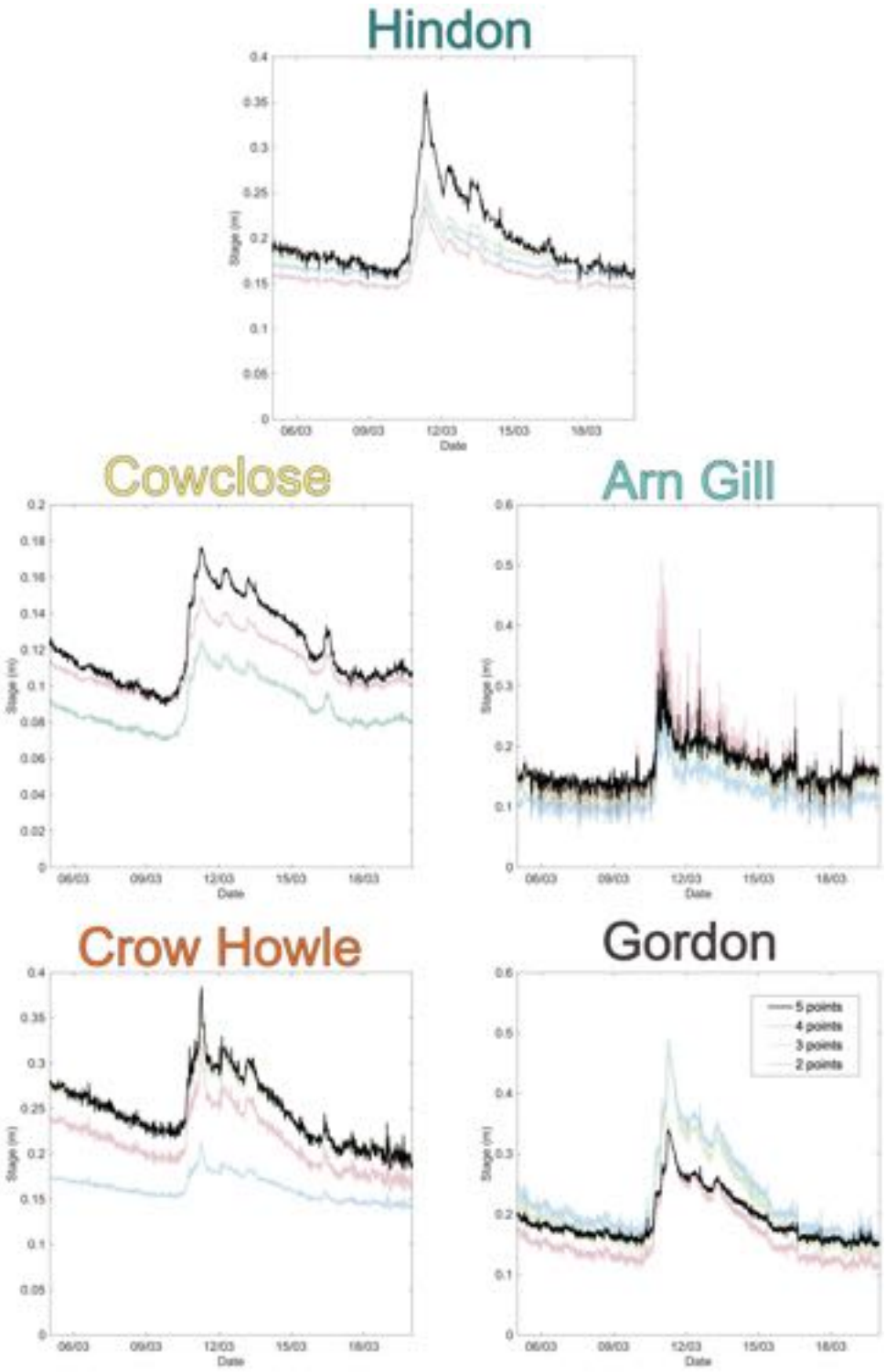

Figure 5.8: Sonohydrographs from the sound-stage rating curves with using all concurrent values in black. The highest stage is removed each time.

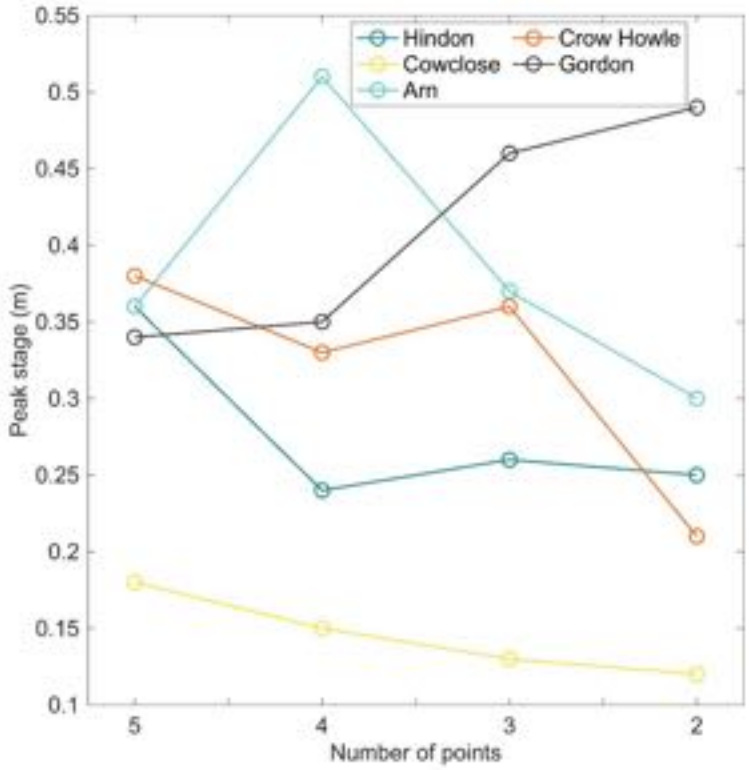

Figure 5.9: Predicted peak stage from the sonohydrographs after the removal of the highest stage from the sound-stage ratings curves.

5.4 Discussion

5.4.1 Peak stage

The Gaunless network is made up of 5 sound-stage monitors, in conjunction with 3 traditional pressure transducer EA gauges. I do not intend that sound-stage monitors are to replace existing gauges but investigate areas in which valuable additional data can be gathered where it cannot be done currently. Hindon, Cowclose Beck and Arn, Steele Gill make up the headwaters of the River Gaunless. Having monitors distributed around the headwaters allows the identification of which of these tributaries is the spatiest, or if they all act in unison, and if they all peak at the same time.

Investigating these smaller streams and tributaries is not a priority for national or regional flood management but could be important for local flood management. By using the data from the EA gauges I am able to verify my data from the flow event on the 11th March 2021, as without it I

would not be able to link the sound-stage monitors to the event. The flow event was not a flood scale event but it can be used to build our argument for exploring the headwater response and subsequent downstream response. By looking at the sound peak time from Table 5.2 and Figure 5.4 the peak does not occur at the same time in any of the sound monitor locations, whereas the EA peak gauge times occur around the same time of around 07:30. A flood peak is expected to happen sequentially downstream, however, the peak occurs earlier at the downstream EA station than the midstream station. Although it does not follow the sequence, it is given that within a margin of error that the peak of the River Gaunless main channel was found around 07:30. The sound-stage monitors do not record the peak at the same time, either being an hour later or 2 hours earlier. The sound peak timing cannot be changed since it is not related to the sound-stage ratings curve. I can observe that sound and stage peak time do not happen at the same time. In Chapter 4 I found that at maximum stage, there was variance within the sound, meaning peak stage and sound does not always match. Due to the mechanism involved in sound creation with relation to RE height, sound can become quieter after submergence. With Steele Gill and Highlands having RE heights at 0.21 m and 0.4 m, and peak stages of 0.29 m and 0.4 m respectively, they are at the point when sound can become quieter, meaning the peak sound may occur earlier or later than the peak stage. In regards to future events, when a flood is expected at these stations the stage will be higher than the RE height and therefore will not have the transitional sound discussed in Section 4.4.3.

With the sound only monitoring stations I cannot determine if the sound and stage peak occur at the same time, but can estimate their reliability with the timings of the EA gauges. The headwater catchments show similarity to the EA timings, with the exception of Arn Gill, which has a sound peak 8 hours earlier than observed at Steele Gill. There may be the effect of the sound transition occurring since Arn Gills' RE height is 0.25 m, and with concurrent measurements being taken at around that height I can assume the river reaches that stage. Another factor may be that the Arn Gill catchment is inherently different to the other headwater catchments.

If the sonohydrographs are to be used, then I can identify that the headwater catchments influence the River Gaunless from confluence at Steele Gill. We are seeing an unsynchronised outflow of the the headwaters meaning we are seeing a reduced peak and a longer duration of the higher

stage at Steele Gill. If the Arn Gill catchment was in sync with the other headwater catchments, then an additional drainage area of $3.6\,\mathrm{km}^2$ would be in combination with the others, leading to a higher combined stage at Steele Gill. By looking at the headwater catchments individually like this we are able to determine if flow is synchronised or unsynchronised. In future flood planning it would be intriguing to know if the peak experienced was due to synchronous flow or not. Meaning that if given a set rainfall, and that the rivers were close to flooding, than if the same rainfall occurred and the rivers were in sync then flooding may occur. Only by real-time monitoring of the headwaters would you be able to determine if flood peaks were occurring.

5.4.2 Water resource management

The River Gaunless catchment was chosen to test using sound as a surrogate measurement for stage due to spatey nature of the headwaters. The general hydrology of the Gaunless is interesting to river monitoring, since there are different pathways that the water can take, with the main tributaries all being significant contributors. Therefore if Crow Howle had a localised shower, then it would cause localised flooding, and propagate downstream in the Gaunless. Whereas monitors upstream of that point would not record a rise in stage.

Flooding has been found within the region of our study with properties employing their own flood prevention measures, such as flood screens and building levees to contain the smaller tributaries. These measures have been taken by the local communities at Crow Howle Beck and Gordon Beck. It is in these areas that a stage gauge would be of benefit, as it would allow both the people to know the state of the river but also to identify at what stages does property damage occur, allowing future mitigation strategies. The sound monitors found in the headwaters are useful for understanding if what is happening downstream, whereas the sound monitors found in community areas are for active flood management. I therefore assess the Crow Howle and Gordon Beck based upon their impact on the local community.

Crow Howle and Gordon Beck are considered to be significant tributaries with drainage areas of $8.5\,\mathrm{km}^2$ and $6.7\,\mathrm{km}^2$. There are 12 homes within the flooding zone of the Crow Howle Beck and 8 homes around Gordon Beck. Understanding therefore what the river is doing can therefore act

as either a reassurance to the homeowners or give them warning to a potential flood. With an R^2 value of 0.95 and 0.96 for the sound-stage ratings curve, I am confident that sound monitoring in these rivers is reliable enough to give an indication for this.

The sound-stage monitors could be used in a range of water resource management scenarios. I identify 3 areas that can use the existing sound-stage monitoring techniques: natural flood management (NFM) verification, the effect of land use on flooding and improvement of flood modelling. NFM has potential benefits, by helping to store and slow the flow of any rainfall event, reducing the peak (Black *et al.*, 2021). The verification of NFM has however heavily relied on modelling to rate the effectiveness, with only around 25% of studies using observed data (Kay *et al.*, 2019; Black *et al.*, 2021). I have shown that peak timing can be identified from sonohydrographs and their duration. By placing a monitor above and below any NFM structure, then the effect can be quantified.

Local land use has an impact at the local scale to flooding, influencing the timing and magnitude of the flood peak (O'Connell *et al.*, 2007). Pattison and Lane (2012) found that land use caused the most impact at small catchment scales, meaning that areas such as headwaters are suitable for monitoring land use impact. The inclusion of local land use in flood sensitivity is not well represented in modelling, and in data sparse areas is not feasible (Ewen *et al.*, 2013; Sanyal *et al.*, 2014). The headwater catchments of the Gaunless have different land uses, with Hindon Beck being a mixture of heather moorland and some farmed grassland, and Cow Close and Arn Gill being mainly farmed grassland according to the UKCEH Land Cover 2020 survey. A difference of land use may be impacting the peak times of the headwater channels discussed, with heather moorland being more retentive than farmed grassland causing a slowing of the peak (Ramchunder *et al.*, 2009). Both the farmed grassland dominant streams reach peak stage earlier than Hindon Beck with the predominantly heather moorland. In reference to the Gaunless' mining heritage, the profusion of EA gauges is to determine the amount of mining waste being transferred downstream. Sound monitoring could be beneficial for observing the spatial differences in peak stage and the hydrograph shape and used to monitor seasonal changes and impact of land use change or practice (Ott and Uhlenbrook, 2004; Mayes *et al.*, 2006).

The main use of the sound-stage monitors is for active flood gauging, giving a calculated stage for that reach, and indicating if the river has reached peak stage. However, that data can be used in flood model calibration and validation to improve future flood resilience and planning (Mazzoleni *et al.*, 2017). Our data is not an absolute value for river stage, and without comparing against in-water stage measuring I cannot guarantee that the stage produced will be highly accurate, but will give an approximate value within 5 cm of the true stage. That begs the question as to why might uncertain data be used in a flood model. Fava *et al.* (2019) found that using additional observed data with errors $\pm$ 10 cm can still improve model forecasting. Real-time monitoring of smaller catchments is useful in flood modelling since as was shown in Table 5.2, the catchments reached peak stage at different times, which subsequently affects the downstream portion. Starkey *et al.* (2017) found that by adding spatial density and ground truth data, not only improved flood forecasting but also localised catchment planning and its response. The network density of the Guanless with the EA gauges was already very high at 1 monitor per $13.8\,\mathrm{km}^2$, given that the UK average is $161\,\mathrm{km}^2$ and the global directive of $1875\,\mathrm{km}^2$ (WMO, 2008). Including the sound-stage monitors the network density of $5.1\,\mathrm{km}^2$ is now found at the Gaunless. I argue that such a high density of stations is a valuable resource, and in terms of cost and infrastructure is minimal for the insights gained.

5.5 Conclusion

Sound-stage monitors offer a new opportunity for flow gauging in areas where traditional gauging methods may be difficult, and as such I target headwater channels which have challenging bed topography. I have shown that the setup of the monitor requires calibration before any stage value can be calculated, with the best improvement of the reliability of data coming from taking stage measurements at both low and high stages. Although a minimum of two points can be used to fit a relationship, I recommend taking as many measurements as possible, to both calibrate and validate the data. The Gaunless network has shown spatial variability of the catchments in terms of peak stage timing, which is assumed to influence the flood peak intensity downstream. Understanding what is happening in the headwaters not only benefits the local communities, but also in future attempts to improve flood resilience and management. I propose that the future of sound-stage monitors is being used in community monitoring schemes in

which real-time data can be fed into local flood action groups. Alternatively additional gauging being used in research activities to validate results of NFM or flood models is feasible. Further work will need to be done to see if adding these extra gauges into a flood model will improve the model or if real-time data from the monitors can be used to update flood forecasting by knowing how the headwater catchments are responding.

> “No man ever steps in the same river twice, for it’s not the same river and he’s not the same man.
>
> Heraclitus ”

Chapter 6

Conclusion

In my thesis my research aim broke down into three main sections: How to monitor sound; Why is sound related to a river and What can sound be used for? Through a combination of fieldwork and experimental work I have addressed each of these questions and hereby give my conclusions on each of these sections.

6.1 How?

The project started with the ambiguous title of "Listening to Rivers", but how does one listen to a river and then extract any data from it? I set out to find a universal method to record and analyse sound data, removing the need to have a sensor positioned at the exact right spot or for it to be suspended over the top of the river. With the goal to have flexibility in mind, I developed the lowest median filter. The filter was designed with the basic principle that the sound of a river is constant, unlike the sound at a beach with the waves coming in and out. If the sound of a river is constant, then any other extraneous noise such as from wind should be able to be removed. In Section 2.2.3 the ability of the filter to take a noisy signal into a meaningful one was shown. The development of the filter is not limited to sub-aerial sound monitoring for rivers, but could also be beneficial to other sound monitoring projects.

Having developed a method to retain only the river sound data, the question of how sound can be measured by a river was explored. The questions of how close by a river do you need to be, or at what part was shown to be important if sound is to be used. The closer to the river you measure, the louder it will be, but if you are not able to be at the river, then a buffer zone of

around 5 m from the river will still be able to be used: as long as you can hear the river, then that area is suitable. Utilising the River Washburn and its planned releases, surveying a long reach of a river during both high and low flow helped to identify the places that generated to most sound. In sections where there was a large RE, the sound generated was far greater than if there were no REs or if they were small. Finding that REs were important to river sound generation means that future site selection for sound monitoring require a RE.

Storm Ciara and Dennis provided data at exactly the correct time, with a 1 in 10 year storm event. The data proves that sound can function during storm condition and that the lowest median filter is capable even during very windy weather. I showed that the frequency at which you monitor a river is not as simple as picking the same for all of them, and that the best frequency range is dependant on the river and the environmental conditions. A frequency range of between 1 - 2 kHz is the range I suggest to be used before any others are chosen, with the absence of any other data. The relationship between sound and stage was shown to be very good, ranging from a R^2 of 0.73 to 0.99.

Having shown that sound and river stage can form a relationship, I focussed on how the sound-stage data could be calibrated for an observer. Using sound by itself, without any concurrent stage measurements, you will not be able to calculate a stage value. You will be able to plot a sonohydrograph, so rising and falling limbs, and peak timings will be known. To assign a depth value to the sound data requires the creation of a sound-depth ratings curve, meaning reference depth and sound values need to be taken. As a general rule, the more data points to form the curve, the better, with a range of stage values being taken as with Chapter 3. This is not so dissimilar to how stage-discharge curves are produced, so should not be taken as a limitation of using sound.

6.2 Why?

Being able to monitor a rivers' sound in relation to depth raised the question, does this work? Using the Tees Barrage I was able to determine the source of river sound and how that links to

RE height and configuration. Knowing if there has to be a certain formulation of REs to have a better sound-depth relationship would be crucial in future deployments of sound monitors. I found that the heights of a RE was more important than the configuration of them. The height of the RE determined how smooth the relationship between sound and stage were, with shorter REs creating more scatter. Of significance was the interface when the stage and RE height met, with over-topping occurring.

With over-topping, the sound experienced a sudden rise in SPL, before falling after the submergence of the RE. Importantly the sound continued to rise after the submergence of an obstacle, meaning that as previously thought the RE does not need to be the same height as the depth that is wanting to be monitored. It is however apparent as the maximum depth of a river increases above an RE, the sound-depth relationship begins to become more scattered at higher depths. It would therefore be prudent to have multiple sound-depth points at these levels to construct a robust sound-depth ratings curve.

In addition to understanding how sound and depth relate to each other, the source of the sound of a river was identified as the white water being generated. By relating sound to the amount of white water in an image, I can add another site selection criteria in which white water must be present. I identified that the sound recorded from a hydrophone, underwater, was not as representative of stage as sub-aerial sound. It is also noted that underwater sound and the amount of white water also relate to each other, meaning that in hydrophone studies the detection of water stage changes may be being measured.

6.3 What?

The purpose of the project was to determine if listening to rivers can be used to infer a rivers' stage, which we have shown in the previous sections to be possible. However, the application of this technology was to address the lack of monitoring in areas deemed to be unnecessary to conventional monitoring, or without adequate gain of information. The headwater channels are a natural location for sound monitoring, and the network study carried out at the River Gaunless

goes some way to showcase what these additional monitoring locations can show. The network of locations took less than a half a day to setup 8 sound locations and then attending the sites over the course of a month to create a sound-stage curve. Showing the ease of deployment of a sound network and with continued calibration of a sound-depth ratings curve is promising. Future work in expanding into larger networks, over a greater area might help to fill in areas of the country that aren't being monitored.

6.4 Future work

In the course of the thesis I answered my three research questions which leaves a crucial one left, where next? In order to make sub-aerial sound a credible method for use in flood monitoring there will need to be long term studies to determine the seasonality of sound. In the UK, the majority of my monitoring occurred during Winter, which came with certain conditions, such as stable temperature. In areas which have larger swings in temperature, the affect on sound might become more pronounced, and skew any sound-stage relationships. Longer study durations will also determine if changes in REs will have any perceivable change in sound-stage relationships. I would therefore like to set-up a long term study on a section of river which has RE measurements being taken and tracked, such as from terrestrial laser scanning or drone imagery. That would answer the long term suitability of sound monitoring and if there is a life-expectancy to any relationships formed.

As a new form of river monitoring there are still questions to be asked around sound monitoring to make it reliable. I have gone some way to answer the main questions regarding sound, such as "will it work in the wind", and "what are the limits on sound". There are certain rivers chosen for sound monitoring that ended up performing poorly, and further data are needed to test my ideas', why they did do, such as Ramshaw on the Gaunless. Modelling, such as computational fluid dynamics, could be utilised to some degree to attempt to understand how a flow behaves over a range of depths, and if there are features of weirs or culverts that make sound monitoring a non-starter at these locations. Further modelling a river reach with the aim of determining the amount of white water produced would enable me to remotely assess a rivers' ability to have sound monitoring and determining the optimal placement of any sound monitor. Having

a model would improve on the work done at the WWC, as model runs similar to the WWC could be trialled to determine if the model is creating the same effect as the real-world. There is potentially a method to extract a rivers' stage using the amount of white water on it's surface, using remote imagery, or translating white water into a proxy for gas exchange.

6.5 Summary

Using sub-aerial sound to monitor a rivers' stage was a novel idea, which over the course of the project has been shown to be productive. The areas in which the insights gained from the project are two fold, research and consumer. The research potential of the devices are that they are easy to install and are cost effective, meaning the coverage of sound monitors can be far greater than that of traditional techniques. Coupled with the ease of deployment, anywhere a river makes a sound, is a potential site. I see sub-aerial sound not being limited to headwater channels, but for example deployed around ephemeral streams for flash flood warnings. Consumer use of sound has both potential benefits and drawbacks, especially if the sound-stage curves are badly calibrated. If advice is followed, then it is not beyond reason that someone can monitor for themselves or at community level a local river that has the potential of flooding.

Bibliography

Aberle, J., Branß, T., Eikenberg, R., Henry, P.-Y., and Olsen, N. R. B. (2022). Directional dependency of flow resistance in an unlined rock blasted hydropower tunnel. *Journal of Hydraulic Research*, 60(3):504–513.

Admiraal, D. M., Stansbury, J. S., and Haberman, C. J. (2004). Case Study: Particle Velocimetry in a Model of Lake Ogallala. *Journal of Hydraulic Engineering*, 130(7):599–607.

Adrian, J. (2005). Twenty years of particle image velocimetry. *Experiments in Fluids*, 39(2):159–169.

Ammari, H., Fitzpatrick, B., Gontier, D., Lee, H., and Zhang, H. (2017). Sub-wavelength focusing of acoustic waves in bubbly media. *Proceedings of the Royal Society A: Mathematical, Physical and Engineering Sciences*, 473(2208).

Anthony, R. E., Aster, R. C., Ryan, S., Rathburn, S., and Baker, M. G. (2018). Measuring Mountain River Discharge Using Seismographs Emplaced Within the Hyporheic Zone. *Journal of Geophysical Research: Earth Surface*, 123(2):210–228.

Atzori, L., Iera, A., and Morabito, G. (2010). The Internet of Things: A survey. *Computer Networks*, 54(15):2787–2805.

Baattrup-Pedersen, A., Larsen, S. E., Andersen, D. K., Jepsen, N., Nielsen, J., and Rasmussen, J. J. (2018). Headwater streams in the EU Water Framework Directive: Evidence-based decision support to select streams for river basin management plans. *Science of the Total Environment*, 613-614:1048–1054.

Bączyk, A., Piwiński, J., Kłoda, R., and Grygoruk, M. (2017). Survey on river water level measuring technologies: Case study for flood management purposes of the C2-SENSE project. *Advances in Intelligent Systems and Computing*, 543:610–623.

Banziger, R. and Burch, H. (1990). Acoustic sensors (hydrophones) as indicators for bed load transport in a mountain torrent. *Hydrology in mountainous regions I*, pages 207–214.

Barr, S. L., Johnson, S., Ming, X., Peppa, M., Dong, N., Wen, Z., Robson, C., Smith, L., James, P., Wilkinson, D., Heaps, S., Laing, Q., Xiao, W., Dawson, R., and Ranjan, R. (2020). Flood-Prepared: a Nowcasting System for Real-Time Impact Adaption To Surface Water Flooding in Cities. *ISPRS Annals of Photogrammetry, Remote Sensing and Spatial Information Sciences*, VI-4/W2-20:9–15.

Barrière, J., Oth, A., Hostache, R., and Krein, A. (2015). Bedload transport monitoring using seismic observations in a low-gradient rural gravel-bed stream. *Geophys. Res. Lett.*, 42:2294–2301.

Barton, J., Slingerland, R. R. L., Pittman, S., and Gabrielson, T. B. (2010). Monitoring coarse bedload transport with passive acoustic instrumentation: A field study. *US Geological Survey Scientific Investigations Report*, pages 38–51.

Barton, J. S., Slingerland, R. L., Gabrielson, T. B., and Johnson, P. a. (2005). Listening to Bedload: A Flume Study Relating Acoustic Response to Bedload Motion. *Proc. Federal Interagency Sediment Monitoring Instrument and Analysis Research Workshop*, pages 9–11.

Bathurst, J. C. (1978). Flow Resistance of Large-Scale Roughness. *ASCE J Hydraul Div*, 104(12):1587–1603.

Bathurst, J. C. (1985). Flow Resistance Estimation in Mountain Rivers. *Journal of Hydraulic Engineering*, 111(4):625–643.

Bathurst, J. C. (2002). At-a-site variation and minimum flow resistance for mountain rivers. *Journal of Hydrology*, 269(1-2):11–26.

Bedard, A. J. (2005). Low-Frequency Atmospheric Acoustic Energy Associated with Vortices Produced by Thunderstorms. *Monthly Weather Review*, 133(1):241–263.

Bedeus, K. and Ivicsics, L. (1964). *Observation of the noise of bed load*. General Assembly, Commission on Hydrometry.

Belleudy, P., Valette, A., and Graff, B. (2010). Monitoring of bedload in river beds with an hydrophone: first trials of signal analyses. *River Flow, Proc. 5th Int. Conf. on Fluvial ...*, pages 67–84.

Benda, L., Hassan, M. A., Church, M., and May, C. L. (2005). Geomorphology of steepland headwaters: The transition from hillslopes to channels. *Journal of the American Water Resources Association*, 41(4):835–851.

Bennett, O. and Hartwell-Naguib, S. (2014). Flood defence spending in England. Technical report, UK Government.

Benson, M. A. (1965). Allocation of Stream-Gauging Stations Within a Country. *IAHS Design of Hydrological Networks Symposium*, (67):222–228.

Bishop, M. P., Young, B. W., Huo, D., and Chi, Z. (2020). Spatial Analysis and Modeling in Geomorphology. In *Reference Module in Earth Systems and Environmental Sciences*. Elsevier.

Black, A., Peskett, L., MacDonald, A., Young, A., Spray, C., Ball, T., Thomas, H., and Werritty, A. (2021). Natural flood management, lag time and catchment scale: Results from an empirical nested catchment study. *Journal of Flood Risk Management*, 14(3):1–16.

Blume, T., van Meerveld, I., and Weiler, M. (2016). The role of experimental work in hydrological sciences – insights from a community survey. *Hydrological Sciences Journal*, pages 1–4.

Bolghasi, A., Ghadimi, P., and Feizi Chekab, M. A. (2017a). Low-frequency sound transmission through rough bubbly air–water interface at the sea surface. *Journal of Low Frequency Noise Vibration and Active Control*, 36(4):319–338.

Bolghasi, A., Ghadimi, P., and Feizi Chekab, M. A. (2017b). Sound attenuation in air–water media with rough bubbly interface at low frequencies considering bubble resonance dispersion. *Journal of the Brazilian Society of Mechanical Sciences and Engineering*, 39(12):4859–4871.

Borga, M., Stoffel, M., Marchi, L., Marra, F., and Jakob, M. (2014). Hydrogeomorphic response to extreme rainfall in headwater systems: Flash floods and debris flows. *Journal of Hydrology*, 518(PB):194–205.

Bradford, R. B. and Marsh, T. J. (2003). Defining a network of benchmark catchments for the UK. *Water Management*, 156(2):109–116.

Bragg, W. (1921). *The World of Sound*. Salzwasser-Verlag GmbH; Illustrated edition.

Brocchini, M. and Peregrine, D. (2001). The dynamics of strong turbulence at free surfaces. Part 1. Description. *Journal of Fluid Mechanics*, 449:225–254.

Burt, P. J. (1981). Fast filter transform for image processing. *Computer Graphics and Image Processing*, 16(1):20–51.

Burtin, A., Bollinger, L., Vergne, J., Cattin, R., and Nábělek, J. L. (2008a). Spectral analysis of seismic noise induced by rivers: A new tool to monitor spatiotemporal changes in stream hydrodynamics. *Journal of Geophysical Research*, 113(B5):1–14.

Burtin, A., Bollinger, L., Vergne, J., Cattin, R., and Nábělek, J. L. (2008b). Spectral analysis of seismic noise induced by rivers: A new tool to monitor spatiotemporal changes in stream hydrodynamics. *Journal of Geophysical Research: Solid Earth*, 113(5):1–14.

Burtin, A., Cattin, R., Bollinger, L., Vergne, J., Steer, P., Robert, A., Findling, N., and Tiberi, C. (2011a). Towards the hydrologic and bed load monitoring from high-frequency seismic noise in a braided river: The "torrent de St Pierre", French Alps. *Journal of Hydrology*, 408(1-2):43–53.

Burtin, A., Cattin, R., Bollinger, L., Vergne, J., Steer, P., Robert, A., Findling, N., and Tiberi, C. (2011b). Towards the hydrologic and bed load monitoring from high-frequency seismic noise in a braided river: The “torrent de St Pierre”, French Alps. *Journal of Hydrology*, 408(1-2):43–53.

Burtin, A., Hovius, N., and Turowski, J. M. (2016). Seismic monitoring of torrential and fluvial processes. *Earth Surface Dynamics*, 4(2):285–307.

Buytaert, W., Dewulf, A., De Bièvre, B., Clark, J., and Hannah, D. M. (2016). Citizen Science for Water Resources Management: Toward Polycentric Monitoring and Governance? *Journal of Water Resources Planning and Management*, 142(4).

Buytaert, W., Zulkafli, Z., Grainger, S., Acosta, L., Alemie, T. C., Bastiaensen, J., De BiÃ¨vre, B., Bhusal, J., Clark, J., Dewulf, A., Foggin, M., Hannah, D. M., Hergarten, C., Isaeva, A., Karpouzoglou, T., Pandeya, B., Paudel, D., Sharma, K., Steenhuis, T., Tilahun, S., Van Hecken, G., and Zhumanova, M. (2014). Citizen science in hydrology and water resources: opportunities for knowledge generation, ecosystem service management, and sustainable development. *Frontiers in Earth Science*, 2:26.

Cameron, D., Beven, K., Tawn, J., Blazkova, S., and Naden, P. (1999). Flood frequency estimation by continuous simulation for a gauged upland catchment (with uncertainty). *Journal of Hydrology*, 219(3-4):169–187.

Camp, L. W. and Farwell, R. W. (1972). Underwater Acoustics. *Physics Today*, 25(1):81–83.

Carbonneau, P. E. and Bergeron, N. E. (2000). The effect of bedload transport on mean and turbulent flow properties. *Geomorphology*, 35(3-4):267–278.

Carling, P. (1992). The nature of the fluid boundary layer and the selection of parameters for benthic ecology. *Freshwater Biology*, 28(2):273–284.

Chacon-Hurtado, J. C., Alfonso, L., and Solomatine, D. P. (2017). Rainfall and streamflow sensor network design: A review of applications, classification, and a proposed framework. *Hydrology and Earth System Sciences*, 21(6):3071–3091.

Chan, K., Schillereff, D. N., Baas, A. C., Chadwick, M. A., Main, B., Mulligan, M., O'Shea, F. T., Pearce, R., Smith, T. E., van Soesbergen, A., Tebbs, E., and Thompson, J. (2020). Low-cost electronic sensors for environmental research: Pitfalls and opportunities. *Progress in Physical Geography: Earth and Environment*, pages 305–338.

Chan, W. H. R., Johnson, P. L., and Moin, P. (2021). The turbulent bubble break-up cascade. Part 1. Theoretical developments. *Journal of Fluid Mechanics*, 912.

Chanson, H. (1996). Free-surface flows with near-critical flow conditions. *Canadian Journal of Civil Engineering*, 23(6):1272–1284.

Chanson, H. (2012). Advective Diffusion of Air Bubbles in Turbulent Water Flows. In *Fluid Mechanics of Environmental Interfaces*, chapter 7. CRC Press.

Chanson, H. and Toombes, L. (1998). Supercritical flow at an abrupt drop: Flow patterns and aeration. *Canadian Journal of Civil Engineering*, 25(5):956–966.

Chaves, H. (2012). A weather independent illumination for field LSPIV 2 . The basic concept of LSPIV. pages 9–12.

Chicharro, R. and Vazquez, A. (2014). The acoustic signature of gas bubbles generated in a liquid cross-flow. *Experimental Thermal and Fluid Science*, 55:221–227.

Clift, R., Grace, J., and Weber, M. (1978). *Bubbles, Drops, and Particles*. Cambridge University Press.

Comiti, F. and Lenzi, M. A. (2006). Dimensions of standing waves at steps in mountain rivers. *Water Resources Research*, 42(3).

Cuff, D., Hansen, M., and Kang, J. (2008). Urban sensing: Out of the woods. *Communications of the ACM*, 51(3):24–33.

Curtis, A. (2015). Valley of River Gaunless.

David, G. C., Wohl, E., Yochum, S. E., and Bledsoe, B. P. (2011). Comparative analysis of bed resistance partitioning in high-gradient streams. *Water Resources Research*, 47(7):1–22.

Deane, G. B. (1997). Sound generation and air entrainment by breaking waves in the surf zone. *The Journal of the Acoustical Society of America*, 102(5):2671–2689.

Del Grosso, V. A. and Mader, C. W. (1972). Speed of Sound in Pure Water. *The Journal of the Acoustical Society of America*, 52(5B):1442–1446.

Demeritt, D., Nobert, S., Cloke, H. L., and Pappenberger, F. (2013). The European Flood Alert System and the communication, perception, and use of ensemble predictions for operational flood risk management. *Hydrological Processes*, 27(1):147–157.

Demir, I. and Krajewski, W. F. (2013). Towards an integrated Flood Information System: Centralized data access, analysis, and visualization. *Environmental Modelling Software*, 50:77–84.

Dey, S., Raikar, R. V., and Roy, A. (2008). Scour at Submerged Cylindrical Obstacles under Steady Flow. *Journal of Hydraulic Engineering*, 134(1):105–109.

Di Baldassarre, G. and Claps, P. (2011). A hydraulic study on the applicability of flood rating curves. *Hydrology Research*, 42(1):10–19.

Di Baldassarre, G. and Montanari, A. (2009). Uncertainty in river discharge observations: a quantitative analysis. *Hydrology and Earth System Sciences*, 13(6):913–921.

Dimakis, A. G., Petrovic, D., and Ramchandran, K. (2006). From Dumb Wireless Sensors to Smart Networks using Network Coding. *arXivcsIT0601130 v1 31*.

Dixon, S. J., Sear, D. A., Odoni, N. A., Sykes, T., and Lane, S. N. (2016). The effects of river restoration on catchment scale flood risk and flood hydrology. *Earth Surface Processes and Landforms*, 41(7):997–1008.

Donratanapat, N., Samadi, S., Vidal, J. M., and Sadeghi Tabas, S. (2020). A national scale big data analytics pipeline to assess the potential impacts of flooding on critical infrastructures and communities. *Environmental Modelling and Software*, 133.

Dramais, G., Le Coz, J., Camenen, B., and Hauet, A. (2011). Advantages of a mobile LSPIV method for measuring flood discharges and improving stage–discharge curves. *Journal of Hydro-environment Research*, 5(4):301–312.

Dziak, R. P., Haxel, J. H., Matsumoto, H., Lau, T. K., Merle, S. G., de Ronde, C. E. J., Embley, R. W., and Mellinger, D. K. (2008). Observations of regional seismicity and local harmonic tremor at Brothers volcano, south Kermadec arc, using an ocean bottom hydrophone array. *Journal of Geophysical Research: Solid Earth*, 113(B8).

Dziewonski, A. and Romanowicz, B. (2015). Deep Earth Seismology: An Introduction and Overview. In *Treatise on Geophysics*, pages 1–28. Elsevier.

Eldwaik, O. and Li, F. (2018). Mitigating Wind Induced Noise in Outdoor Microphone Signals Using a Singular Spectral Subspace Method. *Technologies*, 6(1):19.

Elias, M., Kehl, C., and Schneider, D. (2019). Photogrammetric water level determination using smartphone technology. *The Photogrammetric Record*, 34(166):198–223.

Eltner, A., Elias, M., Sardemann, H., and Spieler, D. (2018). Automatic Image-Based Water Stage Measurement for Long-Term Observations in Ungauged Catchments. *Water Resources Research*, 54(12).

Environment Agency (2011). Hydrometric Data Feed User Manual. pages 1–39.

Environment Agency (2013). Flood risk management: information for flood risk management authorities, asset owners and local authorities - Detailed guidance - GOV.UK. Technical report.

Environment Agency (2015). Cost estimation for flood storage – summary of evidence. page 14.

Ergenzinger, P. and De Jong, C. (2003). Perspectives on bed load measurement. *IAHS-AISH Publication*, (283):113–125.

Escolà, A., Planas, S., Rosell, J. R., Pomar, J., Camp, F., Solanelles, F., Gracia, F., Llorens, J., and Gil, E. (2011). Performance of an ultrasonic ranging sensor in apple tree canopies. *Sensors*, 11(3):2459–2477.

Ewen, J., O'Donnell, G., Bulygina, N., Ballard, C., and O'Connell, E. (2013). Towards understanding links between rural land management and the catchment flood hydrograph. *Quarterly Journal of the Royal Meteorological Society*, 139(671):350–357.

Fava, M. C., Abe, N., Restrepo-Estrada, C., Kimura, B. Y. L., and Mendiondo, E. M. (2019). Flood modelling using synthesised citizen science urban streamflow observations. *Journal of Flood Risk Management*, 12(S2).

Feng, Y. and Sester, M. (2018). Extraction of pluvial flood relevant volunteered geographic information (VGI) by deep learning from user generated texts and photos. *ISPRS International Journal of Geo-Information*, 7(2).

Ferguson, R. (2010). Time to abandon the Manning equation? *Earth Surface Processes and Landforms*, 35(15):1873–1876.

Ferri, M., Wehn, U., See, L., and Fritz, S. (2019). The Value of Citizen Science for Flood Risk Reduction: Cost-benefit Analysis of a Citizen Observatory in the Brenta-Bacchiglione Catchment. *Hydrology and Earth System Sciences Discussions*, pages 1–27.

Ferro, V. (2003). Flow resistance in gravel-bed channels with large-scale roughness. *Earth Surface Processes and Landforms*, 28(12):1325–1339.

Flammer, G. H., Tullis, J. P., and Mason, E. S. (1970). Free Surface, Velocity Gradient Flow Past Hemisphere. *Journal of the Hydraulics Division*, 96(7):1485–1502.

Folz, C. A., Weaver, C., Blumentritt, D., Aufdenkampe, A. K., and Mundahl, N. (2018). Using customizable open source technology to develop a network of stream monitoring stations. Darrell W. Krueger Library.

Fonstad, M. A. and Zettler-Mann, A. (2020). The camera and the geomorphologist. *Geomorphology*, 366:107181.

Fourier, J. B. J. (1878). *The Analytical Theory of Heat*. Cambridge University Press, Cambridge.

Fraternali, P., Castelletti, A., Soncini-Sessa, R., Vaca Ruiz, C., and Rizzoli, A. (2012). Putting humans in the loop: Social computing for Water Resources Management. *Environmental Modelling Software*, 37:68–77.

Freeman, L. a., Carpenter, M. C., Rosenberry, D. O., Rousseau, J. P., Unger, R., and McLean, J. S. (2004). Use of Submersible Pressure Transducers in Water-Resources Investigations. *Techniques of Water-Resources Investigations 8-A3*, Book 8, In:1–65.

Fritz, K., Johnson, R., and Walters, D. (2006). Field Operations Manual for Assessing the Hydrologic Permanence and Ecological Condition of Headwater Streams. *U.S. Environmental Protection Agency, Office of Research and Development, Washington DC.*

Frizzel, W. (1987). *Noise Generation by Air Bubbles in Water: An Experimental Study of Creation and Splitting*. PhD thesis, The University of Minnesota.

Frost, G. L. (2001). Inventing Schemes and Strategies: The Making and Selling of the Fessenden Oscillator. *Technology and Culture*, 42(3):462–488.

Fujita, I., Muste, M., and Kruger, A. (1998). Large-scale particle image velocimetry for flow analysis in hydraulic engineering applications. *Journal of Hydraulic Research*, 36(3):397–414.

Gaál, L., Szolgay, J., Kohnová, S., Parajka, J., Merz, R., Viglione, A., and Blöschl, G. (2012). Flood timescales: Understanding the interplay of climate and catchment processes through comparative hydrology. *Water Resources Research*, 48(4).

Gandomi, A. and Haider, M. (2015). Beyond the hype: Big data concepts, methods, and analytics. *International Journal of Information Management*, 35(2):137–144.

Garcia, C., Laronne, J. B., and Sala, M. (2000). Continuous monitoring of bedload flux in a mountain gravel-bed river. *Geomorphology*, 34(1-2):23–31.

Gaunaurd, G. C. and Überall, H. (1981). Resonance theory of bubbly liquids. *The Journal of the Acoustical Society of America*, 69(2):362–370.

Geay, T., Belleudy, P., Gervaise, C., Habersack, H., Aigner, J., Kreisler, A., Seitz, H., and Laronne, J. B. (2017). Passive acoustic monitoring of bed load discharge in a large gravel bed river.

Geay, T., Michel, L., Zanker, S., and Robert Rigby, J. (2019). Acoustic wave propagation in rivers: An experimental study. *Earth Surface Dynamics*, 7(2):537–548.

Genç, O., Ardıçlıoğlu, M., and Ağıralioğlu, N. (2015). Calculation of mean velocity and discharge using water surface velocity in small streams. *Flow Measurement and Instrumentation*, 41:115–120.

Geng, Y., Edwards, R. M., Davis, J. G., Lepper, P., Pattison, I., Khouakhi, A., Clark, B., Diamantides, K., Dai, C., Kaczmarczyk, M., Licea, V. R., Lopez, J., Cano, O. M., and Santos, R. A. (2019). Impact of Heavy Rain on Signal Propagation in the UK and Mexican 4G and 5G Networks. *13th European Conference on Antennas and Propagation, EuCAP 2019*.

Gilmore, T. E., Birgand, F., and Chapman, K. W. (2013). Source and magnitude of error in an inexpensive image-based water level measurement system. *Journal of Hydrology*, 496:178–186.

Gimbert, F., Tsai, V. C., and Lamb, M. P. (2014). A physical model for seismic noise generation by turbulent flow in rivers. *Journal of Geophysical Research: Earth Surface*, 119:1–30.

Gomi, T., Sidle, R. C., and Richardson, J. S. (2002). Understanding processes and downstream linkages of headwater systems. *BioScience*, 52(10):905–916.

Gordon, R. L. (1989). Acoustic Measurement of River Discharge. *Journal of Hydraulic Engineering*, 115(7):925–936.

Govi, M., Maraga, F., and Moia, F. (1993). Seismic detectors for continuous bed load monitoring in a gravel stream. *Hydrological Sciences Journal*, 38(2):123–132.

Gray, J. R., Laronne, J. B., and Marr, J. D. G. (2010). Bedload-surrogate monitoring technologies. *U.S. Geological Survey Scientific Investigations Report*, 5091:1–37.

Hall, R. O., Kennedy, T. A., and Rosi-Marshall, E. J. (2012). Air-water oxygen exchange in a large whitewater river. *Limnology and Oceanography: Fluids and Environments*, 2(1):1–11.

Hall, S. and Crockford, G. (1973). The Physical Environment. In *Occupational Health Practice*, pages 258–287. Elsevier.

Harris, C. M. (1966). Absorption of Sound in Air versus Humidity and Temperature. *The Journal of the Acoustical Society of America*, 40(1):148–159.

Harvey, A. (1971). Seasonal flood behaviour in a clay catchment. *Journal of Hydrology*, 12(2):129–144.

Hauet, A., Kruger, A., Krajewski, W. F., Bradley, A., Muste, M., Creutin, J.-D., and Wilson, M. (2008). Experimental System for Real-Time Discharge Estimation Using an Image-Based Method. *Journal of Hydrologic Engineering*, 13(2):105–110.

Hayes, B. (2009). Viva Voce. *American Scientist*, 97(6):513.

Herbich, J. B. and Shulits, S. (1964). Large-Scale Roughness in Open-Channel Flow. *Journal of the Hydraulics Division*, 90(6):203–230.

Herschy, R. W. (2008). *Streamflow Measurement*. CRC Press.

Horii, Y., Hong, W., Tamaki, A., and Kitamura, T. (2018). Extraordinary Acoustic Transmission in Human Hearing System. *Progress in Electromagnetics Research Symposium*, 2018-Augus:2393–2398.

Horsburgh, J. S., Caraballo, J., Ramírez, M., Aufdenkampe, A. K., Arscott, D. B., and Damiano, S. G. (2019a). Low-cost, open-source, and low-power: But what to do with the data? *Frontiers in Earth Science*, 7:1–14.

Horsburgh, J. S., Caraballo, J., Ramírez, M., Aufdenkampe, A. K., Arscott, D. B., and Damiano, S. G. (2019b). Low-cost, open-source, and low-power: But what to do with the data? *Frontiers in Earth Science*, 7.

Hortobágyi, B., Perks, M. T., Russell, A. J., and Dussaillant, A. (2019). Handbook for Surface Flow Velocity Measurement. *Preprints 2019*.

Hsu, L., Finnegan, N. J., and Brodsky, E. E. (2011). A seismic signature of river bedload transport during storm events. *Geophysical Research Letters*, 38(13):1–6.

Huang, Z.-G. and Shiu, S.-J. (2015). Design and analysis of diaphragms in dynamic microphones. *Advances in Mechanical Engineering*, 7(7).

Hudspeth, A. J. (1989). How the ear's works work. *Nature*, 341(6241):397–404.

Hughes, D., Greenwood, P., Blair, G., Coulson, G., Pappenberger, F., Smith, P., and Beven, K. J. (2006). An Intelligent and Adaptable Grid-based Flood Monitoring and Warning System. *Proceedings of the UK E-Science All Hands Meeting*, pages 53–60.

Hundt, S. and Blasch, K. (2019). Laboratory assessment of alternative stream velocity measurement methods. *PLoS ONE*, 14(9):1–21.

Hunter, J., Alabri, A., and Van Ingen, C. (2013). Assessing the quality and trustworthiness of citizen science data. *Concurrency Computation Practice and Experience*, 25(4):454–466.

Ibeje, A. O. (2019). Use of Lower-Order and Higher–Order Streams in Modelling the Rating Curve. *Water Resources Management*, 33(2):819–830.

Indoware (2013). Ultrasonic Ranging Module HC - SR04. *Datasheet*, pages 1–4.

IPCC (2014). *Climate Change 2014 Part A: Global and Sectoral Aspects*. IPCC.

Irarrazabal, P. and Nishimura, D. G. (1995). Fast Three Dimensional Magnetic Resonance Imaging. *Magnetic Resonance in Medicine*, 33(5):656–662.

Iskander, M. (2018). Geotechnical Underground Sensing and Monitoring. In *Underground Sensing*, pages 141–202. Elsevier.

Iwahashi, M. and Udomsiri, S. (2007). Water level detection from video with fir filtering. *Proceedings - International Conference on Computer Communications and Networks, ICCCN*, pages 826–831.

Jalbert, J., Mathevet, T., and Favre, A. C. (2011). Temporal uncertainty estimation of discharges from rating curves using a variographic analysis. *Journal of Hydrology*, 397(1-2):83–92.

Jarrett, R. D. (1984). Hydraulics of High-Gradient Streams. *Journal of Hydraulic Engineering*, 110(11):1519–1539.

Javelle, P., Fouchier, C., Arnaud, P., and Lavabre, J. (2010). Flash flood warning at ungauged locations using radar rainfall and antecedent soil moisture estimations. *Journal of Hydrology*, 394(1-2):267–274.

Joo, H., Jun, H., Lee, J., and Kim, H. S. (2019). Assessment of a stream gauge network using upstream and downstream runoff characteristics and entropy. *Entropy*, 21(7).

Jousset, P., Neuberg, J., and Sturton, S. (2003). Modelling the time-dependent frequency content of low-frequency volcanic earthquakes. *Journal of Volcanology and Geothermal Research*, 128(1-3):201–223.

Kavage Adams, R. and Spotila, J. A. (2005). The form and function of headwater streams based on field and modeling investigations in the Southern Appalachian Mountains. *Earth Surface Processes and Landforms*, 30(12):1521–1546.

Kay, A. L., Old, G. H., Bell, V. A., Davies, H. N., and Trill, E. J. (2019). An assessment of the potential for natural flood management to offset climate change impacts. *Environmental Research Letters*, 14(4).

Kean, J. W. and Smith, J. D. (2006). Form drag in rivers due to small-scale natural topographic features: 1. Regular sequences. *Journal of Geophysical Research*, 111(F4):F04009.

Khairetdinov, M. S., Kovalevsky, V. V., Shimanskaya, G. M., Sedukhina, G. F., and Yakimenko, A. A. (2020). Active monitoring technology in studying the interaction of geophysical fields. In *Active Geophysical Monitoring*, pages 207–222. Elsevier.

Kiang, J. E., Gazoorian, C., McMillan, H., Coxon, G., Le Coz, J., Westerberg, I. K., Belleville, A., Sevrez, D., Sikorska, A. E., Petersen-Øverleir, A., Reitan, T., Freer, J., Renard, B., Mansanarez, V., and Mason, R. (2018). A Comparison of Methods for Streamflow Uncertainty Estimation. *Water Resources Research*, 54(10):7149–7176.

Kim, J., Han, Y., and Hahn, H. (2011). Embedded implementation of image-based water-level measurement system. *IET Computer Vision*, 5(2):125.

Kim, S., Mankoff, J., and Paulos, E. (2013). Sensr: Evaluating a flexible framework for authoring mobile data-collection tools for citizen science. *Proceedings of the ACM Conference on Computer Supported Cooperative Work, CSCW*, pages 1453–1462.

Klaus, M., Geibrink, E., Hotchkiss, E. R., and Karlsson, J. (2019). Listening to air–water gas exchange in running waters. *Limnology and Oceanography: Methods*, 17(7):395–414.

Kolmogorov, A. (1949). On the fragmentation of drops in a turbulent flow. *Proceedings of the USSR Academy of Sciences*.

Krein, A., Klinck, H., Eiden, M., Symader, W., Bierl, R., Hoffmann, L., and Pfister, L. (2008). Investigating the transport dynamics and the properties of bedload material with a hydro-acoustic measuring system. *Earth Surface Processes and Landforms*, 33(1):152–163.

Krein, A., Schenkluhn, R., Kurtenbach, A., Bierl, R., and Barrière, J. (2016). Listen to the sound of moving sediment in a small gravel-bed river. *International Journal of Sediment Research*, 31(3):271–278.

Krohn, C. E. and Chen, S. T. (1992). Comparisons of downhole geophones and hydrophones. *GEOPHYSICS*, 57(6):841–847.

Kröhnert, M. and Eltner, A. (2018). VERSATILE MOBILE AND STATIONARY LOW-COST APPROACHES FOR HYDROLOGICAL MEASUREMENTS. *ISPRS - International Archives of the Photogrammetry, Remote Sensing and Spatial Information Sciences*, XLII-2:543–550.

Kruger, A., Krajewski, W. F., Niemeier, J. J., Ceynar, D. L., and Goska, R. (2016). Bridge-mounted river stage sensors (BMRSS). *IEEE Access*, 4:8948–8966.

Krull, B., Tschisgale, S., and Frohlich, J. (2016). An immersed boundary method for complex-shaped bubbles represented by spherical harmonic functions. In *Conference: 9th International Conference on Multiphase Flow (ICMF)*.

Kucukali, S. and Cokgor, S. (2008). Boulder-flow interaction associated with self-aeration process. *Journal of Hydraulic Research*, 46(3):415–419.

Kumar, S. and Brennen, C. E. (1991). Nonlinear effects in the dynamics of clouds of bubbles. *The Journal of the Acoustical Society of America*, 89(2):707–714.

Kummu, M., de Moel, H., Ward, P. J., and Varis, O. (2011). How Close Do We Live to Water? A Global Analysis of Population Distance to Freshwater Bodies. *PLoS ONE*, 6(6).

Kundzewicz, Z. W. (2016). 15 Floods : lessons about early warning systems. pages 347–368.

Lamb, M. P., Brun, F., and Fuller, B. M. (2017). Hydrodynamics of steep streams with planar coarse-grained beds: Turbulence, flow resistance, and implications for sediment transport. *Water Resources Research*, 53(3):2240–2263.

Lauridsen, M., Nguyen, H., Vejlgaard, B., Kovacs, I. Z., Mogensen, P., and Sorensen, M. (2017). Coverage Comparison of GPRS, NB-IoT, LoRa, and SigFox in a 7800 km Area. *IEEE Vehicular Technology Conference*, 2017-June.

Lawrence, D. S. (2000). Hydraulic resistance in overland flow during partial and marginal surface inundation: Experimental observations and modeling. *Water Resources Research*, 36(8):2381–2393.

Le Coz, J., Hauet, A., Pierrefeu, G., Dramais, G., and Camenen, B. (2010). Performance of image-based velocimetry (LSPIV) applied to flash-flood discharge measurements in Mediterranean rivers. *Journal of Hydrology*, 394(1-2):42–52.

Le Guern, J., Rodrigues, S., Geay, T., Zanker, S., Hauet, A., Tassi, P., Claude, N., Jugé, P., Duperray, A., and Vervynck, L. (2021). Relevance of acoustic methods to quantify bedload transport and bedform dynamics in a large sandy-gravel-bed river. *Earth Surface Dynamics*, 9(3):423–444.

Leduc, P., Ashmore, P., and Sjogren, D. (2018). Technical note: Stage and water width measurement of a mountain stream using a simple time-lapse camera. *Hydrology and Earth System Sciences*, 22(1):1–11.

Legleiter, C. J., Kinzel, P. J., and Nelson, J. M. (2017). Remote measurement of river discharge using thermal particle image velocimetry (PIV) and various sources of bathymetric information. *Journal of Hydrology*, 554:490–506.

Leighton, T. (1994). The Sound Field. In *The Acoustic Bubble*, pages 1–66. Elsevier.

Leighton, T., White, P., and Finfer, D. (2005). Possible applications of bubble acoustics in nature (Opening Invited .... *Eprints.Soton.Ac.Uk*, (section 3).

Leighton, T. G. (2012). How can humans, in air, hear sound generated underwater (and can goldfish hear their owners talking)? *The Journal of the Acoustical Society of America*, 131(3):2539–2542.

Lin, I.-C., Hsieh, Y.-R., Shieh, P.-F., Chuang, H.-C., and Chou, L.-C. (2014). The effect of wind on low frequency noise. *Proceedings of INTER-NOISE 2014*, pages 1–12.

Lin, Y.-T., Lin, Y.-C., and Han, J.-Y. (2018). Automatic water-level detection using single-camera images with varied poses. *Measurement*, 127:167–174.

Linke, S., Gifford, T., Desjonquères, C., Tonolla, D., Aubin, T., Barclay, L., Karaconstantis, C., Kennard, M. J., Rybak, F., and Sueur, J. (2018). Freshwater ecoacoustics as a tool for continuous ecosystem monitoring. *Frontiers in Ecology and the Environment*, 16(4):231–238.

Liu, Y., Jia, Y. B., Zhang, X. J., Liu, Z. C., Ren, Y. C., and Yang, B. (2013). Noise Test and Analysis of Automobile Engine. In *Mechatronics and Computational Mechanics*, volume 307 of *Applied Mechanics and Materials*, pages 196–199. Trans Tech Publications Ltd.

Lo, S. W., Wu, J. H., Lin, F. P., and Hsu, C. H. (2015). Cyber surveillance for flood disasters. *Sensors (Switzerland)*, 15(2):2369–2387.

Long, M. (2014). Fundamentals of Acoustics. In *Architectural Acoustics*, pages 39–79. Elsevier.

Lu, J. Y., Su, C. C., and Wang, C. Y. (2006). Application of a portable measuring system with acoustic Doppler current profiler to discharge observations in steep rivers. *Flow Measurement and Instrumentation*, 17(3):179–192.

Lueth, K. L. (2018). State of the IoT 2018 – Analyst Insights from Q1/Q2 2018. Technical report, IoT Analytics.

Lugli, M. and Fine, M. L. (2007). Stream ambient noise, spectrum and propagation of sounds in the goby Padogobius martensii: Sound pressure and particle velocity. *The Journal of the Acoustical Society of America*, 122(5):2881.

MacDonald, L. H. and Coe, D. (2007). Influence of headwater streams on downstream reaches in forested areas. *Forest Science*, 53(2):148–168.

Manasseh, R., Babanin, A. V., Forbes, C., Rickards, K., Bobevski, I., and Ooi, A. (2006). Passive acoustic determination of wave-breaking events and their severity across the spectrum. *Journal of Atmospheric and Oceanic Technology*, 23(4):599–618.

Manasseh, R., Riboux, G., Bui, A., and Risso, F. (2007). Sound emission on bubble coalescence: Imaging, acoustic and numerical experiments. *Proceedings of the 16th Australasian Fluid Mechanics Conference, 16AFMC*, (December):167–173.

Marin-Perez, R., García-Pintado, J., and Gómez, A. S. (2012). A real-time measurement system for long-life flood monitoring and warning applications. *Sensors*, 12(4):4213–4236.

Marineau, M. D., Minear, J. T., and Wright, S. A. (2015). Using hydrophones as a surrogate monitoring technique to detect temporal and spatial variability in bedload transport. *10th Federal Interagency Sedimentation Conference*, page 12.

Marsh, T. (2002). Capitalising on river flow data to meet changing national needs-a UK perspective. Technical report.

Marsh, T. and Hannaford, J. (2008). *UK hydrometric register : a catalogue of river flow gauging stations and observation wells and boreholes in the United Kingdom together with summary hydrometric and spatial statistics*. Centre for Ecology and Hydrology.

Matson, W. (2016). Natural and driven frequencies. In *Earthquakes The sound of multi-modal waves*. IOP Publishing.

Mayes, W., Walsh, C., Bathurst, J., Kilsby, C., Quinn, P., Wilkinson, M., Daugherty, A., and O'Connell, P. (2006). Monitoring a flood event in a densely instrumented catchment, the Upper Eden, Cumbria, UK. *Water and Environment Journal*, 20(4):217–226.

Mazzoleni, M., Verlaan, M., Alfonso, L., Monego, M., Norbiato, D., Ferri, M., and Solomatine, D. P. (2017). Can assimilation of crowdsourced data in hydrological modelling improve flood prediction? *Hydrology and Earth System Sciences*, 21(2):839–861.

McCabe, M. F., Rodell, M., Alsdorf, D. E., Miralles, D. G., Uijlenhoet, R., Wagner, W., Lucieer, A., Houborg, R., Verhoest, N. E. C., Franz, T. E., Shi, J., Gao, H., and Wood, E. F. (2017). The future of Earth observation in hydrology. *Hydrology and Earth System Sciences*, 21(7):3879–3914.

McCuen, R. H., Knight, Z., and Cutter, A. G. (2006). Evaluation of the Nash–Sutcliffe Efficiency Index. *Journal of Hydrologic Engineering*, 11(6):597–602.

McMillan, H., Freer, J., Pappenberger, F., Krueger, T., and Clark, M. (2010). Impacts of uncertain river flow data on rainfall-runoff model calibration and discharge predictions. *Hydrological Processes*, 24(10):1270–1284.

McMillan, H., Krueger, T., and Freer, J. (2012). Benchmarking observational uncertainties for hydrology: Rainfall, river discharge and water quality. *Hydrological Processes*, 26(26):4078–4111.

McMillan, H. K. and Westerberg, I. K. (2015). Rating curve estimation under epistemic uncertainty. *Hydrological Processes*, 29(7):1873–1882.

Mella, D., Brevis, W., Higham, J., Racic, V., and Susmel, L. (2019). Image-based tracking technique assessment and application to a fluid–structure interaction experiment. *Proceedings of the Institution of Mechanical Engineers, Part C: Journal of Mechanical Engineering Science*, 233(16):5724–5734.

Meng, X., Nandagopal, T., Li, L., and Lu, S. (2006). Contour maps: Monitoring and diagnosis in sensor networks. *Computer Networks*, 50(15):2820–2838.

Mennitt, D. and Fristrup, K. (2012). Obtaining calibrated sound pressure levels from consumer digital audio recorders. *Applied Acoustics*, 73(11):1138–1145.

Minnaert, M. (1933). XVI. On musical air-bubbles and the sounds of running water. *The London, Edinburgh, and Dublin Philosophical Magazine and Journal of Science*, 16(104):235–248.

Mishra, A. K. and Coulibaly, P. (2009). Developments in hydrometric network design: A review. *Reviews of Geophysics*, 47(2).

Mitra, P., Ray, R., Chatterjee, R., Basu, R., Saha, P., Raha, S., Barman, R., Patra, S., Biswas, S. S., and Saha, S. (2016). Flood forecasting using Internet of things and artificial neural networks. In *2016 IEEE 7th Annual Information Technology, Electronics and Mobile Communication Conference (IEMCON)*, pages 1–5. IEEE.

Mohd Sabre, M. S., Abdullah, S. S., and Faruq, A. (2019). Flood Warning and Monitoring System Utilizing Internet of Things Technology. *KINETIK: Game Technology, Information System, Computer Network, Computing, Electronics, and Control*, pages 287–296.

Monsalve, A., Yager, E. M., and Schmeeckle, M. W. (2017). Effects of Bed Forms and Large Protruding Grains on Near-Bed Flow Hydraulics in Low Relative Submergence Conditions. *Journal of Geophysical Research: Earth Surface*, 122(10):1845–1866.

Monson, B. B., Hunter, E. J., Lotto, A. J., and Story, B. H. (2014). The perceptual significance of high-frequency energy in the human voice. *Frontiers in Psychology*, 5:587.

Moreno, C., Aquino, R., Ibarreche, J., Pérez, I., Castellanos, E., Álvarez, E., Rentería, R., Anguiano, L., Edwards, A., Lepper, P., Edwards, R. M., and Clark, B. (2019). RiverCore: IoT Device for River Water Level Monitoring over Cellular Communications. *Sensors*, 19(1):127.

Morse, N., Bowden, W. B., Hackman, A., Pruden, C., Steiner, E., and Berger, E. (2007). Using sound pressure to estimate reaeration in streams. *Journal of the North American Benthological Society*, 26(1):28–37.

Moy de Vitry, M., Kramer, S., Wegner, J. D., and Leitão, J. P. (2019). Scalable flood level trend monitoring with surveillance cameras using a deep convolutional neural network. *Hydrology and Earth System Sciences*, 23(11):4621–4634.

Muraro, F., Dolcetti, G., Nichols, A., Tait, S. J., and Horoshenkov, K. V. (2021). Free-surface behaviour of shallow turbulent flows. *Journal of Hydraulic Research*, 59(1):1–20.

Muste, M., Fujita, I., and Hauet, A. (2008). Large-scale particle image velocimetry for measurements in riverine environments. *Water Resources Research*, 44(4).

Muste, M., Yu, K., and Spasojevic, M. (2004). Practical aspects of ADCP data use for quantification of mean river flow characteristics; Part I: moving-vessel measurements. *Flow Measurement and Instrumentation*, 15(1):1–16.

Nardi, F., Cudennec, C., Abrate, T., Allouch, C., Annis, A., Assumpção, T., Aubert, A. H., Bérod, D., Braccini, A. M., Buytaert, W., Dasgupta, A., Hannah, D. M., Mazzoleni, M., Polo, M. J., Sæbø, Ø., Seibert, J., Tauro, F., Teichert, F., Teutonico, R., Uhlenbrook, S., Wahrmann Vargas, C., and Grimaldi, S. (2021). Citizens AND HYdrology (CANDHY):

conceptualizing a transdisciplinary framework for citizen science addressing hydrological challenges. *Hydrological Sciences Journal*, pages 1–18.

Nardone, P. and Koll, K. (2016). Drag force of elements mounted on a rough bed considering relative submergence. pages 1–3.

Nash, J. and Sutcliffe, J. (1970). River flow forecasting through conceptual models part I — A discussion of principles. *Journal of Hydrology*, 10(3):282–290.

Nasution, T. H., Siagian, E. C., Tanjung, K., and Soeharwinto (2018). Design of river height and speed monitoring system by using Arduino. *IOP Conference Series: Materials Science and Engineering*, 308(1).

Nitsche, M., Rickenmann, D., Kirchner, J. W., Turowski, J. M., and Badoux, A. (2012). Macroroughness and variations in reach-averaged flow resistance in steep mountain streams. *Water Resources Research*, 48(12):1–16.

Norbiato, D., Borga, M., Degli Esposti, S., Gaume, E., and Anquetin, S. (2008). Flash flood warning based on rainfall thresholds and soil moisture conditions: An assessment for gauged and ungauged basins. *Journal of Hydrology*, 362(3-4):274–290.

Ocio, D., Le Vine, N., Westerberg, I., Pappenberger, F., and Buytaert, W. (2017). The role of rating curve uncertainty in real-time flood forecasting. *Water Resources Research*, 53(5):4197–4213.

O'Connell, E., Ewen, J., O'Donnell, G., and Quinn, P. (2007). Is there a link between agricultural land-use management and flooding? *Hydrology and Earth System Sciences*, 11(1):96–107.

Ohki, M., Zervakis, M. E., and Venetsanopoulos, A. N. (1995). 3-D Digital filters. In *Control and Dynamic Systems*, volume 69, pages 49–88.

Oppenheim, A. and Weinstein, C. (1972). Effects of finite register length in digital filtering and the fast Fourier transform. *Proceedings of the IEEE*, 60(8):957–976.

Osborne, W. A., Hodge, R. A., Love, G. D., Hawkin, P., and Hawkin, R. E. (2021). Babbling brook to thunderous torrent: Using sound to monitor river stage. *Earth Surface Processes and Landforms*, 46(13):2656–2670.

Ott, B. and Uhlenbrook, S. (2004). Quantifying the impact of land-use changes at the event and seasonal time scale using a process-oriented catchment model. *Hydrology and Earth System Sciences*, 8(1):62–78.

Ottewill, M. (2013). Complex sounds.

Ouro, P., Wilson, C. A. M. E., Evans, P., and Angeloudis, A. (2017). Large-eddy simulation of shallow turbulent wakes behind a conical island. *Physics of Fluids*, 29(12).

Pacholski, C., Sartor, M., Sailor, M. J., Cunin, F., and Miskelly, G. M. (2005). Biosensing Using Porous Silicon Double-Layer Interferometers: Reflective Interferometric Fourier Transform Spectroscopy. *Journal of the American Chemical Society*, 127(33):11636–11645.

Pan, J., Yin, Y., Xiong, J., Luo, W., Gui, G., and Sari, H. (2018). Deep Learning-Based Unmanned Surveillance Systems for Observing Water Levels. *IEEE Access*, 6:73561–73571.

Panda, K. G., Agrawal, D., Nshimiyimana, A., and Hossain, A. (2016). Effects of environment on accuracy of ultrasonic sensor operates in millimetre range. *Perspectives in Science*, 8:574–576.

Papanicolaou, A., Tsakiris, A., and Kramer, C. (2010). Effects of relative submergence on flow and sediment patterns around clasts. *International Conference on Fluvial Hydraulics, River Flow 2010*, pages 793–799.

Patalano, A., García, C. M., Guillén, N., García, C., Díaz, É., Rodriguez, A., and Ravelo, A. (2014). Evaluación Experimental De La Técnica De Velocimetría Por Seguimiento De Partículas A Gran Escala Para La Determinación De Caudales En Ríos Serranos. *Aqua-LAC UNESCO*, 6:17–24.

Patalano, A., García, C. M., and Rodríguez, A. (2017). Rectification of Image Velocity Results (RIVeR): A simple and user-friendly toolbox for large scale water surface Particle Image Velocimetry (PIV) and Particle Tracking Velocimetry (PTV). *Computers and Geosciences*, 109:323–330.

Pattison, I. and Lane, S. N. (2012). The link between land-use management and fluvial flood risk. *Progress in Physical Geography: Earth and Environment*, 36(1):72–92.

Pažourková, E., Křeček, J., Bitušík, P., Chvojka, P., Kamasová, L., Senoo, T., Špaček, J., and Stuchlík, E. (2021). Impacts of an extreme flood on the ecosystem of a headwater stream. *Journal of Limnology*.

Pedersen, Ø. and Rüther, N. (2016). Hybrid Modeling of a Gauging Station Rating Curve. *Procedia Engineering*, 154:433–440.

Perera, D., Seidou, O., Agnihotri, J., Rasmy, M., Smakhtin, V., Coulibaly, P., and Mehmood, H. (2019). Flood Early Warning Systems: A Review Of Benefits, Challenges And Prospects 08. UNU-INWEH Report Series, Issue 08.

Perks, M. T., Russell, A. J., and Large, A. R. G. (2016). Technical Note: Advances in flash flood monitoring using unmanned aerial vehicles (UAVs). *Hydrology and Earth System Sciences*, 20(10):4005–4015.

Perrin, C., Oudin, L., Andreassain, V., Rojas-Serna, C., Michel, C., and Mathevet, T. (2007). Impact of limited streamflow data on the efficiency and the parameters of rainfall—runoff models. *Hydrological Sciences Journal*, 52(1):131–151.

Petersen-Øverleir, A. and Reitan, T. (2009). Accounting for rating curve imprecision in flood frequency analysis using likelihood-based methods. *Journal of Hydrology*, 366(1-4):89–100.

Petrut, T., Geay, T., Gervaise, C., Belleudy, P., and Zanker, S. (2018). Passive acoustic measurement of bedload grain size distribution using self-generated noise. *Hydrology and Earth System Sciences*, 22(1):767–787.

Philip, E. and McLaughlin, J. (2018). Evaluation of Stream Gauge Density and Implementing the Concept of Virtual Gauges in Northern Ontario for Watershed Modeling. *Journal of Water Management Modeling*.

Piégay, H. (2017). Quantitative Geomorphology. In *International Encyclopedia of Geography: People, the Earth, Environment and Technology*, pages 1–3. John Wiley Sons, Ltd, Oxford, UK.

Pool, S. and Seibert, J. (2021). Gauging ungauged catchments – Active learning for the timing of point discharge observations in combination with continuous water level measurements. *Journal of Hydrology*, 598(January):126448.

Powell, D. M. (2014). Flow resistance in gravel-bed rivers: Progress in research. *Earth-Science Reviews*, 136:301–338.

Quinn, A. J. and Bederson, B. B. (2011). Human computation. In *Proceedings of the 2011 annual conference on Human factors in computing systems - CHI '11*, page 1403, New York, New York, USA. ACM Press.

Rabie, A., Peterson, E., Kostelnick, J., and Rowley, R. (2017). Optimizing Digital Elevation Model Resolution Inputs and Number of Stream Gauges in Geographic Information System Predictions of Flood Inundation: a Case Study Along the Illinois River, Usa. *Environmental and Engineering Geoscience*, 23(4):345–357.

Ragnoli, M., Barile, G., Leoni, A., Ferri, G., and Stornelli, V. (2020). An autonomous low-power lora-based flood-monitoring system. *Journal of Low Power Electronics and Applications*, 10(2).

Rahmtalla, A., Mohamed, A., and Wei, W. G. (2014). Real Time Wireless Flood Monitoring System Using Ultrasonic Waves. *International Journal of Science and Research*, 3(8):2012–2015.

Ramchunder, S., Brown, L., and Holden, J. (2009). Environmental effects of drainage, drain-blocking and prescribed vegetation burning in UK upland peatlands. *Progress in Physical Geography: Earth and Environment*, 33(1):49–79.

Ramsbottom, D. M. and Whitlow, C. D. (2003). Extension of Rating Curves at Gauging Stations: Best Practice Guidance Manual. page 257.

Ran, Q. H., Li, W., Liao, Q., Tang, H. L., and Wang, M. Y. (2016). Application of an automated LSPIV system in a mountainous stream for continuous flood flow measurements. *Hydrological Processes*, 30(17):3014–3029.

Ranjan, R., Garg, S., Khoskbar, A. R., Solaiman, E., James, P., and Georgakopoulos, D. (2017). Orchestrating BigData Analysis Workflows. *IEEE Cloud Computing*, 4(3):20–28.

Rapp, B. E. (2017). Conservation of Mass: The Continuity Equation. In *Microfluidics: Modelling, Mechanics and Mathematics*, pages 265–271. Elsevier.

Reichle, R. H. (2008). Data assimilation methods in the Earth sciences. *Advances in Water Resources*, 31(11):1411–1418.

Restrepo-Estrada, C., de Andrade, S. C., Abe, N., Fava, M. C., Mendiondo, E. M., and de Albuquerque, J. P. (2018). Geo-social media as a proxy for hydrometeorological data for streamflow estimation and to improve flood monitoring. *Computers Geosciences*, 111:148–158.

Rickenmann, D. and Recking, A. (2011). Evaluation of flow resistance in gravel-bed rivers through a large field data set. *Water Resources Research*, 47(7).

Rickenmann, D., Turowski, J. M., Fritschi, B., Klaiber, A., and Ludwig, A. (2012). Bedload transport measurements at the Erlenbach stream with geophones and automated basket samplers. *Earth Surface Processes and Landforms*, 37(9):1000–1011.

Riley, W. D., Potter, E. C., Biggs, J., Collins, A. L., Jarvie, H. P., Jones, J. I., Kelly-Quinn, M., Ormerod, S. J., Sear, D. A., Wilby, R. L., Broadmeadow, S., Brown, C. D., Chanin, P., Copp, G. H., Cowx, I. G., Grogan, A., Hornby, D. D., Huggett, D., Kelly, M. G., Naura, M., Newman, J. R., and Siriwardena, G. M. (2018). Small Water Bodies in Great Britain and Ireland: Ecosystem function, human-generated degradation, and options for restorative action. *Science of the Total Environment*, 645:1598–1616.

Rinaldo, A., Marani, A., and Rigon, R. (1991). Geomorphological dispersion. *Water Resources Research*, 27(4):513–525.

Robson, A., Moore, R., Wells, S., Rudd, A., Cole, S., and Mattingley, P. (2017). *Understanding the performance of flood forecasting models*.

Rodi, W. (2010). Large eddy simulation of river flows. *River Flow 2010*, pages 23–32.

Rogger, M., Agnoletti, M., Alaoui, A., Bathurst, J. C., Bodner, G., Borga, M., Chaplot, V., Gallart, F., Glatzel, G., Hall, J., Holden, J., Holko, L., Horn, R., Kiss, A., Kohnová, S., Leitinger, G., Lennartz, B., Parajka, J., Perdigão, R., Peth, S., Plavcová, L., Quinton, J. N., Robinson, M., Salinas, J. L., Santoro, A., Szolgay, J., Tron, S., van den Akker, J. J. H., Viglione, A., and Blöschl, G. (2017). Land use change impacts on floods at the catchment scale: Challenges and opportunities for future research. *Water Resources Research*, 53(7):5209–5219.

Ronan, T. (2017). *Fluvial Seismo-acoustics: Characterizing temporarily dependent river conditions through near river seismic and acoustic signals*. PhD thesis.

Ronan, T. J., Lees, J. M., Mikesell, T. D., Anderson, J. F., and Johnson, J. B. (2017). Acoustic and Seismic Fields of Hydraulic Jumps at Varying Froude Numbers. *Geophysical Research Letters*, 44(19):9734–9741.

Rossing, T. D. and Fletcher, N. H. (2004). Underwater Sound. In *Principles of Vibration and Sound*, pages 294–307. Springer New York, New York, NY.

Roth, D. L., Finnegan, N. J., Brodsky, E. E., Rickenmann, D., Turowski, J. M., Badoux, A., and Gimbert, F. (2017). Bed load transport and boundary roughness changes as competing causes

of hysteresis in the relationship between river discharge and seismic amplitude recorded near a steep mountain stream. *Journal of Geophysical Research: Earth Surface*, 122(5):1182–1200.

Rouse, H. L. (1994). Measurement of bedload gravel transport: The calibration of a self-generated noise system. *Earth Surface Processes and Landforms*, 19(9):789–800.

Royle, J. A. (2018). Modelling sound attenuation in heterogeneous environments for improved bioacoustic sampling of wildlife populations. *Methods in Ecology and Evolution*, 9(9):1939–1947.

Sakaino, H. (2016). Camera-Vision-Based Water Level Estimation. *IEEE Sensors Journal*, 16(21):7564–7565.

Sanyal, J., Densmore, A. L., and Carbonneau, P. (2014). Analysing the effect of land-use/cover changes at sub-catchment levels on downstream flood peaks: A semi-distributed modelling approach with sparse data. *CATENA*, 118:28–40.

Schaefer (1972). Report on Hydrometry—Part I. *Hydrological Sciences Bulletin*, 17(2):145–169.

Schmandt, B., Aster, R. C., Scherler, D., Tsai, V. C., and Karlstrom, K. (2013). Multiple fluvial processes detected by riverside seismic and infrasound monitoring of a controlled flood in the Grand Canyon. *Geophysical Research Letters*, 40(18):4858–4863.

Schmandt, B., Gaeuman, D., Stewart, R., Hansen, S. M., Tsai, V. C., and Smith, J. (2017). Seismic array constraints on reach-scale bedload transport. *Geology*, 45(4):299–302.

Schneider, J. M., Rickenmann, D., Turowski, J. M., and Kirchner, J. W. (2015). Self-adjustment of stream bed roughness and flow velocity in a steep mountain channel. *Water Resources Research*, 51(10):7838–7859.

Seher, W. and Löschner, L. (2018). Balancing upstream-downstream interests in flood risk management: experiences from a catchment-based approach in Austria. *Journal of Flood Risk Management*, 11(1):56–65.

Seibert, J., Strobl, B., Etter, S., Hummer, P., and van Meerveld, H. J. (2019). Virtual staff gauges for crowd-based stream level observations. *Frontiers in Earth Science*, 7(April):1–10.

Shamloo, H., Rajaratnam, N., and Katopodis, C. (2001). Hydraulics of simple habitat structures. *Journal of Hydraulic Research*, 39(4):351–366.

Sheppard, S. A. and Terveen, L. (2011). Quality is a verb. In *Proceedings of the 7th International Symposium on Wikis and Open Collaboration - WikiSym '11*, page 29, New York, New York, USA. ACM Press.

Shin, I., Kim, J., and Lee, S.-G. (2007). Development of an internet-based water-level monitoring and measuring system using CCD camera. *ICMIT 2007: Mechatronics, MEMS, and Smart Materials*, 6794.

Simpfendorfer, C. A., Heupel, M. R., and Hueter, R. E. (2002). Estimation of short-term centers of activity from an array of omnidirectional hydrophones and its use in studying animal movements. *Canadian Journal of Fisheries and Aquatic Sciences*, 59(1):23–32.

Simpson, R. (1989). Turbulent Boundary-Layer Separation. *Annual Review of Fluid Mechanics*, 21(1):205–234.

Slabbekoorn, H. and Ripmeester, E. A. (2008). Birdsong and anthropogenic noise: Implications and applications for conservation. *Molecular Ecology*, 17(1):72–83.

Smith, P. J., Hughes, D., Beven, K. J., Cross, P., Tych, W., Coulson, G., and Blair, G. (2009). Towards the provision of site specific flood warnings using wireless sensor networks. *Meteorological Applications*, 16(1):57–64.

Sood, S. K., Sandhu, R., Singla, K., and Chang, V. (2018). IoT, big data and HPC based smart flood management framework. *Sustainable Computing: Informatics and Systems*, 20:102–117.

Sorensen, J. P. and Butcher, A. S. (2011). Water level monitoring pressure transducers-a need for industry-wide standards. *Ground Water Monitoring and Remediation*, 31(4):56–62.

Starkey, E., Parkin, G., Birkinshaw, S., Large, A., Quinn, P., and Gibson, C. (2017). Demonstrating the value of community-based ('citizen science') observations for catchment modelling and characterisation. *Journal of Hydrology*, 548:801–817.

Strahler, A. N. (1957). Quantitative analysis of watershed geomorphology. *Eos, Transactions American Geophysical Union*, 38(6):913–920.

Sugdon, R. (2004). Developing the Cost-Benefit Framework for the Appraisal of Flood and Coastal Erosion Risk Management Projects. Technical report.

Takagi, Y., Tsujikawa, A., Takato, P., Saito, T., and Kaida, M. (1998). Development of a noncontact liquid level measuring system using image processing. *Water Science and Technology*, 37(12):381–387.

Tauro, F., Petroselli, A., and Arcangeletti, E. (2016). Assessment of drone-based surface flow observations. *Hydrological Processes*, 30(7):1114–1130.

Tauro, F., Piscopia, R., and Grimaldi, S. (2017). Streamflow Observations From Cameras: Large-Scale Particle Image Velocimetry or Particle Tracking Velocimetry? *Water Resources Research*, 53(12):10374–10394.

Tetzlaff, D., Carey, S. K., McNamara, J. P., Laudon, H., and Soulsby, C. (2017). The essential value of long-term experimental data for hydrology and water management. *Water Resources Research*, 53(4):2598–2604.

Thorne, P. D. (1986). Laboratory and marine measurements on the acoustic detection of sediment transport. *The Journal of the Acoustical Society of America*, 80(3):899–910.

Thorne, P. D. and Foden, D. J. (1988). Generation of underwater sound by colliding spheres. *The Journal of the Acoustical Society of America*, 84(6):2144–2152.

Thumser, P., Haas, C., Tuhtan, J. A., Fuentes-Pérez, J. F., and Toming, G. (2017). RAPTOR-UAV: Real-time particle tracking in rivers using an unmanned aerial vehicle. *Earth Surface Processes and Landforms*, 42(14):2439–2446.

Tonolla, D., Lorang, M. S., Heutschi, K., and Tockner, K. (2009). A flume experiment to examine underwater sound generation by flowing water. *Aquatic Sciences*, 71(4):449–462.

Towe, R., Dean, G., Edwards, L., Nundloll, V., Blair, G., Lamb, R., Hankin, B., and Manson, S. (2020). Rethinking data-driven decision support in flood risk management for a big data age. *Journal of Flood Risk Management*.

Trell, E. M., Restemeyer, B., Bakema, M. M., and Van Hoven, B. (2017). *Governing for resilience in vulnerable places: An introduction*.

Tsai, V. C., Minchew, B., Lamb, M. P., and Ampuero, J.-P. (2012). A physical model for seismic noise generation from sediment transport in rivers. *Geophysical Research Letters*, 39(2).

Turowski, J. M. and Rickenmann, D. (2009). Tools and cover effects in bedload transport observations in the Pitzbach, Austria. *Earth Surface Processes and Landforms*, 34(1):26–37.

Ulseth, A. J., Hall, R. O., Boix Canadell, M., Madinger, H. L., Niayifar, A., and Battin, T. J. (2019). Distinct air–water gas exchange regimes in low- and high-energy streams. *Nature Geoscience*, 12(4):259–263.

Unduche, F., Tolossa, H., Senbeta, D., and Zhu, E. (2018). Evaluation of four hydrological models for operational flood forecasting in a Canadian Prairie watershed. *Hydrological Sciences Journal*, 63(8):1133–1149.

Van Den Doel, K. (2005). Physically Based Models for Liquid Sounds. *ACM Transactions on Applied Perception*, 2(4):534–546.

Vaughan, A. A., Belmont, P., Hawkins, C. P., and Wilcock, P. (2017). Near-Channel Versus Watershed Controls on Sediment Rating Curves. *Journal of Geophysical Research: Earth Surface*, 122(10):1901–1923.

Venditti, J. (2013). 9.10 Bedforms in Sand-Bedded Rivers. In *Treatise on Geomorphology*, pages 137–162. Elsevier.

Viglione, A., Merz, B., Viet Dung, N., Parajka, J., Nester, T., and Blöschl, G. (2016). Attribution of regional flood changes based on scaling fingerprints. *Water Resources Research*, 52(7):5322–5340.

Vogel, D. A. (2006). Evaluation of Acoustic Telemetry Equipment for Monitoring Juvenile Chinook Salmon. (March):1–61.

Vračar, M. S. and Mijić, M. (2011). Ambient noise in large rivers (L). *The Journal of the Acoustical Society of America*, 130(4):1787–1791.

Wang, N., Liu, W., Wang, H., Sun, F., Duan, W., Li, Z., Li, Z., and Chen, Y. (2021). Improving streamflow and flood simulations in three headwater catchments of the Tarim River based on a coupled glacier-hydrological model. *Journal of Hydrology*, 603(PC).

Ward, S., Borden, D. S., Kabo-Bah, A., Fatawu, A. N., and Mwinkom, X. F. (2019). Water resources data, models and decisions: International expert opinion on knowledge management for an uncertain but resilient future. *Journal of Hydroinformatics*, 21:32–44.

Weichert, R., Minor, H., and Bezzola, G. (2006). Bed morphology and flow resistance in steep open channels with varying widths. In *River Flow 2006*. Taylor Francis.

Westerberg, I. K., Sikorska-Senoner, A. E., Viviroli, D., Vis, M., and Seibert, J. (2020). Hydrological model calibration with uncertain discharge data. *Hydrological Sciences Journal*, 00(00):1–16.

Wilby, R. L. (2019). A global hydrology research agenda fit for the 2030s. *Hydrology Research*, 50(6):1464–1480.

Wildschut, D. (2017). The need for citizen science in the transition to a sustainable peer-to-peer-society. *Futures*, 91:46–52.

Willert, C. E. and Gharib, M. (1991). Digital particle image velocimetry. *Experiments in Fluids*, 10(4):181–193.

Withers, M. M., Aster, R. C., Young, C. J., and Chael, E. P. (1996). High-frequency analysis of seismic background noise as a function of wind speed and shallow depth. *Bulletin of the Seismological Society of America*, 86(5):1507–1515.

WMO (2008). *Guide to Hydrological Practices Vol I*, volume 53.

Xiao, Y.-X., Feng, X.-T., Chen, B.-R., and Feng, G. (2018). Microseismic Monitoring Method of the Rockburst Evolution Process. In *Rockburst*, pages 301–315. Elsevier.

Yackinous, W. S. (2015). Chapter 15 - Characteristics of Ecological Network Dynamics. In Yackinous, W. S., editor, *Understanding Complex Ecosystem Dynamics*, pages 265–298. Academic Press, Boston.

Yen, B. C. (2002). Open Channel Flow Resistance. *Journal of Hydraulic Engineering*, 128(1):20–39.

Yoo, C., Ku, H., and Kim, K. (2011). Use of a Distance Measure for the Comparison of Unit Hydrographs: Application to the Stream Gauge Network Optimization. *Journal of Hydrologic Engineering*, 16(11):880–890.

Young, D. S., Hart, J. K., and Martinez, K. (2015). Image analysis techniques to estimate river discharge using time-lapse cameras in remote locations. *Computers Geosciences*, 76:1–10.

Yuliandoko, H., Subono, Wardhany, V. A., Pramono, S. H., and Siwindarto, P. (2018). Design of flood warning system based IoT and water characteristics. *Telkomnika (Telecommunication Computing Electronics and Control)*, 16(5):2101–2110.

Zakarauskas, P. (1986). Ambient noise in shallow water: a literature review. *Canadian Acoustics*, 14(3):3–17.

Zeman, O. (1995). The persistence of trailing vortices: A modeling study. *Physics of Fluids*, 7(1):135–143.

Zhang, Zhou, Liu, Zhang, and Wang (2019a). Visual Measurement of Water Level under Complex Illumination Conditions. *Sensors*, 19(19).

Zhang, Z., Wang, X., Fan, T., and Xu, L. (2013). River surface target enhancement and background suppression for unseeded LSPIV. *Flow Measurement and Instrumentation*, 30:99–111.

Zhang, Z., Zhou, Y., Liu, H., and Gao, H. (2019b). In-situ water level measurement using NIR-imaging video camera. *Flow Measurement and Instrumentation*, 67:95–106.

Ziemann, A., Barth, M., and Hehn, M. (2013). Experimental investigation of the meteorologically influenced sound propagation through an inhomogeneous forest site. *Meteorologische Zeitschrift*, 22(2):221–229.

Zoccatelli, D., Borga, M., Viglione, A., Chirico, G. B., and Blöschl, G. (2011). Spatial moments of catchment rainfall: rainfall spatial organisation, basin morphology, and flood response. *Hydrology and Earth System Sciences Discussions*, 8(3):5811–5847.

Image References

Jemima Puddle Duck- The Tale of Jemima Puddle-Duck by Beatrix Potter.

Wind in the Willows- Colorised version of Ernest H. Shepard's 1931 illustration for The Wind in the Willows, from Seth Lerer's The Wind in the Willows: An Annotated Edition.

Winnie the Pooh- A.A. Milne with illustration from E.H. Shepard.

Wind in the Willows- Colorised version of Ernest H. Shepard's 1931 illustration for The Wind in the Willows, from Seth Lerer's The Wind in the Willows: An Annotated Edition.

Mark Twain- Edwin Larson, oil on canvas, 1935.

Eleonora- Illustration by Byam Shaw, 1909.

Heraclitus- Hulton Archive.